Host-microbial interactions: extracellular metabolites with immunomodulatory potential generated by *Escherichia coli* in response to human defensin

Von der Fakultät für Lebenswissenschaften

der Technischen Universität Carolo-Wilhelmina

zu Braunschweig

zur Erlangung des Grades einer

Doktorin der Naturwissenschaften

(Dr. rer. nat.)

genehmigte

D i s s e r t a t i o n

von Andréia Bergamo Estrela
aus Porto Alegre, RS, Brasilien

1. Referent: Professor Dr. Kenneth Nigel Timmis
2. Referentin: Professorin Dr. Katharina Riedel
eingereicht am: 01.08.2011
mündliche Prüfung (Disputation) am: 26.10.2011

Druckjahr 2011

Vorveröffentlichungen der Dissertation

Teilergebnisse aus dieser Arbeit wurden mit Genehmigung der Fakultät für Lebenswissenschaften, vertreten durch den Mentor der Arbeit, in folgenden Beiträgen vorab veröffentlicht:

Publikationen

Estrela, A.B. & Abraham, W.R. Adenosine in the inflamed gut: a janus faced compound. Current Medicinal Chemistry 18: 2791-2815 (2011).

Tagungsbeiträge

Estrela, A.B., Würdemann, D., Molinari, G. & Abraham, W.R.: Low molecular weight metabolites secreted by *Escherichia coli* in response to human beta-defensin (hBD) activity.(Poster) European Molecular Biology Organization (EMBO) Meeting, Amsterdam (2009).

Estrela, A.B., Würdemann, D., Molinari, G. & Abraham, W.R.: Response of *Escherichia coli* to human beta-defensin activity: secretion of low molecular weight metabolites.(Poster) 62. Jahrestagung der Deutschen Gesellschaft für Hygiene und Mikrobiologie (DGHM) und Jahrestagung der Vereinigung für Allgemeine und Angewandte Mikrobiologie (VAAM), Hannover (2010).

Estrela, A.B., Gutierrez, M. & Abraham, W.R. Extracellular compounds from *Escherichia coli* after human beta-defensin-2 treatment and the effects on human intestinal epithelial cells (Caco-2). (Vortrag) 3rd Seeon Conference - Microbiota, Probiota and Host, Seeon/Chiemsee (2010).

Estrela, A.B., Gutierrez, M. & Abraham, W.R. Secretion of small metabolites by *Escherichia coli* in response to human beta-defensin-2 can play a role in host-microbial interactions in the inflamed gut. (Vortrag) International Scientific Conference on Gastro-Intestinal Microbial Ecology (GME), Kosice (2010).

CONTENTS

LIST OF FIGURES

Section 1

Section 3

Section 4

Section 5

Section 6

Section 7

LIST OF TABLES

Section 3

Section 4

Section 7

ABBREVIATIONS

5' NT, 5' nucleotidase

A, adenine

ADA, adenosine deaminase

Ado, adenosine

ADP, adenosine 5' diphosphate

AIEC, adherent-invasive *Escherichia coli*

AMP, adenosine 5' monophosphate

ANOVA, analysis of variance

AP, antimicrobial peptide

AR, adenosine receptor

ATP, adenosine 5' triphosphate

BPC, base peak chromatogram

BSA, bovine serum albumin

BSTFA, N,O-bis(trimethylsilyl)trifluoroacetamide

CC, collision cell

CD, Crohn's disease

CFU, colony-forming units

CNT, concentrative nucleoside transporter

DAD, diode array detector

DAPI, 4',6-diamidino-2-phenylindole

DC, dendritic cells

DCIP, 2,6-dichlorophenolindophenol

DMEM, Dulbecco's modified Eagle's medium

DNA, deoxyribonicleic acid

DSS, dextran sodium sulphate

EDTA, Ethylenediaminetetraacetic acid

EHEC, enterohemorragic *Escherichia coli*

ENT, equilibrative nucleoside transporter

EPEC, enteropathogenic *Escherichia coli*

ESI, electro-spray ionization

FSC, forward scatter

G, guanine

GALT, gut-associated lymphoid tissue

GAS, group-A *Streptococcus*

GC, gas chromatography

Guo, guanosine

hBD, human b-defensin

HD, human a-defensin

HNP, human neutrphil peptide

HPLC, high pressure liquid chromatography

HRP, horseradish peroxydase

IDB, inflammatory bowel diseases

IEC, intestinal epithelial cells

IFN, interferon

Ig, immunoglobulin

IκB, inhibitor of NF-κB

IKK, IκB kinase

IL, interleukin

IRMS, isotopic ratio mass spectrometry

LB, Luria-Bertani broth

LC, liquid chromatography

LPS, lipopolysaccaride

MAMP, microbe-associated molecular pattern

MAPK, mitogen-activated protein kinase

MIC, minimal inhibitory concentration

MRM, multiple reaction monitoring

MS, mass spectrometry

MS/MS, tandem mass spectrometry

NF-kB, nuclear factor κ-light-chain-enhancer of activated B cells

NLR, Nod-like receptor

NMR, nuclear magnetic resonance

NOD, nucleotide-binding oligomerization domain

O.D., optical density

PAGE, polyacrylamide gel electrophoresis

PAMP, pathogen-associated molecular pattern

PBMC, peripheral blood mononuclear cells

PBS, phosphate buffered saline

PFA, paraformaldehyde

PI, propidium iodide

PPAR, peroxisome proliferator-activated receptor

QS, quorum sensing

RNA, ribonucleic acid

SDS, sodium dodecyl sulfate

SFB, segmented filamentous bacteria

SMAP, sheep myeloid antimicrobial peptide

SN, supernatant

SSC, side scatter

TBST, Tris buffered saline - Tween

Tc, T-cytotoxic cell

TCR, T-cell receptor

TE, Tris-EDTA

TEM, transmission electron microscopy

TGF, tumor growth factor

Th, T-helper cell

TIC, total ion current

TLR, Toll-like receptor

TMCS, trimethylchlorosilane

TMS, trimethylsylil

TNF, tumor necrosis factor

U.V., ultra violet

UC, ulcerative colitis

VEGF, vascular endothelial growth factor

ABSTRACT

Host-microbial interactions in the human gut are important determinants of the health status of the system, influencing the development and course of several pathologies, including inflammatory bowel diseases (IBD). Gut inflammation in IBD represents a complex scenario where the inducible epithelial β-defensins are shown to play an important role. They present differential expression in IBD patients and are upregulated in inflamed colonic mucosa, where they act as multifunctional antimicrobial peptides and immunomodulators. The present study investigated the hypothesis that an intestinal bacterium (*Escherichia coli*) responds to increased levels of human β-defensin -2 (hBD-2), generating extracellular small molecules which could have an effect on the host. Using HPLC-MS, we analyzed supernatants from *E. coli* cultures challenged with hBD-2, comparing these to unchallenged controls. Molecules present specifically in the supernatants of challenged cultures were identified by tandem MS. The response was characterized by quantitative HPLC-MS/MS analysis. The general physiological state of challenged bacteria was addressed by microscopic and biochemical tools, and the possible mechanisms leading to the observed response were investigated. Additionally, the effects of extracellular compounds from hBD-challenged *E. coli* upon human intestinal epithelial cell line (Caco-2) were evaluated by assessing the activity of the NF-κB pathway. The major compounds identified in *E. coli* supernatants after hBD challenge were the purine nucleosides adenosine (Ado) and guanosine (Guo). The response was dependent upon hBD-2 dose and cell density, each compound presented distinct variation. Other tested defensins and bacterial strains presented variable outcomes. Interaction of hBD-2 with *E. coli* membrane and intracellular nucleic acids, rather than absolute cell lysis, was found to be the mechanism generating extracellular Ado, and the involvement of a AMP-degrading activity was demonstrated. Results obtained from the experiments in the human cell line indicated that NF-κB pathway activation is enhanced in the presence of Ado and supernatants from hBD-challenged *E. coli* containing Ado. Thus, hBD-2 may alter local levels of Ado as a consequence of its interaction with gut bacteria, which in turn can affect the inflammatory process, mediating host-microbial interactions in the intestinal mucosa of IBD patients.

1. INTRODUCTION

1.1. Host-microbial interactions and the human gut scenario

1.1.1. Characterizing the human gut microbiota

The intestinal lumen is a unique environment in our body. It represents the largest surface of contact with the exterior, receiving a constant income of chemical compounds of many kinds through the diet. Furthermore, it is inhabited by a huge number of highly diverse microbes, collectively called gut microbiota. For more than 3 decades it has been appreciated that in the human gastrointestinal tract there are approximately 10^{14} microbial cells, a number 10-fold higher than the total number of mammalian cells in the body (Luckey, 1972). This finding raised the view of humans and their commensal microorganisms as being an inter-kingdom community, an ecological and evolutionary unit (Luckey, 1972; Savage, 1977).

Our knowledge regarding this community has since then greatly increased, especially since the advent of culture-independent, molecular and computational techniques. Currently, it is known that the great majority of bacterial species are uncultivable under laboratory conditions and, although the isolation of key representatives is of obvious importance for detailed functional studies (Duncan *et al.*, 2007), high throughput sequencing and metagenomic analyses became powerful tools in the exploration of bacterial diversity in the gut (Hattori and Taylor, 2009). Large-scale analyses of the microbial small-subunit (16S) ribosomal RNA gene (16S rDNA) sequences in intestinal mucosal tissue or fecal samples from diverse human subjects were performed (Eckburg *et al.*, 2005; Ley *et al.*, 2006b; Frank *et al.*, 2007). Combining the data together provided an unparalleled picture of the bacterial diversity that could be found, where >98 % belong to only four phyla: *Firmicutes*, *Bacteroidetes*, *Proteobacteria*, and *Actinobacteria* (Frank, *et al.*, 2007). This relative uniformity at higher taxonomic levels confirmed previous molecular analysis (Suau *et al.*, 1999). At lower taxonomic levels, the diversity increases substantially: at least 500 distinct bacterial species are estimated (Eckburg *et al.*, 2005). This number may be in fact much higher, and the richness of human gut microbioma has been suggested to consist of more than 1,800 genera and 15,000 species (Frank, *et al.*, 2007). Figure 1.1 illustrates the most common bacterial genera found in the human gut and their respective phyla.

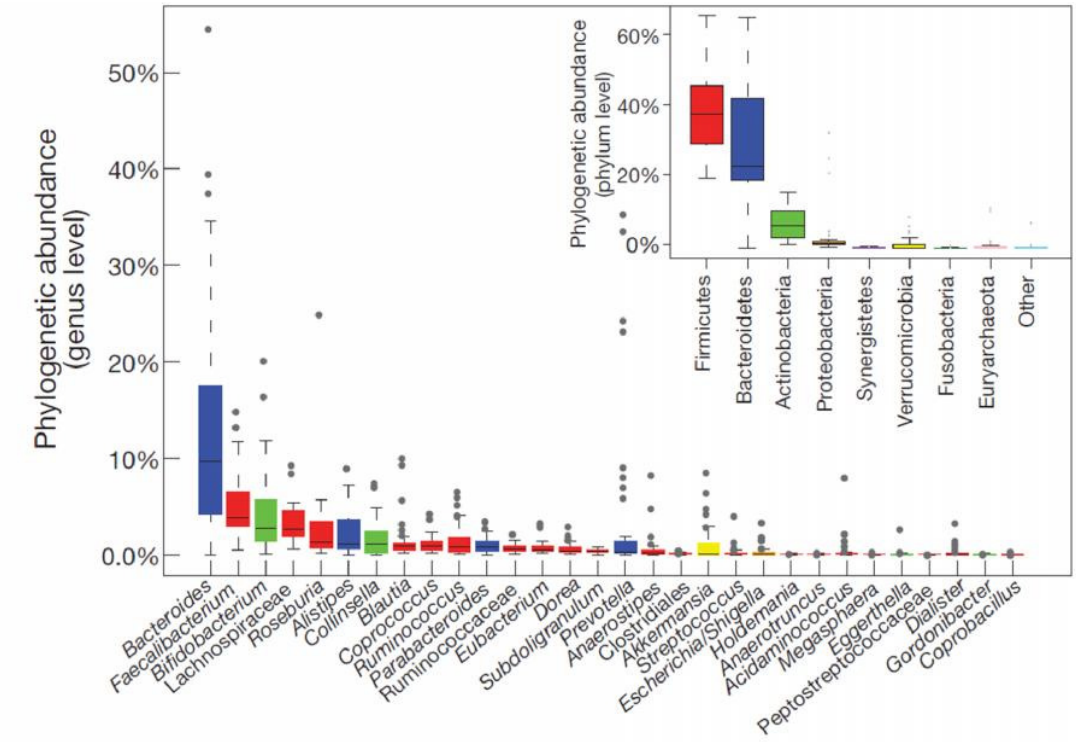

Figure 1.1 - Phylogenetic abundance and variation of the human gut metagenome at genus and phylum levels. The plot shows the 30 most abundant genera identified in the gut metagenome from 35 human subjects. The genera are coloured according to their phyla (inset). Boxes represent the interquartile range (IQR) between first and third quartiles and the line inside represents the median. Whiskers denote the lowest and highest values within 1.53 IQR from the first and third quartiles, respectively. Circles represent outliers beyond the whiskers. Published by Arumugam *et al.*, 2011.

The efforts investigating gut microbiota composition indicated that there is a high degree of individual variation among subjects and several variables can act in shaping the intestinal microbial community including genetic relatedness, environmental factors, obesity and health status (Turnbaugh and Gordon, 2009; Li and Hotamisligil, 2010). Despite such individual variation, recent deep-sequencing metagenomic studies have successfully established a "core gut microbiome", a common set of bacterial genes largely shared among a population (Qin *et al.*, 2010; Arumugam *et al.*, 2011). In this context, a "minimal gut genome" would contain genes necessary for a bacterium to succeed in the gut environment, and a "minimal gut metagenome" would comprise the genes required for the whole system homeostasis (Qin *et al.*, 2010). These studies, like others before, draw attention to the importance of a functional approach to address the intestinal microbiota from another point of view, looking not only for its components, but mainly for their activity and functions. A comprehensive analysis of the collective microbial genome, which is estimated to exceed our

own human genome at least by 100-fold, is therefore a promising tool for exploring the relationships between intestinal bacteria and their human host (Ley *et al.*, 2006a).

1.1.2. Gut microbiota roles in health and disease

Many of the host-microbial relationships in the human intestine are recognized as beneficial interactions. For example, the breakdown of otherwise indigestible compounds from the diet, which is only possible due to the action of the gut microbiota. The diet has indeed a central role in the co-evolution of vertebrates with their symbiotic intestinal microbiota (Ley *et al.*, 2008). The functionality of our gut microbiome could be assessed analyzing the metagenomic data searching for metabolic genes. Gill *et al.*, 2006 identified an enrichment of genes encoding enzymes of glycan metabolism, most of them lacking in the human genome, as well genes involved in the synthesis of essential amino acids and vitamins, and detoxification of xenobiotics. Accordingly, the same functions could be assigned to the "minimal metagenome", as described by Qin *et al.*, 2010, the set of genes necessary for maintenance of homeostasis in the gut ecosystem. Recently, a metatranscriptome analysis, which addresses the actively transcribed genes, rather than the presence of sequences, also highlighted nutrient processing and energy production as main operational roles of the microbiota, and demonstrated that individual variation is lower when considering activity patterns (Gosalbes *et al.*, 2011).

Having in mind the complexity and functional importance of the intestinal bacteria, it is reasonable to infer that this community has a great influence in the host health status. In our intestine, the microbiota is not only rich and diverse, but is also present at high cell density (3.2×10^{11} cells/g in the human colon), another special condition of the gut microbiota when compared to other microbial communities like the one present on our skin (Whitman *et al.*, 1998). Such conditions are at the same time favorable and demanding for an efficient communication system, integrating the activity of different members of the microbiota and the host, in order to keep the balance of a stable and healthy state. In this sense, it is not unexpected that perturbations of the system, like changes in microbial composition have been extensively reported to correlate with conditions of metabolic disorders and gastrointestinal diseases (Backhed *et al.*, 2005).

One well studied example refers to the influence of gut microbes in obesity. Comparing genetically obese and lean mice it was observed a 50 % reduction in the abundance of *Bacteroidetes* in obese animals where the numbers of *Firmicutes* were

proportionally increased (Ley *et al.*, 2005). These findings were also reported in obese and lean humans. Interestingly, the relative abundance of the two dominant phyla could be regulated in obese individuals by either fat-restricted or carbohydrate-restricted diet, approaching the condition found in lean subjects (Ley *et al.*, 2006b). Studies on germ-free mice revealed that colonization of these animals with the gut microbiota from a conventionally raised mice increased the body fat content of germ-free mice, suggesting that the bacteria can influence energy harvest and storage by the host (Backhed *et al.*, 2004). Moreover, germ-free mice were shown to be resistant to diet-induced obesity, presenting an increased fatty acid metabolism (Backhed *et al.*, 2007). Confirming the central role of gut microbiota in obesity, it was demonstrated that the obese phenotype could be transferred to germ-free animals by colonization with the microbiota from an obese donor, this "obese microbiome" having an increased efficiency in energy harvest from the diet (Turnbaugh *et al.*, 2006).

Likewise, other conditions that were already reported to have a microbial component or to be affected by the intestinal biota include type II diabetes, intimately linked to obesity, but also diseases in direct relation to immune functions, like type I diabetes, neonatal necrotizing enterocolitis, celiac disease, colon cancer, *Candida* infection, gastroenteritis, ulcerative colitis and Crohn's disease (Fujimura *et al.*, 2010). Neonatal necrotizing enterocolitis provides a good example of the importance of intestinal colonization for the development of our immune system. It affects mainly premature neonates, in which colonization of the sterile-born gut is delayed. It has been reported that the patients presented lower bacterial diversity and increased *Gammaproteobacteria* abundance in comparison to healthy babies (Wang *et al.*, 2009). The role of colonic bacteria in development of colon cancer has been studied and, although no specific taxa has yet been implicated in oncogenesis, it is suggested that the inflammatory response triggered by bacteria, leading to higher cell division rates, increase the risk of colon cancer (Chang and Parsonnet, 2010).

Inflammation also connects gut microbiota to the development of autoimmune conditions like type I diabetes. Inoculation of MyD88-negative germ-free mice with representative bacteria of the conventional human gut microbiota can attenuate the otherwise higher predisposition to develop type I diabetes (Wen *et al.*, 2008). This illustrates one branch of the "hygiene hypothesis" (the correlation of reduced exposure to pathogens with increased incidence of autoimmune diseases), called the "old friends hypothesis", which highlights a role for the commensal biota in protection against autoimmunity (Rook and

Brunet, 2005). The involvement of intestinal biota in the specific context of Crohn's disease and ulcerative colitis, collectively called inflammatory bowel disease or IBD, is also under intense investigation (Sokol and Seksik, 2010) and will be discussed in more detail in section 1.2.

1.1.3. Signaling events of host-microbial interactions in the gut

The examples of diseases discussed have the common trait of being in close relation to immune processes and therefore, the understanding of their underlying mechanisms, etiology and pathophysiology can be greatly improved by understanding the role of intestinal bacteria in shaping host immunity. The multiple levels of interchange must be considered, which are also related to each other at some degree, for instance: the effects of commensal bacteria in immunoregulation, the host's mechanisms to control the microbial community, the modulation of host responses to pathogens and the bacterial-bacterial interactions taking place within the gut microbiota.

The first two cases represent a bidirectional flow of signals between the two components of the host-microbiota system. Here, there is a clear argumentation behind a rather complex phenomenon: commensal biota and the host immunity must be harmonized to allow colonization and co-existence (Kelly *et al.*, 2005). Moreover, there is an increasing amount of data showing that different properties of commensals and pathogens to interact with host signaling (including surface molecules, pathogenicity factors and all sorts of immunomodulatory traits) are the key to allow the immune system to distinguish between them and respond adequately (Magalhaes *et al.*, 2007; Sansonetti, 2011).

In healthy tissue, the intestinal epithelial cells (IEC) play a central role: they establish the first contact with gut bacteria and their responses upon this contact will dictate how the interaction progresses. IEC recognize bacteria by expressing receptors for microbe-associated molecular patterns (MAMPs), which can engage intracellular signaling pathways tuning the production of antimicrobial factors and cytokines, thereby controlling bacterial population and the recruitment of immune cells to the mucosal sites (Cerf-Bensussan and Gaboriau-Routhiau, 2010). At this point, it is known that the microbiota can interfere with IEC signaling, being able to suppress immune responses and create tolerance. Some already described mechanisms include desensitization by continuous exposure to MAMPs like lipopolysaccharide (LPS) or attenuation by soluble mediators released by the bacteria (Cerf-Bensussan and Gaboriau-Routhiau, 2010).

Specific examples were described for culturable members of the gut microbiota and during investigations of the beneficial effects of certain probiotics. Probiotics are defined as ‘‘living microorganisms which upon ingestion in certain numbers exert health benefits beyond inherent basic nutrition’’ (Guarner and Schaafsma, 1998). This definition has been adopted by the Food and Agricultural Organization of the United Nations and the World Health Organization (WHO, 2001) and encompasses the bacteria that have been described to positively affect host immune responses. For instance, species belonging to the genera *Bacteroides*, *Bifidobacterium*, and *Lactobacillus* have already demonstrated to have modulatory effects on IEC signaling. In many cases, the central target is the nuclear factor kappa-light-chain-enhancer of activated B cells (NF-κB) pathway, a key component for activation of immune responses to several stimuli (Thomas and Versalovic, 2010).

NF-κB pathway is engaged downstream of MAMP receptor activation, for example Toll-like receptors (TLR) and Nod-like receptors (NLR), and it triggers a phosphorylation cascade where the kinase activity of the IκB kinase (IKK) complex phosphorylates the inhibitor of NF- κB (IκB) molecules, resulting in their ubiquitin-mediated degradation. In the unstimulated state, IκB is bound to NF-κB subunits in the cytoplasm, but once IκB is degraded after stimulation, NF-κB is able to dimerize and translocate to the nucleus, where it can regulate the expression of target genes (Razani and Cheng, 2010). Pathogenic and commensal bacteria can interfere with this pathway at several points (Figure 1.2). They can prevent IκB degradation, like is reported for some *Lactobacillus* (Petrof *et al.*, 2009; Ma *et al.*, 2004) and *Salmonella* species (Neish *et al.*, 2000). In turn, *Bacteriodetes thetaiotaomicron* can inhibit transcriptional activity of NF-κB by modulating peroxisome-proliferation-activated receptor γ (PPARγ) pathway and promoting the export of NF-κB from the nucleus back to the cytoplasm (Kelly *et al.*, 2004).

Among the responses regulated by NF-κB in IEC, as well as in immune cells present in the gut mucosa, are many of the functions required for a proper immune response to intestinal bacteria. This brings us to the second component of the bidirectional system: the effects of the host on intestinal bacterial community. The host’s innate mechanisms to keep the microbiota under control include the production of antimicrobial peptides called defensins. Defensin expression is one interesting and much explored tool for homeostasis control in the gut, and will be discussed in more detail in section 1.3. Other compounds produced in the mucosa which have antibiotic properties include cathelicidins, the bactericidal/permeability-increasing protein (BPI), angiogenin and lysozyme (Canny *et al.*,

2006; Hooper *et al.*, 2003; Lehrer and Ganz, 2002; Müller *et al.*, 2005). Besides the direct action of bactericidal products, the production of a physical barrier represented by the mucus and the presence of plasma cell-derived secretory immunoglobulin (Ig)A in this layer also serve as mechanisms for control of excessive and/or undesired bacterial proliferation. Because IgA can induce biofilm formation and the mucus can protect bacteria from soluble immune mediators, they represent at the same time a colonization-favoring factor to be explored by the commensal bacteria (Kelly *et al.*, 2005).

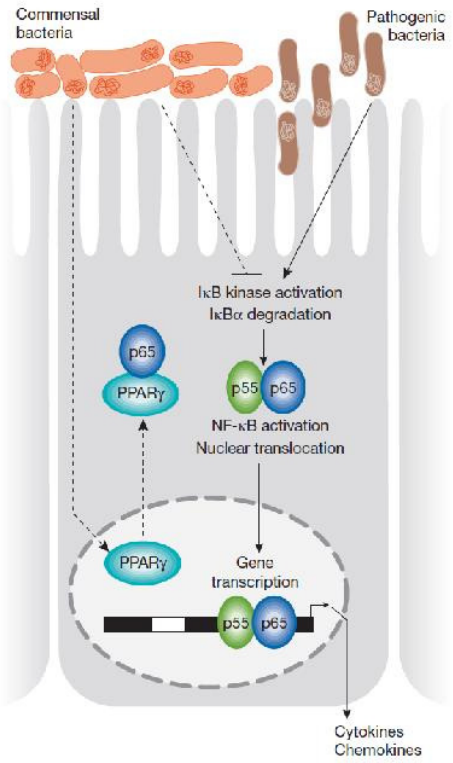

Figure 1.2 - Mechanisms of bacterial modulation of NF-κB pathway in intestinal epithelial cells. Published by O'Hara and Shanahan, 2006

Other target of NF-κB regulation is the secretion of cytokines, which are responsible for cell recruitment to the mucosa and for the triggering of effector functions, linking the first-line innate defense played by IEC to other cellular and adaptative responses (Artis, 2008). For example, an epithelial-specific cytokine, produced by IEC in a NF-κB-dependent pathway, is responsible for inhibition of pro-inflammatory responses in dendritic cells (DC), creating a tissue-specific conditioning that promotes homeostasis (Zaph *et al.*, 2007). The production of cytokines by IEC, represents an important point for controlling mucosal immune responses and are therefore central targets for modulation by bacteria. For instance, pathogenic *Escherichia coli* and *Salmonella* strains can induce the production of pro-inflammatory

cytokines like interleukin (IL)-6 and IL-8 by epithelial cells, whereas non-pathogenic strains were reported to inhibit the secretion of these mediators, both cases involving NF-κB modulation (Savkovic *et al.*, 1997; Ye *et al.*, 2007; Collier-Hyams *et al.*, 2002). Other studies have demonstrated that bacterial ligands interacting with TLR-9 in intestinal epithelial cells exert a complex modulation over production of pro-inflammatory IL-8 via NF-κB inhibition, but only when activation occurred apically, denoting the importance of IEC polarization and barrier integrity in maintenance of tolerance and homeostasis (Lee *et al.*, 2006).

Parallel to the beneficial mechanisms of regulation taking place between the healthy biota and the host, which keep an immune homeostasis environment in the gut, there are the interactions involving potentially harmful pathogenic bacteria also present in the system. These enteric pathogens are frequently strains which differ from the "friendly" gut bacteria by the acquisition of certain genetic and phenotypic traits, or pathogenicity factors, like antibiotic resistance, expression of secretion systems, adhesins and the production of toxins (Pallen and Wren, 2007). As an example, normal commensal *E. coli* strains do not produce Shiga toxin, the main virulence trait of the highly pathogenic enterohemorragic *E. coli* (EHEC) serovar (Kaper *et al.*, 2004), which has recently caused a serious breakout in Northern Germany.

Many of these pathogens reside within the normal community and only cause active infection when the conditions are favorable. Thus, together with the commensal bacteria, the opportunistic pathogens also participate in the host-microbial interactions in the gut. An already described, but yet not fully-understood phenomenon is called colonization resistance. This concept describes the inability of most pathogens to colonize the intestine in the presence of a normal commensal microbiota, which is consistent with the observation that disruption of the normal gut biota by antibiotics increases the risk of enteric infections (Stecher and Hardt, 2008). In some cases, the already mentioned influence of the commensals on the immune responses can turn in the direction of stimulating host defenses to an infection. For example, it has been reported that certain unculturable intestinal bacteria (segmented filamentous bacteria; SFB) when present in the normal murine microbiota community, are associated with stronger antimicrobial responses and the presence of mucosal T-helper cells (Th)17, leading to a more efficient control of the invasive pathogen *Citrobacter rodentium* (Ivanov *et al.*, 2009). On the other hand, the pathogens can also employ their influence on the host to generate and benefit from anti- or pro-inflammatory responses. Those influences include many studied mechanisms of immune evasion (Finlay and McFadden, 2006), but also the

stimulation of responses against the commensal biota as a strategy of competition for colonization niches (Stecher and Hardt, 2008).

Another aspect of the signaling events in the gut ecosystem, the bacteria-bacteria interactions, includes ecological relationships like competition and exclusion. These interactions can be mediated, for instance, by bacterial derived antimicrobial proteins called bacteriocins, from which the colicins from *E. coli* are the best studied examples (Riley and Wertz, 2002). Furthermore, this cross-talk can assume a rather complex character when considering the chemical arsenal available in the context of the human gut. As mentioned above, a very refined communication system to orchestrate the rich interactions in the human gut is needed, and the interface of the mucosal tissue with luminal biota is a favorable environment. Such a system is expected to gather bacterial and host molecules with connecting cross-talk events. Indeed, it is known that the molecules responsible for bacteria-bacteria communication in microbial communities, or the quorum sensing (QS) system, can not only exert their effect on prokaryotic cells, where they are involved in biofilm formation and virulence factor expression, but also mediate communication between bacteria and the host, in a process called inter-kingdom signaling (Hughes and Sperandio, 2008). It has been demonstrated that an *E. coli* strain was able to express virulence genes in response to an eukaryotic signal, even in the absence of its own autoinducer, and the hormones epinephrine and norepinephrine were identified as being responsible for this host induction of bacterial QS (Sperandio *et al.*, 2003). Accordingly, norepinephrine had been shown to correlate with intestinal expression of *Pseudomonas aeruginosa* virulence factor and consequently induction of lethal sepsis in post-surgical stress (Alverdy *et al.*, 2000). Conversely, the acyl homoserine lactones used as autoinducers by many Gram-negative bacteria, have been reported to have immunoregulatory functions in human cells (Shiner *et al.*, 2005).

Taken together, the many interconnected levels of host-microbial interactions taking place in the human gut represent a delicate network, which is usually efficient in maintaining a well-balanced state. In some cases, however, the stability of this complex system is disrupted and the result is an uncontrolled inflammatory response, an equally complex situation, but with detrimental consequences for the human host. Excessive inflammation is one central feature in the pathophysiology of inflammatory bowel diseases and this condition represents a meaningful example of the role of gut microbiota and their interaction with host factors, responsible for the healthy status of the human intestine.

1.2. Inflammatory Bowel Disease (IBD)

Inflammatory bowel disease (IBD) is a lifelong disabling condition characterized by a chronic relapsing inflammatory disorder of the gastrointestinal tract, commonly affecting young adults. It presents two main forms: Crohn's disease (CD) and ulcerative colitis (UC). The prevalence of IBD worldwide is more than 390 cases per 100,000 inhabitants, and the incidence rates demonstrate a great geographical variation: higher numbers are reported in economically developed regions (Northern and Western Europe and North America), whereas lower rates are found in Africa, South America and Asia. The incidence of CD and UC worldwide denote remarkable differences between the two forms of disease. Rates ranging from 0.1 to 16/100,000 for CD and from 0.5 to 24.5/100,000 for UC are reported. Recently, however, epidemiological studies have shown a trend where the predominance of UC over CD seems to be diminishing, and the geographic differences in the incidence of IBD are reduced, with increased rates in developing regions like East Europe and Asia (Lakatos, 2006).

Besides the epidemiological differences, and despite both being characterized by mucosal inflammation, the two forms of IBD present many differences in their clinical presentation. CD can affect any part of the gastrointestinal tract, most typically the terminal ileum, cecum, colon and the peri-anal area. It manifests as a discontinuous inflammation, interposed between segments of unaffected tissue. The histological features include dense lymphocyte and macrophage infiltration with the involvement of the full thickness of the wall and often occurrence of fistulae. General symptoms include pain, diarrhea and bowel obstruction. UC, in turn, presents as a continuous extension of inflamed tissue, always affecting the rectum and generally also the colon. The cellular infiltration is superficial, restricted to the mucosal layer. Patients suffer from bloody diarrhea and progressive loss of motility (Bouma and Strober, 2003; Baumgart and Sandborn, 2007).

The etiology of IBD is a matter of great debate and two main lines of arguments have been proposed. One points to a dysfunctional immune system producing an inappropriate response to the normal intestinal biota, while the other suggests the stimulation of a normally functional immunity by an altered gut microbiota and/or defective epithelial barrier, as the cause of inflammation (Strober *et al.*, 2007). Currently, the most accepted view embraces the two theories and describes IBD as having a multifactorial etiology, including the contribution of environmental, microbial and host factors (Kaser *et al.*, 2010). The environmental aspect is

still very poorly understood and refers to variables which have impact on the host immune responses and on intestinal microbial composition, such as diet, stress, smoking habits and the use of antibiotics or other drugs (Sartor, 2006). Figure 1.3 schematically represents the main components implicated in IBD development. From this view, it is possible to recognize both microbial factors and host-related factors (genetic background, immune system and epithelial barrier status) as well as the interaction events between them, as crucial players in the pathogenesis of IBD (Kaser *et al.*, 2010).

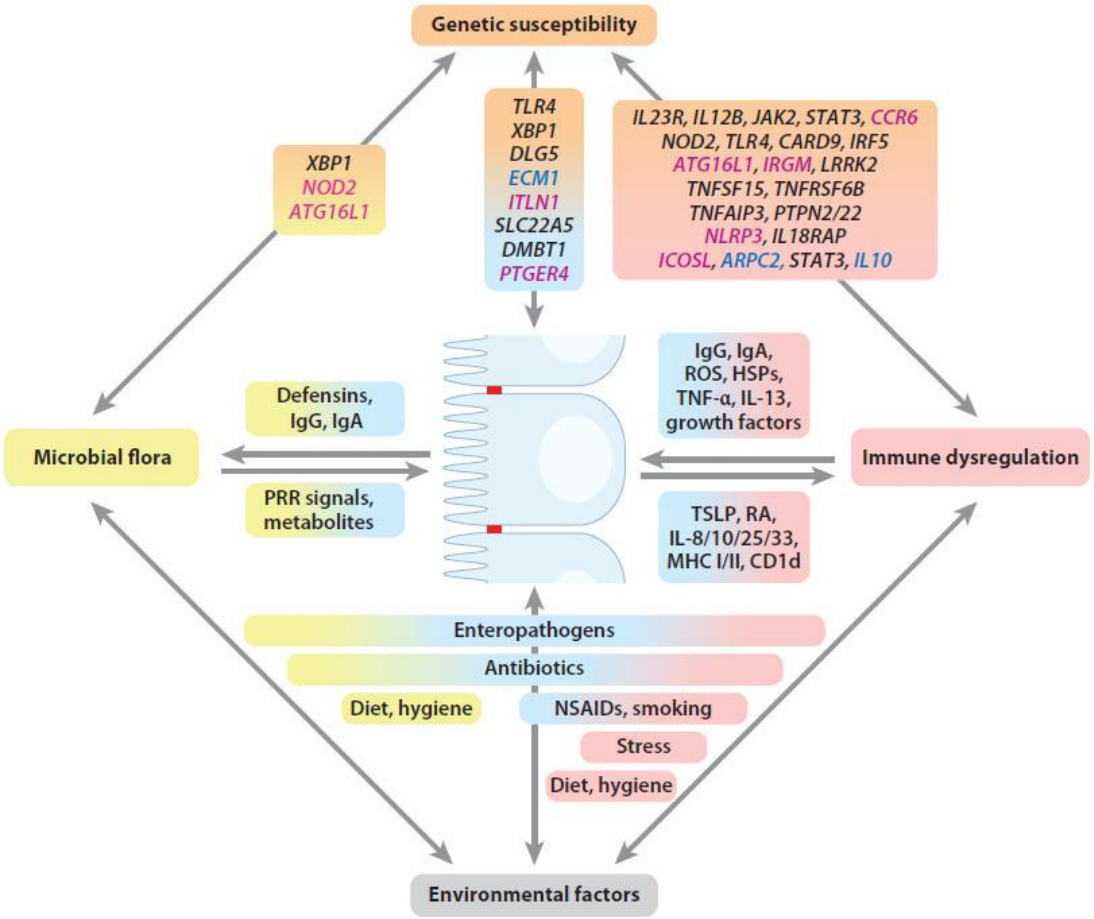

Figure 1.3 - Schematic representation of the different factors affecting IBD development and course, categorized in genetic susceptibility (orange), immune (pink), microbial (yellow) and environmental (grey) factors. Arrows and multicolored boxes indicate the interfaces of mutual influences connecting them to each other, and to intestinal epithelial barrier (blue). Genes of interest are shown in italic text, according to their specificity for Crohn's disease (blue), ulceratice colitis (magenta) or both (black). Abbreviations: HSPs, heat shock proteins; MHC, major histocompatibility complex; NSAIDs, nonsteroidal anti-inflammatory drugs; PRR, pattern-recognition receptor; RA, retinoic acid; ROS, reactive oxygen species; TSLP, thymic stromal lymphopoietin. From Kaser, *et al.*, 2010.

1.2.1. Microbial determinants of IBD development.

The school-of-thought supporting a role for intestinal biota in the etiology of IBD is mainly based on the idea that dysbiosis (changes in the balance between beneficial and pathogenic species) could result in inflammatory phenotype in a susceptible host. Evidence of the contribution of gut bacteria to the pathogenesis of IBD can be found in most animal models of colitis. Rodents which are genetically engineered to develop spontaneous inflammation, for example IL-10 knockout mice, do not develop inflammation in the absence of commensal bacteria, i.e. in a germ-free condition (Sellon *et al.*, 1998). Also, in these models, as well as in human studies with IBD patients, favorable responses have been reported with the use of antibiotic and probiotic treatment (Sartor, 2008). For instance, the successful treatment of IBD patients with probiotic strains have been reported and attributed to the immunomodulatory properties of these species (Hormannsperger and Haller, 2010). Additionally, as discussed above, the importance of commensal bacteria in maintaining gut homeostasis indicate that shifts in the composition and balance of this community can play a role in IBD pathophysiology.

Attempts to identify specific characteristics in gut microbiota of IBD subjects have been undertaken and studies using culture-independent sequencing methods revealed a general reduced bacterial diversity and alteration in the proportion of phylogenetic groups. The first metagenomic investigation of bacterial composition in the human intestine compared fecal samples from healthy volunteers and Crohn's disease patients and demonstrated a marked reduction in the diversity of the *Clostridium leptum* group within the *Firmicutes* in CD subjects (Manichanh *et al.*, 2006). Frank *et al.* (2007) analyzed 16S rRNA genes sequences in 190 tissue samples from IBD and non-IBD control subjects. The results showed a significant difference in the microbial composition in IBD-patients compared to controls: sequences corresponding to *Bacteriodetes* and to the *Lachnospiraceae* subgroup of *Firmicutes* were depleted, whereas the relative abundance of *Proteobacteria* and *Actinobacteria* sequences were enriched in IBD subjects. More recently, deep-sequencing from total DNA in fecal samples showed a clear differentiation among IBD (UC and CD) and healthy individuals when comparing the abundance of 155 selected species (Qin *et al.*, 2010). In this study, the microbiome of IBD patients was reported to contain on average 25 % less genes than found in healthy subjects. Interestingly, an investigation of the bacterial diversity in fecal samples from monozygotic twins which were either concordant or discordant in their health status (healthy or CD patients), demonstrated that changes in microbial composition correlate to disease

regardless of the genetic background and CD subjects presented lower diversity than their healthy twin sibling (Dicksved *et al.*, 2008). This study, as well as the work by Manichanh *et al.*, 2006, chose to analyze samples from patients during remission stage, when inflammation was not active. However, all of these correlations have to consider that alterations in intestinal biota can be a consequence of the inflammatory response, rather than a causative agent of disease (Manichanh, *et al.*, 2006).

The dysbiosis frequently described in IBD patients may not only represent changes in taxonomic composition of their gut microbiota, but also in the functionality and activity patterns within the community. Studies on the metabolic activity of intestinal bacteria in these subjects are of great value and approaches have been proposed. For example, a metabolomic analysis of fecal samples was performed, showing depletion of microbial products as an indication of dysbiosis in IBD patients comparing to healthy controls (Marchesi *et al.*, 2007). Barclay *et al.*, 2008 suggested the use of stable isotope probing to identify those active taxa. Indeed, studies focusing in specific bacterial taxa or phenotypic characteristic complement the metagenomic data in the elucidation of the microbial component in IBD etiology, although no single species has yet been implicated as a cause of the disease, reinforcing the multifactorial character of IBD. On the other hand, an increasing amount of data has been reported which support a role for persistent infection, mainly by opportunistic intracellular pathogens, in the development of chronic inflammation (Chassaing and Darfeuille-Michaud, 2011).

In animal models, individual bacterial species have been demonstrated to be involved in the establishment of intestinal inflammation. For example, IBD-like inflammation can be triggered by colonization of mice with *Salmonella enterica* serovar Thyphimurium (Stecher *et al.*, 2005), *Mycobacterium avium* subspecies *paratuberculosis* (Singh *et al.*, 2007) or enterotoxigenic *Bacteroides fragilis* (Rhee *et al.*, 2009). Also, Campylobacterales species like *Campylobacter jejuni* and *Helicobacter hepaticus* have been reported to induce chronic inflammation in mice, as well as the murine pathogen *Citrobacter rodentium* (Nell *et al.*, 2010). Importantly, the *C. rodentium* mouse infection model is extensively used to study pathogenesis mechanisms of attaching and effacing bacteria, a group which includes the human pathogens EHEC and enteropathogenic *E. coli* (EPEC) (Nell *et al.*, 2010). Higher numbers of *E. coli* were described in the inflamed intestine of IL-10 knockout mice compared to wild-type controls (Wohlgemuth *et al.*, 2009).

In humans, an increased risk of IBD development was reported in patients who presented an episode of *Salmonella* or *Campylobacter* gastroenteritis (Gradel *et al.*, 2009),

supporting the idea that acute infection can contribute to the establishment of a chronic inflammatory process. These results were also in agreement with the aforementioned phylogenetic changes in gut biota composition of IBD patients, which presented higher abundance of *Proteobacteria* sequences. Additionally, the presence of pathogenic *E. coli* strains associated with the intestinal mucosa of IBD patients has been described, and special attention was drawn to enhanced adherence and invasive abilities presented by these isolates, which was consistent with increased numbers of mucosally associated bacteria reported in washed biopsy samples from IBD patients, correlating to disease severity (Masseret *et al.*, 2001; Swidsinski *et al.*, 2002).

The identification of this special phenotypic characteristic in *E. coli* led to the description of a new group of potentially pathogenic *E. coli* called adherent-invasise *E. coli* (AIEC) (Boudeau *et al.*, 1999) and its implication in IBD pathogenesis, particularly in CD, was recently confirmed (Martinez-Medina *et al.*, 2009). Bacteria with an improved colonization, adherence and invasion capacity are able to interact more closely to host cells and potentially generate strong pro-inflammatory responses in the mucosa and they may also take advantage of a deficient epithelial barrier and innate immune response in a susceptible host to promote invasion, generating an amplification loop of colonization and inflammation (Chassaing and Darfeuille-Michaud, 2011). This notion conveys to the mutual influence of the microbial component and the host-related factors implied in IBD pathophysiology.

1.2.2. Host determinants of IBD development

Many of the components and processes of host-origin described to participate in chronic intestinal inflammation in IBD patients were either discovered or confirmed by the assignment of specific genes as genetic susceptibility factors. Family and twin studies of IBD epidemiology show a strong heritable factor in CD and to a lesser extent in UC (Halme *et al.*, 2006). Genome-wide association analysis, employed to identify true statistically significant genetic association to diseases in large cohorts, have been carried comparing IBD patients to healthy controls (reviewed by Cho, 2008). These studies reflect the stronger influence of genetic factors on CD than on UC, in agreement with epidemiological data, and highlight the crucial role of innate immunity defects in the pathophysiology of the disease. Also, they provided molecular evidence of the contribution of innate and adaptative immune mechanisms to both CD and UC (Cho, 2008).

The characteristic cytokine profiles resulting in inflammation in IBD implicate a T-helper (Th) cell-mediated pathway, as can be found in CD or UC patients, and in animal models with corresponding phenotypic traits. It has been suggested that CD includes a Th-1 mediated response, with production of IL-12 and interferon (IFN)-γ and a Th-17 component with involvement of IL-23 and IL-17, whereas UC is driven mainly by a Th-2 like response involving IL-13-producing cells (Strober *et al.*, 2007). In this regard, in both cases mucosal inflammation could result from either an excess stimulation of Th effector cells or from a deficiency in the regulatory mechanisms that normally counter-balance activation (Bouma and Strober, 2003). The latter hypothesis is based on a decreased oral tolerance found in IBD patients (Duchmann *et al.*, 1995), and in several studies with animal models showing the involvement of two important mediators of immunosupression, IL-10 and tumor growth factor (TGF)-β, and of regulatory T-cell subtypes in preventing intestinal inflammation (Sartor, 2006; Izcue *et al.*, 2009). In human studies, most of the data support the case for an exacerbated immune stimulation as central to the inflammatory process. Those include the reporting of genes associated with IBD, represented in Figure 1.3, from which some examples are further described here.

Polymorphisms in the gene encoding IL-23 receptor (*IL23R*) were described to be strongly associated with CD, and are also relevant in UC patients (Duerr *et al.*, 2006). Accordingly, a genome-wide study that identified more than 30 loci associated with CD (Barrett *et al.*, 2008), revealed many components of IL-23 signaling, including *IL23R*, *STAT3*, *JAK2*, *CCR6* and *IL12B*, some already reported to be associated also with UC. IL-23 and IL-12 pathways are closely related. The respective receptors are heterodymers sharing one of the subunits (p40), which has been also identified among the genes associated with both CD and UC (Barrett *et al.*, 2008). Additional evidence of the relevance of IL-23/IL-12 signaling in IBD is the effective reduction in inflammation in animal models of colitis, as well as in CD patients by the use of p40 blocking antibodies, which is in accordance with the involvement of the effectors IFN-γ and IL-17, extensively described as implicated in IBD pathophysiology (Cho, 2008; Kaser *et al.*, 2010). Importantly, these two cytokines represent a central link between innate and adaptative immunity (Langrish *et al.*, 2004).

Because inflammation in IBD is thought to originate from a dysfunctional interaction between the immune system and luminal microbes, it is expected that the first line of defense, the immediate contact point represented by the mucosal barrier and innate immunity, has a prominent role in the development of the disease (Xavier and Podolsky, 2007). Indeed, most

of the therapeutic agents tested in clinical trials which were efficient in the treatment of IBD were the ones directed at innate immune factors (Kaser *et al.*, 2010). Accordingly, many genetic susceptibility factors were identified to be involved in innate functions, mainly in CD patients, for example the autophagy-related genes *ATG16L1* and *IRGM* (Hampe *et al.*, 2007; Parkes *et al.*, 2007). Autophagy has emerged as an important process in antigen processing and presentation by innate immune cells, and this mechanism is also important in epithelial cell-shedding in the gut, where these functions possibly link the autophagy-related genes to the pathogenicity of CD (Levine and Deretic, 2007). Recently, Frank *et al.*, 2011, reported a correlation between shifts in microbial composition and the genotypic features of IBD patients regarding two known innate immunity-related genetic risk factors, *ATG16L1* and *NOD2*.

The first categorical demonstrations of genetic risk factor for CD development were polymorphisms found in *NOD2* (also known as *CARD15*), the gene encoding the nucleotide-binding oligomerization domain (NOD)containing-protein NOD2 (Ogura *et al.*, 2001; Hugot *et al.*, 2001). Those variants are found in 30 % to 40 % of European CD patients and the risk of developing the disease is 2 – 4-fold and 15 – 40-fold higher respectively in heterozygotes and homozygotes for one of the mutations (Lee and Parkes, 2011). NOD2 is a pattern recognition receptor, intracellularly expressed in the gut mucosa by the specialized Paneth cells and also by intestinal epithelial cells, where they play a particularly significant role in bacterial sensing: it has been demonstrated that IEC have a deficient TLR-2 signaling, which was pointed as a mechanism of tolerance to commensal bacteria, giving NOD2 an even greater importance in intestinal defense (Melmed *et al.*, 2003; Kim *et al.*, 2008). In this context, NOD2 is also predicted to have a tolerance function, and different murine models with deficient NOD2 expression were described as being hyperresponsive to bacterial factors and more susceptible to colitis (Watanabe *et al.*, 2006; Maeda *et al.*, 2005).

Upon activation by bacterial peptidoglycan components, like muramyl dipeptide, NOD2 promotes the engagement of NF-κB signaling cascade. As discussed above, NF-κB is a central player in intestinal immunity, and its involvement in the effects of NOD2 mutations on CD pathogenesis is considered, as alterations in the NF-κB pathway have been reported to have complex outcome related to IBD. For example, immunohistochemical and immunofluorescence analysis revealed an increased NF-κB activation specifically in inflamed gut biopsies from CD and UC patients (Rogler *et al.*, 1998). Accordingly, inhibition of NF-κB resulted in attenuation of colitis in different murine models (Neurath *et al.*, 1996; MacMaster

et al., 2003). However, contrasting results have also been reported where NF-κB signaling was protective. For example, the genetic deletion in IEC of NF-κB positive regulators IKKβ and IKKγ caused exacerbated inflammation and increased colitis severity in mice in a cell-context dependent manner (Eckmann *et al.*, 2008; Nenci *et al.*, 2007). These results agree with the evidence of loss-of-function mutations in NOD2 resulting in inflammation via a deficient NF-κB stimulation, and support the involvement of NOD2 in inducing immune tolerance in intestinal epithelia.

Another important aspect to be considered involves NOD2 and NF-κB signaling in antimicrobial peptide production by IEC and Paneth cells. These two cell types, together with the mucus-producing goblet cells, are a major part of the single-cell layer which form the epithelial barrier in the gut, whereas antigen-presenting M cells and DC are present mainly in the areas lining gut-associated lymphoid tissue (GALT) such as the Peyer patches (Rescigno, 2011; Mowat, 2003). Thus, the integrity of the mucosal barrier, necessary for controlling gut microbiota and the inflammatory responses they can trigger, requires the functionality of those cell-types. Evidence has been found for the involvement of altered mucin production by goblet cells in IBD pathophysiology (Heazlewood *et al.*, 2008), as well as of altered regulation of epithelial adhesion molecules implied in bacterial colonization (Barnich *et al.*, 2007). Moreover, the antimicrobial peptides produced by IEC and Paneth cells represent a crucial component of this barrier, and as mentioned above (section 1.1.3), are subject to regulation by NOD-receptors and NF-κB pathways.

An interesting and yet not fully understood story underlies the role of antimicrobial peptides in IBD. NOD2 mutations are suggested to affect antimicrobial production in the ileum of CD patients, where the levels of Paneth cell defensins (human α-defensins or HD) are reduced (Simms *et al.*, 2008; Wehkamp *et al.*, 2005). In contrast, in the colon of IBD patients, the concentration of the peptides are usually enhanced, which may be explained by Paneth cells metaplasia. These cells are abundant in the ileum, particularly in the crypts, but normally very sparsely present in the colon, where they are found in abnormal high numbers in IBD patients (Shi, 2007). Accordingly, colonic expression of Paneth cell defensins has been demonstrated to be significantly increased in UC patients (Lawrance *et al.*, 2001).

The epithelial β-defensins (human β-defensins or hBD), in turn, have also been reported to have a role in IBD pathophysiology, with important differences between CD and UC. While hBD-1 is constitutively expressed in colonic tissue irrespective of inflammation, increased expression of inducible β-defensins 2 and 3 is found in inflamed tissue. In colonic

biopsies, hBD-2 was detected in the mRNA level in 53 % of the UC patients, significantly higher than in CD patients (34 %) and healthy controls (18 %), and these results were confirmed at the protein level (Wehkamp *et al.*, 2002). Similarly, the expression of hBD-3 was found to correlate strongly with hBD-2, and it was upregulated 30-fold in UC patients, and 4-fold in CD patients compared to controls (Wehkamp *et al.*, 2003). Interestingly, hBD-2 expression was found to correlate with degree of inflammation in UC biopsies (Aldhous *et al.*, 2009). Possible explanations for the discrepancy in epithelial β-defensins expression between CD and UC are lower copy numbers of the gene encoding β-defensin-2, *DEFB4*, which is described as a genetic predisposition factor for the colonic form of CD (Fellermann *et al.*, 2006), or the defective NOD2 activation frequently observed in CD patients, as has been suggested by Voss *et al.*, 2006.

These alterations highlight the importance of defensins in IBD, in agreement with the notion that a normally functional mucosal barrier is crucial in maintaining the intestinal health state. The exact mechanisms leading to the observed effects, however, are not completely clear. The direct conclusion that a deficient antimicrobial activity in the gut will result in increased bacterial colonization and consequent inflammation, although correct, has to consider the complexity of defensins and their multiple roles in host defense (Menendez and Brett Finlay, 2007).

1.3. Antimicrobial peptides and the role of human defensins in the inflamed gut

1.3.1. Overview of antimicrobial peptides

Antimicrobial peptides (AP) are small polypeptidic molecules, containing not more than 100 amino acids. They are found in a variety of species throughout the animal and plant kingdoms, having the primary function of protecting against microbial infections, with a diverse range of activity against microbes, including bacteria, fungi, viruses and protozoa (Zasloff, 2002). Currently, there are more than 1,700 sequences described, most of them (> 1,200) from animals, predominantly amphibians, insects and mammals. The great majority of these peptides are active against both Gram-negative and Gram-positive bacteria (The Antimicrobial Peptide Database, APD, Wang and Wang, 2004).

The huge diversity of APs described can be broadly categorized according to their amino acid composition and secondary structure. Based on the net charge, there are a few examples of anionic peptides, often enriched in glutamate or aspartate residues. Cationic peptides are more abundant and structurally diverse: they can be linear, enriched for specific amino acids (generally proline or glycine) or in most of the cases, they assume a secondary structure: either an α-helical conformation or alternatively peptides containing cysteine residues will form disulfide bounds and stable β-sheet structures (Boman, 1995).

The secondary structure seems to have important implications for the antimicrobial activity, as is reported, for example, in many α-helical peptides which have increased antimicrobial activity in correlation with increased α-helical content (Park *et al.*, 2000). However, one common feature that can be identified among most AP from all classes is a tertiary amphipatic conformation, where the hydrophobic and hydrophilic charged residues are spatially separated. This conformation has a functional significance: the antimicrobial activity regardless of the effector mechanism, relies on the interaction of the peptide with plasma membrane of their target organisms, a process facilitated by the amphipatic character of the molecules (Hancock and Rozek, 2002).

AP activity can be studied in natural or artificial membranes, by diverse techniques such as microscopy, circular dichroism, solid-state nuclear magnetic resonance (NMR) spectroscopy and X-ray diffraction. In general, the process that leads to bacterial killing can be divided in three steps: attraction/ attachment, insertion and killing. The first step is mainly

driven by electrostatic bounding between the charged residues in the AP, and the structures in bacteria surface (Matsuzaki, 1999). This process is an important determinant of specificity, because different biological membranes present essential differences in their surface molecules. For example, most of the mammalian cell membranes are composed of neutral phospholipids like phosphatidylcholine and sphingomyelin, making them poor targets for APs. In turn, bacterial surfaces are negatively charged due to the presence of LPS in the outer membrane of Gram-negative species, or lipoteichoic acid in Gram-positive species (Matsuzaki, 1999; Yeaman and Yount, 2003). This first interaction step has another important implication: many of the documented cases of AP resistance involve changes in membrane composition by the target organism, conferring a less negative character (Nizet, 2006). Examples are the LPS modifications such as lipid A acylation reported for several Gram-negative *Enterobacteriaceae* or incorporation of D-alanine to the teichoic acid by Gram-positive bacteria such as *Staphylococcus aureus.* The two-component PhoP/PhoQ regulator system can also promote rearrangements in cell envelope and contribute to AP resistance, as in the case of *Salmonella enterica*, for example (Nizet, 2006).

The second step takes place when a certain ratio of AP/lipid in the membrane is reached, which depends on the peptide and the membrane composition. At this point, the peptide molecules which were first parallel attached to the surface will insert into the lipid bilayer to cause membrane permeability. Three model mechanisms have been proposed (Figure 1.4). The barrel-stave model is based on the formation of barrel-like bundles in the membrane, where several peptide molecules insert perpendicularly, the hydrophobic residues directly interacting with the lipids and forming the lumen of a channel. Alternatively, according to the toroidal-pore model, the peptides induce the lipid layer to bend, forming a hydrophilic core where the lipid head groups are lined by AP molecules. In the third model, called the carpet model, peptides extensively accumulate parallel to the surface, covering in like a carpet and subsequently inducing membrane destabilization in a detergent-like action, with eventual formation of micelles (Brogden, 2005).

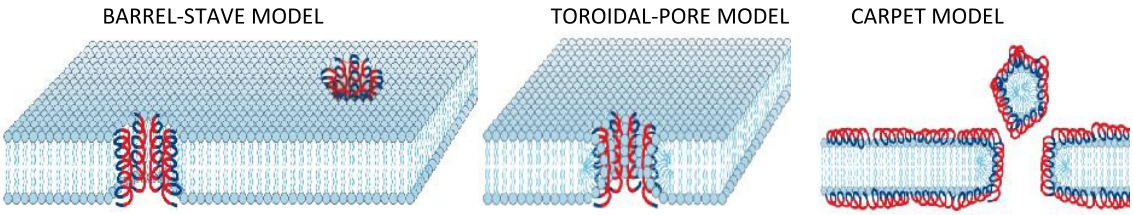

Figure 1.4 - Proposed models for the interaction of antimicrobial peptides with lipid bilayers. Hydrophilic and hydrophobic regions of the peptide structure are represented in red and blue, respectively. Published by Brogden, 2005.

Regarding the cell killing process, the obvious mechanism of damage directly related to membrane permeabilization and eventual cell lysis is probably the general effect contributing to microbial death. The formation of pores and membrane defects cause leakage of metabolites and ions, depolarization and disruption of membrane-coupled respiration. However, evidence has been generated to support the idea that membrane permeabilization does not always necessarily cause cell death, and other mechanisms of killing, involving different non-membrane or intracellular targets are being more frequently described (Yeaman and Yount, 2003). There are peptides capable of inhibiting the synthesis of cell-wall components, for instance mersacidin and seminalplasmin reported to inhibit peptidoglycan synthesis (Brotz *et al.*, 1998; Chitnis and Prasad, 1990). Others have been reported to inhibit chaperone activity, nucleic acid and protein synthesis (Otvos *et al.*, 2000, Patrzykat *et al.*, 2002). Also, direct binding to DNA and RNA has been described as intracellular mechanisms of APs such as buforin II and tachyplesin (Park *et al.*, 1998; Yonezawa *et al.*, 1992).

According to this diversity in the modes of action of APs, microbes also develop resistance mechanisms which are not only related to changes in membrane composition. There is the secretion of AP binding factors, which have been described for *S. aureus* and Group A *Streptococcus* (GAS), able to impair peptide/membrane interaction. Also, GAS, *S. aureus* and many other bacteria including *E. coli*, *S. enterica* and *Enterococcus faecalis* produce and secrete AP degrading proteolytic enzymes of different classes. Additionally, energy-driven efflux systems which are well-known multi-drug resistance factors have been also implicated in AP resistance (Nizet, 2006).

Importantly, although APs represent a rather conserved class of antimicrobials, they present a great sequence diversity. The variable composition and structure of APs, yielding signature conformational characteristics, contribute for the highly diverse activity spectra and mechanisms of action, in a way that, for a satisfactory understanding of their functions, the different peptides must be considered in the context of their individual properties.

1.3.2. Human defensins

The two main classes of antimicrobial peptides expressed in humans and other mammals are the cationic cathelicidins and defensins. They are similar in distribution and abundance in humans, and also in their synthesis mechanisms. In both cases, the polypeptide is expressed as a larger precursor, which is subsequently cleaved by proteolysis to generate the active mature peptide. In the structural properties, a remarkable difference distinguishes cathelicidins from defensins: the α-helical conformation of cathelicidins in contrast to the β-sheet characteristic of defensins.

Cathelicidins include the sheep myeloid antimicrobial peptide SMAP29 and numerous porcine peptides like PR-39, but are represented in humans by one single peptide, LL-37 . The mature LL-37 has 37 amino acids forming one alpha-helical structure. It is found in body fluids, epithelial cells in the skin, gastrointestinal and respiratory tract and in several immune cells including neutrophils, T cells and NK cells. LL-37 presents a broad spectrum of antimicrobial activity against Gram-negative and Gram-positive bacteria, viruses and yeast, and it has been reported to have synergistic action with defensins against *S. aureus* and *E. coli* (Dürr *et al.*, 2006).

In contrast to the single representative of the cathelicidin class in humans, there are more than 10 human AP described pertaining to the class of defensins (The Antimicrobial Peptide Database, APD, Wang and Wang, 2004). They are peptides of 4-6 kDa, having a distinctive triple β-sheet structure, connected by three disulfide bounds. The distance between the cysteine residues in one β-sheet, and the pairing between them defines the two families of human defensins: α-defensins and β -defensins (Figure 1.5). Most of the genes encoding for α- and β -defensins are located in the same chromosome (8p23) and are thought to have a common evolutionary origin (Ganz, 2003).

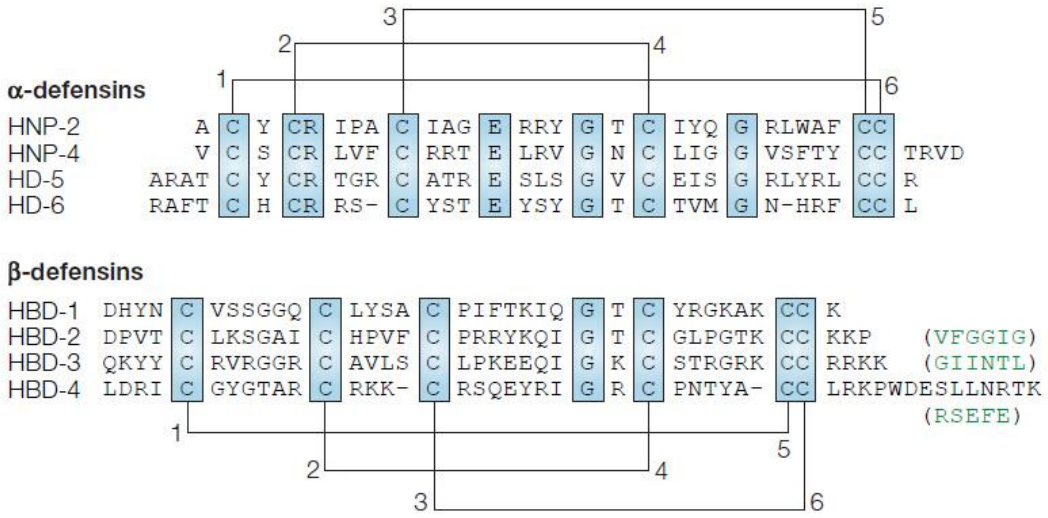

Figure 1.5 - Amino acid sequence of representative human α-defensins and β-defensins, showing the six characteristic cysteine residues and their disulfide pairing, which differentiates the two families. From Lehrer, 2004.

The α-defensin family comprises the peptides produced by neutrophils (human neutrophil peptide HNP 1 to 4) and by Paneth cells in the intestinal crypts (human α-defensin HD 5 and 6). They are generally constitutively expressed as precursors of up to 100 amino acids, with an N-terminal signal sequence, a negatively charged propiece and a C-terminal corresponding to the mature peptide of 29-35 amino acids with high arginine content. The presence of the anionic propiece may be important in preventing intracellular cytotoxicity during the synthesis process (Schneider *et al.*, 2005; Valore *et al.*, 1996). In neutrophils, defensins are synthesized early during the cell differentiation process (promyelocytes) and stored in the mature form inside primary granules which will later fuse with phagocytic vacuoles (Gullberg *et al.*, 1999). In Paneth cells, they are stored as propeptides, and only cleaved to the mature form after release in intestinal lumen. Metalloprotease matrilysin and trypsin, produced by the same Paneth cells, have been decribed as responsible for HD processing (Wilson *et al.*, 1999; Ghosh *et al.*, 2002).

The antimicrobial activity of neutrophil α-defensins includes a wide range of Gram-negative and Gram-positive bacteria, which are killed *in vitro* at concentrations between 10-100 $\mu g \cdot mL^{-1}$ (Lehrer *et al.*, 1993). Physiologically, these defensins are present in the granules at concentrations over 10 $mg \cdot mL^{-1}$, and their phagocyted targets will be exposed to minimally diluted content (Ganz, 2003). In turn, the main Paneth cell defensin HD5, present

also a broad antimicrobial activity with minimal inhibitory concentration for *E. coli*, *S. thyphimurium* and *Lysteria monocytogenes* in the nanomolar range (Schneider *et al.*, 2005).

The β-defensin family is produced predominantly by epithelial cells. They include at least 10 peptides, many of them restricted to a few cell types. The most widely distributed peptides are human β-defensin (hBD) 1, 2 and 3. These are peptides with 36-45 amino acids present in the skin, urinary and respiratory epithelia and in the gastrointestinal tract (Pazgier *et al.*, 2006). hBD genes have a common organization consisting of one intron and two exons: one encoding the signal sequence and the second the mature peptide. In post-translational processing, the larger precursors are cleaved by proteolysis for removal of the signal sequence and secreted into the adjacent milieu of epithelial cells (Pazgier *et al.*, 2006). The average concentration of defensins in epithelial surface is in the micromolar range, although local concentrations can be higher due to differential distribution (Ganz, 2003).

hBD-1 is more abundant in urinary and respiratory tract, where it has been reported to be inducible by inflammatory stimuli (Zhu *et al.*, 2003), whereas lower, constitutive expression is found in the intestine (Zhao *et al.*, 1996). It is reported to have salt-sensitive antimicrobial activity, mostly against Gram-negative bacteria, being able to kill *E. coli* and *P. aeruginosa* at micromolar concentrations (Schroder, 1999).

In the human gut, together with Paneth cell α-defensins, hBD-2 reinforces the host innate defence. It is normally expressed at low basal levels and can be upregulated by a variety of microbial and inflammatory stimuli. Particularly, in the intestinal epithelium, hBD-2 can be induced by IL-1β and bacterial flagellin, in a process mediated by NF-κB pathway (O'Neil, 2003). Like hBD-1, it also salt-sensitive and generally more potent against Gram-negative bacteria, and it has been shown that ~10 $\mu g \cdot mL^{-1}$ doses are effective against *E. coli* and *P. aeruginosa*, whereas concentrations as high as 100 $\mu g \cdot mL^{-1}$ are required to prevent growing of *S. aureus* (Schneider *et al.*, 2005).

Another important enteric β-defensin, hBD-3, is also subject to induction by bacterial components and inflammatory cytokines, but the exact mechanism seems to be different from hBD-2, and is thought to be independent of NF-κB (Ganz, 2003). The antimicrobial activity of hBD-3 is markedly different form the other two hBD: in addition to killing Gram-negative species at similar concentration ranges, it is also active against Gram-positive bacteria like *Streptococcus pyogenes*, *Enterococcus faecium* and *S. aureus*, including the aggressive multi-resistant strains (Harder *et al.*, 2001).

This brief description gives a general idea of the similarities and differences regarding structure, expression and antimicrobial activity among the defensins which are important in the context of the human intestine. For several reasons already presented, their antimicrobial activity is clearly a central feature of the innate defense mechanisms, being at the same time important targets and mediators in host-microbial interactions in health and disease. In addition, other diverse biological activities are often reported, with relevant consequences for the inflammatory responses in the gut.

1.3.3. Diverse functions of human defensins in the gut

One important role of human defensins in the intestinal mucosa, which is directly related to their antimicrobial activity, regards the shaping of the microbial community and protection against infections. A recent study using two complementary transgenic mouse systems, one expressing HD5 and the second with deficient processing of the indigenous mouse defensin, demonstrated a shift in the gut microbiota: the ratio of *Bacteriodetes/Firmicutes* was higher in the presence of HD5, and accordingly lower in the absence of mouse defensin, without affecting the total numbers of bacteria (Salzman *et al.*, 2010). These mouse models had been used before to demonstrate the effect of Paneth cell defensins in intestinal infections. Mice lacking the mature peptide were more susceptible to oral challenge with *Salmonella thyphimurium* (Wilson *et al.*, 1999), whereas mice expressing HD5 were markedly resistant to salmonellosis (Salzman *et al.*, 2003). Definitive proof of the role of one specific defensin *in vivo*, however, is difficult to access due to overlap and redundancy of their antimicrobial effects (Menendez and Brett Finlay, 2007).

Both α- and β-defensins were also described to act as chemoatractants to immune cells including monocytes, mast cells, neutrophils, T cells and dendritic cells (Territo *et al.*, 1989; Yang *et al.*, 2000; Niyonsaba *et al.*, 2002; Niyonsaba *et al.*, 2004). In particular, direct interaction of hBD with chemokine receptor CCR6, expressed by some subsets of immune cells has been characterized (Yang *et al.*, 1999). The chemotatic properties of hBDs are not inhibited by physiological concentrations of salts, unlike their microbicidal activity, which except for hBD-3, is substantially higher in low-salt microenvironment found in epithelial surfaces (Pazgier *et al.*, 2006).

Several reports described a function for human defensins in modulating inflammatory responses by changing the expression of cytokines. For instance, hBD1, 2 and 3 were able to differentially modulate the expression of IL-1β, IL-5, IL-6, IL-8 and IL-10, among others, in

human peripheral blood mononuclear cells (PBMC), and the induction by hBD-2 of IL-1β production, which in turn upregulates the expression of the defensin, represents a response amplification mechanism (Boniotto *et al.*, 2006). In contrast, HD5 was able to block the release of IL-1β from monocytes (Shi *et al.*, 2007). In intestinal epithelial cells, an upregulation of TLR-7 and IL-8 was found in response to hBD-2 (Stroinigg and Srivastava, 2005). Also, mouse Paneth cell defensin was shown to induce IL-8 in intestinal cells *in vitro* (Lin *et al.*, 2004). According to a pro-inflammatory role found for defensins in some models, HNPs and hBDs demonstrated adjuvant properties, enhancing antibody responses in mice against *Porphyromonas gingivalis* antigens (Kohlgraf *et al.*, 2010a). An induction of adaptative immunity was also reported for murine β-defensin-2 acting as a ligand for TLR-4 in dendritic cells (Biragyn *et al.*, 2002).

The interaction of defensins with bacterial components may as well have implications in their immunomodulatory properties. Despite the pro-inflammatory potential, especially after antibiotic treatment, of released bacterial molecules such as membrane components or DNA, the activity of defensins has been reported to counteract the induction of inflammation (Hancock and Scott, 2000). For example, binding of *P. gingivalis* hemagglutinin by hBD-3 attenuated pro-inflammatory induction in human dendritic cells (Pingel *et al.*, 2008). Furthermore, interaction of defensins with bacterial membranes and products like LPS, adhesins and toxins can account for attenuated inflammatory responses to these molecules (Kohlgraf *et al.*, 2010b). Interestingly, the binding of neutrophil defensins to molecules of the complement system has been reported, with possible implications for the control of inflammation and of the cytotoxic effect of the defensins, an important player in tissue injury due to the high concentrations of defensins found in inflamed sites (Panyutich *et al.*, 1994; van den Berg *et al.*, 1998). Another recognized paracrine effect of intestinal defensins is induction of Cl^- secretion from epithelial cells, and the consequent water secretion and mucosal flushing could also be important to avoid cytotoxicity (Lencer *et al.*, 1997).

The myriad functions of the different defensins in the human intestine and their intricate regulation, particularly during inflammation, add complexity to the host-microbiota system and highlight these peptides as interesting subjects of studies for improving the current understanding on intestinal inflammation and related pathologies.

2. APPROACH AND OBJECTIVES

The current knowledge about IBD highlights the interplay between bacteria and the host, reciprocally modulating responses in a scenario where disturbances in this system will lead to pathological inflammation of the gut. This study intended to improve the understanding of IBD pathophysiology, considering that one factor of disturbance is the deregulated expression of defensins by the host. These antimicrobial peptides can exert a variety of effects on the immune system itself, and especially on the intestinal microbial community, where the classical membrane disruption killing is an important, but not the only mechanism. Thus, we hypothesized that the effect of defensin challenge on intestinal bacteria would trigger the release of specific soluble small molecules which could in turn have a consequence on the host.

The detection, identification and characterization of small molecules (or metabolites) from a given organism is an area of great interest in medical and biological sciences, which has long been recognized as a tool for phenotypic characterization and clinical diagnostic purposes. Recently, it has gained additional recognition with the development of metabolomics as a functional complement to the genomic, transcriptomic and proteomic studies (Villas-Boas *et al.*, 2005). In its strict definition, the metabolome of an organism should include all of the low-molecular mass compounds it synthesizes. This is an extremely hard task to accomplish, given the diversity of chemical structures that compose this set of molecules, implying that a combination of different methods is usually necessary to achieve the desired coverage (Werner *et al.*, 2008). Other ways to answer scientific questions by the characterization of metabolites in a biological sample deal with sets of molecules of interest, either metabolites of a specific chemical class (metabolite target analysis) or an overview of metabolites present in a sample under specific conditions using a particular analytical tool (metabolic profiling). In the case of microbiology, the later can be further directed to assess molecules from the intracellular pool, defining a metabolic fingerprint, or metabolites present in the extracellular space, or metabolic footprint (Villas-Boas *et al.*, 2005; Fiehn, 2002; Mashego *et al.*, 2007).

Currently, several analytical platforms employed for metabolite-based investigations rely on mass-spectrometry (MS) tools, often in combination with other detection methods like U.V. or infra-red spectral data or NMR. Furthermore, the coupling of different chromatographic separation systems with a variety of ionization techniques and mass

analyzers, so-called hyphenated technologies, such as gas chromatography (GC)-MS, liquid chromatography (LC)-MS, represent powerful tools for the characterization of metabolites in microbial samples (Mashego *et al.*, 2007). They support the acquisition of at least two layers of information about the compounds: the chromatographic retention time, which is related to the physic-chemical properties of the molecules, like size or hydrophobicity, depending on the kind of separation matrix used; and their mass spectra characteristics. Using these data, one proposed strategy for the identification of molecules of interest from MS-based profiles can be simplified in four steps, according to Werner *et al.*, 2008: 1) data acquisition (retention time and mass spectra); 2) database search; 3) diagnostic ions and fragment spectra determination by tandem-MS (MS/MS); 4) confirmation using commercial or synthetic compounds with matching retention time and mass spectra.

Because our aim was to identify metabolites with potential significance for host-microbial interactions, this general strategy was employed in the analysis of extracellularly available coumpouds, rather than intracellularly trapped molecules, by liquid chromatography coupled to a triple quadrupole mass analyzer. One advantage of such a footprint approach, directly applying cell-free supernatants to the liquid chromatography, is to avoid many quenching and extraction steps which would otherwise be demanded (Kell *et al.*, 2005). The triple quadrupole analyzer is a reliable method to screen for characterized metabolites, and it is also a powerful quantification tool, offering the possibility of combining qualitative and quantitative analysis (Soler *et al.*, 2007).

Thus, the experimental approach used in this study was to search for metabolites enriched in the extracellular medium of *Escherichia coli* cultures, specifically after defensin (hBD-2) challenge. This setup was chosen based on the prominent role of hBD-2 in IBD pathophysiology, and relying on a well-studied organism, which is at the same time a known component of the gut microflora and also a player during IBD development. The investigation largely employed the LC-MS technique as a central tool for finding molecules with potential physiological relevance, following a trend where “the focus of metabolomic studies is shifting from cataloging chemical structures to finding biological stories” (Baker, 2011).

2.1. Specific aims and questions

The research project aimed to investigate:

1) the presence of small extracellular metabolites released by *E. coli* in response to human β-defensin activity;
2) the mechanisms involved in this bacterial response; and
3) the potential effects of the major identified molecules as immunomodulators in the human host.

Specific questions addressed during this study were:

→ How does human β-defensin affect *E. coli*?
→ Are there bacterial metabolites differentially present in the culture medium after defensin stress?
→ How is this extracellular response characterized in terms of dose-dependence, temporal-dynamics and specificity?
→ What is the source of the generated compounds?
→ Can the identified extracellular metabolites have an effect on human intestinal cells? Do they have an influence on inflammatory responses in the host?

By answering these questions, this work intended to contribute to the current understanding of host-microbial interactions taking place during in the inflammation in the human intestine.

3. MATERIALS AND METHODS

3.1. Summary of the experimental design

The methodology used in this research was centered in the comparative investigation of *Escherichia coli* cultures in the presence or absence of human defensin (hBD-2). The analyses included determination of bacteriological parameters in the defensin challenged vs. unchallenged cultures, as well as investigation of the cell-free bacterial supernatants for the presence of small metabolites. Additionally, the studied supernatants were tested for their *in vitro* effect on human intestinal epithelial cells. Figure 3.1 illustrates the approach and experimental procedures described in detail in the following sections.

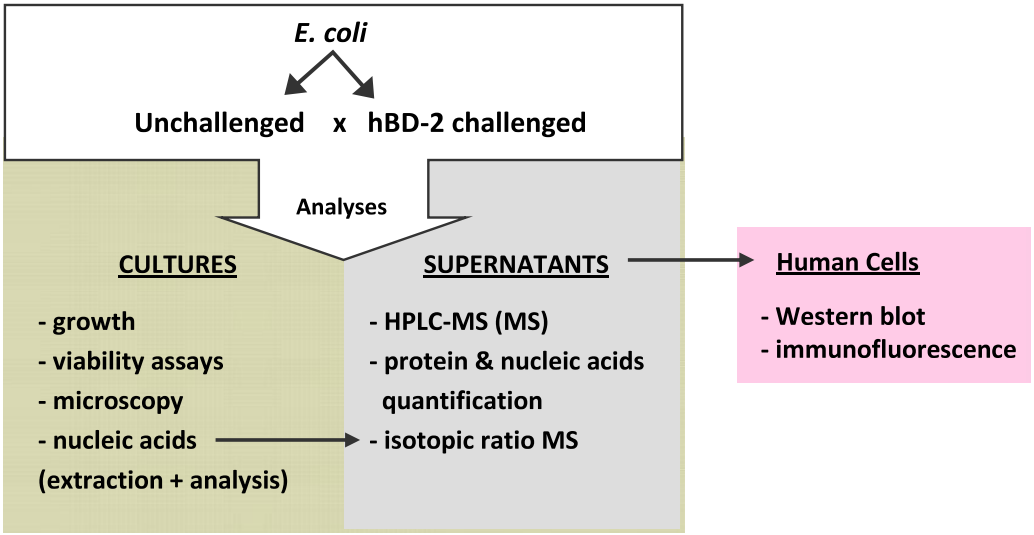

Figure 3.1 - Summarized experimental design.

3.2. Chemicals

Antimicrobials: Lyophilized synthetic human beta-defensin-2, human beta-defensin-3 and human alfa-defensin-5 were purchased from Peptide Institute Inc. (Osaka, Japan). Sheep Myeloid Antimicrobial Peptide 29 (SMAP29) was purchased from AnaSpec Inc. (Fremont, CA, USA). Magainin I was purchased from Sigma-Aldrich (St. Louis, MO, USA).

Nucleotides, nucleosides and nitrogen bases: All compounds used as standards in GC or HPLC-MS analysis were purchased from Sigma-Aldrich unless otherwise stated. Adenosine was purchased from MP Biomedicals, LLC (Santa Ana, CA, USA). ATP was purchased from Promega (Madison, WI, USA) and AMP was supplied by Michael Morr (Helmholtz Zentrum für Infektionsforschung)

HPLC solvents: Methanol and acetonitrile (HPLC grade) were purchased from J.T. Baker (Deventer, Holland). Formic acid was purchased from Carl Roth GmBH (Karlsruhe, Germany). MilliQ® water was used in the preparation of all solvent solutions.

Enzymes: Nuclease P1 from *Penicillium citrunum* and phosphatase alkaline from *Escherichia coli* were purchased from Sigma-Aldrich. Lysozyme from chicken egg white was purchased from Serva Electrophoresis GmBH (Heidelberg, Germany).

Trimethylsilylation reagents: N,O-bis(trimethylsilyl)trifluoroacetamide (BSTFA), 1 % trimethylchlorosilane (TMCS) was purchased from Supelco Analytical (Bellefonte, PA, USA) and pyridine was purchased from Fluka (Buchs, Switzerland).

Lipopolysaccharide (LPS), cytokines and antibodies: LPS purified from *Klebsiella pneumoniae* was purchased from Sigma-Aldrich. Recombinant human interleukin-1β (IL-1β) was purchased from Millipore (Temecula, CA, USA), and human recombinant tumor necrosis factor-α (TNF-α) was purchased from R&D Systems, Inc. (Minneapolis, MN, USA). Anti-IκBα rabbit IgG, anti-p65 rabbit IgG and anti-p65 mouse IgG were purchased at 0.2 $mg \cdot mL^{-1}$ from Santa Cruz Biotechnology (Santa Cruz, CA, USA). Anti-phospho-p65 (Ser563) rabbit polyclonal antibodies were purchased from Cell Signaling Technology, Inc. (Danvers, MA, USA). Anti-βactin mouse IgG was purchased at 0.6 $mg \cdot mL^{-1}$ from Abcam (Cambridge, UK). Horseradish peroxidase (HRP) conjugated goat anti-rabbit-IgG and HRP conjugated goat anti-mouse-IgG antibodies were purchased at 0.4 $mg \cdot mL^{-1}$ from Jackson ImmunoReasearch Laboratories, Inc. (West Grove, PA, USA). Alexa Fluor ® 546 conjugated goat anti-rabbit-IgG antibody was purchased at 2 $mg \cdot mL^{-1}$ from Invitrogen /Molecular Probes (Eugene, OR, USA).

Other chemicals used in this work, as well as specific laboratory supplies and equipment, are mentioned together with the respective supplier in the corresponding method's description below. A list of the equipments used can be found in Supplementary Material section 7.3

3.3. Analytical Methods

3.3.1. High Pressure Liquid Chromatography - Mass Spectrometry (HPLC-MS and HPLC-MS/MS)

Mass spectrometric analysis was performed in a 6460 TripleQuad LC-MS system (Agilent Technologies, Santa Clara, CA, USA) with electro-spray ionization (ESI) coupled to a 1200 series LC system and operated by the Data Acquisition MassHunter software (Agilent Technologies). Figure 3.2 shows an overview of the system. The compounds are separated by liquid chromatography, ionized and analyzed in two sequential mass filters, the first quadrupole (Q1 or MS1) and the last quadrupole (Q3 or MS2). The intermediate collision cell (CC) is a hexapole, designated as Q2. The combination can be operated in three different configurations: total ion scan at MS2 (Figure 3.2a); or ion selection at MS1 and fragmentation in the CC followed by either fragment scan at MS2 (Figure 3.2b) or by specific fragment(s) monitoring (multiple reaction monitoring, MRM; Figure 3.2c).

The samples were injected (2 to 10 μL) on a reversed-phase C_{18} column Zorbax SB (50 mm x 2.1 mm ID; 1.8 μm particle size; Agilent Technologies) and isocratically eluted with 95 % water, 5 % methanol, 0.1 % formic acid at a flow of 0.1 $mL \cdot min^{-1}$ for 10 min. The U.V. absorbance spectrum of effluent was continuously monitored in a diode array detector (DAD) before entering the MS. Ionization was performed in the positive mode, with the following ion source parameters: N_2 flow 9 $L \cdot min^{-1}$ and temperature 300 ºC, nebulizer pressure 25 psi, sheath gas (N_2) flow 7 $L \cdot min^{-1}$ and temperature 300 ºC, capillary voltage 4000 V and charging voltage 1000 V. Fragmentor voltage applied to lead the ions into the mass analyzer was 135 V.

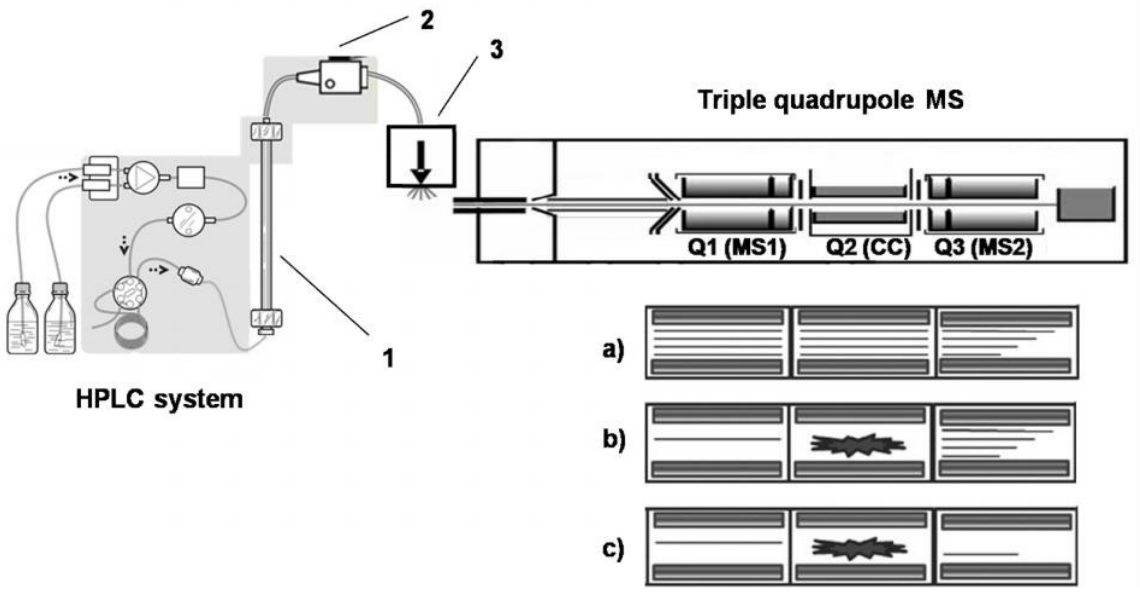

Figure 3.2 - HPLC-MS instrument view. 1-HPLC separation column; 2-diode array detector (DAD); 3-ESI ion source. Three possible operation modes of the triple quadrupole MS are represented: a) MS2 scan; b) product ion scan; and c) multiple reaction monitoring (MRM). Adapted from Chalkley, 2010 and UC Davis ChemWiki (University of California, Davis).

For the comparative investigation, where the compounds differentially present in a specific experimental condition were recognized, first the MS2 Scan mode was used. In this mode, the ions were analyzed in a single quadrupole, according to their mass-to-charge ratio (*m/z*), scanning for all masses between 20 and 2,000 atomic mass units in 0.1 unit steps. Total ion current (TIC) and base peak chromatograms (BPC) were compared in the Qualitative Analysis MassHunter software (Agilent Technologies). Ions of interest were selected for a MS/MS analysis of fragmentation patterns. The MS was set to the Product Ion Scan mode, where the target ions were filtered in the first quadrupole, fragmented in the collision cell at collision energy of 30V, and the product ions were then scanned in the next quadrupole. Fragment spectra were compared to a database (METLIN, from Scripps Center for Metabolomics) and the identity of the metabolites was further confirmed by the U.V. spectra and retention time comparison with the corresponding commercially available pure compounds.

Quantitative analysis of the identified extracellular metabolites was performed by MS/MS in the multiple reaction monitoring (MRM) mode. Here, the target parent ions were selected and fragmented as described above, and the two most intense product ions from each selected parent ion were then monitored in the second quadrupole. Standard curves were generated using selected commercial standards and used to calculate the concentration of the

metabolites in the samples by the Quantitative Analysis MassHunter software (Agilent Technologies).

3.3.2. Gas Chromatography - Mass Spectrometry (GC-MS) and Gas Chromatography - Isotopic Ratio Mass Spectrometry (GC-IRMS)

GC-MS was used for confirmation of the presence of target compounds before IRMS determination. Analysis was performed in Varian GC-MS system 450GC/240MS ion trap mass spectrometer (Varian Inc., Agilent Technologies) equipped with a PAL autosampler (Varian) and operated by the software MS Workstation 6.9.3 (Varian). In this method, volatile derivatives of the compounds of interest are separated by gas chromatography before ionization and scanning of mass spectra in an ion trap analyzer (Figure 3.3). Samples (1 μL) were applied with injector temperature of 230 ºC on a FactorFour VF 5ms column (30 m x 0.25 mm ID, 0.25 μm film thickness, Varian) with helium as carrier gas (1 $mL \cdot min^{-1}$). The temperature of the column-oven was programmed as follows: from 150 ºC to 290 ºC (20 ºC $\cdot min^{-1}$). Positive ions were obtained using electron ionization at 70 eV and the mass spectra were generated by scanning ions of up to *m/z* 700. Retention times of the compounds and *m/z* values of the most abundant ions were compared to those of commercially available nucleosides.

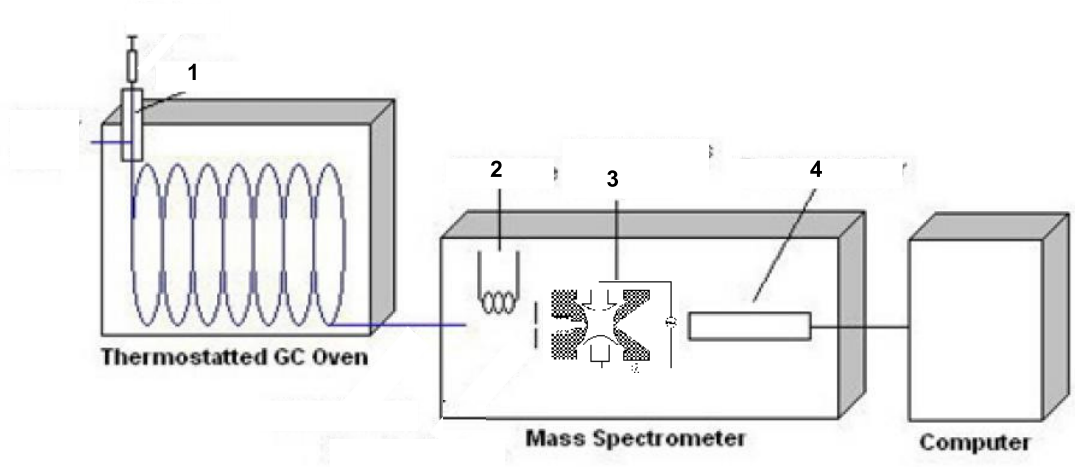

Figure 3.3 - Diagram of the GC-MS instrument. 1-sample injector to the GC column; 2-electron ionization source; 3- ion trap mass analyzer; 4-electron multiplier detector. Adapted from UC Davis ChemWiki, (University of California, Davis).

Determination of $^{13}C/^{12}C$ ratios was performed using the GC IsoLink system connected via a combustion interface to a MAT 253 stable isotope ratio MS (Thermo Scientific, Rockford, IL, USA). This system analyses the volatile derivatives of the target compounds by gas-chromatography separation followed by combustion and detection of the resulting carbon dioxide according to the mass (Figure 3.4). Samples were injected on an Optima-5 column (5 % Phenyl – 95 % Methylpolysiloxan, 50 m x 0.32 mm ID; 0.25 μm film thickness, Macherey-Nagel, Düren, Germany) with helium as the carrier gas and column oven-temperature program as described above for GC-MS. Column effluent was combusted on-line in an oxidation oven at 1030 ºC. The combustion gas was dried by a sulfonated fluoropolymer (Nafion^{TM}) water-permeable membrane. Subsequently, the resulting CO_2 was ionized and separately detected by the IRMS as *m/z* 44, corresponding to $^{12}CO_2^+$ and *m/z* 45, corresponding to $^{13}CO_2^{+\cdot}$ The intensity was determined for each ion and used by the software Isodat 3.0 (Thermo Scientific) to calculate the $^{13}C/^{12}C$ ratio (R).

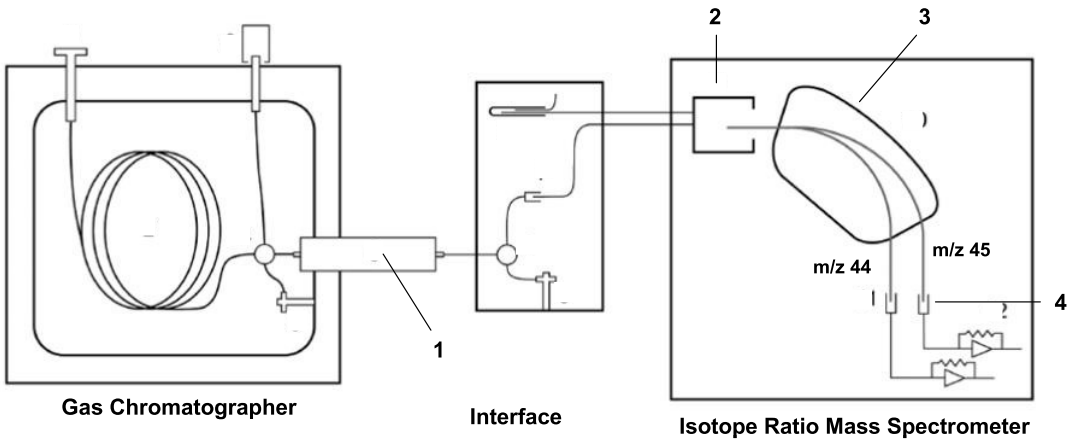

Figure 3.4 - Diagram of the GC-IRMS instrument showing the GC system, the interface and the IRMS analyzer. 1-combustion reactor; 2- electron ionization source; 3- magnetic-sector mass analyzer; 4-Faraday detectors. From Sessions, 2006.

According to the standard notation used to express gas isotope ratio results, calculations where carried as follows:

Eqn. (1) $$\delta\,^{13}C = [(\frac{R_{SAMPLE}}{R_{PDB}})-1] \times 10^3$$

where R_{SAMPLE} is the $^{13}C/^{12}C$ ratio of the measured compound, and R_{PDB} is the $^{13}C/^{12}C$ ratio of the international standard PeeDee Belemnite, a ^{13}C rich carbonate (R_{PDB} = 0.0112372 ± 0.0000090). Thus, the higher ^{13}C content of the sample, the higher the calculated $\delta\,^{13}C$ value. Because the derivatization process (trimethylsilylation) introduces additional carbons to the molecule, the $\delta\,^{13}C$ values of the target compounds ($\delta^{13}C_c$) were corrected to adjust for the number of trimethylsylil (TMS) groups added, according to Rieley, 1994. For ^{13}C-enriched compounds, the fractional abundance (F) must be used in the correction, being defined as:

Eqn. (2) $$F = \frac{^{13}C}{(^{12}C + ^{13}C)}$$

Eqn. (3) $$F_{dc} = \frac{R}{(1 + R)}$$

where F_{dc} corresponds to the fractional abundance of ^{13}C in the derivatized compound, calculated from the measured R. The trimethylsylilation reaction does not involve carbon-containing bounds and hence, a suitable correction can be achieved with a mass balance equation, as follows:

Eqn. (4) $$F_c = \frac{[(n_{dc}F_{dc}) - (x n_d F_d)]}{n_c}$$

where subscripts c and d represent respectively the compound of interest and the derivatization group (TMS), n is the number of carbon moles in each compound and ***x*** is the number of TMS groups introduced. Fractional abundance of ^{13}C in TMS was calculated from R obtained by measuring the derivatization reagent alone in the GC-MS (R_{TMS} = 0.10823).

Finally, $\delta\ ^{13}C$ can be calculated from the corrected F_c for the compound of interest, using the relationships expressed in equations 1 - 3, giving:

Eqn. (5) $$R_c = \frac{F_c}{(1 - F_c)}$$

Eqn. (6) $$\delta\ ^{13}C_c = [(\frac{R_c}{R_{PDB}})-1] \times 10^3$$

After these corrections, the ^{13}C enrichment in the different target compounds expressed in the standard notation, $\delta^{13}C$ per mille (‰), could be properly compared.

3.3.3. Microscopy

Transmission Electron Microscopy (TEM). A TEM910 transmission electron microscope (Carl Zeiss, Oberkochen) was used at an acceleration voltage of 80 kV. Images were taken at calibrated magnifications using a line replica and recorded digitally with a Slow-Scan CCD-Camera (ProScan, 1024x1024, Scheuring, Germany) with ITEM-Software (Olympus Soft Imaging Solutions, Münster, Germany).

Fluorescence Microscopy. Bacterial cells were visualized using one of the two following systems: a Axio Imager A1 epifluorescence microscope using the AxioVision rel 4.6.3 software (Zeiss Imaging Solutions GmBH, Göttingen, Germany) with filters set to excitation/emission of 480/500 nm and 490/635 nm; or a Zeiss Photo microscope (Carl Zeiss) with filter set No. 49 (365 nm excitation, 445/450 emission). Images were recorded with AxioVision software 7.2 . Contrast and brightness were adjusted with Adobe Photoshop CS 5 (Adobe Systems Incorporated, San Jose, CA, USA).

Human cells were visualized using a DMI6000 CS microscope (Leica Microsystems GmbH, Wetzlar, Germany) and a confocal unit Leica TCS SP5 with acousto-optical beam splitter (AOBS) and acousto-optical tunable filters (AOTF), operated by Leica Application Suit (LAS, Leica Microsystems). Single focal plane was monitored in xy scanning mode

using 63x/1.4 HCX-PLAPO oil objective, Argon Laser (488 nm) and DPSS Laser (561 nm), scanner frequency 400 Hz; line averaging 4.

3.3.4. Flow Cytometry

A Becton Dickinson FACSCalibur (BD Bioscience, San Jose, CA, USA) in low flow mode (12 $\mu L \cdot min^{-1}$), operated by BD CellQuest Pro software was used for flow cytometry analysis of bacterial cultures. Total cells were first gated by scatter (side scatte SSC vs. forward scatter FSC) and then analyzed according to their fluorescence in channel 1 and 3 (FL1 vs. FL3 plot). Gates were defined using mid-logarithmic phase growing *E. coli* cultures as reference for intact cells, and the same cultures, after incubation at 100 ºC in a water bath for 20 min, were used as reference for membrane-disrupted cells. Blank values for each sample were considered as the total events counted in unstained replicates. The concentration of cell populations were calculated from the number of events in the gate (subtracting the corresponding blank value), multiplied by the dilution factor and divided by the volume injected.

3.3.5. Agarose gel eletrophoresis

Eletrophoresis of nucleic acids in agarose gel was performed to verify the integrity of bacterial DNA or RNA. Typically, 10 µL of DNA (1 $ng \cdot mL^{-1}$) or RNA (10 $ng \cdot mL^{-1}$) were added to 2 µL of 6 x Loading Dye (Ferramentas Molecular Biology Tools, Thermo Scientific) and applied for separation in a 2 % agarose gel for 30 min at 100 V using a Horizontal Gel System (Starlab International, GmbH, Ahrensburg Germany). GeneRuler™ 1 kb DNA Ladder (Ferramentas) was used as the molecular mass marker. The gel was incubated in EtBr for 30 min and visualized under U.V. light using E.A.S.Y. Win32 gel documentation system (Herolab GmbH, Wiesloch, Germany).

3.3.6. Western blot

Samples were applied in sodium dodecyl sulfate-polyacrylamide gel electrophoresis (SDS-PAGE, 12 % acrylamide, unless otherwise indicated) using Mini-Protean ® Tetra system (Bio-Rad Laboratories, Inc., Hercules, CA, USA) for aprox. 3 h at 100 V. Pre-stained BenchMark® protein ladder (Invitrogen) was applied as the molecular mass marker. Proteins separated in the gel were electrically transferred to a nitrocellulose membrane Protran™ 0.45

μm pore (Whatman) for 1 h at 100 V in Mini Trans-Blot cell (Bio-Rad). The membrane was incubated at 4 ºC overnight for blocking with 5% bovine serum albumine (BSA) in Tris buffered saline-Tween (TBST: 0.1 M Tris-HCl, 0.1 M NaCl, 0.25 mM $MgCl_2$, 0.05 % Tween 20), and then split in two parts for antibody probing, according to the molecular mass marker. The upper part, containing proteins above 64 kDa, was probed for p65 and phospho-p65, and the lower part, containing proteins below 64 kDa, was probed for IκB and actin. Incubations with antibodies were performed at room temperature in a platform shaker as follows:

1) primary antibodies: rabbit IgG anti- IκB or rabbit IgG anti-phospho-p65, 1:500 in TBST for 1 h;
2) washing: TBST for 3 times 10 min;
3) secondary antibody: anti-rabbit IgG – HRP conjugate, 1:10,000 in TBST for 1 h.
4) washing: TBST for 3 times 10 min.

Finally, the proteins were detected using Amersham™ ECL™ Plus Western-blotting detection system (GE Healthcare Bio-Sciences AB, Uppsala, Sweden). The reagent contains a chemoluminescent HRP substrate and the reaction was visualized by exposing a Hyperfilm ECL™ in a Hypercassete (GE Healthcare) to the probed membrane. The film was developed in an Optimax Typ TR developing machine (MS-L GmbH, Wiesloch, Germany).

For relative quantitation purposes, the same membrane was treated with pH 2.2 stripping buffer (15 $g \cdot L^{-1}$ glycine, 1 $g \cdot L^{-1}$ SDS, 1% Tween 20) 2 times for 20 min for removal of antibodies, then washed with phosphate buffered saline (PBS; sodium phosphate 8 mM, sodium chloride 150 mM, pH 7.4) and TBST (2 times for 10 min each), blocked and probed again as described above, except that the antibodies and dilutions used were: primary antibodies - mouse IgG anti-actin (1: 2,000) or mouse IgG anti-p65 (1:250); secondary antibody - anti-mouse IgG – HRP conjugate (1:10,000). After developing, the films were digitalized and the images were compared in a densitometry analysis using the public domain software ImageJ 1.43u.

3.4. Microbiology methods

3.4.1. Bacterial strains and culture conditions

Strains: The bacterial strains used in this study are listed in Table 1. *E. coli* strains were kindly provided by Dr. Gabriella Molinari (Environmental Microbiology, HZI). Strains *E. coli* Nissle 1917 (EcN) and LF82 were obtained from HZI collection in a previous work. *E.*

coli 7145A was isolated by Dr. Alexander Swidsinski (Medical Clinic of the Humboldt-University Berlin Charité). *E. coli* HZI 2-6 was isolated by Dr. Dieco Würdemann (Environmental Microbiology, HZI) from IBD patients' biopsy obtained at the University-Hospital Schleswig-Holstein (UKSH, Kiel). *E. coli* strain W, *Pseudomonas aeruginosa* and *Klebsiella pneumoniae* were purchased from the Deutsche Sammlung von Mikroorganismen und Zellkulturen (DSMZ, DSM strains). Species identification was confirmed by 16S rRNA gene sequencing as described previously (Abraham *et al.*, 1999). Briefly, DNA extracted from solid grown colonies was amplified in four polymerase chain reactions (PCR) using one of the following primers: 16R1087 (5'-ACT GGC GGA CGG GTG AGT AA-3'), 16F945 (5'-TAC GGY TAC CTT GTT ACG ACT T-3'), 16R518 (AGA GTT TGA TCM TGG CTC AG-3'), 16F357 (5'-CCG CTT GTG CGG GCC CCC GTC-3'). PCR products were purified with DyeEx 2.0 Spin Kit (Qiagen, Hilden, Germany) following manufacturer's instructions, dried in a vacuum centrifuge and sequenced in a 3130*xl* Genetic Analyzer (Applied Biosystems, Darmstadt). Sequences were analyzed in Sequencher™ 4.8 (Gene Codes Corporation, Ann Arbor, USA) and compared to Genbank database using basic local alignment tool (BLAST; NCBI).

Table 3.1 - Bacterial strains used in this study.

Strain	Description
Escherichia coli strain W	DSM1116; quality control strain
E. coli Nissle 1917	probiotic strain, therapeutic potential for IBD [a]
E. coli 7145A	clinical isolate from IBD biopsy
E. coli HZI 2-6	clinical isolate from IBD biopsy
E. coli LF82	adherent-invasive (AIEC) reference strain, CD-associated [b]
Pseudomonas aeruginosa	DSM1707 (PAO1)
Klebsiella pneumoniae	DSM30102

a - Schultz, 2008; b - Boudeau *et al.*, 1999

Cultures: Unless otherwise indicated, bacteria were cultivated in sterile filtered defined minimal medium, herein referred as M4 ($MgSO_4$ 0.02 $g \cdot L^{-1}$, Citric Acid 0.2 $g \cdot L^{-1}$, K_2HPO_4 1 $g \cdot L^{-1}$, $NaNH_4HPO_4$ 0.32 $g \cdot L^{-1}$), supplemented with glucose (0.2 %), in a shaker incubator (37 ºC, 100 rpm). Bacteria from frozen stocks were grown in M4 up to 18 h (late stationary-phase pre-culture). Alternatively, strains showing reduced growth in M4 were pre-cultured in autoclaved Luria-Bertani (LB) broth (tryptone 10 $g \cdot L^{-1}$, yeast extract 5 $g \cdot L^{-1}$, NaCl 10 $g \cdot L^{-1}$). From the pre-cultures, 200 to 500 µL were transferred to 5 mL M4 medium, grown

for 1h, and then used to inoculate the main culture. The optical density (O.D., absorbance at 600 nm) was measured in 10 mm-path disposable cuvette (Ratiolab GmBH, Dreieich, Germany) using a NanoDrop 2000c spectrophotometer (Thermo Scientific).

3.4.2. Antimicrobial challenge experiments

For antimicrobial challenge experiments, cultures were inoculated at start O.D. 0.005 (unless otherwise indicated) in 100-wells "Honeycomb" plates (Oy Growth Curves Ab Ltd, Helsinki, Finland) with 160 μL in each well. Growth was monitored by measuring O.D. at 15 min intervals in a BioscreenC automated microbiology growth analysis system (Oy Growth Curves) using incubation temperature control at 37 ºC and continuous shaking mode (medium amplitude). Alternatively, 20 mL of main culture in M4 was grown in 100 mL Erlenmeyer flasks and bacterial growth was monitored by measuring O.D. in 10 mm-path disposable cuvette using NanoDrop 2000c spectrophotometer at different time-points. It is important to note that the O.D. values reported by the BioscreenC system, as a result of vertical absorbance reading, are related to the culture volume and consequent path length in each well, therefore not corresponding to usual measurements in cuvette photometers.

At mid-logarithmic phase (O.D. 0.1 ± 0.005) the cultures in 100-well plates (160 μL) were challenged with 40 μL of antimicrobial peptide solution in water to the final peptide concentration used in the different experiments, as indicated (typically 20 $\mu g \cdot mL^{-1}$). Unchallenged cultures (controls) were always handled in parallel by adding 40 μL of sterile autoclaved water at the same time-point as the peptide. In indicated experiments, a lysis challenge was included, where the cultures were submitted to one of the following lysis protocols: incubation with TE buffer (10 mM Tris-HCl, 1 mM EDTA, pH 7.5) containing lysozyme (10 $mg \cdot mL^{-1}$) and Triton X-100 (1.2 %, Sigma-Aldrich); or freeze/thaw cycles (5 times for 1 min each) using liquid nitrogen and a 100 ºC water bath. Two to three cultures (wells) for each condition (control or treatment) were tested in every experiment. The cultures were then further incubated under the same start conditions in BioscreenC system. At sampling point (2 h after treatment unless otherwise indicated), the cultures (200 μL) were filtered through 0.22 μm pore centrifuge tube filter (Corning Inc., Corning, NY, USA) for 2 min at 13,000 rpm for cell removal. Supernatants were transferred to glass HPLC-vial insets for immediate analysis, or stored at -20 ºC for further use. Alternatively, whole cultures were processed for cell-viability determinations or electron transmission microscopy as described

below. Two to three culture replicates of each condition were always kept in the BioscreenC system for >20 h for following the growth curves.

3.4.3. Colony-Forming Units (CFU) counts

CFU counts were performed in M4-agar or LB-agar plates. Cultures were diluted (10-fold series: 10^3, 10^5 and 10^4) in phosphate buffer (Na_2HPO_4 10 mM, pH 7.4). In each plate, 10 µL of culture dilutions were spread using sterile Drygalski loops. After 24 h to 48 h, plates containing between 30 and 300 distinguishable colonies were used for colony counting under a stereomicroscope (Carl Zeiss AG, Oberkochen, Germany). A minimum of two plates were counted for each culture and the average number of CFU *per* mL was calculated according to the initial dilution.

3.4.4. Metabolic activity assays

Metabolic activity of bacterial cultures was determined using the BacTiter-Glo™ microbial cell viability assay (Promega) according to manufacturer's instructions. Briefly, 75 µL of culture was transferred to a 96-well plate with black opaque walls (Greiner Bio-One GmBH) and 75 µL of reconstituted BacTiter-Glo™ substrate was added to each sample. The formulation of the reagent causes ATP release from the cells and a luminescent signal proportional to ATP concentration is generated by luciferase activity. After 5 min incubation at room temperature, luminescence was recorded in a Victor™ X3 2030 multilabel reader (PerkinElmer, Turku, Finland). A standard curve was performed simultaneously with varying concentrations (0, 10 pM, 100 pM, 1 nM, 10 nM, 100 nM and 1 µM) of ATP (Promega) in M4 minimal medium, and used to calculate ATP concentration released from the tested cultures.

As an alternative approach to estimate bacterial metabolic activity applying a technique not directly dependent upon ATP concentration, the redox dye 2,6-dichlorophenolindophenol (DCIP) was used. DCIP presents a blue color when oxidized, turning colorless when reduced. The protocol was adapted from Yoshida *et al.*, 2002, where DCIP is reported as an efficient method to determine biochemical oxygen demand in Gram-negative bacteria. DCIP was mixed to the cultures to a final concentration of 40 µM, at different time-points after challenge, in a clear 96-well plate (Greiner Bio-One GmBH). The reaction was incubated for 30 min at room temperature and the change in color observed was

measured in a μQuant microplate spectrophotometer (Bio-Tek Instruments, Inc., Winooski, VT, USA) with KCjunior software (Bio-Tek Instruments, Inc.).

3.4.5. Sample preparation for fluorescence microscopy, flow cytometry and TEM

Bacterial membrane integrity was microscopically verified using the LIVE/DEAD® BacLight ™ kit (Invitrogen/Molecular Probes). The reagent was prepared by mixing component A (1.5 μL) and B (3 μL) in 95.5 μL of water. From each culture, 100 μL were transferred to a 96-well plate (Greiner Bio-One GmBH, Frickenhausen, Germany) and 3 μL of the freshly mixed reagent was added. The plate was incubated for 15 min at room temperature protected from light. The samples were then filtered through Nuclepore™ Track-Etched 0.2 μm pore filter membrane, (Whatman/GE Healthcare, Piscataway, NJ, USA) with the aid of a vacuum pump. Membranes were placed onto suitable microscopy glass lamina and covered with one drop of BacLight ™ mounting oil (kit component C) for visualization under an Axio Imager A1 epifluorescence microscope (Zeiss Imaging Solutions) as described in section 3.3.3. The staining is based on the combination of two fluorescent dyes: SYTO® 9 and propidium iodide, with excitation/emission maxima of 480/500 nm and 490/635 nm respectively. SYTO 9 is a green-fluorescent nucleic acid stain able to generally label bacteria, irrespective of membrane integrity. Propidium iodide, a red-fluorescent nucleic acid stain, is in turn not able to penetrate intact bacterial membrane and only labels bacteria with membrane damage, reducing the green-fluorescence from SYTO 9 when both dyes are present. The resulting image shows intact cells in green, whereas membrane-damaged cells appear in red.

For flow cytometry, a Becton Dickinson Cell Viability Kit (BD Biosciences) was used, which employs thiazole orange (TO) as the permeant dye for all cells, and propidium iodide (PI) to differentially stain only membrane-compromised cells. Cultures were diluted 1:10 in PBS containing 0.01% Tween® -20 (Sigma-Aldrich) to a final volume of 500 μL, gently mixed to 1 μL of TO 42 μM and incubated for 10 min at room temperature protected from light. Next, 1 μL of PI 4.3 mM was added and incubated for 1 min at room temperature, again protected from light. Samples were then analyzed in a BD FACSCalibur (BD Biosciences) as described in section 3.3.4. According to the manufacturer's instructions, TO

fluorescence is detected primarily in FL1 and FL2, and PI primarily in FL3. A FL1 vs. FL3 plot was used for discrimination of intact or damaged cell populations.

For direct imaging of bacterial DNA, cells were incubated in 10 $mg \cdot mL^{-1}$ aqueous 4',6-diamidino-2-phenylindole (DAPI) for 5 min, washed twice with TE buffer (Tris 20 mM, 0.1 M EDTA, pH 6.9) and mounted onto glass slides for analysis under a Zeiss Photo microscope (Carl Zeiss) as described in section 3.3.3.

For investigation of morphological features of *E. coli* cultures by electron microscopy, 3 mL of cultures at each condition were collected by pooling cultures from 15 wells (200 µL) after the challenge experiment. The cells were fixed 2 h after treatment by the direct addition of paraformaldehyde to the cultures (20 % v/v), thus avoiding damage that could result from centrifugation. Here, Bacteria were further processed with 2 % glutaraldehyde and 3 % formaldehyde in cacodylate buffer for 1 h on ice, washed with cacodylate buffer, and osmificated with 1 % aqueous osmium for 1 h at room temperature. Samples were then dehydrated with a graded series of acetone (10 %, 30 %, 50 %, 70 %, 90 %, and 100 %) for 30 min at each step. Dehydration in the 70% acetone step was done with 2% uranyl acetate overnight. Samples were then infiltrated with an epoxy resin (1 part acetone/1 part resin; 1 part acetone/2 parts resin, pure resin alternating) according to the Spurr's formula (Spurr, 1969). Ultrathin sections were cut with a diamond knife, picked up with formvar-coated grids, counterstained with uranyl acetate and lead citrate, and examined under a TEM910 transmission electron microscope (Carl Zeiss) as described in section 3.3.3.

3.4.6. Quantification of cellular components in bacterial supernatants

Proteins: The bicinchoninic acid (BCA) method (Smith *et al.*, 1985) was employed for determination of total protein content. This technique is based on the reduction of Cu^{+2} to Cu^{+1} by protein in an alkaline medium, combined to the colorimetric detection of the Cu^{+1} by the bicinchoninic acid in the reagent. The assay was performed using the Pierce ® BCA Protein Assay Kit (Pierce Biotechnology, Rockford, IL, USA) according to manufacturer's instructions. The reagent was prepared by mixing 50 parts of component A to 1 part of component B, and 200 µL were added in clear 96-well plates (Greiner Bio-One GmBH) to 25 µL of the filtered supernatants resulting from challenge experiments (as described above). BSA (Pierce Biotechnology) was used to prepare the standard curve (0.05, 0.1, 0.25, 0.5, 1 and 2 $mg \cdot mL^{-1}$ in M4 minimal medium). After 30 min incubation at 37 ºC, absorbance at 562 nm was recorded in a µQuant microplate spectrophotometer (Bio-Tek Instruments, Inc.) with

KCjunior software (Bio-Tek Instruments, Inc.). The mean value obtained for the reaction with M4 alone was used as a blank and subtracted from the experimental results.

DNA: Supernatants were analyzed using the Quant-iT™ PicoGreen® dsDNA Reagent kit (Invitrogen/Molecular Probes). The reagent was prepared immediately before use by diluting the supplied DMSO stock solution 200-fold in TE buffer (10 mM Tris-HCl, 1 mM EDTA, pH 7.5). The samples (50 μL) were transferred to a 96-well plate with black opaque walls (Greiner Bio-One, GmBH), and the volume was adjusted to 100 μL by addition of 50 μL of TE buffer. Finally, 100 μL of the reagent was added to each sample and the reaction was incubated for 2-5 min at room temperature, protected from light. Fluorescence was read in a VICTOR^2 Wallac 1420 multilabel counter (PerkinElmer) using filters for excitation at 485 nm and emission at 535 nm. A standard curve was processed simultaneously using lambda DNA standard (Invitrogen/Molecular Probes) at 0.05, 0.5, 5, and 50 $ng \cdot mL^{-1}$. The mean value obtained for the reaction with M4 alone was used as a blank and subtracted from the experimental results.

ATP: The concentration of ATP in filtered supernatants from experimental cultures was measured using BacTiter-Glo™ microbial cell viability assay (Promega) as described above (section 3.4.4).

3.4.7. Nucleic acids extraction

Bacterial cells from 7 mL of culture were harvested by centrifugation (10 min, 4,000 rpm at 4 ºC). For RNA extraction, harvested cells were resuspended in RNAprotect® Bacteria Reagent (Qiagen, Hilden, Germany), then again centrifuged (10 min, 4,000 rpm) for removal of excess reagent, before further processing. Total DNA was extracted and purified using the DNeasy® Blood and Tissue kit (Qiagen), according to the protocol for Gram-negative bacteria, as provided by the manufacturer. RNA was extracted and purified using the RNeasy mini kit (Qiagen), according to the protocol for enzymatic lysis of bacteria, as provided by the manufacturer. In both cases, the purified nucleic acids were eluted with water. The yield of each extraction was monitored by spectrophotometric quantification (absorbance at 260 nm and 280 nm) using Nanodrop2000c (Thermo Scientific).

3.4.8. Sample preparation for isotopic labeling studies

^{13}C Labeling. Bacteria were labeled by the addition of 0.5 $g \cdot L^{-1}$ [U-^{13}C]-glucose (99 % ^{13}C) ($^{13}C_6$-Glu; Euriso-Top, Gif-sur-Yvette, France) to the culture medium M4. Pre-cultures and inoculums were prepared in normal M4 as described above (section 3.4.1) and the main cultures (20 mL) were grown in either in normal M4 or in ^{13}C-Glu M4. In this case, the challenge experiments were performed using 3 mL of culture. For preparation of nucleosides for IRMS, bacterial cells from 7 mL of each culture were harvested by centrifugation (10 min, 4,000 rpm at 4 ºC) and the pellets were stored at -70 ºC until further processing. For RNA extraction, harvested cells were resuspended in RNAprotect® Bacteria Reagent (Qiagen, Hilden, Germany), then again centrifuged (10 min, 4,000 rpm) for removal of excess reagent, before the pellet was stored at -70 ºC.

Preparation of nucleosides. Nucleic acids were extracted as described above (section 3.4.7), and subsequent enzymatic degradation into the corresponding nucleosides was performed according to Crain, 1990. Extracted nucleic acids (100 µL) samples were denaturated (2-3 min at 100 ºC in a water bath) and immediately cooled down in crashed ice. Then, ammonium acetate 0.1 M, pH 5.3 (10 µL) and 2 units of Nuclease P1 were added, and the reaction was incubated for 2 h at 45 ºC. Alkaline phosphatase (0.5 units), and 12 µL of freshly prepared ammonium bicarbonate 1 M for alkalinization were added to each sample before further incubation for 1 h at 37 ºC. Hydrolysis products were stored at -20 ºC until use.

Trimethylsilylation. In order to be analyzed by gas chromatography (GC), as described above, nucleosides were converted into volatile trimethylsilyl (TMS) derivatives. The reaction replaces active hydrogen from hydroxyl or amine groups of the nucleoside by TMS groups. Before derivatization, hydrolysis products were lyophilized in a Christ Alpha 1-2 Plus freeze-drier (Martin Christ Gefriertrocknungsanlage GmbH, Osterode am Harz, Germany). Dried samples were resuspended in 100 µL derivatization reagent (BSTFA 4:1 in pyridine) and incubated at 100 ºC for 1 h, according to the protocol reported by Macallan *et al.*, 1998. After filtering through a 0.2 µM pore syringe filter unit (Spartan 13, Whatman GmbH, Dassel, Germany) the TMS-nucleosides were ready to be applied to gas-chromatography.

3.5. Cell biology methods

3.5.1. Human intestinal epithelial cell line cultures

Human intestinal epithelial cell line (Caco-2) was kindly provided by the group of Dr. Lothar Jänsch (Cellular Proteome Research, HZI). The cells were cultivated in Dulbecco's modified Eagle's medium (DMEM), 4.5 $g \cdot L^{-1}$ glucose (PAA Laboratories GmBH, Pasching, Austria) supplemented with L-glutamine (2 mM) and 10 % heat-inactivated fetal calf serum (FCS), herein referred only as DMEM. . The culture was grown at 37 ºC, 5 % CO_2 in 75 cm^2 flasks (Sarstedt, Newton, NC, USA) until forming a confluent monolayer. For propagation, cells were washed 3 times with PBS, detached by treatment with trypsin (0.5 $mg \cdot mL^{-1}$) and EDTA (0.22 $mg \cdot mL^{-}1$) in PBS (1 mL) and transferred to a new culture flask, typically at a 1:10 dilution. Sub-cultures at passage number between 5 and 30 were used for experiments as described below, in which case, cell density was determined by staining of the cell suspension (20 µL) with 20 µL of Trypan blue (Fluka/Sigma-Aldrich) and counting in a Neubauer chamber under the light microscope (Nikon Eclipse TS100, Nikon Instruments, Inc., Melville, NY, USA)

3.5.2. NF-κB activation assay

To investigate the level of activation of the NF-κB pathway in Caco-2 cells, the cells were seeded (0.075 x 10^6 cells *per* well) in 24-wells plate (Sarstedt) and grown for 24 h. In cases where the cells would be further analyzed by fluorescence microscopy, a sterile cover slip was placed in the bottom of each well before cell attachment. The culture medium was exchanged for serum-free DMEM during 3 h before beginning of the experiment. First, to establish the optimal assay conditions, IL-1β (10 $ng \cdot mL^{-1}$), TNFα (50 $ng \cdot mL^{-1}$) or LPS (20 $\mu g \cdot mL^{-1}$) were tested as positive controls for NF-κB activation. The treatment was added to cells in duplicated wells (always keeping two wells as untreated controls) and after 20 min or 40 min of incubation, the cultures were processed for analysis as described below. The same experimental setup with 40 min incubation was used to test the effect or bacterial supernatants (200 µL per 800 µL of serum-free DMEM) on Caco-2 cells, with IL-1β (10 $ng \cdot mL^{-1}$) as the positive activation control. In a alternative experiment, a pre-incubation time of 30 min was performed in the presence or absence of bacterial supernatants, and the cells were subsequently incubated in the presence or absence of IL-1β (10 $ng \cdot mL^{-1}$). After 40 min, the

cells were collected for analysis. For Western blot, the cells in each well were washed with PBS and harvested in 100 μL of reducing sample load solution (50 mM Tris-HCl pH 6.8, 4.5 % glycerin, 1.1 % β-mercaptoethanol, 11 $g \cdot L^{-1}$ SDS, 58 $mg \cdot L^{-1}$ bromophenol blue), the duplicates were pooled together. For fluorescence microscopy cells attached to the glass slips were washed one time with PBS and immediately fixed as described below.

3.5.3. Immunofluorescence staining

Cells attached to glass slips were fixed by incubation with paraformaldehyde (PFA) 3 % in PBS at room temperature for 15 min. At this point, the PFA solution was removed and the samples could be stored in PBS at 4 ºC until further processing. Before staining, samples were treated with glycine 50 mM in PBS for 15 min, to quench PFA-derived fluorescence. All steps were performed at room temperature. The samples were incubated for 15 min in the blocking solution: PBS containing 1 % BSA, and 0.05 % saponine as permeabilizing agent. Slips were covered with the primary antibody solution (rabbit IgG anti-p65, 1:200 in PBS) and incubated for 1 h, after which they were washed 3 times for 10 min in PBS. Next, the slips were covered with the secondary antibody solution (anti-rabbit IgG-Alexa546 conjugate, 1:800 in PBS) and incubated for 1 h. Samples were washed again 3 times for 10 min in PBS and the nuclear staining was performed by incubation for 10 min with Hoechst 33258 (2′-(4-hydroxyphenyl)-5-(4-methyl-1-piperazinyl)-2,5′-bi-1*H*-benzimidazole trihydrochloride hydrate; Sigma-Aldrich) 1:1,000 in PBS. After a final PBS wash (2 times 10 min), slips were placed onto microscope slides with one drop of fluorescent mounting medium (Dako, Glostrup, Denmark) left at room temperature for drying before analysis under a DMI6000 CS microscope (Leica Microsystems) as described in section 3.3.3.

3.6. Statistical analysis

Data obtained in three or more replicates were tested for statistically significant differences between means by one way analysis of variance (ANOVA), with $\alpha = 0.01$, using Holm-Sidak Test for pairwise comparison. The analyses were performed using SigmaPlot 11.0 (Systat Software, Inc., Chicago, IL, USA).

4. RESULTS

RESULTS I

4.1. Extracellular metabolites from *Escherichia coli* in response to human defensin

4.1.1. Effect of human β-defensin-2 on E. coli *and identification of extracellular metabolites*

The first fundamental question to be answered in this study was whether the activity of human β-defensin-2 (hBD-2) on *Escherichia coli* could generate extracellular soluble compounds, potentially involved in host-microbial interaction, which would not be present in a normally-growing, unchallenged culture. To address this question, a laboratory quality control *E. coli* strain (DSM1116) grown in minimal medium (M4) was used. The composition of the medium was carefully chosen to support bacterial growth at low salt content, thus being suitable for the salt-sensitive activity of hBD-2, and low complexity, facilitating further analysis by mass spectrometry. The cultures were either challenged or not at mid-logarithmic phase with hBD-2 50 $\mu g \cdot mL^{-1}$, a concentration able to irreversibly impair *E. coli* growth under these experimental conditions. The cell-free supernatants from both cultures were collected 2 h after the challenge to be analyzed by mass spectrometry. Figure 4.1 shows the representative growth curves of the unchallenged (control) culture and the effect of hBD-2 challenge on bacterial growth.

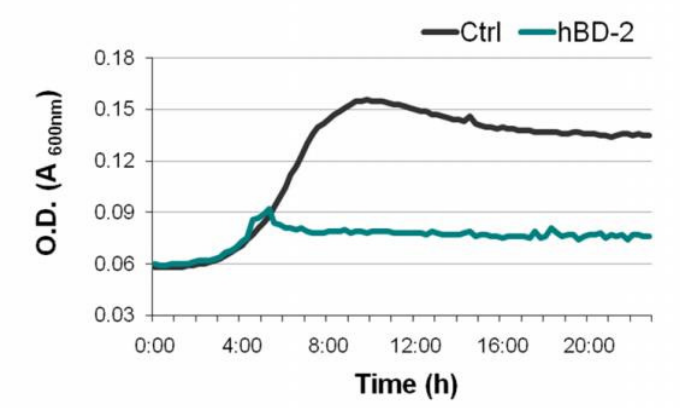

Figure 4.1 - Growth curves of *E. coli* (DSM1116) starting from inoculum (approx. $5x10^6$ $CFU \cdot mL^{-1}$) in M4 medium and incubated for 23 h at 37 °C in the BioscreenC system using medium amplitude shaking. Ctrl (black line): unchallenged culture; hBD-2 (green line): challenged with 50 $\mu g \cdot mL^{-1}$ hBD-2 at 4 h as described in Materials and Methods.section 3.4.2

Before analyzing the culture supernatants, an HPLC-MS scan evaluation of M4 alone was performed, in order to determine the peaks corresponding to medium components rather than bacterial products. The analysis of the base peak chromatogram (BPC) demonstrated the presence of two major peaks at retention times of 1 and 1.3 min (Figure 4.2a, number 1 and 2, respectively). The mass spectrum of each peak was generated by scanning ions of mass-to-charge ratio (*m/z*) up to 2,000. Figure 4.2a insets show the ions detected at *m/z* values lower than 700 as no ions were detected at higher *m/z* values. The mass spectrum of the first peak (Figure 4.2a, inset 1) presented a major ion of *m/z* 203, likely corresponding to glucose sodium adduct, which can be formed during the positive ionization process. In this case, instead of forming the H^+ protonated molecular ion (*m/z* = M+1), the molecule acquires a positive charge by coupling with Na^+, forming a sodium adduct (*m/z* = M+23). Thus, glucose (M=180) was detected as *m/z* 203 (180 + 23). Similarly, the mass spectrum of the second peak (Figure 4.2a, inset 2) presented a major ion of *m/z* 215, likely representing the sodium adduct for citric acid (M= 192; *m/z* = M + 23 = 215).

Next, the supernatants sampled from the experimental cultures were analyzed by the HPLC-MS scan. As expected, the two peaks already identified as medium components were present in the BPC of both samples (Figure 4.2b). Additionally, two peaks at retention time 2.1 and 2.6 min (numbered 3 and 4, respectively) were detected exclusively in the supernatant from hBD-2 challenged culture (Figure 4.2b, green line). As demonstrated by the mass spectra (Figure 4.2b, insets 3 and 4), peak number 3 was composed of two main ions of *m/z* 136 and *m/z* 268, whereas peak number 4 corresponded to one major ion of *m/z* 152. Again, only ions with *m/z* < 700 are shown as no other ions were detected up to *m/z* 2,000.

To further investigate the identity of the compounds present in peaks 3 and 4, tandem mass spectrometry analysis (HPLC-MS/MS) of the supernatants was performed. Here, following HPLC separation, the target ions (*m/z* 268, *m/z* 136 and *m/z* 152) were selected and submitted to collision induced fragmentation. The resulting fragments (product ions) were then scanned and a fragment spectrum for each target (parent) ion was generated. Figure 4.3 shows the product ion chromatogram and the corresponding fragment spectra of ions of *m/z* 268 (a), *m/z* 136 (b) and *m/z* 152 (c). The supernatant from unchallenged culture (Ctrl, black lines) was also analyzed to confirm that the target ions were not present in any region of the chromatogram. From challenged culture supernatants (green lines), fragmentation of *m/z* 268 ions resulted in a single product of *m/z* 136 (Figure 4.3a) at retention time 2.1 min, indicating that the two major ions present in the corresponding peak 3 derived from the same compound.

This was further confirmed by fragmentation of *m/z* 136 ions, yielding one peak with the exact retention time as *m/z* 268, in addition to an earlier peak at 1.1 min, both presenting identical fragment spectra represented in the inset (Figure 4.3b). Similarly, fragmentation of *m/z* 152 ions resulted in a peak at 2.6 min (corresponding to peak 4, as expected) and an additional peak at 1.1 min, both presenting identical fragment spectra (Figure 4.3c, inset).

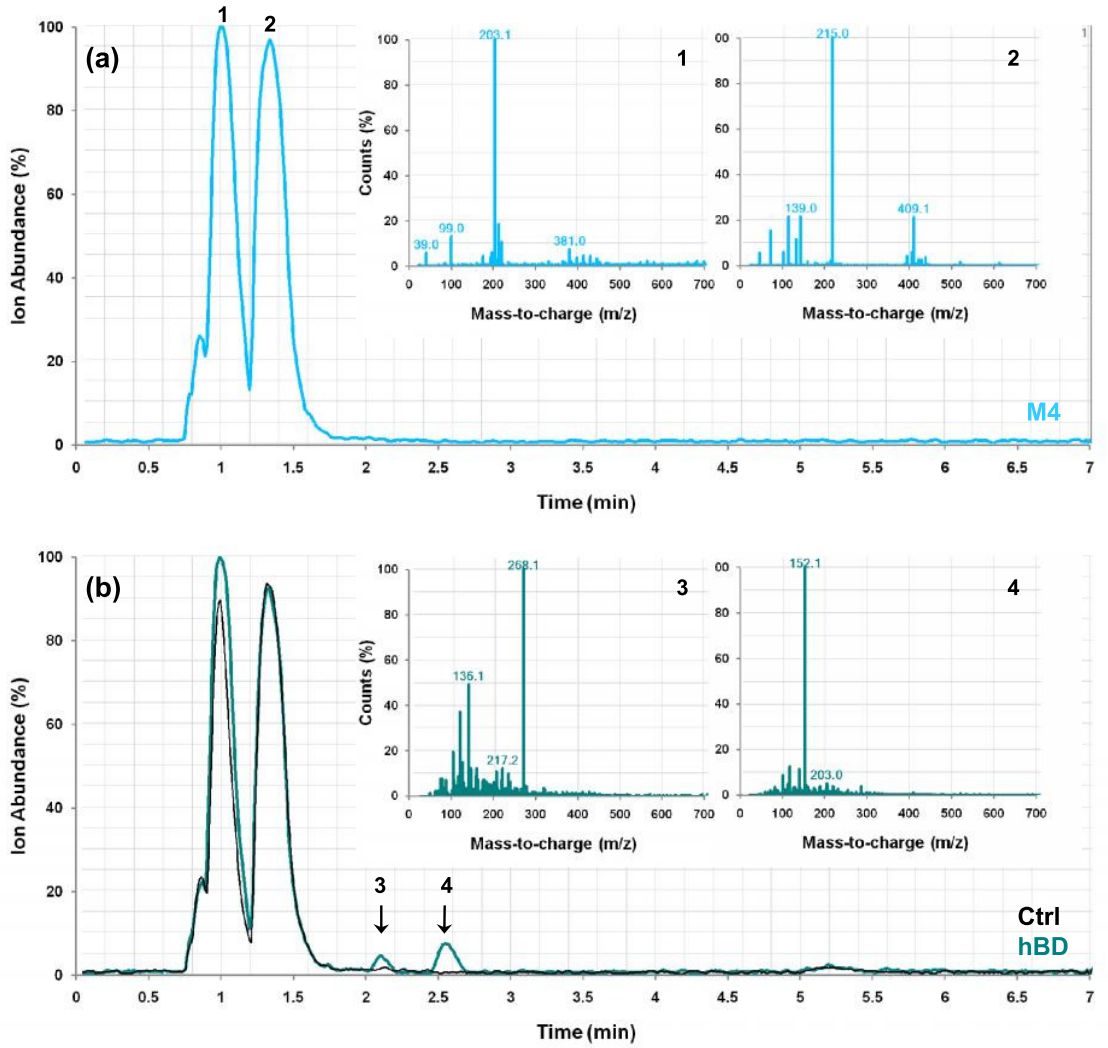

Figure 4.2 - HPLC-MS analysis (scan base peak chromatogram) of (a) sterile M4 medium (blue line) or (b) supernatants from *E. coli* (DSM1116) cultures unchallenged (Ctrl; black line) or challenged with hBD-2 50 µg·mL-1 (hBD, green line). Challenge was performed as described in Materials and Methods section 3.4.2 and supernatants were collected 2 h after hBD-2 addition. Samples (5 µL) were injected in reversed-phase chromatography and analyzed by MS scan mode as described in Materials and Methods section 3.3.1. Insets show the mass spectra (average scan of minimum 7 points at peak maxima) of peaks found in all samples (a, 1 and 2) and peaks found exclusively in supernatants from hBD-2 challenged cultures (b, arrows 3 and 4).

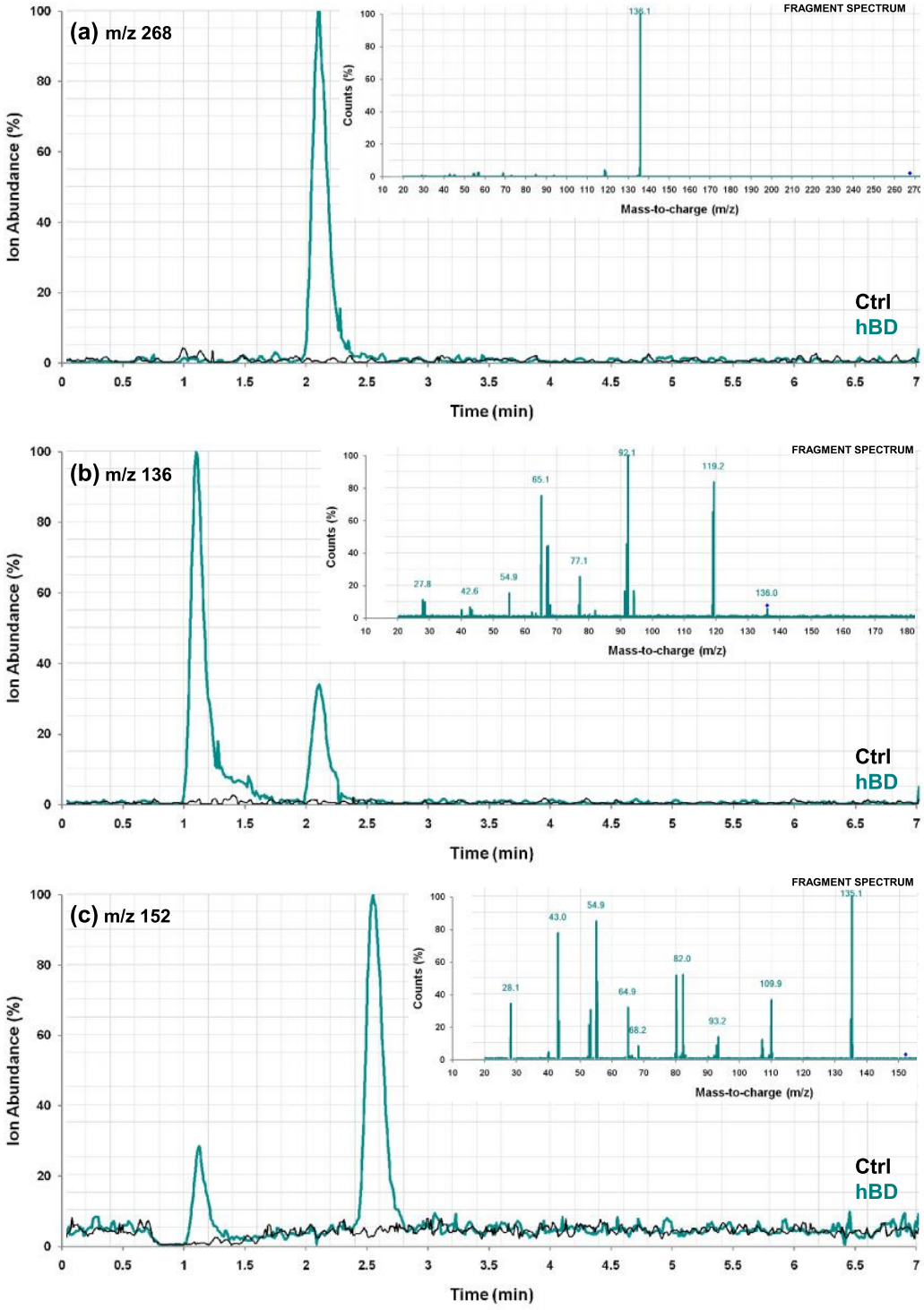

Figure 4.3 - HPLC-MS/MS analysis (product ion base peak chromatogram) of target ions of *m/z* 268 (a) *m/z* 136 (b) and *m/z* 152 (c) in supernatants from *E. coli* (DSM1116) cultures unchallenged (Ctrl, black line) or challenged with hBD-2 50 $\mu g \cdot mL^{-1}$ (hBD, green line). Challenge was performed as described in Materials and Methods section 3.4.2 and supernatants were collected 2 h after hBD-2 addition. Samples (5 µL) were injected in reversed-phase chromatography and analyzed by MS/MS product ion scan mode as described in Materials and Methods section 3.3.1. Insets show representative fragment spectra (C.E. 50 V) of each targeted parent ion.

The main product ions generated from parent ion *m/z* 136 (*m/z* 119, *m/z* 92 and *m/z* 65) and from parent ion *m/z* 152 (*m/z* 135, *m/z* 110, *m/z* 55 and *m/z* 43) were used to search the web-based data repository METLIN for metabolites presenting matching fragments, considering the precursors were molecular ions of compounds with M=135 and M=151, respectively. The purine nucleobases adenine (A, M=135) and guanine (G, M=151) were identified as possible matches for the mass spectrometry data. However, having observed an ion of *m/z* 268 as a precursor of *m/z* 136, with identical fragment spectra, peak 3 was identified as the purine nucleoside adenosine (Ado, M=267). In turn, the molecular ion for the corresponding guanine nucleoside guanosine (Guo, M=283) was not detected in peak 4. Nevertheless, according to the polarity of the compounds, and taking into account that the fragmentation pattern of Guo would possibly also match the one of its constituent base (G), peak 4 was recognized as the nucleoside (Guo). Polarity is a determinant factor of retention time in reversed-phase chromatography, where more polar molecules elute earlier. This was considered here to complement mass spectrometry data in compound identification, as it was unlikely that G presented a higher retention time than Ado in the conditions used. The presence of two peaks of *m/z* 136 and *m/z* 152 (b and c) at earlier (1.1 min) retention time was also acknowledged, but not targeted at this first screening, which aimed only at identifying peaks 3 and 4 (Figure 4.2b). Thus, to confirm that the ions detected in hBD-challenged culture supernatants corresponded to the presence of Ado and Guo in these samples, the two nucleosides were purchased as pure compounds, prepared as aqueous solutions and evaluated in the same HPLC-MS/MS analysis (Figure 4.4). Ado eluted at a similar retention time as peak 3 and yielded ions of *m/z* 136 and *m/z* 268, with a fragmentation pattern identical to the ones observed for the same parental ions in the sample (Figure 4.4a). Accordingly, Guo retention time and fragment spectrum matched those of peak 4 (Figure 4.4b). Additionally, as measurements of U.V. absorbance were always taken by the in-line diode array detector in the HPLC system, the U.V. absorbance spectra of peaks 3 and 4 from hBD-challenged culture supernatants could be compared to the U.V. absorbance spectra of the pure nucleosides, also confirming the identity of the compounds (Figure 4.5).

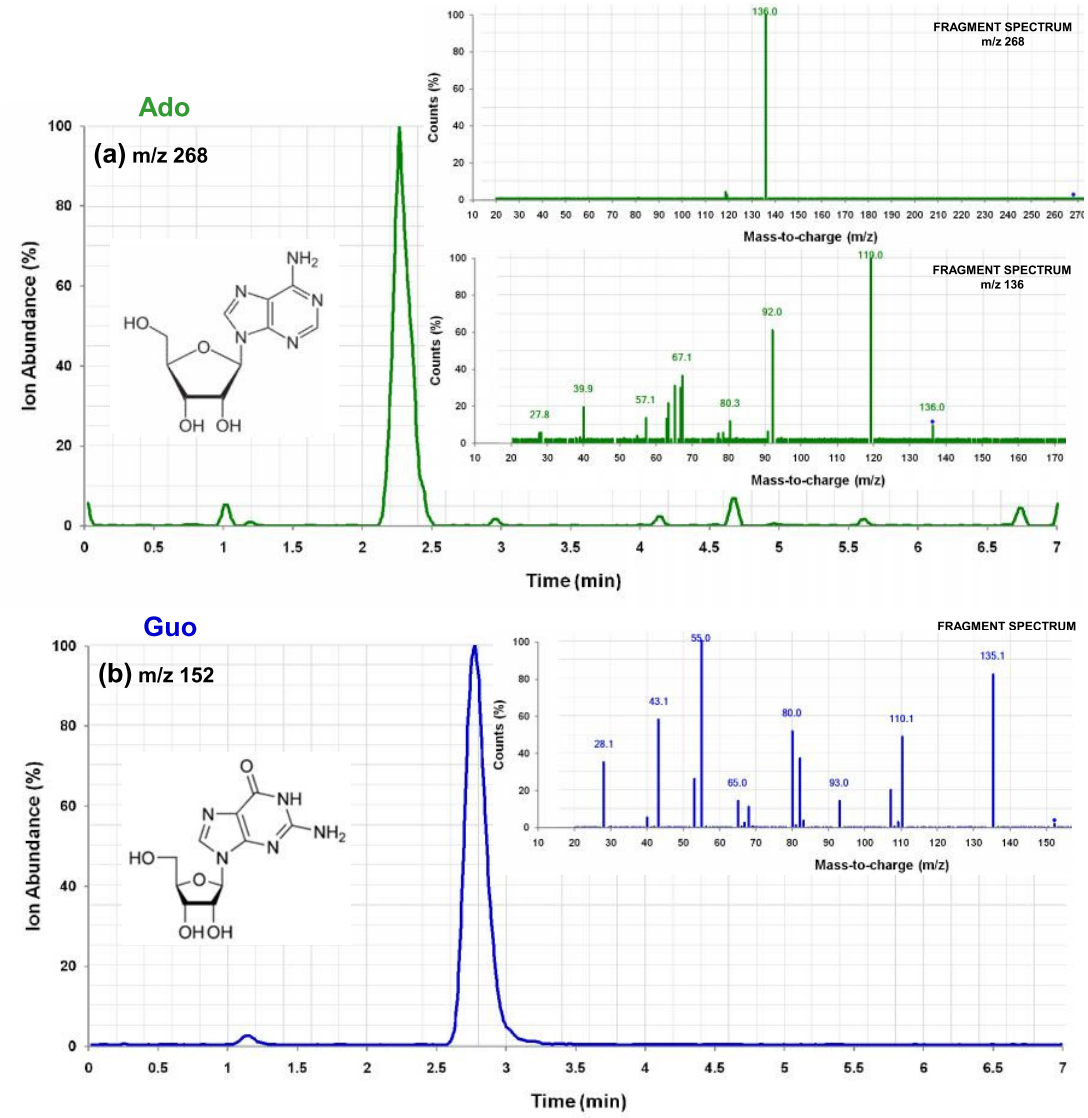

Figure 4.4 - HPLC-MS/MS analysis (product ion base peak chromatogram) of commercial nucleosides (a) adenosine (Ado; target ion *m/z* 268) and (b) guanosine (Guo; target ion *m/z* 152). Solutions (5 µL, 1 $mg \cdot mL^{-1}$) were injected in reversed-phase chromatography and analyzed by MS/MS product ion scan mode as described in Materials and Methods section 3.3.1. Insets show representative fragment spectra (C.E. 50 V) of the targeted parent ions. Additional fragment spectrum for ion of *m/z* 136 from Ado is also shown. The chemical structure of each compound is depicted.

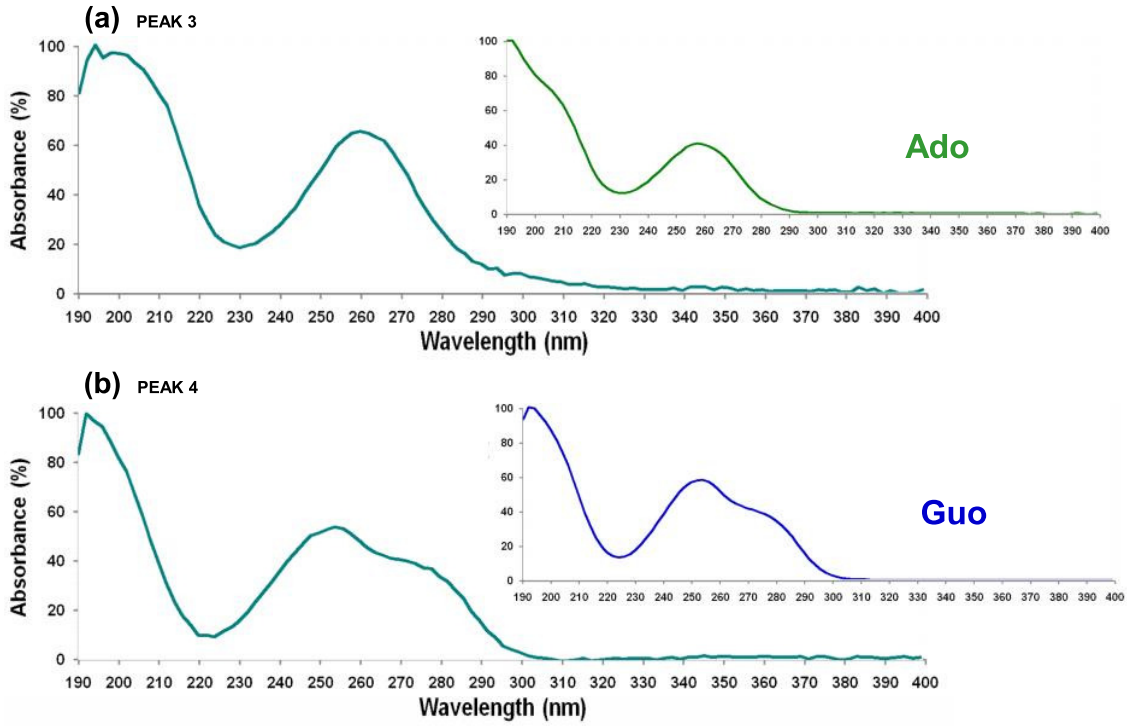

Figure 4.5 - U.V. absorbance spectra of peaks found in HPLC-MS analysis of supernatants from hBD-challenged *E. coli* (DSM1116) culture (Figure 3.2) numbered as peak 3 (a) and 4 (b), measured by the in-line diode array detector in the HPLC system, as described in Materials and Methods section 3.3.1. Insets show the U.V. spectra of the purine nucleosides adenosine (Ado) and guanosine (Guo) used to confirm compounds identity.

As mentioned above, the presence of more polar compounds with the same *m/z* values and the same fragmentation pattern as the identified nucleosides indicated the nucleobases adenine and guanine were also present in the studied supernatant. This hypothesis was further investigated by analyzing the chromatogram showing absorbance at 260 nm (Figure 4.6a). Besides the expected peaks at retention times corresponding to Ado and Guo (2 min and 2.5 min, as detection at DAD occurs a few seconds earlier than the ion detection at the MS), the analysis confirmed the presence of at least two additional compounds absorbing U.V. light at this wavelength in the hBD-challenged culture supernatants (hBD, green line), which were not present in the unchallenged supernatants (Ctrl, black line).

The identity of the first peak at retention time 1 min, which was already shown to contain the ions of *m/z* 136 and *m/z* 152 (Figure 4.3), was confirmed by comparative analysis of pure solutions of adenine (A) and guanine (G), showing matching retention times (Figure 4.6b and c). Accordingly, the fragment spectra generated from the target ions of *m/z* 136 for adenine and *m/z* 152 for guanine (Figure 4.6b and c insets) were equivalent to the fragment spectra of the corresponding nucleosides (Figure 4.6), as well as to the fragment spectra of the two peaks found for each target ion in the supernatant sample (Figure 4.3). Together, these results indicated that the product ions of the nucleosides derive from their nitrogen bases, and that both purine nucleosides and bases were present in the hBD-challenged culture supernatants.

In an attempt to determine if the 260 nm absorbance peak at 1.4 min (Figure 4.6a) corresponded as well to a nucleoside or a nucleobase, a directed search was performed in the MS scan data of both culture supernatants. The molecular ions of uridine (*m/z* 245), cytidine (*m/z* 244), deoxyadenosine (*m/z* 252), thymidine (*m/z* 243), deoxycytidine (*m/z* 228) and thymine (*m/z* 127) were either not present or detected at very low counts equally in both samples. In turn, the pyrimidines uracil (*m/z* 113) and cytosine (*m/z* 112) were found exclusively in the hBD-challenged culture supernatants(data not shown), however, the very low ion abundance and lack of correspondence of the retention times indicated they were not contained in the 1.4 min peak and prevented further analysis.

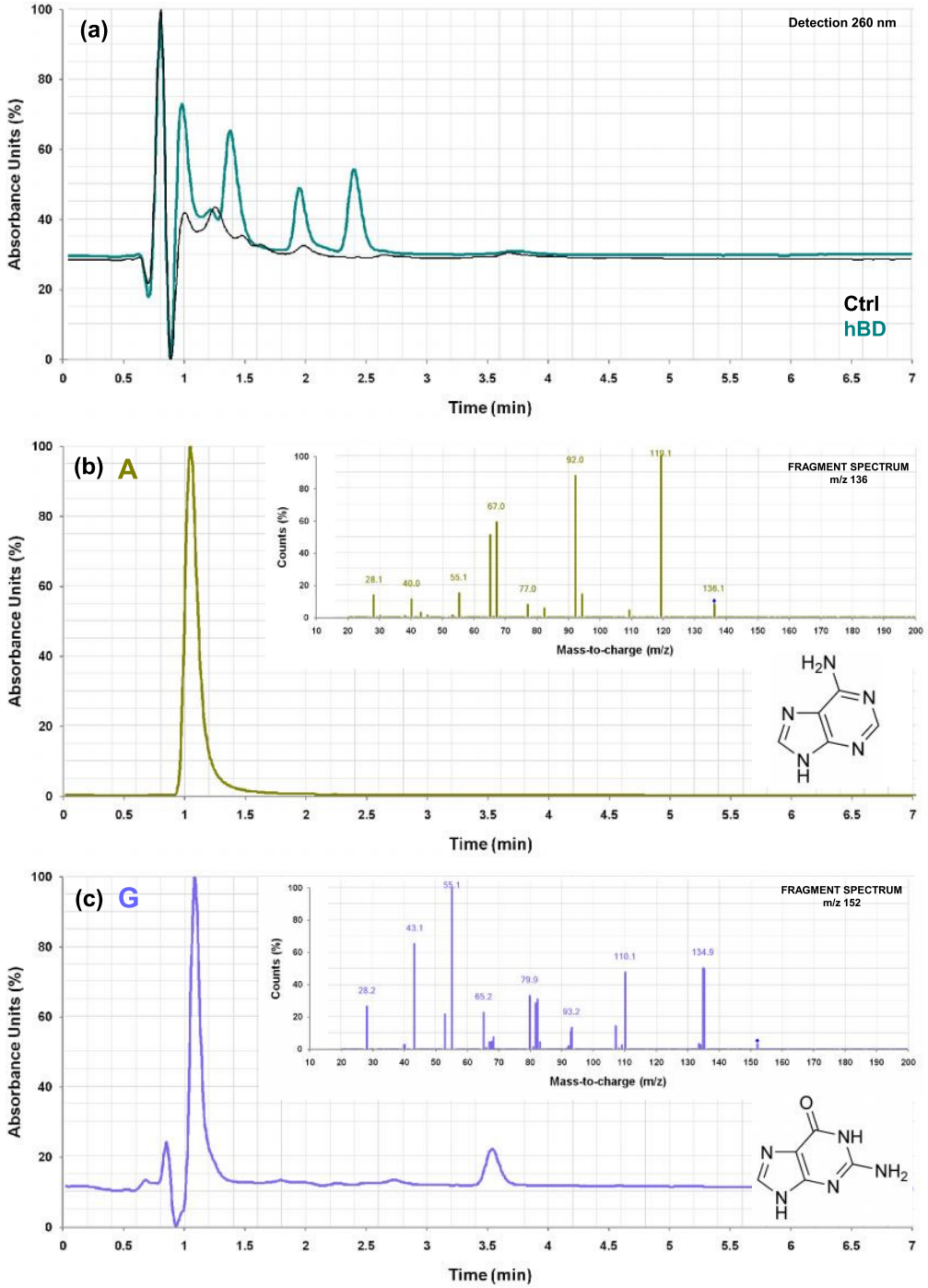

Figure 4.6 - HPLC chromatograms of absorbance at 260 nm of: (a) supernatants from *E. coli* (DSM1116) unchallenged cultures (Ctrl; black line) or challenged with hBD-2 50 $\mu g \cdot mL^{-1}$ (hBD, green line); (b) adenine or (c) guanine solution, 1 $mg \cdot mL^{-1}$. Challenge was performed as described in Materials and Methods section 3.4.2 and supernatants were collected 2 h after hBD-2 addition. Samples (5 µL) were injected in reversed-phase chromatography and analyzed as described in Materials and Methods section 3.3.1. Insets in b and c show the fragment spectra (C.E. 50 V) of adenine and guanine, respectively. Chemical structure of each compound is depicted.

4.1.2. Quantitative characterization of the extracellular metabolites from E. coli *after hBD-2 challenge*

After identification of the purine nucleosides Ado and Guo and their corresponding nitrogen bases (A and G) as major compounds present in culture supernatants of *E. coli* cultures challenged with hBD-2, but not in the supernatants of unchallenged cultures, quantitative analyses of these four compounds were performed. Concentration of the compounds in the sample was determined by HPLC-MS/MS in the multiple reaction monitoring (MRM) mode, as described in Materials and Methods section 3.3.1, using the commercially available compounds to generate the standard curves. The MRM transitions used for each compound and the corresponding curves can be found in Supplementary Material section 7.1. In these analyses, to focus the investigation on the response generated specifically after defensin stress, the concentrations found in hBD-challenged culture supernatants were corrected by subtracting the lower concentrations occasionally detected in the corresponding unchallenged control. This was typically performed for the quantitative HPLC-MS/MS results described in the following sections, except in the cases where the values for the unchallenged control is also presented.

E. coli cultures were grown using the same experimental setup described for the first experiment (section 4.1.1), except that the hBD-2 concentration used in the challenge was 20 $\mu g \cdot mL^{-1}$. This concentration was also able to impair bacterial growth and resulted as well in the presence of the same extracellular compounds identified. The supernatants from both cultures were again collected 2 h after the challenge and the concentrations determined for A, Ado, G and Guo. As shown in Figure 4.7 the compounds were present at low μM range. The nucleosides were more abundant than the bases, and Ado was present at a higher concentration than Guo.

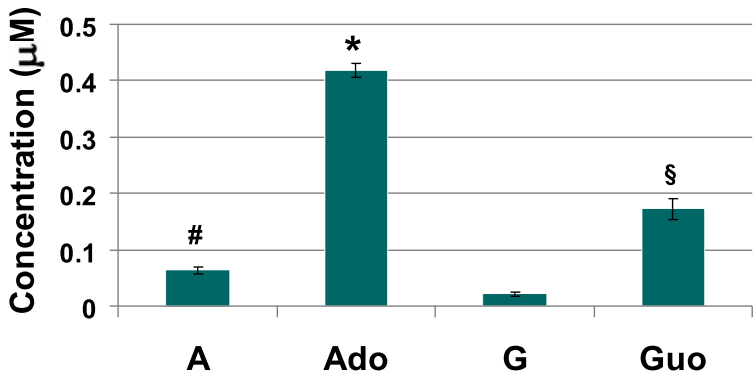

Figure 4.7 - Concentration of adenine (A), adenosine (Ado), guanine (G) and guanosine (Guo) present in supernatants from *E. coli* (DSM1116) cultures after challenged with hBD-2 (20 $\mu g \cdot mL^{-1}$) at O.D. 0.1 as described in Materials and Methods section 3.4.2. Supernatants were collected 2 h after the challenge and analyzed by HPLC-MS/MS in the MRM mode as described in Materials and Methods section 3.3.1. A symbol (*, # or §) indicates significant differences ($p<0.001$) from the lowest value, and different symbols indicate significant difference ($p<0.001$) between compounds in pairwise ANOVA as described in Materials and Methods section 3.6.

The extracellular response, in terms of concentration of the four purine compounds in the challenged culture supernatant, was then characterized as a function of hBD-2 dose (Figure 4.8) and of time after challenge (Figure 4.9). The dose-curve was performed in the range of 2.5 $\mu g \cdot mL^{-1}$ to 100 $\mu g \cdot mL^{-1}$. Figure 4.8a shows an interesting pattern of dose-response, where each of the four compounds presented a different behavior. In all of the cases, the concentrations varied with defensin dose and an accentuated increase was first detected at 20 $\mu g \cdot mL^{-1}$. Whereas for the bases (A and G) the level of response was mantained low throughout the higher defensin doses, the concentration of nucleosides increased in a dose-dependent manner. Confirming the first quantification data, Ado tended to be more abundant than Guo at the intermediate dose (20 $\mu g \cdot mL^{-1}$). It was interesting to note, by analyzing the growth curves at each tested hBD-2 dose (Figure 4.8b) that the lower defensin doses of 2.5 and 5 $\mu g \cdot mL^{-1}$, which caused only a transient inhibition of *E. coli* growth, were not able to induce significant increases in extracellular concentration of the compounds. However, comparing the doses from 10 to 100 $\mu g \cdot mL^{-1}$, the concentration of nucleosides still increased with hBD-2 dose, even though an equivalent effect on bacterial growth was seen at this dose range.

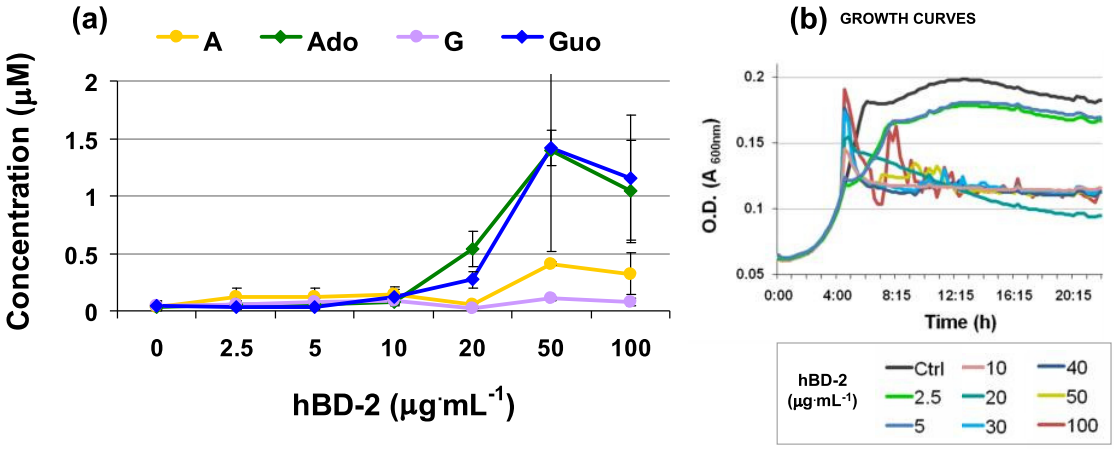

Figure 4.8 - Effect of increasing hBD-2 doses on *E. coli*. (a) Extracellular concentration of adenine (yellow line), adenosine (green line), guanine (purple line) and guanosine (blue line) after challenge with hBD-2 (0, 2.5, 5, 10, 20, 30, 40, 50 or 100 $\mu g \cdot mL^{-1}$). *E. coli* (DSM1116) was challenged at O.D. 0.1, as described in Materials and Methods section 3.4.2. The supernatants were collected 2 h after challenge for quantitative analysis by HPLC-MS/MS in the MRM mode as described in Materials and Methods section 3.3.1. Mean ± SD for three to five replicates from two independent experiments. (b) Representative growth curves of *E coli* cultures unchallenged (Ctrl) or challenged with increasing doses of hBD-2.

The variation in the extracellular response over time after hBD-2 challenge also demonstrated clear differences among the four purine compounds analyzed (Figure 4.9). The bases presented both a similar trend, being present at constant lower concentrations from 6 up to 48 h. The concentration of nucleosides in turn, increased more rapidly in the first 2 h. Interestingly, the differences between Ado and Guo are greatly accentuated after 24 and 48 h: the concentration of Guo approached those found in the unchallenged cultures (which reached 0.14 and 0.45 µM at 24 and 48 h respectively), whereas the concentration of Ado significantly increased exclusively in the hBD-2 challenged culture.

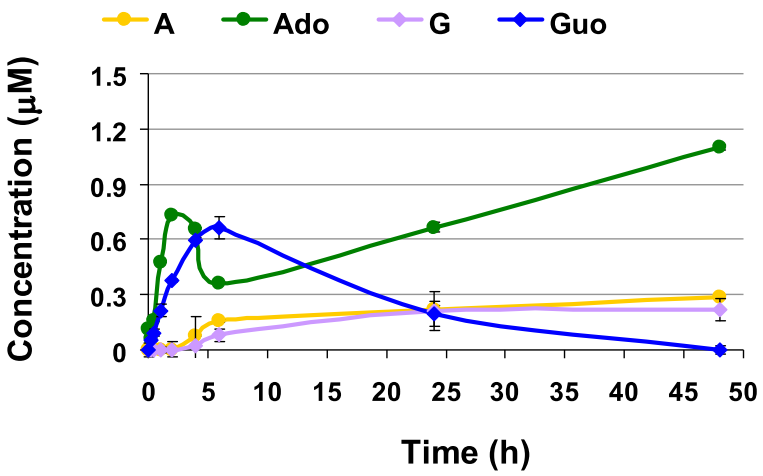

Figure 4.9 - Variation in the extracellular concentration of adenine (yellow line), adenosine (green line), guanine (purple line) and guanosine (blue line) over time after challenge with hBD (20 $\mu g \cdot mL^{-1}$). *E. coli*(DSM1116) was challenged as described in Materials and Methods section 3.4.2. The supernatants were collected at different time-points for quantitative analysis by HPLC-MS/MS in the MRM mode as described in Materials and Methods section 3.3.1. Data are representative from three independent experiments. Mean ± SD of three replicates.

4.1.3. Investigation of cell viability and metabolic activity of hBD-2 challenged E.coli *cultures and the influence of cell density on the extracellular response*

The results obtained by quantitative analysis of the extracellular metabolites present in *E. coli* cultures after hBD-2 challenge indicated they were a result of independent processes, as the variation on the detected concentrations was not uniform for the four compounds. Interestingly, as mentioned, the dose-dependence of the response appeared to be not directly correlated to the effect on bacterial growth. Additionally, and particularly in the case of Ado, the concentration continuously increased up to 48 h after the challenge, even when the O.D. of the cultures was unchanged. This led to the question whether these cultures were still viable or metabolically active. Different approaches were employed, including re-inoculation in liquid medium, CFU counts in agar plates, evaluation of membrane integrity by fluorescent staining, and quantification of ATP and reducing potential of the cultures.

As a first attempt, cells challenged with hBD-2 20 $\mu g \cdot mL^{-1}$ were separated from the culture medium after 2 h and resuspended in the same volume of fresh M4 or LB media, free of hBD. No growth was observed after incubation at 37 °C for 24 h, as the O.D. of the cell

suspensions did not change. Accordingly, the hBD-challenged cultures were unable to grow further either in M4- or in LB- agar plates. No colony was formed on the plates inoculated 2 h after the challenge, irrespective of the dilution factor used. In contrast, the mean CFU value of the unchallenged *E. coli* cultures at late logarithmic phase (same time point) was $125x10^6$ $CFU \cdot mL^{-1}$, with a standard deviation of ± $31x10^6$ $CFU \cdot mL^{-1}$ in 4 determinations from two independent cultures on M4-agar plates.

The level of membrane damage, expected from the known membrane-targeted mechanism of action by hBD was assessed by fluorescence microscopy (Figure 4.10). Bacteria were harvested 2 h after challenge with hBD-2 (5 or 50 $\mu g \cdot mL^{-1}$) or at normal logarithmic growth in unchallenged cultures, and stained with the Live/Dead BacLight kit as described in Materials and Methods section 3.4.5. The results showed that, in comparison to the unchallenged control (Ctrl; Figure 4.10a), hBD-2 at a low dose (5 $\mu g \cdot mL^{-1}$) caused the occurrence of membrane compromised cells (stained red by PI), although cells with intact membrane (stained green by permeant Syto9) still represented a great proportion of the culture (Figure 4.10b). However, at 50 $\mu g \cdot mL^{-1}$, all cells presented membrane damage (Figure 4.10c).

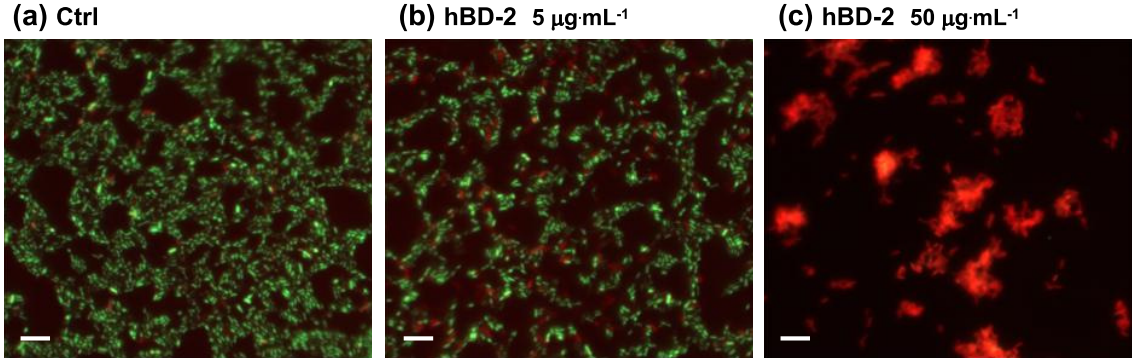

Figure 4.10 - Fluorescence microscopy showing membrane integrity of *E. coli* (DSM1116) cultures unchallenged (a; Ctrl) or challenged with hBD-2 at 5 $\mu g \cdot mL^{-1}$ (b) or 50 $\mu g \cdot mL^{-1}$ (c). Cultures were challenged as described in Materials and Methods section 3.4.2. Cells were harvested 2 h after challenge, stained with the Live/Dead BacLight kit as described in Materials and Methods section 3.4.5 and analyzed using Axio Imager A1 epifluorescence microscope with filters for excitation/emission of 480/500 nm and 490/635 nm. Representative overlaid images are shown. Bars represent 10 µm.

In an alternative approach, flow cytometry was applied to determine the level of membrane damage caused by hBD-2 challenge on *E. coli* using the same principle of fluorescence staining as described in Materials and Methods section 3.4.5. In this case, the ratio between the fluorescence of the permeant dye (TO, detected in channel FL1) and of the non-permeable dye (PI, detected in channel FL3) was used to compare the hBD-2 challenged culture to the normally growing unchallenged culture and to a culture lysed by a standard bacterial-cell disruption protocol (lysozyme 10 $mg \cdot mL^{-1}$ in TE buffer with Triton X-100 1.2 %). The dot-plots generated (Figure 4.11) show the cellular events counted in the gates defined for intact cells (R2, high FL1, low FL3) and for membrane damaged cells (R4, low FL1, high FL3). In the unchallenged control (Ctrl, Figure 4.11a) the majority of cells were detected in R2. In contrast, challenge with hBD-2 (50 $\mu g \cdot mL^{-1}$) caused the cells to shift from R2 to R4 (Figure 4.11b), similar to the effect caused by the lysis protocol (Figure 4.11c). It is interesting to note, however, that although the high PI staining (high FL3/FL1 ratio) confirmed that the hBD-2 challenged cells presented damaged membranes, the dot-plot differs somewhat from the cells disrupted by the standard lysis protocol, a result that could not be explained within this experiment, but possibly indicated a difference in the process of membrane permeabilization. A quantitative analysis of the cellular events counted in each gate for the three conditions is presented in Table 4.1.

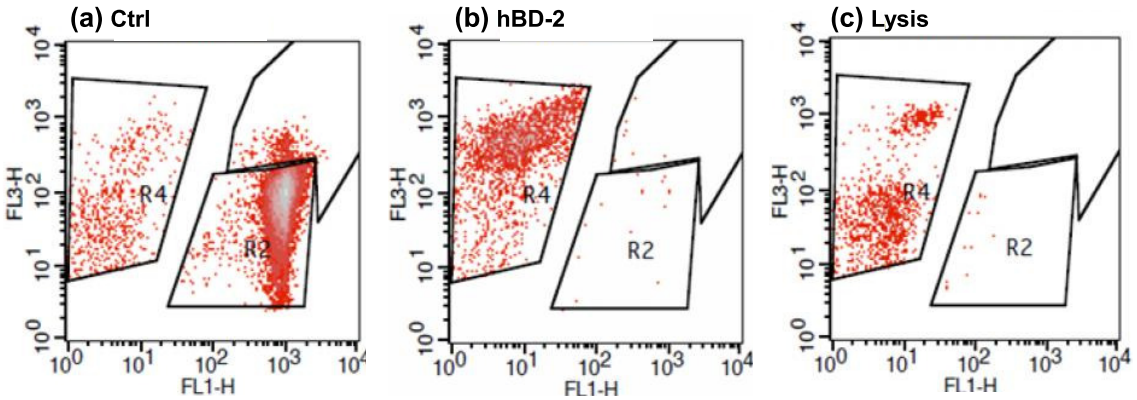

Figure 4.11 - Flow cytometry dot-plots showing membrane integrity of *E. coli* (DSM1116) cultures (a) unchallenged (Ctrl); (b) after challenged with 20 $\mu g \cdot mL^{-1}$ hBD-2; or (c) after lysis by treatment with lysozyme/Triton. Cultures were challenged at as described in Materials and Methods section 3.4.2. Cells were harvested 2 h after challenge, stained with BD Cell Viability kit as described in Materials and Methods section 3.4.5 and analyzed in BD FACSCalibur at low flow mode (12 $\mu L \cdot min^{-1}$).

Table 4.1 - Relative quantification of intact and membrane-damaged cells in *E. coli* cultures unchallenged (Ctrl), challenged with hBD-2 or submitted to lysis by lysozyme/Triton and analyzed by fluorescence staining and flow cytometry (Figure 4.11)

	EVENTS·mL^{-1}				
	Total (100%)	R2		R4	
Ctrl	*11195000*	*10260833*	***(91.6%)***	*-492083*	
hBD-2	*1726250*	*-339583*		*1706666*	***(98.8%)***
Lysis	*956667*	*-35833*		*947500*	***(99%)***

Both fluorescence-based techniques indicated that hBD-2 caused membrane breach already at a dose of 50 μg·mL^{-1}, in accordance to the growth arrest effect observed. However, as demonstrated by the dose-response curve, it did not result in a stabilization of the extracellular nucleosides concentration detected at higher hBD-2 doses. Therefore, the next experiments aimed to verify if those membrane-compromised cells were still metabolically active. A luminescence-based assay was employed, which estimates the metabolic activity by the amount of ATP in the whole cultures. Also, a colorimetric assay was performed, which was based in the conversion of a blue dye (DCIP) to its colorless reduced form. In both cases, it was clear that hBD-2 challenge (20 μg·mL^{-1}) caused significant inhibition of the bacterial metabolism. When ATP was assessed, the effect was immediate, but appears to be complete only after the first hour of exposition (Figure 4.12). Accordingly, the reduction of DCIP by challenged cultures was completely abolished, but only 2 h after the addition of hBD-2, and the metabolic activity seems to be even enhanced within the first hour (Figure 4.13).

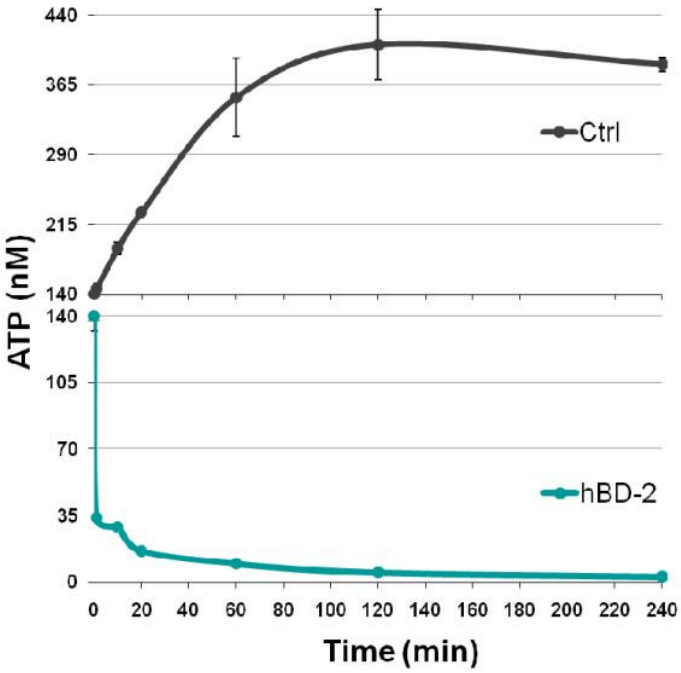

Figure 4.12 - Metabolic activity measured by the quantification of ATP in *E. coli* (DSM1116) cultures after challenged with hBD-2 20 $\mu g \cdot mL^{-1}$ (green line) or by unchallenged cultures (Ctrl; black line). Cultures (75 µL) were analyzed at different time-points after challenge (performed as described in Materials and Methods section 3.4.2), using BacTiter-Glo kit as described in Materials and Methods section 3.4.4. Mean ± SD of four determinations from two independent cultures.

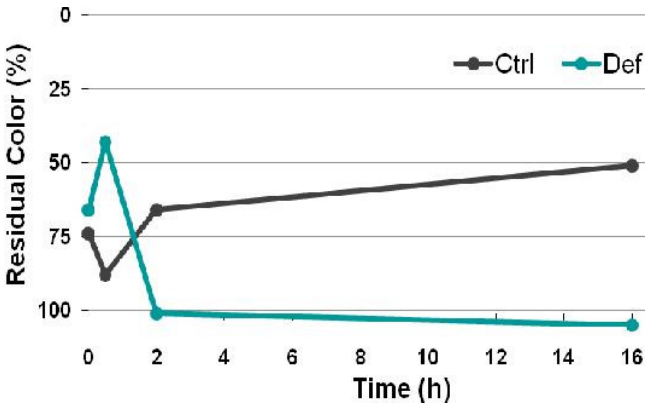

Figure 4.13 - Metabolic activity measured by the reduction of DCIP by *E. coli* (DSM1116) cultures after challenged with hBD-2 20 $\mu g \cdot mL^{-1}$ (green line) or by unchallenged cultures (Ctrl; black line). Cultures (75 µL) were analyzed at different time-points after challenge (performed as described in Materials and Methods section 3.4.2) by addition of DCIP (40 µM final concentration) and determination of the residual blue color by absorbance readings at 600 nm as described in Materials and Methods section 3.4.4.

The effect of sequential hBD-2 challenges on the same culture was also investigated. These results could verify whether the challenged cultures would be responsive to a second pulse of hBD-2. This was tested by two different experiments. In one case, the cultures received one dose of hBD-2 (20 $\mu g \cdot mL^{-1}$) at 4 h, and 1 h later a second cumulative dose (20 $\mu g \cdot mL^{-1}$) was either applied or not. Supernatants were collected as usually 2 h after the first challenge and the concentration of extracellular metabolites were compared (Figure 4.14a). In the other experiment, cultures that were either unchallenged or challenged at 4 h with hBD-2 (20 $\mu g \cdot mL^{-1}$) were harvested after 2 h, reacclimated in fresh, defensin-free M4 medium, and 1 h later received a second hBD-2 dose (20 $\mu g \cdot mL^{-1}$). In this case, the supernatants were collected after 18 h for quantification of the metabolites (Figure 4.14b). In both experiments, it was clear that once affected by a first hBD pulse, the cultures were no longer responsive. The concentrations of extracellular nucleosides were identical when applying either one (D) or two times (D+D) 20 $\mu g \cdot mL^{-1}$ hBD-2 (Figure 4.14a). When cultures were transferred to a fresh medium before the second hBD dose, no metabolites were detected in the supernatants of previously challenged cultures (defensin/defensin or D/D), in contrast to what happened to the cultures that did not receive the first hBD pulse (control/defensin or C/D) (Figure 4.14b).

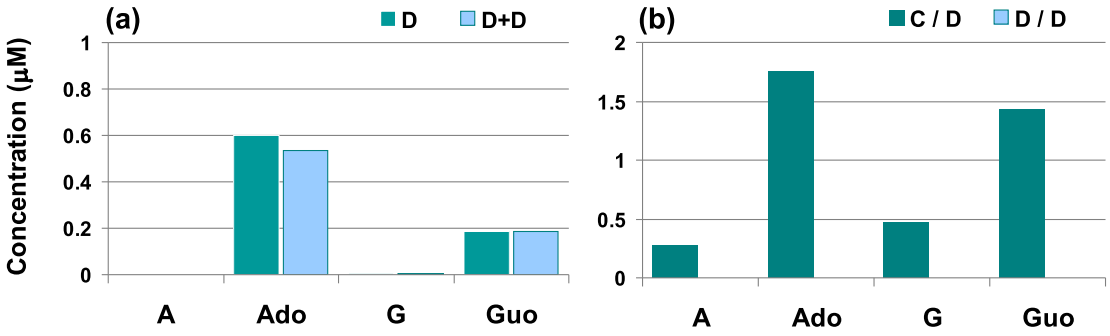

Figure 4.14 - Effect of a second hBD-2 pulse on previously challenged *E. coli* (DSM1116) cultures. (a) Extracellular concentration of adenine (A), adenosine (Ado), guanine (G) and guanosine (Guo) after one or two cumulative doses (D or D+D, respectively) of hBD-2 (20 $\mu g \cdot mL^{-1}$) applied with 1 h interval, the first applied at O.D. 0.1. Supernatants were collected 2 h after the first pulse for quantitative analysis by HPLC-MS/MS in the MRM mode as described in Materials and Methods section 3.3.1. (b) Extracellular concentration of adenine (A), adenosine (Ado), guanine (G) and guanosine (Guo) after hBD-2 challenge (20 $\mu g \cdot mL^{-1}$) applied to unchallenged cultures (control/defensin or C/D) or to cultures previously challenged with hBD-2 (20 $\mu g \cdot mL^{-1}$, defensin/defensin or D/D). Two hours after the first dose was applied (at O.D. 0.1), the cells were transferred to fresh M4 medium and incubated for 1 h before the second challenge. Supernatants were collected 21 h after the first pulse for quantitative analysis by HPLC-MS/MS in the MRMmode.

To further understand how the presence of extracellular purine compounds was related to the effect of hBD-2 on bacterial metabolism and growth, *E. coli* cultures were challenged with hBD-2 (20 $\mu g \cdot mL^{-1}$) at different points of their growth curves, meaning that cultures at increasing cell densities (O.D.) were challenged with the same dose of hBD-2. Figure 4.15a shows the concentration of extracellular A, Ado, G and Guo as a function of the cell density at the challenge point, whereas Figure 4.15b shows the representative growth curves of cultures inoculated at increasing initial O.D. and challenged at 4 h. The O.D. of each culture at this point is indicated in the inset boxes and corresponds to the category axis in panel (a). CFU counts of each culture were performed 2 h after the challenge and are presented in Table 4.2. The results demonstrated that the concentration of extracellular metabolites was proportional to the number of cells in the early and mid-logarithmic phase, when the given dose of hBD was still able to completely arrest bacterial growth (the first three cultures, challenged at O.D. 0.075, 0.092 and 0.13). When the cultures were challenged at late-exponential growth (O.D. 0.16), being able to partially recover, the extracellular concentration of A, G and Guo was reduced, whereas the concentration of Ado was the highest, highlighting again the differences in the response of this particular compound. In the last case, where the cultures were challenged at the beginning of the stationary phase (O.D. 0.22) and the effect of hBD in growth was mild, the concentration of Ado found in the supernatants was not optimal, but still significantly higher than the other purine compounds. Interestingly, challenging the stationary-phase cultures with increasing doses of hBD demonstrated that also in this case, the presence of extracellular nucleosides was proportional to the dose, and that the differences between Ado and Guo were greater when the culture was able to recover from challenge (Figure 4.16).

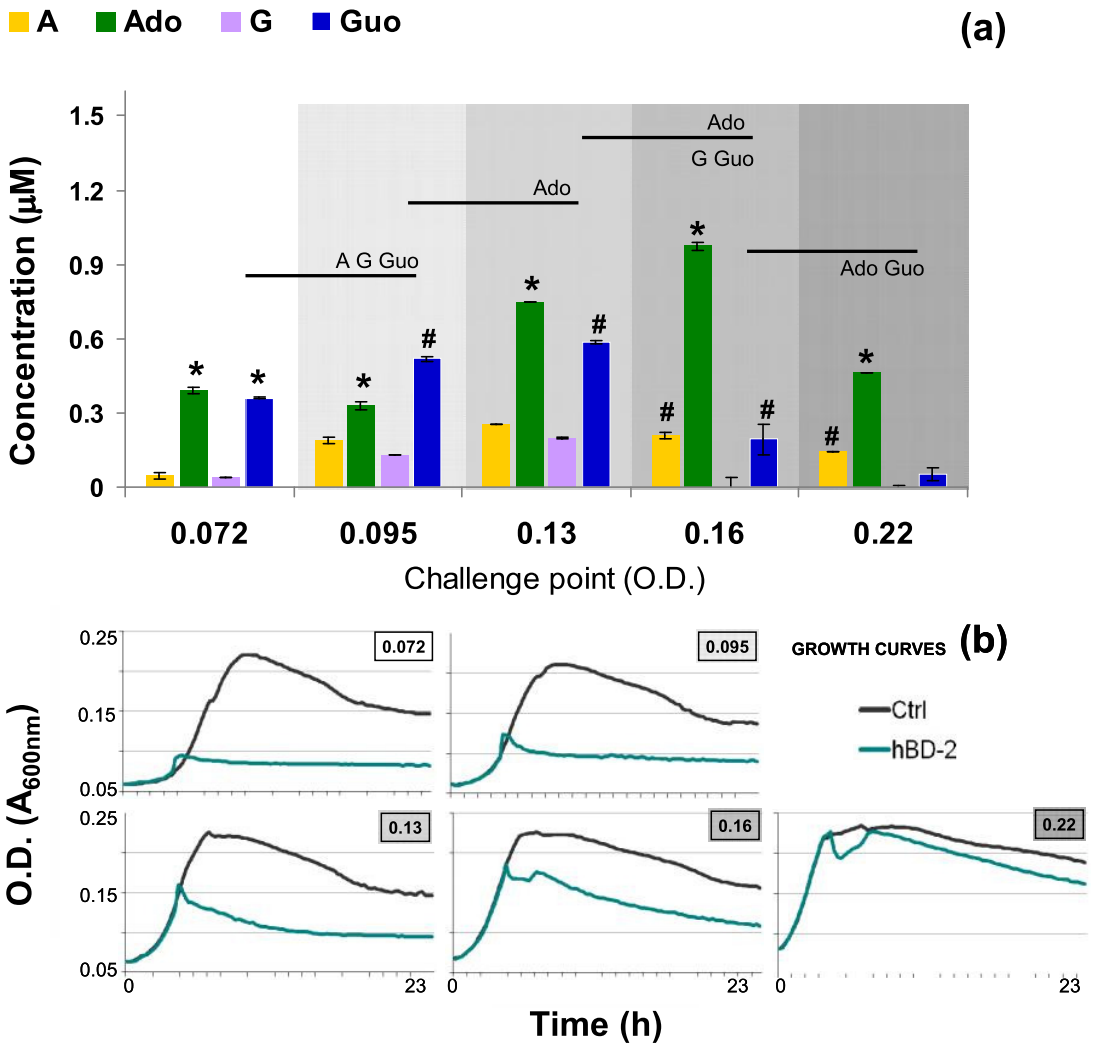

Figure 4.15 - Effect of hBD-2 on *E. coli* (DSM1116) cultures at different cell densities. (a) Concentration of extracellular adenine (yellow bars), adenosine (green bars), guanine (purple bars) and guanosine (blue bars) in cultures challenged at different O.D. values.; (b) representative growth curves for each culture, inoculated with increasing cell densities (O.D. 0.001, 0.002, 0.005, 0.01 and 0.02) at time 0 and challenged (green lines) or not (Ctrl, black lines) at 4 h with 20 $\mu g \cdot mL^{-1}$ hBD-2. Boxed numbers indicate the O.D. at challenge point. Supernatants were collected 2 h after challenge for quantitative analysis by HPLC-MS/MS in the MRM mode as described in Materials and Methods section 3.3.1. Results in (a) represent the mean ± SD of three replicates. Within each category (O.D.), a symbol (* or #) indicates significant differences ($p<0.001$) from the lowest value, and different symbols indicate significant differences ($p<0.001$) between compounds in pairwise ANOVA as described in Materials and Methods section 3.6. Between adjacent categories, black lines indicate significant differences ($p<0.001$), when the concentration of a given compound is higher (indicated above the line) or lower (indicated below the line) than in the preceding category in pairwise ANOVA.

Table 4.2 - Viability of *E. coli* cultures of increasing cell densities, as determined by CFU counts in M4-agar plates 2 h after challenged with hBD-2.

CFU ($x10^6 \cdot mL^{-1}$)	Challenge point (O.D.)				
	0.072	0.095	0.13	0.16	0.22
Ctrl	*23.5*	*40*	*100*	*140.5*	*180*
hBD-2	*0*	*0*	*0*	*32*	*54.7*

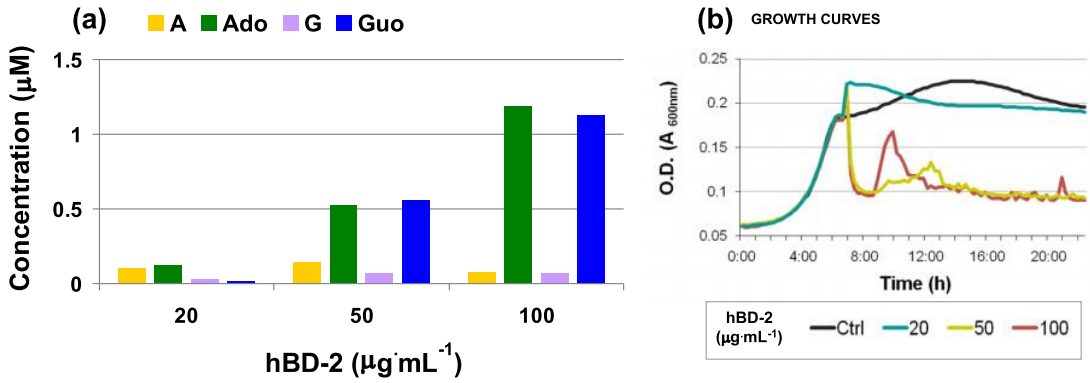

Figure 4.16 - Effect of increasing hBD-2 doses on *E. coli* (DSM1116) at stationary growth-phase. (a) Extracellular concentration of adenine (yellow bars), adenosine (green bars), guanine (purple bars) and guanosine (blue bars) after addition of hBD-2 (20, 50 or 100 $\mu g \cdot mL^{-1}$). (b) Representative growth curves of *E. coli* cultures unchallenged (Ctrl) or challenged with increasing doses of hBD-2 at 6 h. The supernatants were collected 2 h after the challenge for quantitative analysis by HPLC-MS/MS in the MRM mode as described in Materials and Methods section 3.3.1.

4.1.4. Comparison of extracellular response to different antimicrobial peptides and the effect of hBD-2 on different E. coli *strains or other Gram-negative bacteria.*

The presence of extracellular purine compounds induced by antimicrobial peptide challenge was investigated using different antimicrobial peptides to verify if the response was related to a specific class of peptide or to their specific structural features. The challenge experiment was performed with cultures at same O.D. (0.1) and using identical conditions and peptide dose (20 $\mu g \cdot mL^{-1}$), comparatively testing hBD-2, human β-defensin-3 (hBD-3), human α-defensin-5 (HD5), sheep myeloid antimicrobial peptide (SMAP) and magainin I.

Figure 4.17 shows the concentration of A, Ado, G and Guo in the culture supernatants 2 h after challenged with the different antimicrobial peptides, and the corresponding effect on *E. coli* growth is shown in the inset. While the growth-inhibition ability seemed to be similar among the peptides under these conditions, the concentration of purine compounds in the supernatants after the challenge showed remarkable differences. HBD-2 was the most efficient peptide to induce the extracellular response for all four compounds analyzed. The closely related β-sheet peptide hBD-3 also resulted predominantly in the presence of Ado in the supernatants, although at lower concentrations than induced by hBD-2. However, this response seems not to be exclusive for β-sheet peptides, as the α-helical sheep cathelicidin SMAP29 was also able to induce the presence of extracellular Ado. In contrast, the human defensin (HD5) as well as the frog defensin (magainin I) were unable to promote increased concentrations of extracellular Ado.

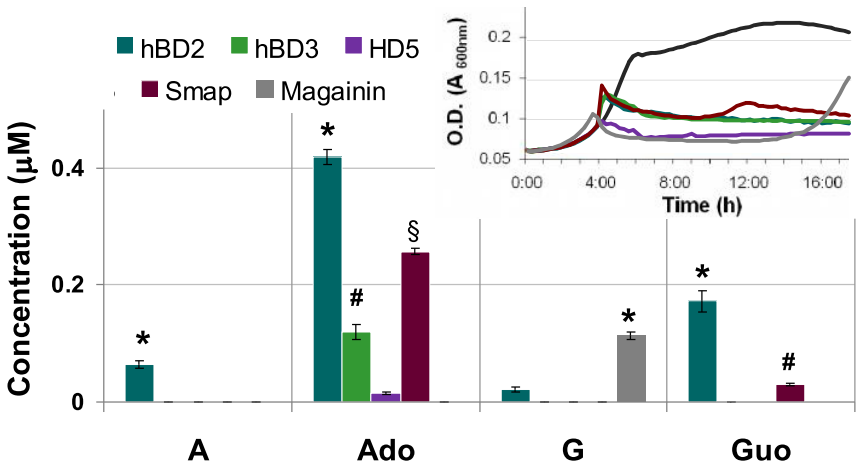

Figure 4.17 - Effect of different antimicrobial peptides on *E. coli* (DSM1116). Extracellular concentration of adenine (A), adenosine (Ado), guanine (G) and guanosine (Guo) after addition of 20 $\mu g \cdot mL^{-1}$ of: human β-defensin-2 (hBD-2, green), human β-defensin-3 (hBD-3, light-green), human α-defensin-5 (HD5, purple), sheep myeloid antimicrobial peptide 29 (SMAP, dark-red) or magainin I (grey). Inset shows the representative growth curves of *E. coli* cultures unchallenged (Ctrl, black line) or challenged at 4 h (O.D. 0.1) with different antimicrobial peptides (colors according to the bar-chart). The supernatants were collected 2 h after the challenge for quantitative analysis by HPLC-MS/MS in the MRM mode as described in Materials and Methods section 3.3.1. Mean ± SD of three replicates. Within each category (compound), a symbol (*, # or §) indicates significant differences ($p<0.001$) from the lowest value, and different symbols indicate significant differences ($p<0.001$) between peptides in pairwise ANOVA as described in Materials and Methods section 3.6.

Next, the effect of hBD-2 was tested on five different strains of *E. coli*, in comparison to the laboratory reference strain (DSM1116), including a probiotic strain (*E. coli* Nissle 1917, EcN), two clinical isolates from IBD patients (7145A and HZI 2-6) and one reference enteroinvasive strain (LF82). The experimental setup described in Materials and Methods section 3.4.2 was used for all strains. Cultures were inoculated at O.D. 0.005, except for *E. coli* Nissle 1917 (start O.D. 0.01), HZI 2-6 and LF82 (start O.D. 0.02), which presented delayed growth in M4 medium. The cultures were challenged with hBD-2 (20 $\mu g \cdot mL^{-1}$) at mid-exponential phase (O.D. 0.1). The results are presented in Figure 4.18, showing the extracellular concentration of the compounds on the left charts, and the corresponding effect on bacterial growth on the right panels. It is important to note that the strans were challenged with the same hBD dose and at the same O.D. The CFU counts 2 h after challenge (data not shown) yielded the same results for the five strains (absence of colonies, indicating none of them were able to grow further). Yet, remarkable differences were observed in the concentration of the four compounds found in the supernatants (Figure 4.18). The probiotic strain (EcN) and the laboratory reference (DSM1116) strain presented the highest extracellular Ado concentrations, whereas in the supernatants from the pathogenic strain LF82, the concentrations of the four compounds were much lower, and Ado was not predominant. Interestingly, from the two clinical isolates, 7145A was found to respond more similarly to the DSM1116 strain, while HZI 2-6 presented a lower response, comparable to LF82.

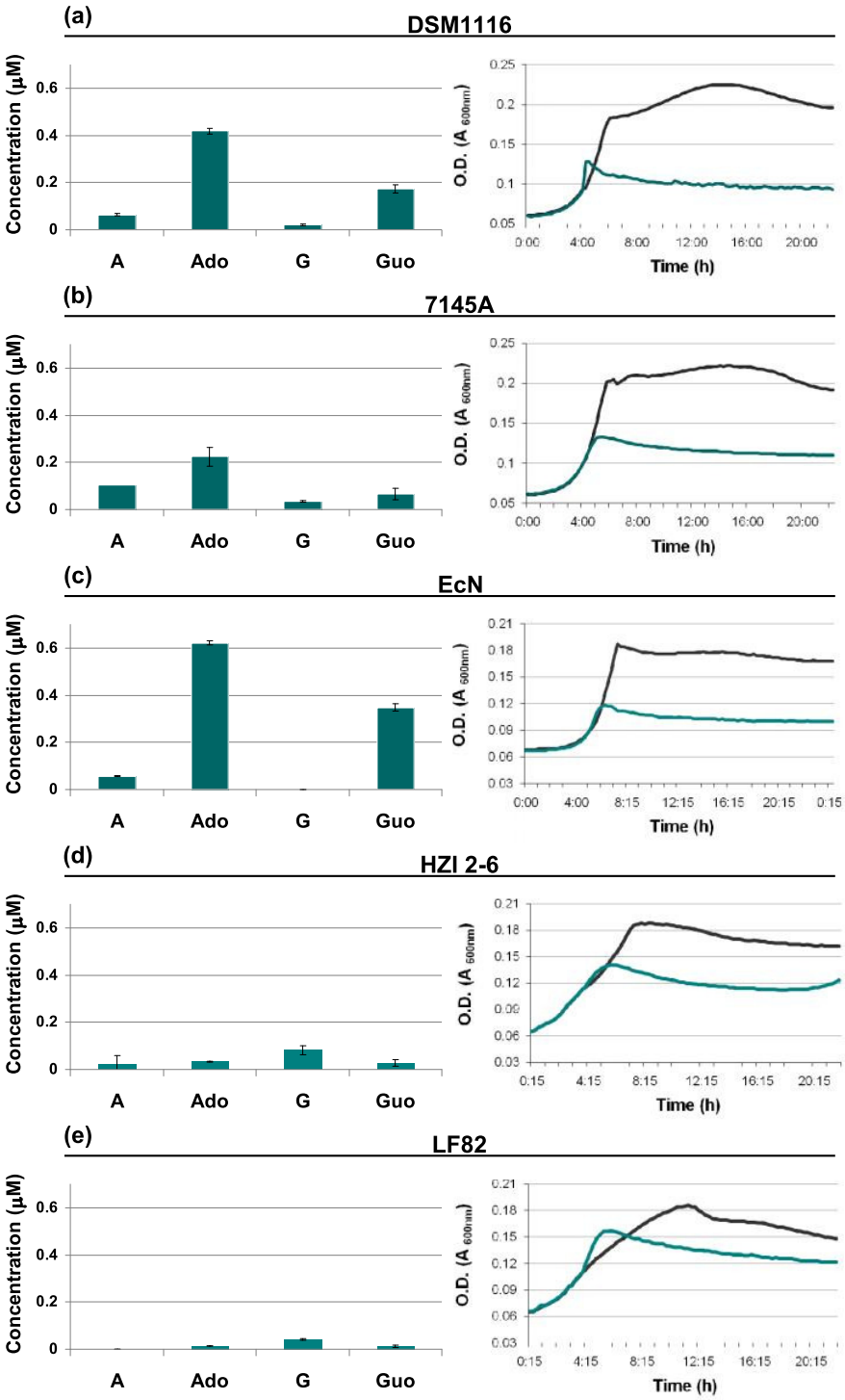

Figure 4.18 - Effect of hBD-2 on *E. coli* strains DSM1116 (a), 7145A (b), *E. coli* Nissle 1917 (EcN, c), HZI 2-6 (d) and LF82 (e). Extracellular concentration of adenine (A), adenosine (Ado), guanine (G) and guanosine (Guo) after challenge with hBD-2 (20 $\mu g \cdot mL^{-1}$). Strains were challenged at ~4 h (O.D. 0.1) and the supernatants were collected 2 h after challenge for quantitative analysis by HPLC-MS/MS in the MRM mode as described in Materials and Methods section 3.3.1. Mean ± SD for three replicates. Representative growth curves of *E coli* cultures unchallenged (Ctrl, black line) or challenged with hBD-2 (green line) are shown right.

As the results with *E. coli* strains showed, the extracellular response to hBD-2 challenge was not generally the same for different bacteria and thus it would be interesting to investigate whether other species could as well be induced to release purine compounds to the medium when facing hBD-2 challenge. Therefore, two Gram-negative species, *Klebsiella pneumoniae* and *Pseudomonas aeruginosa* were tested in the same experimental setup described for *E. coli*, except that the start inoculum for *P. aeruginosa* was adjusted to O.D. 0.01. The challenge point for both species was at O.D. 0.1 and two doses of hBD-2 were compared. Challenging *K. pneumoniae* cultures with 20 $\mu g \cdot mL^{-1}$ hBD-2 (Figure 4.19a, left) resulted in a transient effect in bacterial growth and a poor extracellular response compared to *E. coli* DSM1116. The concentration of the compounds was increased at a higher hBD-2 dose (100 $\mu g \cdot mL^{-1}$, Figure 4.19a, right), where the effect on growth was accentuated. However, the proportion of the four metabolites at this dose was similar as at the lower dose-challenge, different from what was observed in *E. coli*. Also, the concentrations of nucleosides Ado and Guo was much lower than detected in *E. coli* cultures after challenged with hBD-2 at the same dose (Figure 4.8). The effect of hBD-2 on *P. aeruginosa* growth (Figure 4.19b) showed that the response to hBD-challenge differed substantially from the response of *E. coli* and accordingly, none of the purine compounds were detected in the supernatants.

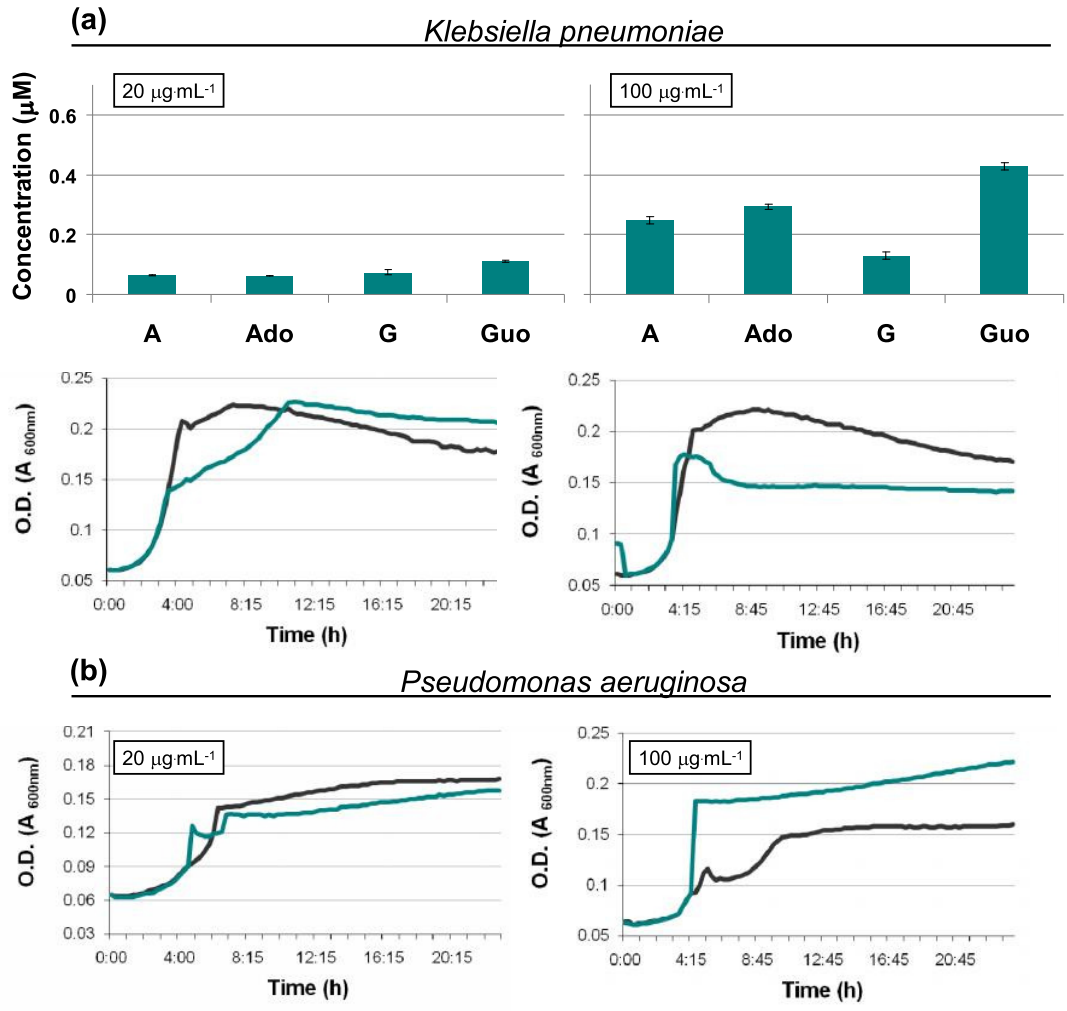

Figure 4.19 - (a) Effect of hBD-2 on *Klebsiella pneumoniae*. Extracellular concentration of adenine (A), adenosine (Ado), guanine (G) and guanosine (Guo) after challenge with hBD-2 20 $\mu g \cdot mL^{-1}$ (left) or 100 $\mu g \cdot mL^{-1}$ (right). Cultures were challenged at ~4 h (O.D. 0.1) and the supernatants were collected 2 h after challenge for quantitative analysis by HPLC-MS/MS in the MRM mode as described in Materials and Methods section 3.3.1. Mean ± SD for three replicates. Representative growth curves of unchallenged cultures (Ctrl, black line) or challenged with hBD-2 (green line) are shown below the corresponding bar chart. (b) Effect of hBD-2 on *Pseudomonas aeruginosa*. Cultures were challenged at ~4 h (O.D. 0.1) and the supernatants were collected 2 h after challenge for quantitative analysis by HPLC-MS/MS in the MRM mode. The target compounds were not detected. Representative growth curves are shown from unchallenged controls (black lines), or cultures challenged with hBD-2 20 $\mu g \cdot mL^{-1}$ (left) or 100 $\mu g \cdot mL^{-1}$ (right).

RESULTS II

4.2. Underlying mechanisms for the release of adenosine from defensin challenged *Escherichia coli*

4.2.1. Lysis hypothesis

With the aim of elucidating the mechanisms responsible for the presence of extracellular purine compounds, particularly adenosine in *E. coli* cultures challenged with hBD-2, the hypothesis that the extracellular response could be a consequence of peptide mediated cell-lysis was investigated. General lysis processes, as triggered by standard laboratory protocols for bacterial cell disruption (e. g. freeze-thaw cycles, enzymatic digestion in the presence of surfactants or mechanic disruption using a French-press) are known to cause the release of macromolecules from the cell into the culture medium. This effect was measured in *E. coli* cultures by determination of protein and DNA concentration in the supernatants of hBD-2 challenged cultures, in comparison to unchallenged controls or to supernatants from cultures submitted to freeze-thaw lysis (Figure 4.20). It was clearly observed that, as opposed to what happened in the lysed cultures, hBD-2 challenged cultures presented no increase in extracellular protein and DNA content, with results comparable to the unchallenged controls. It is important to note that, regarding the presence of extracellular Ado (as well as A, G and Guo), the cultures submitted standard lysis protocols did not produce any response (data not shown).

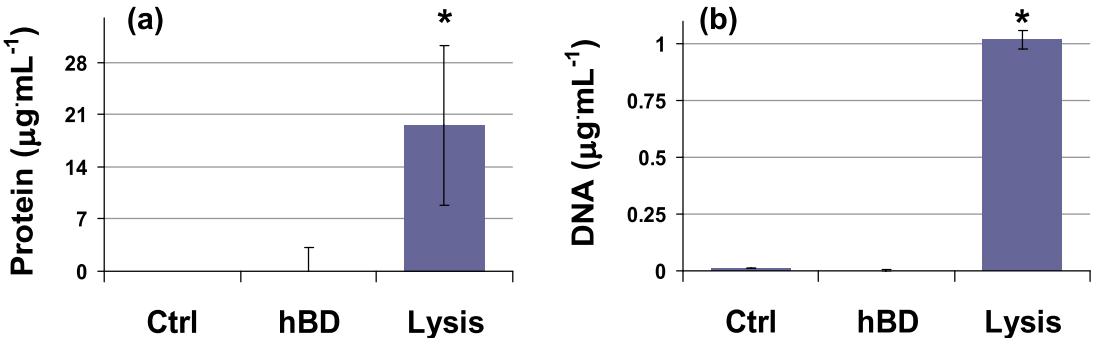

Figure 4.20 - Presence of proteins (a) and DNA (b) in the supernatants of *E. coli* (DSM1116) cultures unchallenged (Ctrl) or after challenged with hBD-2 (hBD, 20 $\mu g \cdot mL^{-1}$) or submitted to freeze-thaw cycles (Lysis). Cultures were challenged as described in Materials and Methods section 3.4.2 and the supernatants were collected 2 h after challenge. Protein concentration was determined by the bicinchoninic acid method and DNA concentration was determined by fluorescent detection using Quant-iT™ PicoGreen® Reagent as described in Materials and Methods section 3.4.6. Mean ± SD for four replicates from two independent cultures. * indicates significant differences ($p<0.001$) in pairwise ANOVA as described in Materials and Methods section 3.6.

Because the results with differential fluorescent staining (section 4.1.3) indicated the membrane of hBD-2 challenged cells were indeed damaged, but apparently, the presence of extracellular Ado could not be explained solely by general leakage of intracellular contents, transmission electron microscopy (TEM) was employed to visualize cellular structures in the bacteria after hBD-2 addition in comparison to normally growing cultures. The ratio of intact and membrane altered/disrupted cells was estimated by counting the events in 10 different sections (50-250 cells per section) for each condition. Representative images (Figure 4.21) show unchallenged *E. coli* cells grown in M4 medium (a-c) with intact membranes and cytoplasm organization. The electron-lucent DNA content could be discerned (arrow 1), as well as electron-dense cytoplasmic material, for instance ribosomes. The presence of small areas of plasmolysis (arrow 2) was observed in few cells (~ 8 %) and less than 1 % of these bacteria were lysed. In contrast, hBD-2-challenged bacteria (d-f) presented high levels of membrane alteration. Nevertheless, intracellular contents were largely retained, except for ~ 8 % of lysed cells detected, in which the intracellular material was lost (arrow 3). From the remaining cells, around 10 % were observed with intact membranes (arrow 4) and circa 82 % presented extensive plasmolysis, most with complete dissociation of the outer and inner membranes forming a large periplasmic space (arrow 5).

As a further confirmation that intracellular content was not generally released, unchallenged cultures, hBD-2 challenged or freeze-thaw lysed cells were analyzed by fluorescence microscopy after DAPI staining (Figure 4.22). It was possible to see that, similar

to the unchallenged controls (a-c), challenged bacteria (d-f) kept its DNA content inside individually distinguishable cells, whereas a standard lysis procedure (g-i) causes visible loss of cellular integrity. This was evident in representative overview images (a, d and g), and more clearly when the fluorescence signal of individual cells (b, e and h) was compared to the corresponding phase-contrast images (c, f and i).

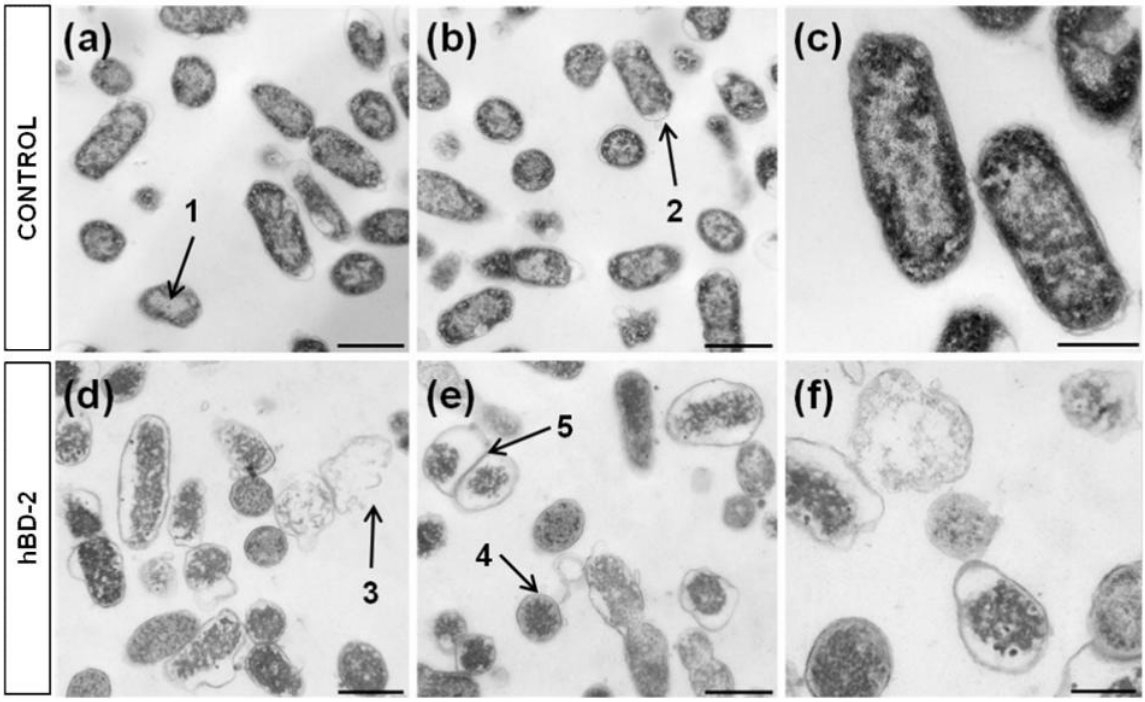

Figure 4.21 - Effect of hBD-2 challenge on *E. coli* (DSM1116) visualized by transmission electron microscopy (TEM), comparing unchallenged cultures (Control: a, b and c) to defensin-challenged cultures (20 $\mu g \cdot mL^{-1}$ hBD-2: d, e and f). Bacteria were challenged at O.D. 0.1, as described in Materials and Methods section 3.4.2. Cells were fixed 2 h after challenge, as described in Materials and Methods section 3.4.5, and examined in a TEM910 transmission electron microscope (Carl Zeiss) at an acceleration voltage of 80 kV. Representative images from each condition are shown. Arrows indicate: 1) electron-lucent DNA content; 2) low-extent plasmolysis; 3) lysed bacteria; 4) intact bacteria; 5) high-extent plamolysis with enlarged periplasmic space. Scale bars represent 1 µm (a, b, d and e) or 0.5 µm (c and f).

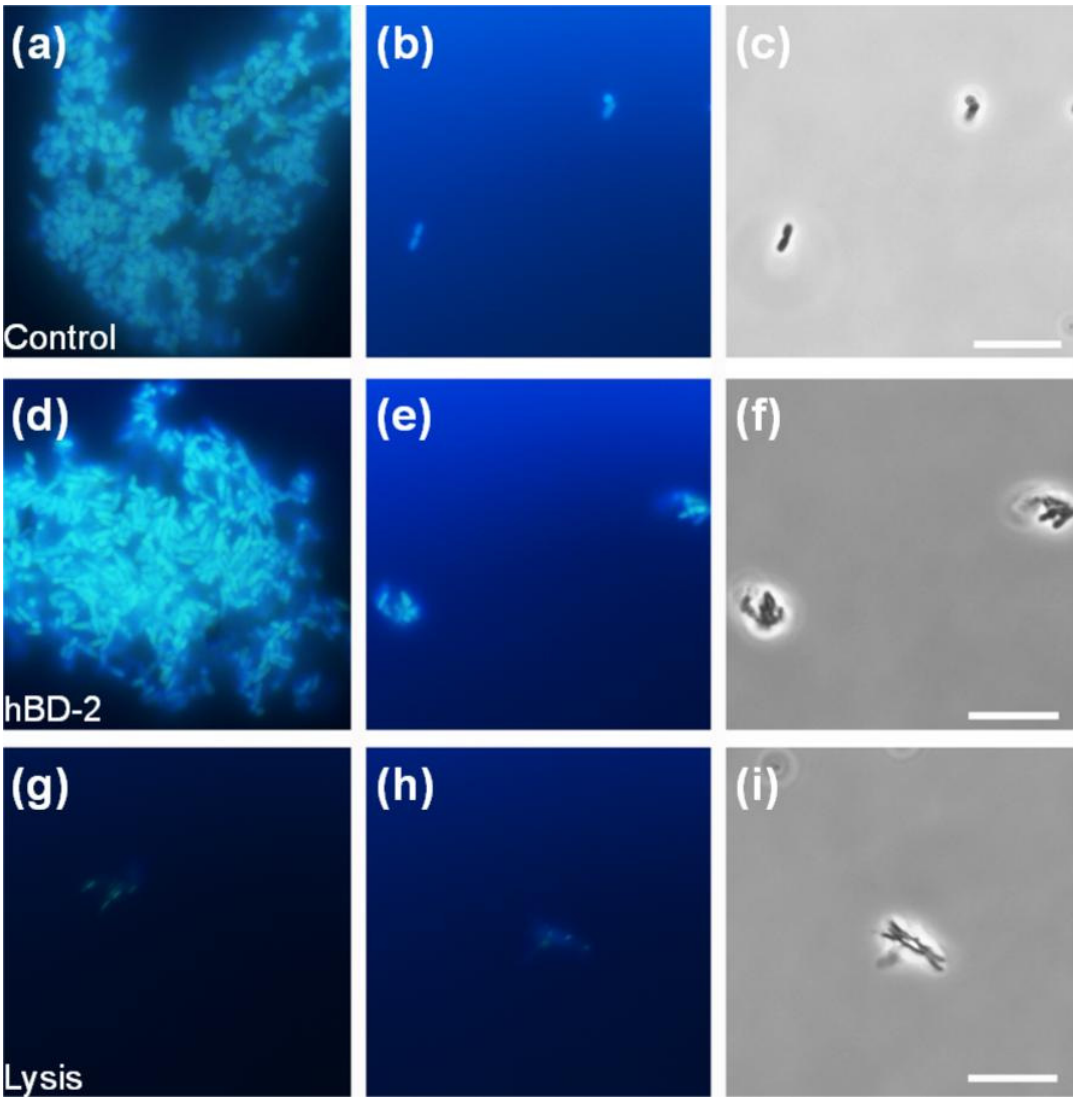

Figure 4.22 - Staining of DNA in hBD-2-challenged *E. coli* (DSM1116) visualized by fluorescence microscopy comparing unchallenged cultures (Control: a, b and c) to defensin-challenged cultures (20 $\mu g \cdot mL^{-1}$ hBD-2: d, e and f) and to cultures submitted to freeze-thaw lysis. Bacteria were challenged at O.D. 0.1, as described in Materials and Methods section 3.4.2. Cells were harvested 2 h after challenge, stained as described in Materials and Methods section 3.4.5, and examined in a Zeiss Photo microscope with filter set No. 49 (365 nm excitation, 445/450 emission). Representative fluorescence images are shown from unchallenged controls (a and b), hBD-2 challenged (d and e) and lysed cells (g and h). Phase-contrast images corresponding to (b), (e) and (h) are shown in panels (c), (f) and (i) respectively. Scale bars represent 5 µm.

4.2.2. Possible sources of extracellular Ado

Having confirmed that indiscriminate lysis was not the immediate cause of extracellular Ado accumulation, the next hypothesis to be tested was whether the extracellular Ado was a result of *de novo* synthesis processes triggered by hBD challenge, or derived from pre-existent cell components. The first possibility was tested by an experiment using culture medium (M4) containing either habitual, unlabeled (^{12}C) glucose or carbon isotope (^{13}C) labeled Glu (Figure 4.23). *E. coli* cultures were grown in each of the two above mentioned media for 4 h (mid-logarithmic phase, O.D. 0.1). At this point, the cultures were separated from the medium by filtration and resuspended either in ^{12}C- or in ^{13}C- containing M4, in order to have the 4 possible combinations (^{12}C-^{12}C, ^{12}C-^{13}C, ^{13}C-^{12}C and ^{13}C-^{13}C). The cultures were immediately challenged as described in Materials and Methods section 3.4.2. After 2 h the supernatants were collected and processed for analysis by HPLC-MS in scan mode. Comparing the presence of ions of *m/z* 268 (Ado) and *m/z* 269 (Ado containing one ^{13}C), this analysis would indicate if the molecule was synthesized previously, or only after addition of hBD-2. Figure 4.23 shows that irrespective of the presence of ^{13}C in the culture medium after hBD challenge, ^{13}C Ado was detected exclusively in the cultures that were previously grown with labeled Glu. The result indicated that extracellular Ado derived from compounds formed prior to hBD-2 addition.

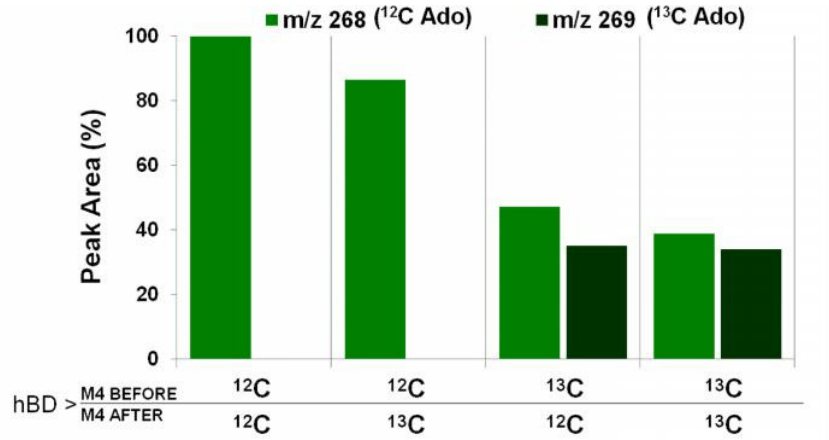

Figure 4.23 - Presence of ^{13}C-containing Ado in supernatants from *E. coli* (DSM1116) grown with different combinations of unlabeled M4 medium and/or ^{13}C-containing M4 medium and challenged with hBD-2 (20 $\mu g \cdot mL^{-1}$). The cultures were either grown in the absence or presence of ^{13}C-Glu for 4 h at which point the medium was either exchanged or not before the addition of hBD-2. Supernatants were collected 2 h after the challenge and analyzed by HPLC-MS in Scan mode (described in Materials and Methods section 3.3.1) for determination of the peak areas corresponding to ions of *m/z* 268 and *m/z* 269.

The identification of the purine ribonucleosides Ado and Guo, and of the four bases constituents of RNA (A, G, C and U) in the supernatants of *E. coli* cultures in response to hBD challenge, as reported in section 4.1.1, suggested that this response could be related to a nucleic acid degrading activity, and this was further supported by the results described in Figure 4.23. One approach chosen to verify the nucleic acid origin of extracellular Ado was the simultaneous addition of RNA or DNA (extracted from *E. coli* as described in Materials and Methods section 3.4.7) at the moment of hBD challenge. For this experiment, the bacterial cells and the supernatants were separated immediately after hBD addition (20 $\mu g \cdot mL^{-1}$), and the cells were resuspended in fresh M4 medium before the addition of the nucleic acid. By analyzing the cellular and soluble components separately, it was also possible to obtain information about the contribution of each component to the final response. Two hours after the challenge, samples were taken and analyzed by agarose (2 %) gel electrophoresis, to verify the presence of the added nucleic acid, and by HPLC-MS/MS to quantify the corresponding extracellular Ado resulting from each experimental condition. The results are summarized in Figure 4.24. The first and rather unexpected result from this experiment was that hBD-2 seemed to have DNA- and RNA-degrading activity, independent of any bacterial factor. This was evident by the absence of EtBr detection when the nucleic acids were incubated with hBD-2 in sterile M4 (Figure 4.24, upper left panel, hBD) in comparison to the incubation with M4 alone (control, C). The result was confirmed afterwards by more than five independent repetitions using different hBD-2 batches and DNA and RNA from different sources (data not shown). In *E. coli* cultures, it was possible to observe that the bacterial cells were able to degrade RNA irrespective of hBD-2 presence, whereas degradation of DNA was only observed in hBD-2 challenged cells (Figure 4.24, upper middle panel). The presence of hBD-2 triggered DNA and RNA degradation in the cell-free supernatants of challenged cultures (Figure 4.24 upper right panel).

These observations were in accordance with a nucleic acid degrading activity by hBD-2. The degradation of nucleic acids by hBD-2 alone, however, did not result in the production of Ado, as measured by HPLC-MS/MS and shown in Figure 4.24 (bar chart, “M4”). The concentration of extracellular Ado resulting from 2 h incubation of the challenged cells in a fresh medium (Figure 4.24 bar chart, “Cells”) or from 2 h incubation of the cell-free supernatants from challenged cultures (Figure 4.24 bar chart, “SN”), was analyzed in comparison to the response in the whole cultures where the components were not separated after challenge (Figure 4.24 bar chart, “Culture”). The reduced Ado concentration found in

the separated cells or supernatants (6 % and 30 %, respectively) indicated that both components were necessary for the total response, although the supernatants seemed to present a relatively higher autonomy. The importance of the soluble factors to Ado generation was evident upon addition of DNA or RNA to the system: the degradation of nucleic acids resulted in 2.5 times higher Ado concentration exclusively in the cell-free supernatants, and not in the cellular component. Taken together, these data indicate that the presence of extracellular Ado in hBD-2 challenged *E. coli* cultures may result from a combination of nucleic acid degrading activity by hBD-2 and a bacterial soluble factor present in the supernatants after defensin challenge.

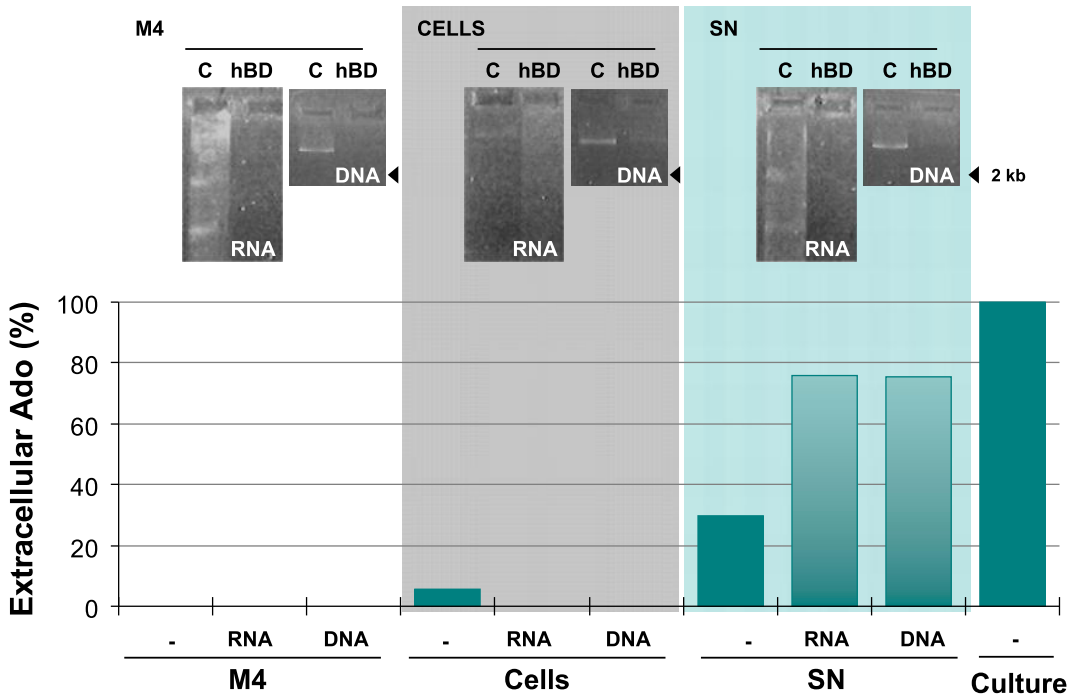

Figure 4.24 - Interaction of hBD-2 with nucleic acids extracted from *E. coli* and its effect on the generation of extracellular Ado by hBD-challenged cultures. Upper panels show detection of added RNA (10 $ng \cdot mL^{-1}$) and DNA (1 $ng \cdot mL^{-1}$) after 2 h incubation in the absence (control; C) or presence (hBD) of hBD-2 (20 $\mu g \cdot mL^{-1}$). Left: in sterile M4 medium; Middle: in *E. coli* (DSM1116) cells harvested by filtration immediately after hBD addition and resuspended in fresh M4 medium; Right: in the cell-free supernatants from hBD-2-challenged cultures. Challenge was performed as described in Materials and Methods section 3.4.2. Sample aliquots (10 µL) were analyzed by agarose (2 %) gel electrophoresis and stained with EtBr, as described in Materials and Methods section 3.3.5. Bar chart show the relative concentration of extracellular Ado generated in the systems in the absence (-) or presence of the added nucleic acids (RNA or DNA), as determined by HPLC-MS/MS analysis in the MRM mode (described in Materials and Methods section 3.3.1) The values are expressed relative to extracellular Ado levels from whole *E.coli* cultures after the same hBD challenge.

To confirm the nucleic acid origin of extracellular Ado in hBD-challenged *E. coli* cultures, a second experiment using ^{13}C labeling of bacterial cells was performed. The cultures were grown in either in ^{12}C- or ^{13}C-Glu containing M4 up to mid-logarithmic phase (4 h) and challenged with hBD-2 (20 $\mu g \cdot mL^{-1}$) in the same medium. In this experiment, instead of qualitatively detecting the isotopic labeled product, a quantitative determination of the isotopic ratio in extracellular Ado was performed and compared to the isotopic ratio in RNA and DNA extracted from the cultures immediately before the challenge, and similar ^{13}C ratios would indicate a common origin. This was achieved by submitting the sampled supernatants and the extracted, purified nucleic acids, in parallel with commercial nucleoside standards, to the same trimethisilylation protocol and analysis by GC-MS and GC-IRMS, as described in Materials and Methods sections 3.3.2 and 3.4.8. To obtain enough material for the analyses, 20 mL cultures were grown in duplicate for each medium.

GC-MS was used to confirm the presence of TMS derivatives in the samples. Table 4. 3 shows the obtained retention times and *m/z* values for standard adenosine (Ado), guanosine (Guo), deoxyadenosine (dAdo) and deoxyguanosine (dGuo), together with a description of the derivatives represented by the detected ions, i. e. the molecular mass of the nucleoside plus the TMS groups incorporated. The generation of tri-, tetra- and penta-TMS for dAdo, dGuo and Guo, respectively, was in accordance to the expected replacement of each active hydrogen atom in the molecule by one TMS group. For Ado, the ion lacking one methyl group was found. Accordingly, in the supernatants and RNA samples, peaks corresponding to Ado and Guo were detected, and in the DNA samples, peaks corresponding to dAdo and dGuo were present (data not shown).

Table 4. 3 - Characteristics of trimethylsilylated nucleosides analyzed by GC-MS.

	R.T. (min)	**Mass (*m/z*)**	**Description**
Ado	*10.15*	*540*	*Ado + 4(TMS) - CH_3*
Guo	*10.95*	*644*	*Guo+ 5(TMS)*
dAdo	*10.13*	*467*	*dAdo + 3(TMS)*
dGuo	*11.06*	*555*	*dGuo + 4(TMS)*

After the first scanning by GC-MS to find the optimal conditions for GC separation, the samples were submitted to analysis by GC-IRMS. The same temperature program was used in the GC to separate the compounds, but because the capillary column used in this equipment was different in length from the column in the GC-MS, the small changes in retention time of the compounds were monitored by parallel injection of the commercial standards, and corrected accordingly. The results of the IRMS calculations (Figure 4.25) are expressed in the standard notation for isotopic ($^{13}C/^{12}C$) ratio, $\delta^{13}C$ per mille, after correction according to the carbons added during the derivatization process. Details on the calculations and measured values can be found in Supplementary Table 6 (section 7.2). The results show that the ^{13}C isotope is incorporated both in adenine nucleosides forming DNA (dAdo) and RNA (Ado). The isotopic ratio in extracellular (SN) Ado after hBD challenge was found to be in the same range as DNA and RNA, supporting the hypothesis that this compound derives from the degradation of bacterial ribonucleic acids.

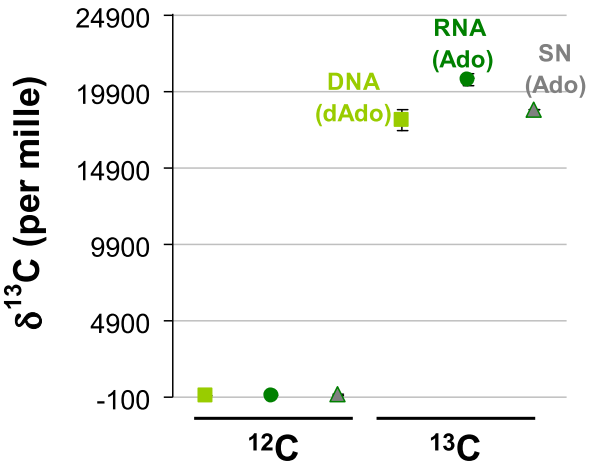

Figure 4.25 - Isotopic (^{13}C) enrichment in adenine nucleosides from *E. coli* total DNA and RNA and in extracellular adenosine generated after hBD-2 challenge. *E. coli* (DSM1116) was grown either in normal, unlabeled M4 medium or in [^{13}C]Glu-containing M4 medium and challenged with hBD-2 (20 $\mu g \cdot mL^{-1}$) at mid-logarithmic phase (4 h). DNA and RNA were extracted and digested (as described in Materials and Methods section 3.4.8) from two culture replicates immediately before challenge. hBD-2 challenge was performed as described in Materials and Methods section 3.4.2, and supernatants were collected 2 h after challenge. The samples were derivatized by trimethylsilylation and analyzed by GC-IRMS as described in Materials and Methods sections 3.4.8 and 3.3.2. Values were normalized according the number of carbon atoms and of TMS groups included in the derivatization process. Details on the correction and measured values can be found in Materials and Methods section 3.3.2 and in Supplementary Table 6 (section 7.2). Mean $\delta^{13}C \pm$ SD for four replicates from two independent cultures.

One possible direct pathway for the generation of Ado from RNA starts with the action of nucleotidyltransferases (E.C. 2.7.7.), which can catalyze the formation of nucleoside tri- or diphosphates from RNA, and phosphotransferases (E.C. 2.7.4.) which will finally produce AMP as a precursor for the formation of Ado by 5'-ribonucleotide phosphohydrolase (E.C. 3.1.3.5). The presence of adenosine nucleotides in the supernatants of hBD-2 challenged *E. coli* cultures was investigated. First, the luminescence based method for quantifying ATP in bacterial cultures was applied to the cell-free supernatants at different time-points after the hBD challenge. Different to the kinetics found in the unchallenged cultures (Figure 4.26, black line) the results showed a slight increase in extracellular ATP concentration in the first 10 to 20 min after hBD challenge, followed by gradual depletion up to 4 h (Figure 4.26, green line). As a comparison, the solid symbols show ATP concentrations in total cultures at time 0 and 4 h after challenge. Additionally, the concentration of ATP determined in cultures submitted to freeze-thaw lysis, represented by the blue symbols, show that the total ATP in the cultures (solid circle) was found extracellularly (open diamond) immediately after lysis, different to what was observed in the hBD-challenged culture (green symbols).

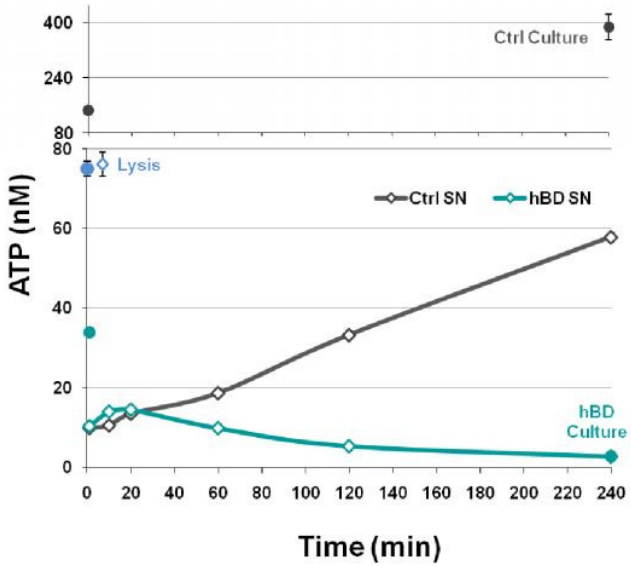

Figure 4.26 - Quantification of extracellular ATP in *E. coli* (DSM1116) supernatants after challenge with hBD-2 20 $\mu g \cdot mL^{-1}$ (green line) or in unchallenged cultures (Ctrl; black line). The presence of ATP in whole cultures at 0 and 240 min is represented by filled symbols with the same color code. Immediate effect of freeze-thaw lysis on ATP concentration and release is indicated by blue symbols. hBD-2 challenge was performed as described in Materials and Methods section 3.4.2. Supernatants (75 µL) were analyzed at different time-points after challenge using BacTiter-Glo kit (as described in Materials and Methods section 3.4.6). Mean ± SD of four determinations from two independent cultures.

In addition, the identification of adenine nucleotides in defensin challenged supernatants was also attempted by HPLC-MS, using the same approach employed for the identification of Ado. The presence of neither ATP nor ADP could be demonstrated by this method, as ions of corresponding *m/z* were not detected. The cyclic purine nucleotides were also not found in our analysis (data not shown). In turn, the presence of extracellular AMP in the cultures could be clearly observed and quantified. Figure 4.27 shows the extracted ion chromatograms for *m/z* 348 in synthetic AMP (pink line) and in the sampled *E. coli* supernatant 2 h after hBD-2 (20 $\mu g \cdot mL^{-1}$) challenge (green line) and in the unchallenged control (black line). The inset displays the ions produced from the fragmentation of *m/z* 348, the same spectrum was found for standard AMP and for the same ions present in the samples. As described above for the other purine compounds (section 4.1.2), the fragment ions were used for quantification of AMP in the supernatants by HPLC-MS/MS in the MRM mode.

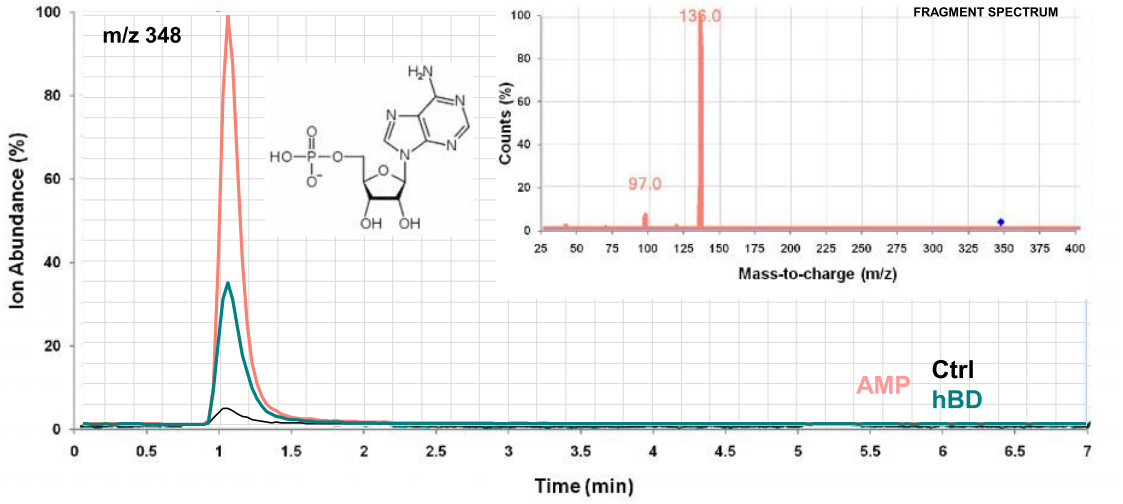

Figure 4.27 - HPLC-MS/MS analysis (product ion base peak chromatogram) of target ion (*m/z* 348) in supernatants from *E. coli* (DSM1116) cultures unchallenged (black line) or challenged with hBD-2 20 $\mu g \cdot mL^{-1}$ (green line), and in synthetic AMP (0.6 $\mu g \cdot mL^{-1}$, pink line). Challenge was performed as described in Materials and Methods section 3.4.2 and supernatants were collected 2 h after hBD-2 addition. Samples (5 µL) were injected in reversed-phase chromatography and analyzed by MS/MS product ion scan mode as described in Materials and Methods section 3.3.1. Inset shows representative fragment spectrum (C.E. 50 V) of the targeted parent ion. The chemical structure of AMP is depicted.

Quantitative analysis of the presence of extracellular AMP in *E. coli* cultures was performed by HPLC-MS/MS analysis in the MRM mode. The MRM transitions used the standard curves can be found in Supplementary Table 5 (section 7.1). The results allowed insight on the involvement of this precursor on the generation of extracellular Ado by hBD-2 challenged bacteria. For a matter of comparison, some of the results on quantification of Ado described in section 4.1 are included in the following figures. The concentration of AMP in the supernatants as a function of time after the challenge is presented in Figure 4.28a. In comparison to the Ado concentration, there seems to be a similar increase in extracellular AMP in the first 6 h after hBD challenge. From 6 h to 48 h, an inverse correlation was observed, indicating the conversion of AMP into Ado, in contrast to the accumulation of AMP observed in the unchallenged cultures. The formation of Ado from AMP was found to occur also when supernatants collected 30 min after hBD challenge were re-incubated for 18 h (Figure 4.28b), suggesting that the reaction was taking place in the extracellular medium.

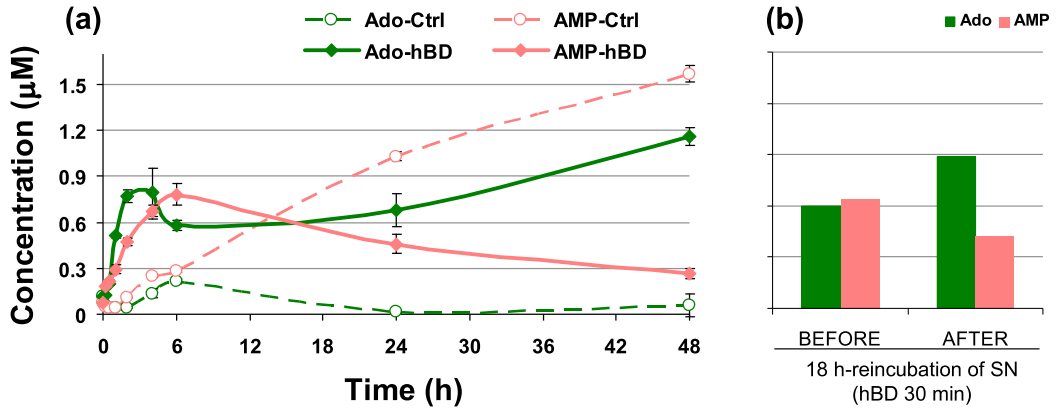

Figure 4.28 - (a) Variation in the extracellular concentration of adenosine (Ado, green lines) and AMP (pink lines) over time after challenge with hBD-2 at 20 $\mu g \cdot mL^{-1}$ (solid lines) or in unchallenged cultures (dashed lines). *E. coli* (DSM1116) cultures were challenged as described in section 3.4.2 and the supernatants were collected at different time-points for quantitative analysis by HPLC-MS/MS in the MRM mode as described in Materials and Methods section 3.3.1. Data are representative from three independent experiments. Mean ± SD of three replicates. (b) Effect in adenosine and AMP concentration of incubating (for 18 h at 37° C) a supernatant sample collected from challenged culture 30 min after hBD-2 addition.

When investigating the effect of hBD-2 dose on AMP concentration in the supernatants (Figure 4.29), the comparison to the concentration of extracellular Ado demonstrated an interesting correlation: lower hBD-2 doses, which did not result in the formation of Ado, were found to induce extracellular AMP accumulation. At higher doses, AMP concentration in the supernatants was reduced, while Ado levels were increased. This inverse correlation was also observed by comparing the effect of different antimicrobial peptides (Figure 4.30). A higher accumulation of AMP resulted from challenge with magainin I and human α-defensin-5, both found to be unable to induce generation of extracellular Ado.

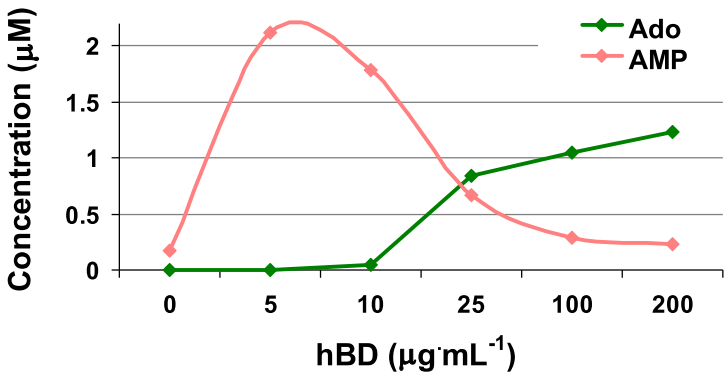

Figure 4.29 - Effect of increasing hBD-2 doses (0, 2.5, 5, 10, 20, 30, 40, 50, 100 or 200 $\mu g \cdot mL^{-1}$) on extracellular concentration of adenosine (Ado, green line) and AMP (pink line). *E. coli* (DSM1116) cultures were challenged as described in section 3.4.2 and supernatants were collected 2 h after challenge for quantitative analysis by HPLC-MS/MS in the MRM mode as described in Materials and Methods section 3.3.1. For representative growth curves of *E. coli* in each condition, refer to Figure 4.8.

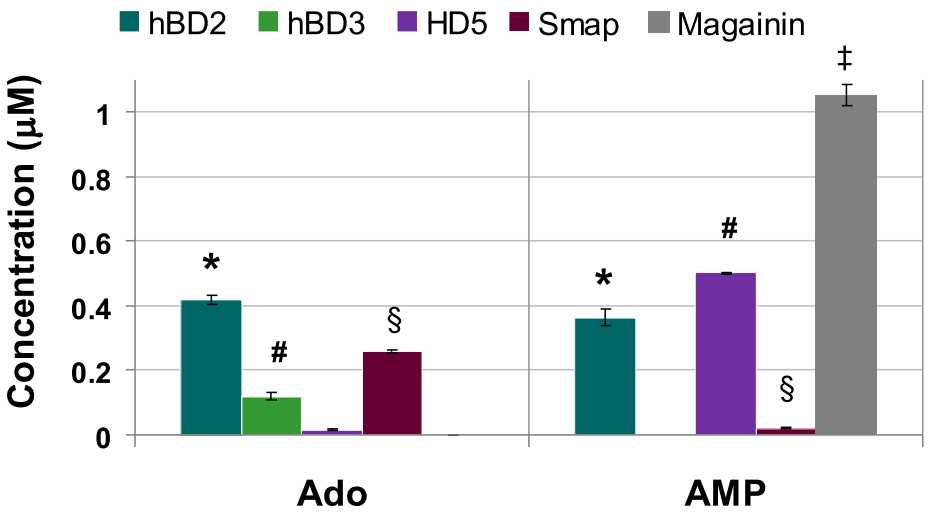

Figure 4.30 - Effect of different antimicrobial peptides on extracellular concentration of adenosine (Ado) and AMP in *E. coli* (DSM1116) cultures. The supernatants were collected 2 h after addition of 20 $\mu g \cdot mL^{-1}$ of: human β-defensin-2 (hBD-2, green), human β-defensin-3 (hBD-3, light-green), human α-defensin-5 (HD5, purple), sheep myeloid antimicrobial peptide 29 (SMAP, dark-red) or magainin I (grey). Concentration of the target compounds was determined by quantitative analysis by HPLC-MS/MS in the MRM mode. Mean ± SD of three replicates. Within each category (compound), a symbol (*, #, § or ‡) indicates significant differences ($p<0.001$) from the lowest value, and different symbols indicate significant difference ($p<0.001$) between peptides in pairwise ANOVA as described in Materials and Methods section 3.6. For representative growth curves of *E. coli* in each condition, refer to Figure 4.17.

Using the same experimental design described in Figure 4.24, provided additional evidence that accumulation of AMP corresponded to a deficiency in the formation of Ado. Quantification of extracellular AMP generated by hBD-2 challenged cultures, in comparison to the concentrations observed when the cells were separated from the supernatant immediately after defensin addition, demonstrated again that accumulation of AMP occured in situations where Ado formation was impaired, in this case, in the challenged cells in the absence of their original challenged supernatants (Figure 4.31, "Cells"). The concentrations were even higher upon addition of purified RNA or DNA, which presented no effect on the generation of Ado by these cells (see Figure 4.24). In contrast, the cell-free supernatants from challenged cultures presented lower levels of AMP, unaffected by RNA or DNA addition (Figure 4.31, "SN"). The same supernatants were able to generate higher amounts of Ado than the cells alone, particularly after addition of nucleic acids (see Figure 4.24). Importantly, the incubation of nucleic acids with hBD-2 alone in sterile medium did not result in formation of AMP (Figure 4.31 "M4"). Finally, as a confirmation of the conversion of AMP to Ado by

hBD-2 challenged culture supernatants, extracellular Ado concentration was measured after addition of exogenous AMP to the challenged cells or cell-free supernatants after hBD-2 challenge (Figure 4.32). Cells separated from their supernatants after defensin challenge, as well as sterile M4 were unable to generate Ado, irrespective of AMP addition. In turn, when AMP was added to cell-free supernatants from challenged cultures, Ado levels were greatly increased.

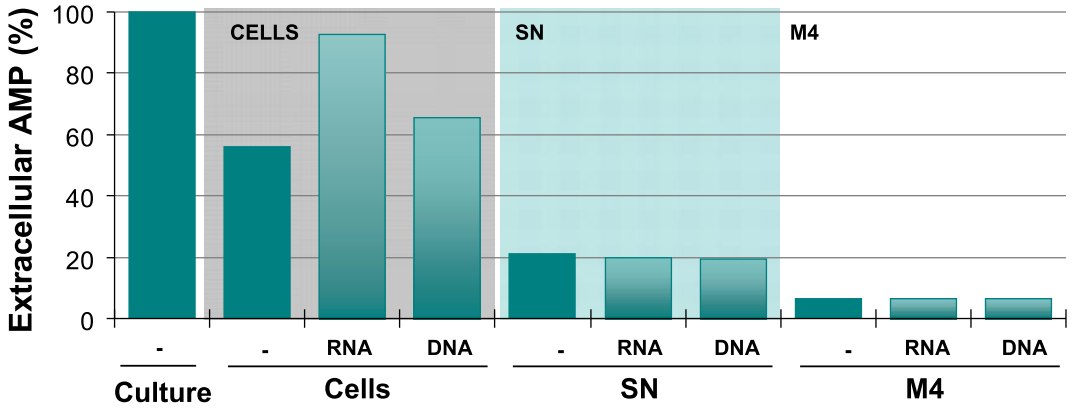

Figure 4.31 - Effect of added nucleic acids on the generation of extracellular AMP: in sterile medium (right, M4); in cell-free supernatants from hBD-2 challenged *E. coli* (DSM1116) (middle, SN); or in harvested cells resuspended in fresh M4 medium (left, Cells). Bacteria were separated from the supernatants by filtration immediately after nucleic acid addition and hBD challenge (performed as described in Materials and Methods section 3.4.2). The relative concentration of extracellular AMP generated in the systems in the absence (-) or presence of the added nucleic acids (RNA or DNA) was determined 2 h after the challenge, by HPLC-MS/MS analysis in the MRM mode (as described in Materials and Methods section 3.3.1). The values are expressed relative to extracellular AMP levels from whole *E.coli* cultures after the same hBD challenge.

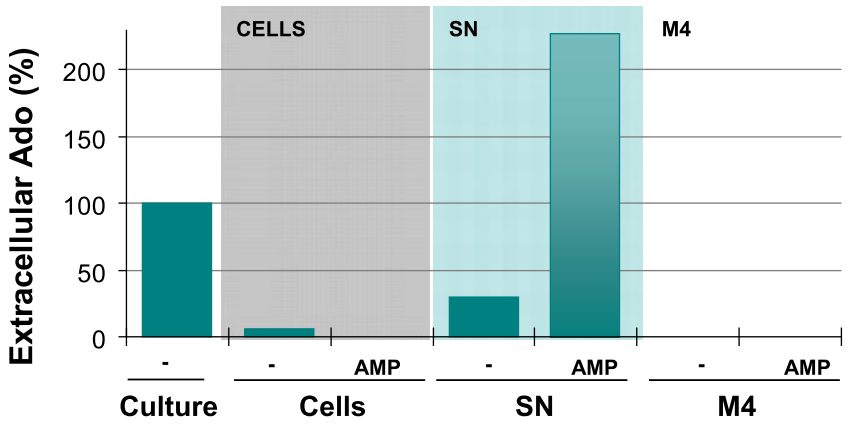

Figure 4.32 - Effect of added AMP on the generation of extracellular adenosine: in sterile medium (right, M4); in cell-free supernatants from hBD-2 challenged *E. coli* (DSM1116) (middle, SN); or in harvested cells resuspended in fresh M4 medium (left, Cells). Bacteria were separated from the supernatants by filtration immediately after AMP addition and hBD challenge (performed as described in Materials and Methods section 3.4.2). The relative concentration of extracellular Ado generated in the systems in the absence (-) or presence of added AMP was determined 2 h after the challenge, by HPLC-MS/MS analysis in the MRM mode (as described in Materials and Methods section 3.3.1). The values are expressed relative to extracellular Ado levels from whole *E.coli* cultures after the same hBD challenge.

RESULTS III

4.3. Defensin induced *E. coli*-derived compounds as potential immunomodulators

4.3.1. NF-κB activation in Caco-2 cells

To address the hypothesis that extracellular metabolites released from *E. coli* after hBD-2 challenge have a role in host-microbial interactions in the intestine, the activity of NF-κB pathway in a human intestinal epithelial cell-line (Caco-2) was investigated as a possible target. NF-κB is a key cell-signaling component involved in inflammatory responses (Razani and Cheng, 2010). As indicators of the activation of this pathway in the cells, both the degradation of the inhibitor IκB and the nuclear translocation/phosphorylation of the effector p65 were monitored. These events are long recognized to be interconnected and responsible for the transcriptional activity of NF-κB (Naumann and Scheidereit, 1994). First, for validation of the method, the human cells were incubated in serum-free DMEM for 20 min or 40 min in the absence of stimuli, or in the presence of different inflammatory mediators. Western blot analysis (Figure 4.33) shows satisfactory detection of IκB in control cells extract (-). The protein was absent in cells which were stimulated with TNF-α or IL-1β, indicating the activity of the pathway in these cultures already after 20 min and being stable to up 40 min. Incubation with LPS, however, was not able to induce IκB degradation, in accordance to previous reports demonstrating that Caco-2 cells are generally less sensitive to LPS (Abreu *et al.*, 2001). The degradation of IκB in TNF-α and IL-1β treated cells was accompanied by nuclear translocation of p65 as assessed by immunofluorescence microscopy (Figure 4.34). The immunostaining of p65 is restricted to the cytoplasm in untreated cells, whereas it is clearly co-localized with the nuclear staining (Hoechst) in some, but not all stimulated cells (indicated by arrows).

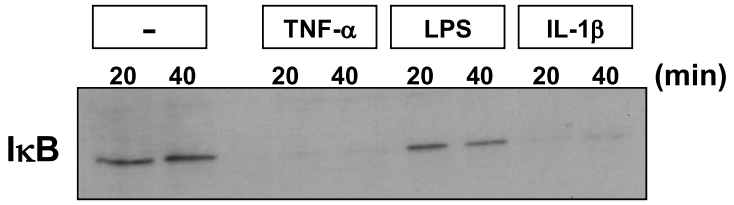

Figure 4.33 - Degradation of IκB protein in Caco-2 cells after inflammatory stimuli. Cells were assayed as described in Materials and Methods section 3.5.2, with TNF-α (50 ng·mL^{-1}), LPS (20 µg·mL^{-1}) or IL-1β (10 ng·mL^{-1}), or in the absence of stimuli (-), and harvested after 20 or 40 min. Western blot analysis was performed as described in Materials and Methods section 3.3.6 using primary rabbit antibody anti-IκB (1:500) and secondary antibody anti-rabbit IgG-HRP conjugate (1:10,000).

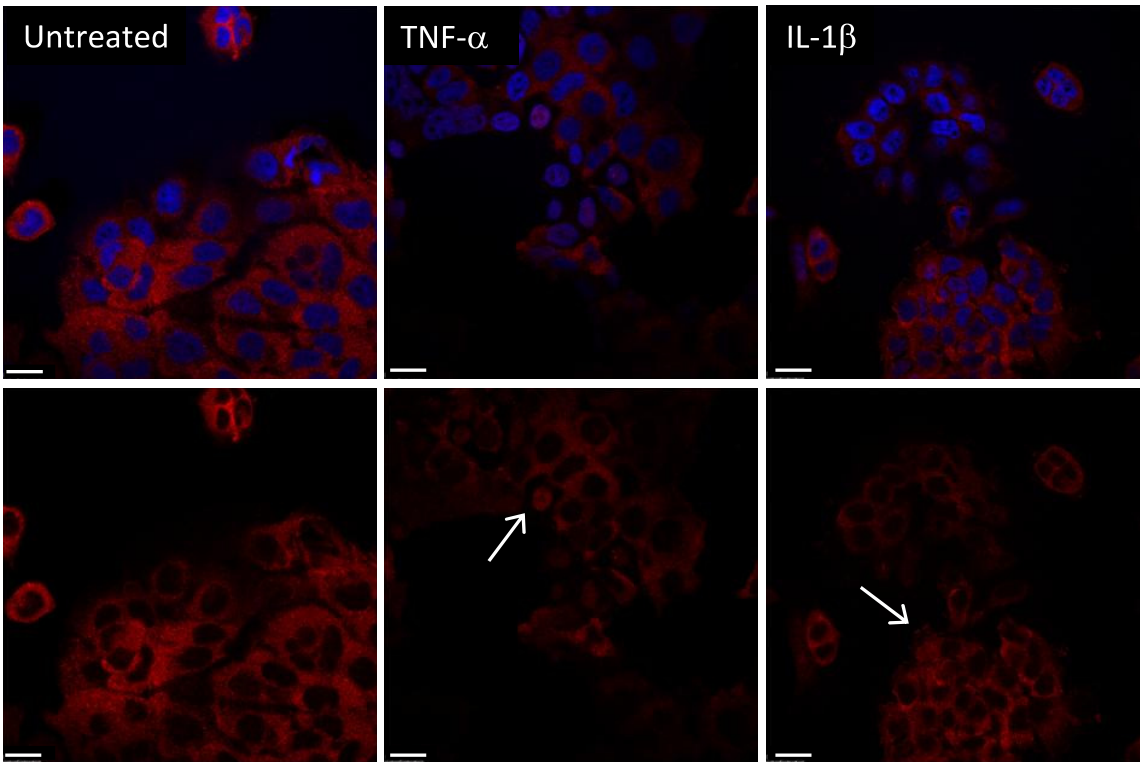

Figure 4.34 - Subcellular distribution of transcription factor NF-κB subunit p65 in Caco-2 cells after inflammatory stimuli. Cells were assayed as described in Materials and Methods section 3.5.2, with TNF-α (50 ng·mL^{-1}) or IL-1β (10 ng·mL^{-1}), or in the absence of stimuli (Untreated), and fixed after 40 min. Immunofluorescence staining was performed as described in Materials and Methods section 3.5.3 using primary rabbit antibody anti-p65 (1:200) and secondary antibody anti rabbit IgG-Alexa546 conjugate (1:800). Nuclear material was stained with Hoechst 33258. Cells were observed under DMI6000 CS microscope with confocal unit Leica TCS SP5. Bars represent 25 µm. Arrows indicate nuclear localization of p65 protein.

4.3.2. Effect of E. coli *supernatants on NF-κB activation in Caco-2 cells*

Using IL-1β as a positive control for the activation of NF-κB, and in comparison to unstimulated Caco-2 cells, the effect of *E. coli* supernatants on the human cells was investigated. Western blot for the detection of IκB (Figure 4.35) revealed that supernatants from control, unchallenged *E. coli* (1), culture lysates (2) or sterile M4 medium (3), as well as supernatants from hBD-2 challenged cultures collected after 30 min (4) or 2 h (5), did not substantially change levels of inhibitor protein in comparison to unstimulated cells (-). Additionally, pure commercial Ado was tested at the concentration range produced by defensin challenged *E. coli* (150 $ng \cdot mL^{-1}$, 0.56 μM), but no effects were observed. The expression of adenosine receptors by Caco-2 cells has been already reported but studies demonstrating general effects of Ado signaling in this cell line, which include for example induction of cell proliferation, modulation of cytokine production and apoptosis, usually employ much longer incubation times or higher dosages (Gessi *et al.*, 2007; Frick *et al.*, 2009; Yasuda *et al.*, 2009).

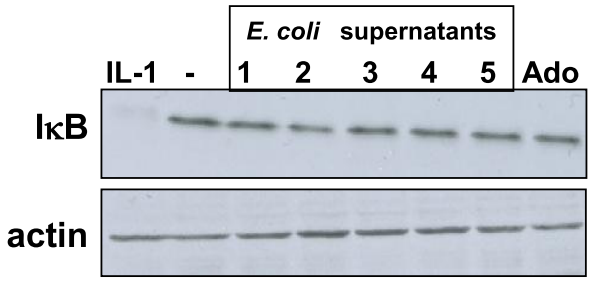

Figure 4.35 - Degradation of IκB protein in Caco-2 cells after stimulation with IL-1β or in the presence of *E. coli* (DSM1116) supernatants. Cells were assayed as described in Materials and Methods section 3.5.2, in the presence of IL-1β (10 $ng \cdot mL^{-1}$), in the absence of stimuli (-), or in the presence of the following preparations: 1- supernatants from normally growing *E. coli* cultures at mid-logarithmic phase; 2- filtered *E. coli* lysates; 3- sterile bacteriological culture medium M4; 4- and 5- supernatants from hBD-2 challenged *E. coli* cultures (collected respectively 30 min or 120 min after defensin addition), Ado- pure commercial adenosine solution (0.56 μM). Cells were harvested after 40 min and Western blot was performed as described in Materials and Methods section 3.3.6. Upper panel: detection of IκB using primary rabbit antibody anti-IκB (1:500) and secondary antibody anti-rabbit IgG-HRP conjugate (1:10,000). Lower panel: detection of β-actin using primary mouse antibody anti-βactin (1:2,000) and secondary antibody anti-mouse IgG-HRP conjugate (1:10,000).

According to previous work (Jijon *et al.*, 2005) a pre-treatment with Ado prior to stimulation has a modulatory effect on NF-κB signaling in intestinal epithelial cells. Our experimental setup was re-designed to include pre-incubation of the cells for 30 min in the presence or absence of tested samples before addition of IL-1β. Additionally, as an option to address p65 activation simultaneously with IκB degradation, the presence of phosphorylated (active) form of the protein (P-p65) was also determined by Western blot. Figure 4.36 shows that P-p65 protein is detected as expected in IL-1β stimulated (2-4), but not in unstimulated cells (1, 5, 6), and that pre-incubation with commercial Ado (0.56 μM, 4) resulted in an enhanced response to IL-1β regarding IκB degradation. Again, the addition of Ado in the absence of IL-1β presented no relevant effect (5-6). In this experiment, different concentrations of IκB in the samples showed the presence of two proteins recognized by the antibody, likely corresponding to two forms of IκB differing by their phosphorylation state. The phosphorylation of IκB precedes its polyubiquitination and degradation in the proteasome pathway, but phosphorylation alone does not lead to degradation of the inhibitor (Alkalay *et al.*, 1995).

Finally, the same experimental setup including pre-incubation was used to test supernatants from *E. coli* cultures challenged or not with hBD-2, in comparison to commercial Ado and sterile M4 medium as a control (Figure 4.37). The content of IκB and P-p65 protein in Caco-2 cells stimulated or not with IL-1β after each pre-treatment condition was verified. For normalization before quantitatively comparing the effects of the different treatments, detection of total p65 and actin was performed in parallel, and a lower acrylamide concentration (10 %) in the electrophoresis gel was used for better separation. Regarding the presence of IκB, the effect of pure Ado was confirmed and could be visualized in the Western blot, but the differences were less clear for the bacterial samples tested. In turn, the content of phosphorylated p65 seems to be higher when Caco-2 cells were pre-incubated with supernatants from hBD-2 challenged *E. coli* followed by stimulation with IL-1β. Relative quantitation analysis performed by densitometry could further clarify the effects observed in the Western blot. The results shown in Table 4.4 are expressed as ratio IκB/actin and P-p65/total p65. The amount of IκB after IL-1β stimulation was strongly reduced by the presence of Ado and it seems to be affected to a lesser extent by bacterial supernatants and medium. In contrast, p65 ratios showed a response specific to pre-treatment with supernatants from hBD-challenged bacteria, as well as to pure Ado, where a marked induction of p65

phosphorylation after IL-1β stimulation was observed. This induction was not observed when cells were instead pre-treated with unchallenged bacterial supernatants or medium.

Higher level of phosphorylated (active) p65 in stimulated cells after pre-incubation with Ado was in accordance with lower level of the inhibitor IκB found in this condition. Interestingly, extracellular compounds from hBD-2 challenged *E. coli* were also able to enhance NF-κB activation, althought it was unclear if IκB degradation was specifically affected. Taken together, these results indicate an enhancing effect of Ado in NF-κB pathway activation after IL-1β stimulation in Caco-2 cells, and that this effect can be mimicked by *E. coli*-derived compounds (including Ado) generated in response to defensin challenge.

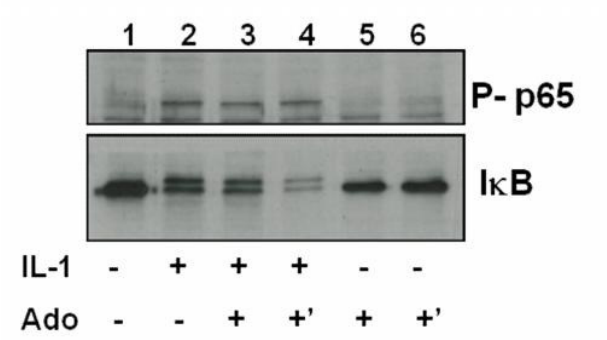

Figure 4.36 - NF-κB pathway activation in Caco-2 cells after stimulation with IL-1β and effect of adenosine. Cells in serum-free DMEM were stimulated or not with IL-1 β (10 $ng \cdot mL^{-1}$) in the absence (1 -2), or in the presence (3-6) of Ado (0.56 μM). Ado was added either simultaneously (3 and 5) or 30 min before IL-1β stimulation (4 and 6, indicated by '). Cell extracts were harvested 40 min later and Western blot was performed as described in Materials and Methods section 3.3.6. Upper panel: detection of phosphorylated p65 using primary rabbit antibody anti-p65 (phospho Ser563) (1:500) and secondary antibody anti-rabbit IgG-HRP conjugate (1:10,000). Lower panel: detection of IκB using primary rabbit antibody anti-IκB (1:500) and secondary antibody anti-rabbit IgG-HRP conjugate (1:10,000).

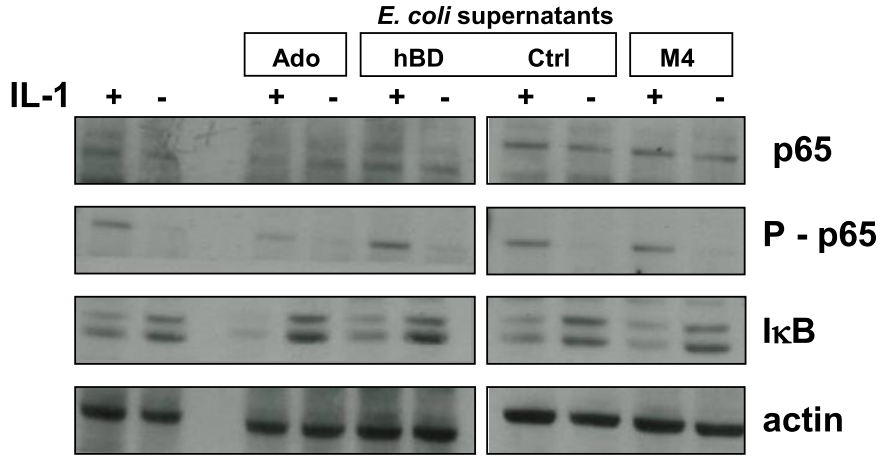

Figure 4.37 - NF-κB pathway activation in Caco-2 cells after stimulation with IL-1β and effect of *E. coli* (DSM1116) supernatants. Cells in serum-free DMEM were stimulated or not with IL-1 β (10 $ng \cdot mL^{-1}$) after 30 min pre-incubation in the absence or in the presence of different preparations as follows: pure commercial Ado (0.56 μM), supernatants from defensin challenged *E. coli* cultures (collected 2 h after addition of hBD-2 20 $\mu g \cdot mL^{-1}$), supernatants from mid-logarithmic unchallenged *E. coli* cultures (Ctrl) or sterile bacteriological M4 medium. Cell extracts were harvested 40 min after IL-1β stimulation and Western blot was performed as described in Materials and Methods section 3.3.6. Top panel: detection of total p65 using primary mouse antibody anti-p65 (1:250) and secondary antibody anti-mouse IgG-HRP conjugate (1:10,000). Middle-upper panel: detection of phosphorylated p65 using primary rabbit antibody anti-p65 (phospho Ser563) (1:500) and secondary antibody anti-rabbit IgG-HRP conjugate (1:10,000). Middle-lower panel: detection of IκB using primary rabbit antibody anti-IκB (1:500) and secondary antibody anti-rabbit IgG-HRP conjugate (1:10,000). Bottom panel: detection of β-actin using primary mouse antibody anti-βactin (1:2,000) and secondary antibody anti-mouse IgG-HRP conjugate (1:10,000).

Table 4.4 - Presence of IκB and phosphorylated p65 in Caco-2 cells relative to β-actin and total p65 content, estimated by densitometry analysis of the image in Figure 3.37.

		PRE-TREATMENT				
	IL-1β	-	Ado	SN_{hBD}	SN_{Ctrl}	M4
IκB/actin	-	*0.314*	*0.374*	*0.32*	*0.353*	*0.331*
	+	*0.152*	*0.032*	*0.122*	*0.11*	*0.08*
P-p65/p65	-	*0.293*	*0.33*	*0.394*	*0.069*	*0.143*
	+	*3.083*	*3.589*	*4.121*	*1.12*	*1.153*

5. DISCUSSION

5.1. Response of *Escherichia coli* to hBD-2 challenge

5.1.1. Experimental setup

One of the main goals of this study was to search for metabolites of bacterial origin present in the extracellular space under conditions of high defensin stress found in inflamed tissue. The approach chosen was to analyze supernatants from defensin challenged *Escherichia coli* cultures by HPLC-MS, which is a powerful technique widely used in the characterization of microbial metabolites (Mashego *et al.*, 2007). The specific method employed here, the comparative analysis of whole cell-free supernatants from bacterial cultures, referred to as the metabolic footprint, has been used in microbiology for different applications. The molecules present in bacterial supernatants are considered to reflect the intracellular metabolism, and used in biotechnology, for example, to develop, monitor and optimize bioprocesses. In other cases, the extracellular metabolites represent bacterial secretory activity, and can be used to characterize strains, or to accelerate the identification of intercellular communication (quorum sensing) systems (Mapelli *et al.*, 2008). However, to date, only few studies focused on this approach to identify compounds directly involved in host-microbial networks, mostly in the field of plant-pathogen interactions (Allwood *et al.*, 2010). This novel concept was successfully employed here in the context of a human gut bacterial species.

One fundamental issue of directly analyzing culture media by HPLC-MS is that the composition of the medium should be kept as simple as possible, to avoid interference of high background signals that would result from a complex medium and avoid time consuming optimization of the chromatographic separation procedure. The medium of choice for this study was based on the paper by Kaderbhai *et al.*, 2003, who described the metabolites secreted by different *E. coli* mutants grown in minimal medium with glucose as the primary carbon source. This composition was suitable for HPLC-MS analysis, as demonstrated by the two peaks with defined mass spectra found in the sterile medium, which could be readily distinguished in the supernatants (Figure 4.2). An additional concern here was that the medium should be compatible with the salt-sensitive defensin activity, which was achieved by reducing 10-fold the concentration of all components except glucose. In a physiological

context, the local concentrations of salts at the site of defensin action are not known, and ionic microenvironments and regional variations are expected to exist in the interface between gut epithelia and the lumen (O'Neil *et al.*, 1999; Selsted and Ouellette, 2005). Generation of such differences is mostly controlled at the level of ion transport by epithelial cells, a tightly regulated process which is altered during inflammation (Eisenhut, 2006).

A similar puzzle concerns the concentration of defensin at the intestinal epithelial surface. It is reported that most of the antimicrobial activity secreted by the intestinal mucosa is retained in the mucus layer (Meyer-Hoffert *et al.*, 2008), which contributes to an uneven distribution and variable local concentrations of defensin. The average value for defensin concentration in epithelia in general is estimated to be 1-100 $\mu g \cdot mL^{-1}$ (Ganz, 2003). In the gut, secretion of hBD-2 by human colonic biopsies *ex vivo* was in the range of 20-100 $pg \cdot mL^{-1}$ (Aldhous *et al.*, 2009), and in human fecal samples, concentrations of > 50 $ng \cdot mL^{-1}$ of hBD-2 were found, estimated to be a dilution reflecting the luminal content, indicating that indeed much higher concentrations can be found in the mucosa (Mondel *et al.*, 2009).

In the experimental setup developed in this study, a dose of 50 $\mu g \cdot mL^{-1}$ of hBD-2 was selected, in the range estimated to be found in the epithelium and being able to irreversibly impair *E. coli* growth in the described low-salt medium (Figure 4.1). The correlation of our selected conditions to the literature reports on the antimicrobial activity of hBD-2 over *E. coli* is not straightforward. There are different methods used to estimate this kind of activity, many involving incubation in buffers, microdilution and solid growth (Lehrer *et al.*, 1991; Giacometti *et al.*, 2000), which would not fulfill our requirement of an actively growing culture for evaluating the response at metabolite levels. Still, effective concentrations reported employing CFU counts are not far from the ones used here, the LC_{90} (concentration of hBD-2 resulting in 90 % reduction in CFU counts) ranging from 10 to 50 $\mu g \cdot mL^{-1}$ for different *E. coli* strains (Harder *et al.*, 1997; Routsias *et al.*, 2010). Accordingly, determination by culture turbidity of the lowest peptide dose resulting in no increase in O.D. after 12 h, calculated 60 $\mu g \cdot mL^{-1}$ as a minimal inhibitory concentration (MIC) of hBD-2 for *E. coli* (Bals *et al.*, 1998).

For this work, in order to assure reliable reproducibility of the experiments, it was important that the effect of hBD over bacterial growth was stable, which guided the choice of defensin dose and ionic environment. Also for this reason, the defensin challenge was applied to mid-logarithmic phase cultures always at the same O.D. It is known that growth-phase is one of many factors influencing bacterial susceptibility to antimicrobial peptides (Yeaman and Yount, 2003), and that inability of bacterial cells to replicate, as inferred by unchanged

O.D. measurement over time, is one of many variables to consider when determining the viability state of a culture (Davey *et al.*, 2004). However, to achieve our first aim of comparative analysis between normally growing *E. coli* and defensin-challenged bacteria for the release of differential extracellular metabolites, the experimental design was appropriate, and the implications on the physiological state of the challenged cultures will be discussed later.

5.1.2. Identification of extracellular nucleosides

The central finding of this study was the identification of purine nucleosides adenosine (Ado) and guanosine (Guo) as bacterial metabolites present in the extracellular medium after defensin challenge (Figures 4.2 to 4.5). Evidence of the identity of the compounds were collected, including retention time in reversed-phase chromatography, U.V. absorbance spectra, mass and fragmentation patterns. These results were extremely interesting and raised a number of questions regarding the origin of such compounds in the sample. It could be possible that the detection of nucleosides in the MS reflected the presence of other, more complex molecules which could be fragmented during the ionization process, in a similar way as the ions corresponding to the base component were present in the nucleoside's spectra. Thus, it was justifiable to consider searching for other nucleoside-related molecules to understand the nature of the observed HPLC-MS signal.

For instance, we first considered whether the presence of bacterial nucleic acids in the culture medium could result in the detection of the nucleosides. The GC % content of *E. coli* DSM1116 genomic DNA is 50 % (Accession No: PRJNA48011). The composition of the different classes of RNA in turn is variable, influenced for example, by gene expression activity and codon usage patterns (Ermolaeva, 2001). Interestingly, it has been shown in *E. coli* that the GC % content of each single DNA strand also contains equal amounts of the four bases (Rudner and LeDoux, 1974), and that the base composition of different parts of the genome (protein coding genes, structural RNA genes and spacers) correlate with total genomic GC % content, ranging from 40-60 % (Muto and Osawa, 1987). Thus, a similar rate of the four nucleosides would be expected in the HPLC-MS analysis. The presence of nucleosides other than Ado and Guo, as well as deoxynucleosides and bases was investigated in the defensin-challenged culture supernatants and indicated not to be proportionally relevant. This suggested that the mere presence of bacterial nucleic acids in the supernatants would not directly account for the detection of purine nucleosides in these samples. The

possibility that analytical parameters could favor the detection of some molecules over the others cannot be completely excluded, although it is unlikely in the case of similar chemical structures. Additionally, the comparison to commercially available standards Ado and Guo demonstrated a retention-time and U.V. spectra match that would not be observable if the ions resulted from ESI-induced fragmentation of oligonucleotides, for example.

The same was true for other purine compounds which are important signaling mediators, like cyclic AMP (cAMP), cGMP and cyclic-di-GMP, as well as the purine mono-, di, or tri-phosphates and guanosine tetraphosphate (ppGpp). All these molecules have recognized functions in bacterial metabolism and communication. For example, c-di-GMP can regulate bacterial virulence, adhesion, motility and biofilm formation, being responsible for numerous changes in the *E. coli* transcriptional profile (Méndez-Ortiz *et al.*, 2006). Also cAMP is known to be an important messenger in both prokaryotes and eukaryotes, whereas cGMP seems not to be ubiquitous among bacteria (Botsford and Harman, 1992; Linder, 2010; Daniel *et al.*, 1998). The presence of such messengers in the hBD-challenged cultures could have different implications for our study, however, none of them was detected in our analyses. Taken together, this evidence corroborates the conclusion that adenine, adenosine, guanine and guanosine were specifically present in the culture medium in response to hBD-2 challenge.

The quantitative analysis of the four compounds provided further information helping in the interpretation of the data. The rather high price of synthetic hBD-2 peptide was a major bottleneck for these analyses, and therefore, the defensin dose was adjusted to 20 $\mu g \cdot mL^{-1}$, which would have an equivalent effect in *E. coli* growth as at 50 $\mu g \cdot mL^{-1}$, but allowing a higher number of samples to be tested. It was clear that the nucleosides were much more abundant than the corresponding bases, and that Ado was the dominant compound in the challenged culture supernatants (Figure 4.7). It is of course likely that the bases present in the supernatant were derived from the extracellular nucleosides, but this was not specifically addressed in the present study, and the four compounds were always analyzed in the quantitative experiments as a comparison. Although a rather high variation in the calculated absolute concentrations was found among independent experiments, the biological replicates within experiments yielded always similar results, and the relative concentration of the compounds was kept constant in individual repetitions. Moreover, it was interesting to observe that each compound presented a singular correlation to different doses of hBD-2 and followed different kinetics over time after defensin challenge (Figure 4.8 and Figure 4.9). In

particular, the dose- and time-curves of extracellular Ado underlined a distinct character: its presence in the supernatants was dominant at lower doses of defensin, it was the fastest response in the first minutes after challenge, and it presented a sustained increase for up to 48 h after addition of hBD-2. These results raised the interest in determining the mechanism responsible for the presence of the nucleosides in the extracellular medium after defensin stress, as they suggest a specific process was taking place, related but not restricted to the effect on bacterial growth.

5.1.3. Viability and metabolic activity

A first step to elucidate the effect of hBD-2 on *E. coli* and how did this effect result in the presence of extracellular nucleosides was to determine the viability/activity state of the challenged cultures. Commonly, the ability to replicate in a liquid or solid bacteriological medium is regarded as a reliable indication of bacterial viability (Nyström, 2001) and can be assessed with methods like O.D. measurements and CFU counts. Applying such methods in this study, it was clear that hBD-challenged cultures were unable to replicate, even after removal of the stress agent, or replacement of the minimal medium by a rich-medium. However, despite being the gold-standard for determination of antimicrobial activity, this culture-based concept of bacterial viability is sometimes considered too strict since it is known that many bacteria can show limited or even lacking culturability (Strauber and Muller, 2010). Particularly, bacteria submitted to stress conditions can be temporarily non-culturable, or the culture conditions may become unfavorable, even harmful for those cells. In addition, intermediate states of cell injury are difficult to detect by culturing methods (Berney *et al.*, 2007).

The term “viable but non-culturable” (VBNC) is often used to describe such states, when bacteria are unable to replicate but are still intact and active at some level, suggested to be a survival strategy for bacteria facing unfavorable environments. This definition and its use to differentiate live and dead bacteria is a theme of debate, as is the concept of “live” or “dead” bacteria itself (Nyström, 2001). There are at least two other approaches to address bacterial viability which are culture-independent. One is the use of fluorescent dyes and the principle of permeability/exclusion to determine membrane integrity; the most used techniques apply propidium iodide (PI) as a nucleic acid stain which is only able to enter the cells when severe membrane damage is present. The second includes numerous methods to measure specific enzymatic reactions or energy state of the cells, as indicators of their

metabolic activity (Strauber and Muller, 2010). These techniques provide information that complements the culture-based methods in determining the state of a bacterial population as being dead or not. Still, a clear unique definition for microbial death is not easy to achieve, and a combination of methods is desirable to better describe specific states (Breeuwer and Abee, 2000).

The results with the "Live/Dead" fluorescent probes (Figure 4.10 and Figure 4.11) show that hBD-2 caused membrane permeabilization in *E. coli* cultures under the conditions tested. This is consistent with the idea that interaction and destabilization of microbial membranes is the core of defensin antimicrobial activity. According to these data, either using fluorescence microscopy or flow cytometry to address the permeability of the cell to PI, the challenged cultures were regarded as "dead", already at 2 h after hBD-2 addition. The conclusion that these cultures are completely inactive at this point, however, is not immediate. In the cytometry analysis it was possible to see that PI fluorescence of hBD-2 challenged cells seems to be different than that of heat-inactivated cultures. Moreover, some authors have already reported that subpopulations of stressed bacterial cells could be stained with PI while at the same time retaining an intracellularly loaded dye, showing that intermediate states of membrane damage can be formed which allow PI entry, without complete loss of membrane structure. Therefore, assuming that staining with PI is always associated with severe and irreparable membrane breaches may be a simplistic view, and the results could reflect the complexity of the process investigated, rather than a clear death estimation (Graca da Silveira *et al.*, 2002).

Eventually, the question whether the cultures still presented metabolic activity was pivotal to determine if cellular processes were taking place in the non-culturable, membrane compromised cells after defensin challenge. There are several different methods described for the detection of viable bacteria based on their metabolic activity, for example the use of tetrazolium salts as electron acceptors to detect cellular respiration, or detection of esterase activity using fluorescein (Breeuwer and Abee, 2000). Additionally, quantification of ATP extracted from bacterial cultures has been extensively used for decades as a very sensitive technique to enumerate metabolically active cells (Stanley, 1989). We relied on this method to detect even low amounts of ATP indicating the energy status of hBD-challenged cells. We also employed a respiration-based method (using DCIP) to confirm the results obtained with ATP. Taken together, these data (Figures 4.12 and 4.13) indicated that respiration and energy-related processes were severely impaired by the effect of hBD. It is important to note that this

effect was not immediate. Interestingly, it has been described that a related β-defensin which can completely impair *E. coli* growth in CFU assays within 15 min of exposure, still caused general cellular damage 120 min after peptide addition (Yenugu *et al.*, 2004).

Our results on bacterial viability did not provide evidence that cellular activity was correlated to the continued generation of extracellular nucleosides, and rather suggested that the severe damage inflicted by hBD-2 in *E. coli* cells was triggering this response. This was consistent with the fact that once damaged, the cells were unresponsive to a second exposure to defensin (Figure 4.14). In this case, it was expected that the ratio of peptide/cell in the challenged cultures would be a critical issue. Thus, not only increasing doses of hBD-2 would generate higher levels of extracellular response, as observed, but also cell density at the moment of challenge would have an influence on the outcome. This was verified in two additional experiments: one compared the effect of the same hBD-2 dose on *E. coli* cultures of increasing O.D. (Figure 4.15); the second compared the effect of the higher doses on late-logarithmic, high O.D. cultures (Figure 4.16). The results indicated again an independent behavior in the concentration of the extracellular purine compounds. For Guo and the bases, the curves show an optimum at the highest O.D. at which hBD-2 was able to completely impair bacterial growth, supporting the idea that the presence of these compounds in the extracellular medium was a result of severe cellular damage. In turn, the presence of Ado seems to be favored at lower peptide/cell ratios, where intermediate levels of damage would occur.

The interpretation of these results should bear in mind that the growth phase of the target microorganism can influence the activity of defensins. It has been shown that susceptibility of *Staphylococcus aureus* to hBD-3 is higher in the stationary phase, and this was correlated to changes in the expression of two important mediators of membrane changes which lead to resistance (Matsuo *et al.*, 2011). On the other hand, both hBD-2 and -3 were reported to have antimicrobial activity against *Campylobacter jejuni* which was not influenced by growth-phase (Zilbauer *et al.*, 2005). Also, some highly cationic α-defensins seem to have equal potency against metabolic energetic or quiescent bacteria, whereas others are more active against highly energized cells. This reflects the influence of membrane energetics on the interaction of defensins with their targets, and can explain differences in the antimicrobial activity in different physiological states (Yeaman and Yount, 2003).

Also important to consider is that the peptide concentration, together with membrane parameters, will determine the threshold concentration, the amount of peptide molecules

accumulated in the target surface necessary to drive the initial electrostatic interaction into a permeabilization process (Yeaman and Yount, 2003). Interestingly, it is appreciated that sublethal concentrations of antimicrobial peptides can cause distinct and selective responses from bacteria which are not necessarily involved in their mechanism of microbial killing. Such responses have been investigated at the transcriptional level in *E. coli* and demonstrated that changes in transcript levels are observed when bacteria were treated with sublethal doses of an insect antimicrobial peptide, which are not paralleled by the changes induced using lethal concentrations (Hong *et al.*, 2003).

5.1.4. Specificity of the response

Taken together, the comparative quantification of the extracellular compounds in response to hBD challenge suggest that, at least in the case of Ado, this response presented traits which were independent of the purely membrane-targeted antimicrobial activity. From another point of view, if the presence of extracellular nucleosides would be an unspecific, passive consequence of the killing effect of hBD, it would be expected that other antimicrobial peptides active against *E. coli* would trigger a similar reaction. This was verified by testing four other antimicrobial peptides (Figure 4.17), and demonstrated that they clearly differ in their ability to induce the extracellular metabolites. Interestingly, this activity seems not to be related to a specific structural class. Three representatives of the β-sheet folded human defensins relevant in the context of intestinal epithelia were tested (hBD-2, hBD-3 and α-defensin-5) and hBD-2 demonstrated the strongest induction of extracellular nucleosides. Given the important role described for this defensin in IBD, especially in UC patients (Wehkamp *et al.*, 2003), this result supports a relevance for this bacterial-host interaction in the inflamed gut.

In turn, the mammalian (sheep) α-helical peptide SMAP-29 resulted as well in the distinct presence of Ado in the extracellular medium, whereas this was not observed with the amphibian α-helical peptide magainin. While a more detailed investigation would be necessary to correlate specific structural features to the observed response, these results indicated that generation of extracellular nucleosides is not a general property of different or even closely related peptides. Indeed, it is known that secondary structuring is an important player in the membrane-targeted effects of antimicrobial peptides but the interactions with other cellular targets and sometimes alternative mechanisms of action are found in peptides belonging to different structural classes (Powers and Hancock, 2003).

Conversely, we hypothesized whether the response could be triggered by hBD-2 in different strains of *E. coli*, or different bacterial species. It was evident that even though the parameters which we have determined to influence the response, namely peptide concentration and cell density, were equal for all different strains tested, as was the replication-impairing effect measured by CFU counts, the extracellular response was different among the strains tested (Figure 4.18). The results have to be taken carefully, as a more complete characterization of the response for each strain was not performed as in the case of DSM1116. The differences observed can reflect the fact that the effector mechanism of one peptide can be different for different bacteria (Powers and Hancock, 2003). Particularly, in the case of hBD-2 –*E. coli* interactions, testing the susceptibility of 18 different clinical isolates of *E. coli* to hBD-2 (10-50 $\mu g \cdot mL^{-1}$) revealed differences and similarities in the survival curves among the strains (Routsias *et al.*, 2010).

The five strains tested in the present study represent some of the different ecological roles of *E. coli*, which is a facultative anaerobe species highly adapted to the human intestine. It is also a very versatile species including a diversity of environmental, commensal, probiotic and pathogenic strains, most of them with an extracellular lifestyle, but some pathogens are also found as truly intracellular organisms (Kaper *et al.*, 2004). Recently, an interesting study analyzed metabolic networks reconstructed from the available genomes of 29 *E. coli* strains, including commensal and pathogenic variants. The authors described a high proportion of reactions which were common to all strains, revealing the low level of diversity in metabolism is in contrast to the higher variation found in their genomes. Yet, they were able to identify sets of reactions which were related to specific pathogenic or commensal phenotypes (Vieira *et al.*, 2011). This suggests that further investigations comparing strains of different lifestyles in their extracellular responses to defensin could improve the understanding of the physiological role of such responses.

In the present work, in comparison to the *E. coli* laboratory reference strain (DSM1116), we tested two uncharacterized clinical isolates (7145A and HZI 2-6), one adherent-invasive intestinal pathogen (LF82) and one probiotic strain (*E. coli* Nissle 1917, EcN). It was interesting to observe the apparent lower responsiveness of the pathogenic strain regarding the generation of extracellular compounds, which was paralleled by one of the isolates (Figure 4.18). In turn, it was clear that hBD-2 induced a distinctively high response in the probiotic strain. We currently do not know the exact relevance of the observed differences, which could result from different adaptability of each strain to the growth

conditions, with possible effects in the interaction with the defensin itself. Still, it seems noteworthy that the interaction of hBD-2 with EcN yielded a clear response, with high concentration of Ado present in the supernatant. This probiotic strain has a prominent role in modulating host immune system. Importantly, it has been already successfully employed in clinical trials as a therapy for IBD (Schultz, 2008). Among the immunomodulatory activities described are upregulation of TLR receptors and adaptor proteins, as well as modulation of cytokine profiles in intestinal epithelial cells (Hafez *et al.*, 2010; Huebner *et al.*, 2011). The ability of *E. coli* Nissle 1917 to induce hBD-2 production by intestinal epithelial cells, a NF-κB dependent response triggered by bacterial flagellin, has been reported as a possible mechanism by which this strain contributes to enhanced barrier function with beneficial consequences for IBD patients (Wehkamp *et al.*, 2004; Schlee *et al.*, 2007). Moreover, *E. coli* Nissle 1917 can inhibit *in vitro* epithelial adherence and invasion by LF82 as demonstrated by co-infection studies in Caco-2 and ATCC CCL6 cell lines (Boudeau *et al.*, 2003; Huebner *et al.*, 2011). The partially sequenced genome of *E. coli* Nissle 1917 (Sun *et al.*, 2005), as well as the complete available genome of DSM1116 (= strain W = ATCC 9637; Accession No: PRJNA48011) and LF82 (Accession No: PRJNA33825) can be valuable tools for further exploration of strain-specific responses to defensins.

The Gram-negative *Klebsiella pneumoniae* and *Pseudomonas aeruginosa* were not susceptible to hBD in the conditions tested, as shown by the growth curves. Indeed, other studies had already reported a general lower susceptibility of *K. pneumonia* strains to hBD-2 compared to *E. coli*, although the same study actually pointed a higher susceptibility for *P. aeruginosa* (Routsias *et al.*, 2010). In our experiments, those species did not produce an equivalent extracellular response, when compared to the corresponding situation of partial growth inhibition in *E. coli*. Whereas *K. pneumonia* seemed to be able to produce the compounds but was much less responsive, *P. aeruginosa* was completely devoid of such response. Importantly, the effect of hBD-2 on *P. aeruginosa* growth in our assay was also rather peculiar, and further investigation would be demanded to better understand these results.

In conclusion, the presence of extracellular purine compounds was demonstrated as a consequence of bacterial challenge with antimicrobial peptide, which was dependent on the peptide and the bacterial species. In particular, the generation of extracellular Ado was accentuated among the compounds identified and it seems to involve a response correlated to cell damage, but at least partially independent of the bacteriocidal effect. Considering this,

and the fact that Ado is a very versatile molecule already known to play a variety of roles in host-microbial interactions and immunomodulation in humans, we were prompted to focus on this compound to further investigate the mechanisms implied in the observed microbial response to defensin, as well as the possible consequences for the host.

5.2. Putative mechanisms for the generation of extracellular Ado

5.2.1. Multiple activities of defensin

The exact mechanism of action of antimicrobial peptides has been extensively debated. The general concept is that they primarily interact with microbial membranes, however in some cases, the membrane is not the main target of the bacteriocidal activity (Brogden, 2005; Nicolas, 2009). The interaction and permeabilization of *E. coli* inner and outer membrane by defensins has been shown in early studies with HNP-1 (Lehrer *et al.*, 1989) and more recently with hBD analogues (Krishnakumari *et al.*, 2006). Our data using fluorescence staining revealed extensive membrane damage, but the response kinetics and the results with cultures at different growth-phase argued that a mechanism beyond cell disruption was triggering the generation of extracellular Ado. This was further confirmed by the absence of intracellular macromolecules in the challenged culture supernatants (Figure 4.20), together with the evidence that by using disruption protocols no extracellular purine compounds could be detected.

Furthermore, transmission electron microscopy (TEM), as well as DAPI-stain imaging analysis (Figure 4.21 and Figure 4.22) showed that a large population of hBD-2 challenged cells indeed kept their intracellular contents at a time point when high levels of extracellular Ado were already detected. In contrast to our findings, clear areas of discontinuity in the cell wall, along with leakage of intracellular material have been observed by TEM as the main consequences of β-defensin analogs activity at micromolar concentrations on *E. coli* (Krishnakumari *et al.*, 2006). For other Gram-negative species (*Moraxella catarrhalis* and *Haemophilus influenza*) the formation of membrane blebs after incubation with hBD-2 (10 $\mu g \cdot mL^{-1}$) has been described (Lee *et al.*, 2004). The high level of plasmolysis observed in our results has not been reported in any of those cases, however, a retraction of the cytoplasmic membrane has been observed in *Salmonella typhimurium* treated with sub-lethal concentrations of porcine β-defensin (Veldhuizen *et al.*, 2008). Changes in the periplasmic environment of *E. coli* and other Gram-negative bacteria can trigger envelope stress

responses, mediated by the alternative σ-factor E, which in turn regulates a number of cellular processes, including nucleic acid metabolism (Ades, 2008; Rhodius *et al.*, 2006). Interestingly, the induction of plasmolysis by mannitol in *E. coli* revealed that dissociation of outer and inner membrane protected bacteria from killing by HNP-1, probably impairing the access of the defensin to the cytoplasmic membrane, the disruption of which likely being the final lethal event (Lehrer *et al.*, 1989).

Also the formation of pores as postulated for many antimicrobial peptides could not be observed in our samples. The interaction of α-defensins with membranes have been modeled (Wimley *et al.*, 1994), but experimental data on most defensins are still not readily available (Ganz, 2003). According to the models proposed by Wimley *et al.*, 1994 for HNPs in unilamellar vesicles, pores of maximum 25 Å diameter could be formed, as the peptide allowed total diffusion of a 400 Da molecule (6 Å) and, to a lesser extent, of a 4,400 Da dextran (18 Å), but only partially induced the leakage of a bigger dextran (19,000 Da, 29 Å). However, X-ray crystallography studies on hBD-2 revealed that this peptide is unlikely to arrange in channel forming oligomers, and that the carpet-like model of membrane interaction would better explain the mode of action for this defensin. In model vesicles, hBD-2 (0.125 μM) caused release of the small (400 Da) marker, but not of molecules of 3,000 Da or more (Hoover *et al.*, 2000). This model would support the conclusion that small metabolites could be released from *E. coli* following hBD challenge independent of a general lysis event. However, this effect alone would not explain the differential presence of Ado in the studies supernatants.

In addition to the action on the target membrane, it is possible that other intracellular effects of hBD-2 are involved in the generation of extracellular purine compounds by *E. coli*. Evidence for a membrane-independent action mechanism of antimicrobial peptides comes from the temporal dissociation between membrane permeabilization event and the effective killing of the target (Nicolas, 2009). This was observed for example by the effect of the amphibian linear peptide temporin L on *E. coli* (Mangoni *et al.*, 2004). Indeed Pazgier *et al.*, 2006, based on the narrow range of bacterial species where the whole net charge has been correlated to susceptibility for β-defensins, suggested that other membrane-independent mechanisms might be implicated in the antimicrobial activity of these peptides. The recognition of alternative modes of action has been hampered in many cases because high concentrations of peptide are demanded for structural studies. The use of peptide concentrations close to the lethal dose for mechanism characterization, as has been done in the

present study, may favor the identification of different mechanisms and intracellular targets (Nicolas, 2009).

One such mechanism already described for some cationic antimicrobial peptides and highly relevant in the context of the present study involves direct interactions with bacterial nucleic acids (Lan *et al.*, 2010). This activity would be consistent with the relatively strong negative charge of nucleic acids. Here we demonstrated that hBD-2 is able to interact *in vitro* with genomic DNA and total RNA isolated from *E. coli* (Figure 4.24). The description of small peptides interacting to nucleic acids dates back from early 90's, when it has been reported that the β-sheet tachyplesin I binds to DNA and implications for its antimicrobial activity have been inferred (Yonezawa *et al.*, 1992). In addition, similar activity was found as well in β-sheet human defensin α-1 associated with DNA fragmentation in the unicellular protozoan parasite *Trypanosoma cruzi* (Madison *et al.*, 2007). Also, the α-helical antimicrobial peptide buforin II has been reported to bind *E. coli* DNA and RNA (Park *et al.*, 1998). The α-helix structure seems not to be required for the binding property, and the analogous α-helical magainin II has a much lower ability to bind bacterial nucleic acids (Lan *et al.*, 2010). This may be related to our observations that challenge with the closely related magainin I was not able to induce extracellular nucleosides in *E. coli* cultures and argues that the capacity of hBD-2 to interact with *E. coli* nucleic acids has a role in the observed extracellular response. Moreover, the present data represent to our knowledge the first description of a nucleic acid interaction activity for hBD-2.

5.2.2. Source of extracellular Ado

Interestingly, the generation of Ado was substantially increased by addition of either DNA or RNA to the soluble component of the *E. coli*-hBD-2 system, but not to the challenged cells or pure hBD-2. This indicated that a bacterial factor present in the supernatants was necessary to accomplish Ado accumulation following hBD-2 interaction with the nucleic acids. In this regard, it was unclear how the addition of DNA also resulted in the formation of the ribonucleoside and not deoxyribonucleoside, and it might involve enzymatic reactions and regulatory mechanisms which were not addressed in this study. Also, co-elution of RNA in DNA purification process cannot be excluded. A deeper investigation of the nature of hBD-2 interaction with *E. coli* nucleic acids remains to be done employing, for example, thiazole orange fluorescence intercalator displacement (TO-FID), circular dichroism

or comet assay, which could further elucidate whether nucleic acid binding and/or fragmentation by hBD-2 are involved.

A very powerful method that can be used to track the origin or fate of a molecule of interest is the use of stable isotope labeling. It is widely employed in the study of complex communities, for example, to probe biomarkers of taxonomic relevance, such as membrane lipids and nucleic acids, as well as to indicate substrate consumption (Neufeld *et al.*, 2007; Evershed *et al.*, 2006; Friedrich, 2006; Abraham *et al.*, 1998). Other authors have reported the efficiency of ^{13}C labeling of DNA and RNA in *E. coli*, which is an approach of choice for producing isotopically labeled nucleic acids and nucleotides for structural studies (Thakur *et al.*, 2010; Dayie and Thakur, 2010). In the present work, the method was applied to test the hypothesis that the extracellular Ado generated by hBD-2 challenged cultures was directly derived from bacterial nucleic acids. This approach represents a simplified application for the established use of ^{13}C labeling in metabolic flux analysis, which aims at the characterization of networks within the central carbon metabolism of microorganisms (Wiechert, 2001). Here, we measured ^{13}C enrichment ($\delta\ ^{13}C$) in *E. coli* nucleic acids and compared it to the values found in extracellular Ado (Figure 4.25). The results support the conclusion that Ado was not newly synthesized after hBD challenge, but instead derived from the intracellular RNA pool.

To gain insight into the events resulting in the observed accumulation of extracellular Ado, the corresponding adenosine nucleotides were investigated as possible precursors. Figure 5.1 shows an overview of purine metabolic pathways in *E. coli*, with emphasis for the reaction addressed in this study. The majority of purines are found intracellularly as nucleotides, most of them as part of RNA or DNA, which represent respectively ~ 20 % and 3 % of the total biomass in *E. coli* grown in glucose minimal medium. Synthesis of nucleic acids, together with the utilization of ATP and GTP as energy sources, create the greatest net demand for nucleotides (Castellanos *et al.*, 2004; Domach *et al.*, 1984).

In intact cells, the flux of purine nucleotides across the outer membrane is not fully understood, but believed to be mediated by two major porines, OmpF and OmpC. These are channel forming proteins present in outer membrane of Gram-negative bacteria which allow the passive diffusion of hydrophilic molecules of up to 700 Da (Watanabe *et al.*, 2011). In the periplasmic space of *E. coli*, three enzymes have been found involved in purine metabolism. Adenylate kinase (E.C. 2.7.4.3) can interconvert ADP into ATP and AMP, and 5' nucleotidase (E.C. 3.1.3.5) dephosphorylates AMP to Ado. Ado can be further metabolized to adenine free base by purine-nucleoside phosphorylase (E.C. 2.4.2.1), or directly taken up via

nucleoside transporters (NupC and NupG) present in the cytoplasmic membrane (Watanabe *et al.*, 2011).

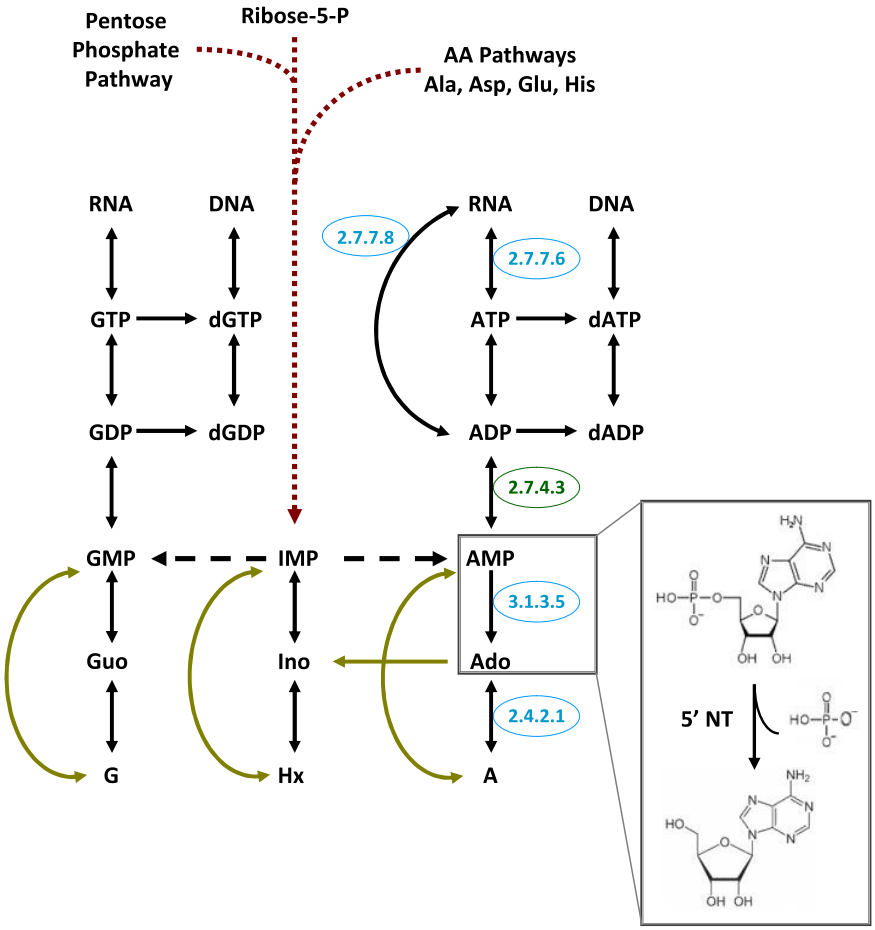

Figure 5.1 - Overview of purine metabolism in *E. coli*. Reactions of the de novo synthesis and salvage pathway are represented by red and yellow arrows, respectively. Dashed arrows indicate that more than one enzymatic step is involved. E.C. numbers are given for the enzymes discussed in sections 4.2.2 and 5.2.2. Enzymes represented in blue are common for guanine and adenine compounds, whereas the enzyme in green is exclusive for adenine nucleotides. EC 2.7.7.6: RNA polymerase; EC 2.7.7.8: polynucleotide phosphorylase/polyadenylase; EC 2.7.4.3: adenylate kinase; EC 3.1.3.5: 5' nucleotidase; EC 2.4.2.1: purine-nucleoside phosphorylase. In detail, the reaction catalized by 5' nucleotidase (5'NT). Ino: inosine; Hx: hypoxanthine. Source: Kyoto Encyclopedia of Genes and Genomes (KEEG,) Pathway Database.

We have found indications that Ado was generated from AMP in hBD-2 challenged *E. coli* supernatants. AMP was rapidly produced by challenged cultures in the first 6 h and its subsequent depletion was found to correlate with formation of Ado in whole cultures, as well as in cell-free supernatants (Figure 4.28). In contrast, intact *E. coli* accumulated extracellular AMP, a reaction which was not explained in the present experiments, but might be related to RNA degradation and purine excretion documented in stationary-growth phase *E. coli* (Okamura *et al.*, 1973; Rinas *et al.*, 1995). Unchallenged cultures also showed accumulation of extracellular ATP (Figure 4.26), whereas in hBD-2 challenged culture supernatants the presence of ATP, as well as ADP, was not evident. Particularly concerning ATP, it is important to consider that the presence and/or depletion of this molecule could directly influence the host's immune system. Extracellular ATP is largely recognized for its functions in cell-cell communication and as potent inflammatory mediator acting via P2 purine receptors in human cells (Trautmann, 2009). For instance, bacterial derived ATP in the intestinal lumen has been implicated in mucosal T-cell differentiation and exacerbated inflammation in murine colitis model (Atarashi *et al.*, 2008). Interestingly, it has been appreciated that the membrane-permeabilizing effect of certain antimicrobial peptides can trigger ATP release from microbial cells, generating an additional signal for enhancing immune responses (Vylkova *et al.*, 2007). In addition, extracellular ATP can also induce responses in bacterial cells, promoting biofilm formation and epithelial adherence by *E. coli* (Xi and Wu, 2010).

However, in our analysis ATP could not be detected, and we have focused on investigating the involvement of AMP as a precursor for Ado formation in defensin-challenged *E. coli*. Further evidence was obtained at lower doses of hBD-2 (< 10 $\mu g \cdot mL^{-1}$) and by comparing the different antimicrobial peptides for AMP accumulation (Figures 4.29 and 4.30). It seems that the inability to induce extracellular Ado is a consequence of impaired AMP dephosphorylation, which would implicate 5' nucleotidase as a central player in hBD-2 induced extracellular Ado production. As a periplasmic enzyme, *E. coli* 5' nucleotidase is readily released in the extracellular medium under conditions of osmotic stress and it is possible that a similar response is triggered by defensin-induced membrane damage. In this regard, the differences in the response observed for *P. aeruginosa* and *K. pneumonia* in comparison to *E. coli* could be explained by differences in the distribution of their respective 5' nucleotidases. In *E. coli*, > 90 % of the 5' nucleotidase activity is located in the periplasmic space and released by osmotic shock (Watanabe *et al.*, 1986; Broad and Smith, 1981). In

contrast, less than 50 % of the enzyme can be recovered by this treatment from *K. pneumonia* and *P. aeruginosa*, and it has been suggested that *P. aeruginosa* nucleotidase is bound in the periplasmic space in a manner distinct to those of other periplasmic enzymes (Neu, 1968; Glick and Garber, 1983; Bhatti *et al.*, 1976). On the other hand, indications have been found that an elongated character of *E. coli* 5'nucleotidase may facilitate its release from cells in conditions where other globular proteins of similar molecular mass would be retained, irrespective of their subcellular localization (Broad and Smith, 1981), and this agrees with the hypothesis that this enzyme is present in the supernatants of hBD-challenged cultures even when no increase in the total extracellular protein content is observed.

The differences in the ability of other antimicrobial peptides tested to induce extracellular Ado are still unclear. Observing that accumulation of AMP in the medium is more strongly induced by peptides which were not able to promote Ado generation, points to the notion that a combination of membrane effects and intracellular (nucleic acids) targets determines the final outcome. Importantly, mechanically induced disruption of *E. coli* cells does not result in the presence of either Ado or AMP in the medium (data not shown). The processes that lead to AMP formation in the defensin challenged cultures remain to be characterized, as it is speculated whether the direct interaction of hBD-2 with bacterial nucleic acid can cause degradation or induce other enzymatic mechanisms to do so. The accumulation of extracellular AMP upon addition of nucleic acids to the system (Figure 4.31) was observed in the cellular fraction of the challenged cultures, where the subsequent conversion to Ado was deficient, as opposed to what was seen in the soluble component. In turn, direct addition of exogenous AMP to the cultures boosts the generation of extracellular Ado by the cell-free supernatants to higher extents than addition of nucleic acids (Figure 4.32), suggesting that the generation of AMP from nucleic acids is a limiting step.

Taken together, the data presented here allow the suggestion of a novel mechanism by which hBD-2 cause accumulation of extracellular Ado by bacteria during the bacteriocidal process, and opens new questions regarding the interaction of the antimicrobial peptide with its targets. For instance, investigating the relative contribution of DNA or RNA as precursors of the extracellular nucleosides, as well as the reasons leading to distinct proportion of purines and pyrimidines can be valuable for understanding the whole process. These questions were not addressed in the present study and go beyond the scope of this discussion. Considering the complete pathway of nucleotide metabolism in *E. coli,* the role of enzymes which are known to have differential activity towards adenine nucleotides, or a preference for ribonucleotides

instead of deoxyribonucleotides, as well as the involvement of DNA repair mechanisms and stress responses, represent interesting targets for further analysis.

5.3. Adenosine in the inflamed gut

The present work reported the generation of extracellular Ado by an intestinal bacterium in response to a host defense peptide. A series of experiments using the human intestinal epithelial cell line (Caco-2) was performed to investigate possible effects of the bacterial products on host signaling, specifically the NF-κB pathway. The results represent initial indications of a putative role for the described microbial compounds in modulating epithelial cells responses. The highlighted presence of extracellular adenosine in the studied bacterial supernatants draws attention to the diversity of biological activities presented by Ado and to the prominent role of this compound in inflammatory processes. Many studies have already addressed different aspects of Ado signaling, as well as its involvement in gastrointestinal inflammation, infection and host-microbial interactions. The following discussion, which has been edited and partially published in a review article (Estrela and Abraham, 2011), presents an integrated summary of this knowledge, particularly focusing on the consequences of Ado signaling modulation for the outcome of IBD and related conditions.

5.3.1. Diverse effects of Ado in inflammation

Ado is a very versatile signaling molecule, with biological activity in many different tissues and cell types. In human tissues, the levels of extracellular Ado are estimated around 1μM under physiological conditions, and are increased up to 100-fold in situations of cellular stress, such as ischemia, trauma, hypoxia or inflammation (Hasko and Cronstein, 2004). The main source of extracellular Ado is the catabolism of ATP released from stressed cells. Extracellular ATP is degraded to Ado by the action of membrane ectonucleotidases like CD39 (ENTPD1 or apyrase, which converts ATP to ADP and AMP) and CD73 (ecto-5'-nucleotidase, which converts AMP to adenosine). The presence of Ado in the extracellular space can be limited by conversion to inosine catalyzed by adenosine deaminase (ADA), or by intracellular phosphorylation to AMP by adenosine kinase (Hasko and Cronstein, 2004). Membrane nucleoside transporters of two types are also important regulators of extracellular Ado levels: the active, sodium-dependent concentrative nucleoside transporters (CNT) and the

passive, diffusion-driven equilibrative nucleoside transporters (ENT) (Loffler *et al.*, 2007, Ye and Rajendran, 2009).

There are four cell surface receptors known to respond to Ado, namely A_1, A_{2A}, A_{2B} and A_3 adenosine receptor (AR). They contain seven transmembrane domains and are intracellularly coupled to GTP-binding proteins. A_1 and A_3 receptors couple to and activate $G_{i/o}$ proteins that inhibit adenylate cyclase, leading to decreased cAMP levels, while A_{2A} and A_{2B} receptors couple to G_s proteins, stimulating cAMP accumulation (Fredholm *et al.*, 2001a). cAMP, in turn, is a very important second messenger involved in numerous cellular functions, like regulation of gene expression via protein kinase A (PKA) and the cAMP response element binding (CREB) protein. Other pathways engaged by ARs include phospholipase C (PLC) and Ca^{2+} signaling, mitogen-activated protein kinase (MAPK), phosphoinositide 3-kinase (PI3K), protein kinase B (PKB or Akt) and NF-κB-mediated gene regulation (Jacobson and Gao, 2006). ARs can modulate all these different processes in a cell type-, time- and concentration-dependent fashion. Importantly, during inflammation, all four AR subtypes have been reported to be upregulated (Sundaram *et al.*, 2003, Kolachala *et al.*, 2005a, Fortin *et al.*, 2006).

The role of Ado during inflammation in the gut is a result of its different effects on intestinal epithelium and immune cells present in the mucosa. Here it is important to highlight that each cell-type usually expresses more than one receptor subtype, and that there are many variables contributing to the final effect of Ado signaling. Ado changes cAMP levels with EC_{50} 0.3 μM for A_1 and A_3 receptors and 0.7 μM for A_{2A} receptor, which means they are responsive to physiological concentrations of extracellular Ado. The potency of A_{2B} AR, however, is much lower (EC_{50} 24 μM) and it can be activated mainly in pathophysiological conditions (Fredholm *et al.*, 2001b). In intestinal epithelial cells A_{2B} is the predominant Ado receptor expressed (Strohmeier *et al.*, 1995). Immune cells, in turn, express A_1 and A_{2A} AR, which has been extensively linked to the anti-inflammatory properties of Ado (Gessi *et al.*, 2000; Panther *et al.*, 2001; Koshiba *et al.*, 1997; Deaglio *et al.*, 2007). In neutrophils, for example, at low Ado levels, activation of A_1 receptor promotes chemotaxis and tissue infiltration. At higher concentrations present at the site of inflammation, Ado is known to inhibit effector functions via A_{2A} receptor, attenuating tissue damage. Adherence to endothelium is also regulated by these two receptors in a way that A_1 stimulates and A_{2A} suppresses the process (Cronstein *et al.*, 1990; Cronstein *et al.*, 1992). Similarly, in dendritic cells (DC) expression pattern of different Ado receptors subtypes changes during maturation.

In immature DC, Ado signaling, mainly through A_1 AR promotes chemotaxis. After LPS-induced maturation, A_{2A} AR responds to Ado resulting in reduced IL-12 production (Panther *et al.*, 2001).

Further interactions between different receptor subtypes also need to be considered. Studies in human peripheral-blood mononuclear cells (PBMC) demonstrated that Ado-induced reduction of pro-inflammatory cytokine production is reversed by A_{2A} blockage, but enhanced by inhibition of A_1 or A_3 receptors. Agonists for A_1 and A_3 receptors, in turn, could abolish the effect on cytokine levels when A_{2A} was activated by a selective agonist in a similar way as the A_{2B} antagonist (Takahashi *et al.*, 2007). Such interactions may result from the opposite effect of A_1 and A_3 versus A_2 receptors in intracellular cAMP concentration and reflect the differential modulation of signal transduction pathways by each receptor subtype. Also dealing with the paradoxal effect of Ado in immune responses, a recent study indicated that, despite the supressive effect on T-cell activation, a pre-exposure to Ado leads to desensitization of cAMP signaling, resulting in enhanced T-cell responses (Yang *et al.*, 2010). A similar mechanism had also been described for dendritic cells, Ado pre-exposed cells presenting subsequently higher activation by pathogen-associated molecular patterns (PAMPs) and also higher capacity of stimulating T-cells (Flach *et al.*, 2009). In this context, the different characteristics of Ado-affinity presented by the different receptors and their expression patterns in different cell-types define the importance of Ado levels and its temporal-dynamics during inflammation as crucial players in the overall effect of Ado signaling, ranging from a protective, anti-inflammatory modulation to a strong pro-inflammatory induction.

Anti-inflammatory effects. The protective effects of Ado in inflammation and consequent tissue damage were known, but poorly understood until a study with A_{2A} adenosine receptor knockout mice showed a striking inflammatory phenotype, with extensive liver damage in response to concanavalin A in the absence of the receptor (Ohta and Sitkovsky, 2001). Those results drew attention to the therapeutic potential of modulating A_{2A} signaling to control inflammation. There are a number of studies describing inhibitory effect of Ado on pro-inflammatory cytokine production by different immune cells. For example, Ado can reduce IL-12 and TNF-α production by murine macrophages, an effect partially mediated by A_{2A} receptor (Hasko *et al.*, 2000). Conversely, in two independent reports, A_{2B} and A_3 receptors had also been implicated in suppression of TNF-α production by murine

macrophages (Kreckler *et al.*, 2006; Martin *et al.*, 2006). Furthermore, A_{2B} receptor activation in LPS-stimulated mouse macrophages is responsible for increased anti-inflammatory IL-10 production, by mediating the relief of a posttranscriptional repression mechanism (Nemeth *et al.*, 2005). Interestingly, A_{2B} knockout mice developed enhanced inflammation after an intestinal ischemia/reperfusion event, while A_{2B} agonist treatment protected wild-type mice from intestinal injury (Hart *et al.*, 2009).

A_{2A} receptors, in turn, are able to mediate the inhibition of IL-12 and simultaneous induction of IL-10 production by human monocytes (Link *et al.*, 2000). In murine $CD4^+$ T cells, signaling through T-cell receptor (TCR) increase A_{2A} transcription and the consequent accumulation of cAMP, which in turn reduce TCR-mediated IFN-γ production (Lappas *et al.*, 2005). Also important for T cell activation are the effects of Ado in dendritic cells and regulatory T cells (Treg). As discussed above, the expression of A_{2A} receptors in mature DC has anti-inflammatoy effects. Moreover, A_{2B} receptors were reported to play an important role in Ado-induced inhibition of pro-inflammatory cytokines, as well as in enhanced IL-10 production and reduced levels of major histocompatibility complex (MHC) II and CD86 expression by DC, resulting in less effective T-cell activation (Wilson *et al.*, 2009). Indeed, adenosine deaminase activity is an important mechanism of dendritic cells to maintain their activation in the high-Ado environment of inflamed tissues (Desrosiers *et al.*, 2007). In Tregs, the generation of Ado by expression and activity of CD39 and CD73 is essential to maintaining their anergic state and suppression of T cell responses (Deaglio *et al.*, 2007; Kobie *et al.*, 2006).

An anti-inflammatory role for A_1 receptors had also been demonstrated in murine macrophages and mesothelial cells. The preconditioning with A_1 agonists reduced sera levels of TNF-α and IL-6 in response to bacterial inoculation. This effect could be reversed not only by A_1, but also by A_{2A} antagonists. Interestingly, activation of A_1 receptor was shown to induce A_{2A} expression. These observations, together with the absence of preconditioning effect in A_{2A} knockout mice, indicated that A_1 agonists can reduce inflammation by induction of A_{2A} (Nakav *et al.*, 2008). In human intestinal epithelium, using HT-29 cells as a model, a reduction of MAPK phosphorylation and IL-8 expression and secretion in response to pro-inflammatory stimuli, including TNF-α, IL-1 and LPS, was observed when the cells were pre-incubated with Ado, showing a negative-regulation effect on the inflammatory process (Jijon *et al.*, 2005). Also, attenuation of hypoxia-induced inflammation in intestinal mucosa could be observed with inhibition of ENT-2, which is responsible for Ado uptake by epithelial cells

limiting extracellular Ado levels, demonstrating a protective effect of intestinal Ado in this condition (Morote-Garcia *et al.*, 2009).

Pro-inflammatory effects. Ado acting through the A_{2B} receptor in T84 cells stimulates luminal secretion of IL-6 in similar levels as induced by pro-inflammatory agents like TNF-α or *Salmonella typhimurium* colonization. Interesting to note is that the concentration of IL-6 released is able to induce intracellular Ca^{++} influx and subsequent degranulation in neutrophils (which are a source of AMP, converted to Ado by intestinal ectonucleotidase), resulting in a pro-inflammatory signaling loop (Sitaraman *et al.*, 2001). Expression of IL-6 is also induced by A_{2B} activation in the epithelial-like cell line U373 MG (Fiebich *et al.*, 2005). Another study found indications of a pro-inflammatory role for A_{2B} receptors, observing that under stimulation with the stable Ado analog NECA (5'-N-ethylcarboxamidoadenosine), the production of IL-6 by macrophages *ex vivo*, and also IL-6 levels in blood plasma *in vivo*, were enhanced. This effect could be reversed by genectic ablation of the receptor, as well as by selective A_{2B} antagonists. In contrast, the anti-inflammatory effect of NECA in this model, supression of TNF-α release after LPS-activation, was not inhibited in the absence of A_{2B} activation, indicating this effect is mediated by a different receptor (Ryzhov *et al.*, 2008a). Accordingly, A_{2B} receptor has also been implicated in stimulation of pro-inflammatory responses in human mast cells, like secretion of IL-4 and IL-13. Indeed, genetic ablation of A_{2B} receptors in mast cells, as well as pharmacological inhibition, impaired Ado-induced degranulation and secretion of IL-6, IL-13 and vascular endothelial growth factor (VEGF) (Ryzhov *et al.*, 2008b). Stimulation in mast cells of angiogenic factors secretion, like VEGF and IL-8, links Ado signaling to angiogenesis, another important feature of chronic inflammation (Jackson *et al.*, 1997). Selective activation of A_{2B} receptors induced IL-8 and VEGF in human mast cells, whereas the A_3 receptor was responsible for enhanced angiopoietin-2 expression. The ability of mast cells to induce capillary formation *in vitro* was optimal when both receptors were activated, denoting a cooperative function in promotion of angiogenesis (Feoktistov *et al.*, 2003). Moreover, a complex regulation of dendritic cells maturation has been attributed to A_{2B} receptors, its activation during monocyte differentiation leading to the formation of a phenotipically distinct DC subtype. Besides the anti-inflammatory effects observed (in accordance to Wilson *et al.*, 2009 as discussed above), DC generated in the presence of Ado displayed increased expression of pro-inflammatory factors

such as IL-6 and cyclooxygenase-2, as well as increased secretion of VEGF and IL-8, therefore being more angiogenic as compared to the conventional DC (Novitskiy *et al.*, 2008).

Regulation of Ado receptors expression. On the other hand, cytokines can also regulate Ado signaling at several levels. For example, it has been demonstrated that the expression of A_{2B} receptor in T84 cells is upregulated by TNF-α , highly present in chronic inflammatory diseases (Kolachala *et al.*, 2005a) whereas IFN-γ, another important mediator in chronic inflammation, is implicated in downregulation of adenosine-mediated signaling, not affecting receptor expression, but by direct inhibition of adenylate cyclase (Kolachala *et al.*, 2005b). However, in murine macrophages, IFN-γ presented a direct enhancing effect in A_{2B} expression, which in turn mediated the inhibition of IFN-γ -induced pro-inflammatory responses, suggesting a negative-feedback loop for controlling macrophage activity (Xaus *et al.*, 1999). The expression of A_{2A} receptor is upregulated by the Th1 pro-inflammatory cytokines TNF-α and IL-1β in human neutrophils (Fortin *et al.*, 2006) and in THP-1 cells, where these two cytokines enhanced the effect of A_{2A} agonist in suppression of IL-12 and stimulation of IL-10 production (Khoa *et al.*, 2001). The responses were instead attenuated with IFN-γ treatment, which reduced A_{2A} expression by these cells (Khoa *et al.*, 2001). Similarly, TNF-α and IL-1β were reported to increase expression of A_{2A} and A_{2B} receptors in human dermal microvascular endothelial cells (HMVEC), in contrast to INF-γ, which was able to up regulate only A_{2B} expression and presented a suppressor effect on A_{2A} levels. This differential regulation is also clear at a functional level: the increase in cAMP in response to A_{2A} activation is higher in TNF-α treated cells, while in IFN-γ treated cells, the response to Ado-receptor stimulation is in turn mediated by A_{2B} (Nguyen *et al.*, 2003).

5.3.2. Ado in animal models of intestinal inflammation

The intricacy of Ado signaling in intestinal inflammation not surprisingly reflects the results obtained by manipulating such pathways in established animal models for inflammatory diseases. The use of an A_{2B} selective antagonist (ATL-801) in the diet of colitic mice, induced either by dextran sodium sulphate (DSS) or piroxicam in IL-$10^{-/-}$ mice, resulted in significant atteuation of the disease, with reduced clinical symptoms and histological scores. Effects were observed in terms of suppression of pro-inflammatory cytokines, neutrophil infiltration and epithelial hyperplasia (Kolachala *et al.*, 2008a). The protective

effect of impaired A_{2B} signaling against induced colitis was also evident in knockout mice were the A_{2B} receptor had been deleted (Kolachala *et al.*, 2008b). In contrast, a similar study found that knockout mice for A_{2B} AR displayed an increase in DSS-induced colitis severity, which was also the case when a selective A_{2B} inhibitor (PSB1115) was administered to the wild-type mice. Here, IL-10 deficiency caused by the absence of A_{2B} activity appears as the cause of exacerbated inflammation, implicating IL-10 modulation by adenosine on epithelial cells as a central protective effect in acute inflammation (Frick *et al.*, 2009).

Activation of the A_{2A} receptor is generally accepted to have anti-inflammatory properties after activation on immune cells. Its role in colitis was studied using a murine model where inflammation is induced by adoptive transfer of pathogenic Th cells (Naganuma *et al.*, 2006). In this model, co-transfer of regulatory Th cells was able to prevent disease development. The authors observed that regulatory cells from A_{2A} knockout mice were not able to suppress T cell-mediated colitis and that conversely, A_{2A} deficient pathogenic Th cells were not inhibited by wild-type regulatory cells. Moreover, it was shown that the A_{2A} agonist ATL202 modulates cytokine production in both regulatory and pathogenic Th cells, reducing the production of pro-inflammatory cytokines while leaving anti-inflammatory cytokines unchanged (Naganuma *et al.*, 2006). A_{2A} receptor activity also resulted as being protective against mucosal inflammation during *Clostridium difficile* toxin A-induced murine ileal enteritis, where the selective agonist (ATL313) was able to reduce mucosal edema, disruption and neutrophil infiltration (Cavalcante *et al.*, 2006). Another selective A_{2A} agonist, ATL-146e, exerted anti-inflammatory effects in different models of inflammatory bowel disease (Odashima *et al.*, 2005). The treatment reduced inflammatory tissue damage in acute rabbit colitis and was able to reduce immune cell infiltration in colonic mucosa in the chronic model of rabbit colitis. In the mouse model of spontaneous ileitis, activation of A_{2A} signaling also improved histological scores and reduced the production of pro-inflammatory cytokines (TNF, IFN-γ and IL-4). Adoptively transferred ileitis induced by injection of T-cells from spontaneous ileitic mice in immunodeficient acceptors was also ameliorated by administration of ATL146e (Odashima *et al.*, 2005). Another A_{2A} AR agonist (CGS 21680) showed anti-inflammatory activity by reducing secretion of IL-2 and TNF-α by Th-1 and T-cytotoxic (Tc)-1 cells *in vitro* (Erdmann *et al.*, 2005). However, when tested in DSS-induced colitis in mice, intraperitonial administration of the compound was unable to improve disease parameters like bodyweight and colon length and was ineffective as well in preventing the increased levels of macrophage inflammatory proteins and IL-1β (Selmeczy *et al.*, 2007).

The involvement of Ado signaling in regulation of motility has been demonstrated in healthy intestine (Christofi *et al.*, 2001) and some studies aimed to investigate this involvement during inflammatory conditions. In this regard, A_{2A} AR agonist (CGS 21680) was reported to reduce contractile responses to electrical stimulation on rat colon, and the effect was significantly enhanced in inflamed tissue, when colitis was induced by 2,4-dinitrobenzenesulfonic acid (DNBS) administration. Possible causes for the higher activity of A_{2A} AR in colitic rats are increased receptor density and increased recruitment caused by inflammation-induced changes in endogenous Ado levels (Antonioli *et al.*, 2006). Interestingly, in this model of rat colitis, expression of A_{2A} AR and CD73 is higher in inflamed colon than in healthy tissue (Antonioli *et al.*, 2011).

IB-MECA, a selective agonist for the A_3 receptor, demonstrated protective role for this receptor subtype in murine DSS-induced and IL-$10^{-/-}$ spontaneous colitis (Mabley *et al.*, 2003a). In trinitrobenzene sulphonic acid (TNBS)-induced colitis, an A_3 agonist was also reported to ameliorate inflammation, improving clinical and histological parameters. In this model, a microarray technique revealed that IB-MECA was able to prevent the dysregulation of gene expression induced by TNBS (Guzman *et al.*, 2006). However, DSS-induced colitis model in A_3 AR knockout mice showed that the absence of this receptor has a protective effect, with improved disease parameters like body weight, colonic motility and histological scores, raising the hypothesis that the previously observed beneficial effect of agonist IB-MECA results from high-dosage and unspecific receptor stimulation (Ren *et al.*, 2011).

The conversion of adenosine to inosine by adenosine deaminase (ADA) is one important reaction limiting Ado biodisponibility. Activity of purine deaminases (including ADA) in blood and colonic tissue was observed to correlate inversely with inflammation in rat experimental colitis (Al-Awadi and Khan, 1999), while the levels of circulating adenosine is also reduced with inflammation, possibly due to an increased demand in the inflamed mucosa (Al-Awadi and Khan, 2001). Therefore, some studies in animal models aimed at the modulation of this enzyme activity to determine the effects on intestinal inflammation. ADA inhibitors were able to attenuate inflammation in DNBS-induced colitis (Antonioli *et al.*, 2007) and in a model of murine enteritis induced by *C. difficile* toxin-A, where ileal ADA activity is upregulated (de Araujo Junqueira *et al.*, 2011). General mechanisms involved in the effects of ADA inhibition include reduction in pro-inflammatory cytokine production, oxidative damage and lymphocyte depletion. Inhibition of NF-κB pathway in ileal tissue was observed, probably a result from the increased Ado concentration in the inflamed sites (de

Araujo Junqueira *et al.*, 2011). Moreover, it was reported that the beneficial effects of ADA inhibitors are impaired by blokage of A_{2A} and A_3, but not A_1 and A_{2B} receptors (Antonioli *et al.*, 2010). It is important to note that the product of ADA, inosine, also possesses anti-inflammatory activity in monocytes, neutrophils as well as in epithelial cells *in vitro* and shows beneficial effects in animal models of colitis (Mabley *et al.*, 2003b; Rahimian *et al.*, 2010).

Another enzyme involved in adenosine metabolism is adenosine kinase, which catalyzes the phosphorylation of adenosine to form AMP, limiting cytosolic Ado concentration. When this reaction is inhibited, an increase in intracellular Ado results in enhanced Ado export, thus raising extracellular Ado levels. In fact, an adenosine kinase inhibitor GP515 has been investigated for its effects in experimental murine colitis. A significant improvement in clinical and histological scores was observed in colitic mice receiving the inhibitor i.p., parallel to decreased INF-γ production and splenocyte activation (Siegmund *et al.*, 2001). On the other hand, the nucleotidases that convert ATP to AMP (e. g. CD39) and subsequently generate Ado from AMP (e. g. CD73) are also interesting targets for the modulation of Ado-mediated effects in inflammation. TNBS colitis in mice resulted in an induction of CD73 transcripts in colonic mucosa and this enzyme presented a protective role in inflammation, as indicated by the increased severity of the disease in CD73 knockout mice. This study pointed to the induction of IL-10 via IFN-αA production as the mechanism by which CD73 dampened inflammation (Louis *et al.*, 2008).

It has been demonstrated that genetic deletion of CD39 resulted in more severe inflammation in mice with DSS-induced colitis, an effect that could be prevented by restoring enzymatic activity. This observation indicated a protective role for CD39 and was reinforced by single-nucleotide polymorphism analysis demonstrating that a tag for low expression of CD39 was associated with increased susceptibility to Crohn's disease (Friedman *et al.*, 2009). Paradoxally, an increase in CD39 expression in inflamed colonic tissue was reported in another study in DSS-induced colitic mice. In this case, a decrease in ATP levels impairs purinergic sympathetic regulation, a possible cause of altered blood flow in IBD (Neshat *et al.*, 2009).

Practical examples of the importance of Ado regulation in inflammatory diseases and their treatment are found in some currently used immunosuppressant drugs. For instance, Methotrexate (Mtx) is commonly applied for induction of remission and maintenance therapy in IBD patients (van Dieren *et al.*, 2006). Its mechanism of action has been investigated and

there is evidence that an induction of Ado release has a central role in anti-inflammatory properties of Mtx (Chan and Cronstein, 2002). Mtx inhibits 5-aminoimidazole-4-carboxamide ribotide (AICAR) transformylase, leading to AICAR accumulation. AICAR in turn can cause inhibition of adenosine deaminase and AMP deaminase, resulting in increased levels of Ado (Baggott *et al.*, 1986). Further anti-inflammatory properties of AICAR were reported in TNBS-induced murine colitis, possibly through the activation of AMPK (Bai *et al.*, 2010). The activity of the ecto-5'-nucleotidase CD73 and activation of Ado receptors are also implicated in the anti-inflammatory effect of Mtx in animal models (Montesinos *et al.*, 2003; Montesinos *et al.*, 2007). Importantly, Mtx treatment has been reported to modulate Ado levels *in vivo* in humans (Riksen *et al.*, 2006). Sulfasalazine, also used in the treatment of IBD and other inflammatory disorders, shares with Mtx the ability to induce Ado accumulation in inflamed tissue (Gadangi *et al.*, 1996). Tacrolimus, or FK506, and Cyclosporin A, other drugs indicated to treat some cases of IBD, have been shown to inhibit adenosine uptake and adenosine kinase activity in endothelial cells and T-cells (Hwang *et al.*, 2001; Spychala and Mitchell, 2002).

5.3.3. Ado in host-microbial interactions

The unique scenario found in the gut adds an important component to the complexity of the Ado signaling system in immune responses. Here, the bacterial community plays a critical role and Ado signaling is in many cases included in the plethora of host-microbial interaction strategies. Several examples of mutual influence were investigated, mainly concerning intestinal pathogens and infectious diseases. Mechanisms involving Ado signaling can link distinct Ado receptor subtypes to an increase in the efficiency of bacterial infection. For example, the anti-inflammatory effects of A_{2A} activation in Th cells in the gastric mucosa has been reported to cause increased colonization and persistence of *Helicobacter pylori*, an effect driven by expression of CD73 in regulatory Th cells (Alam *et al.*, 2009a; Alam *et al.*, 2009b). A_{2B}, in turn, was shown to be responsible for extracellular Ado-induced delay in intracellular *Chlamydia trachomatis* development in epithelial cells, also leading to persistent infection (Pettengill *et al.*, 2009). In intestinal epithelia, A_{2B} signaling stimulates fibronectin expression, enhancing adhesion and invasion of *Salmonella typhimurium* (Walia *et al.*, 2004).

Gastrointestinal infections represent the most common cause of diarrhea, as a consequence of electrolyte imbalance and increase intestinal secretion. Ado has been implicated as a mediator of those effects through activation of A_{2B} receptor and subsequent

induction of ion secretion. The stimulation of Cl^- secretion in intestinal epithelial cells (T84) by neutrophils, for example, is a result of the conversion of neutrophil-derived AMP to Ado by the nucleotidase CD73 expressed by epithelia (Strohmeier *et al.*, 1997). Accordingly, a more recent study using a high throughput gene expression analysis, identified higher expression of A_{2B} receptor gene as one of the susceptibility factors in a model of infectious colitis induced by *Citrobacter rodentium*, pointing to severe diarrhea as a cause of mortality in this model (Borenshtein *et al.*, 2008). In EPEC infection (but not nonpathogenic *E. coli*) the killing of host cells results in ATP release, which is converted to Ado generating a secretory response. Moreover, EPEC is able to activate the phosphatidylinositol-specific phospholipase C (PI-PLC) and the consequent release of CD73 from T84 cell surface, responsible for the formation of Ado and the Cl^- secretion observed. Those results indicate an important role for Ado in EPEC-induced diarrhea (Crane *et al.*, 2002; Crane *et al.*, 2007). Interestingly, the same group had shown later that host-derived adenosine have a direct effect on EPEC cultures, stimulating growth, changing adherence patterns and regulating virulence factors expression (Crane and Shulgina, 2009).

Given the critical importance of extracellular Ado levels in the control of immune responses, it is not unexpected that pathogens develop strategies to manipulate Ado signaling during infection and evade host defenses. A study on *Mycobacterium avium* infected macrophages, using a cDNA expression array to address infection-induced changes in gene regulation, identified a sustained decrease in Ado receptor expression (2.5-fold). In this model, in the absence of T cells mediators, macrophages were not able to eliminate *M. avium*, however the significance of the modulation of this particular gene in bacterial growth and survival was not specifically discussed (Greenwell-Wild *et al.*, 2002). Another clear example of such strategies is a study identifying the surface protein adenosine synthase A (AdsA) as a key virulence factor in *Staphylococcus aureus*. It was shown that the generation of Ado by the 5'-nucleotidase activity of AdsA causes an inhibition of *S. aureus* killing by neutrophils in the blood of infected mice. A strain with a mutation in *adsA* presented reduced survival in the blood and was unable to form kidney abscesses, in contrast to the wild-type strain. The phenotype could be rescued by complementation with *adsA* expressing plasmid, and by exogenous Ado addition. The protein was shown to be expressed by other Gram-positive pathogens and is also involved in enhanced survival of *Bacillus anthracis* in rat blood (Thammavongsa *et al.*, 2009).

Clearly, the Ado signaling system represents a prominent target for immunoregulation by bacteria. In this study Ado was identified as a predominant *E. coli* product in response to a host defense peptide, with related consequences on host cell signaling. Recognizing the manifold effects of Ado in intestinal inflammation, it seems plausible that bacterial-derived Ado generated under defensin stress can be an additional player in this scenario. Thus, the results obtained not only delineate a novel mechanism of action for a human defensin, but also broaden the prospect of host-microbial interactions in the inflamed gut.

6. CONCLUDING REMARKS

The dynamic cross-talk between gut microbiota and the host immunity has been shown to have numerous aspects. The present research dealt with the hypothesis that a host defense peptide (hBD-2) could trigger an extracellular response in *E. coli*, and that such response, regarding soluble small molecules, could have a feedback influence on the host. Special interest was focused on the pathophysiology of inflammatory bowel disease, a condition where the homeostasis between the microbial community and host immune system is disturbed. This hypothesis was proven to be valid with the identification of purine compounds (including adenosine) as extracellular metabolites generated specifically by hBD-challenged bacteria. We then postulate that a deregulated expression of hBD-2 in the intestinal mucosa of IBD patients leads to altered local levels of adenosine, as a consequence of its interaction with gut bacteria, which in turn can affect the inflammatory process (Figure 6.1).

Our study represents a so far undisclosed link between two recognized elements of the IBD-puzzle: the interplay between bacteria and epithelial cells antimicrobials, and the central role of Ado in controlling inflammation. The former can be appreciated, for instance, in researches addressing the effectiveness of probiotic *E. coli* (strain Nissle 1917) as a therapy for IBD (reviewed by Hormannsperger and Haller, 2010). Regarded as one of the beneficial mechanisms of *E. coli* Nissle 1917 in IBD patients, the induction of β-defensin production in intestinal epithelial cells, via modulation of NF-κB pathway by this strain has been described (Wehkamp *et al.*, 2004; Schlee *et al.*, 2007; Mondel *et al.*, 2009). On the other hand, the relevance of Ado signaling in intestinal inflammation is supported by extensive evidence found in the literature, including studies *in vitro* and in animal models of colitis. Importantly, the expression of several genes involved in purine metabolism and signaling was reported to be differentially regulated in IBD patients (Rybaczyk *et al.*, 2009), and the therapeutic potential of modulating the Ado signaling system in these patients is largely recognized (Antonioli *et al.*, 2008; Hasko *et al.*, 2008).

In conclusion, besides contributing to the understanding of host-microbial interactions, particularly during gut inflammation, we believe this work offers a new perspective to the mechanism of action of human β-defensins, which must be considered beyond its bacteriocidal effect, as a component of the interkingdom signaling network. The search for bacterial-derived molecules in response to defensin challenge has been shown here as a valid

approach, and is therefore an interesting tool for continued investigation in this context. Additionally, the integrated understanding of the molecular mechanisms responsible for the observed phenomenon, addressing both the peptide properties and the bacterial elements involved, will further improve the comprehension and strengthen the view where a host defense peptide acting in concert with intestinal bacteria can influence the inflammatory outcome in the gut.

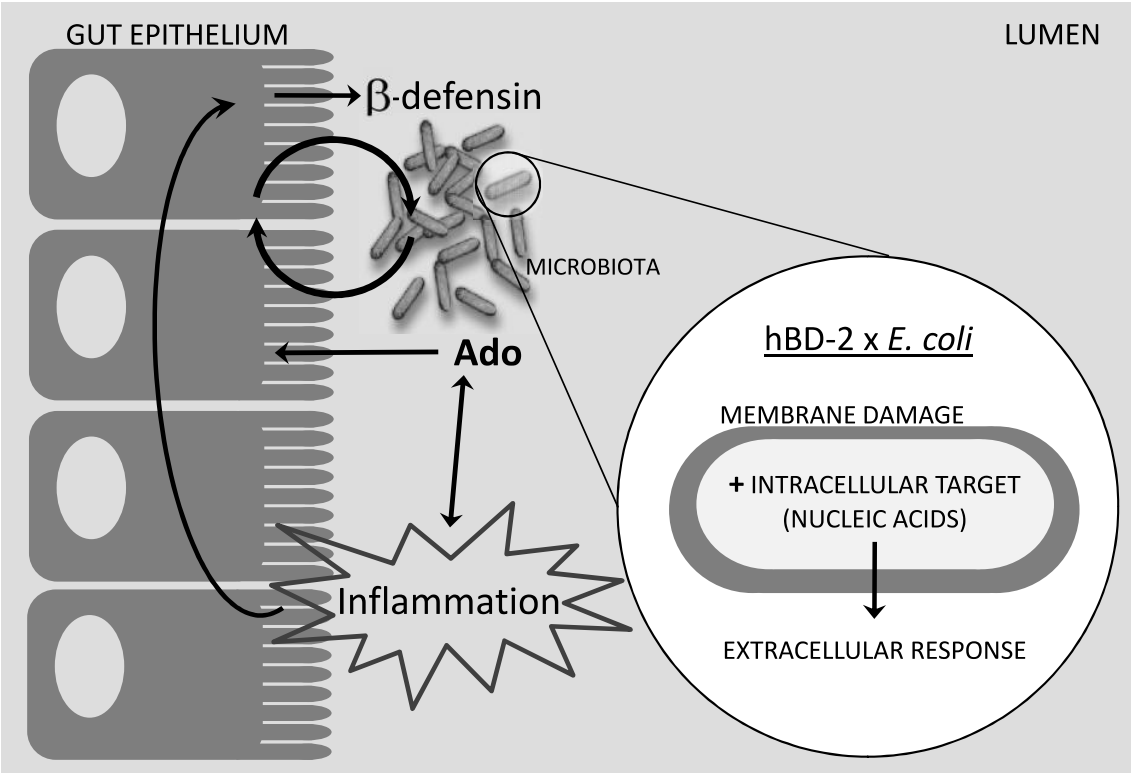

Figure 6.1 - Schematic representation of the proposed role for hBD-2 interaction with *E. coli* in influencing intestinal inflammation. Multi-target effect of hBD-2 on *E. coli* generates extracellular purine nucleosides, including adenosine (Ado), which is a key regulator in inflammatory processes.

7. SUPPLEMENTARY MATERIAL

7.1. Quantitative HPLC-MS/MS standard curves

Supplementary Table 1 - Standard curve for adenine. MRM: 136 → 119 (qualifier 136→92).

Concentration		MRM Response
$ng \cdot mL^{-1}$	μM	(peak area)
7.8125	0.06	5179.712403
15.625	0.12	10447.64593
31.25	0.23	22707.28798
62.5	0.46	42203.90141
125	0.93	81687.53942
250	1.85	152863.4303
500	3.70	281026.7611

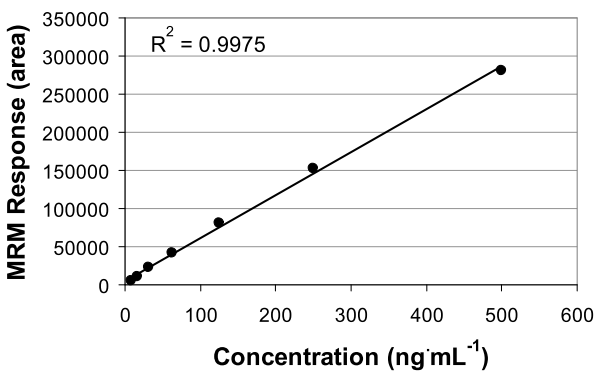

Supplementary Figure 1 - Standard curve for adenine performed as described in section 3.3.1.

Supplementary Table 2 - Standard curve for adenosine. MRM: 268 → 136 (qualifier 268→119).

Concentration		MRM Response
$ng \cdot mL^{-1}$	μM	(peak area)
7.8125	0.03	14725.91633
15.625	0.06	26523.43369
31.25	0.12	47986.43353
62.5	0.23	96018.63147
125	0.47	190221.2346
250	0.94	364304.0695
500	1.87	685734.5591

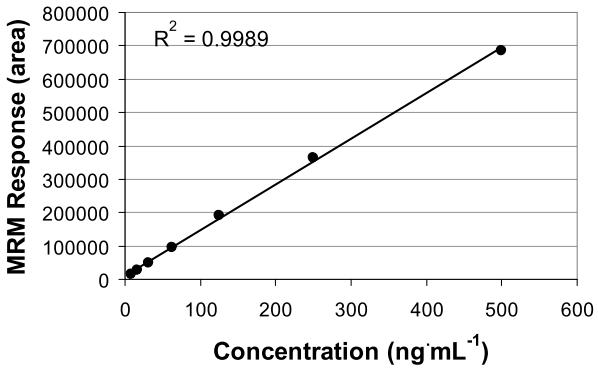

Supplementary Figure 2 - Standard curve for adenosine performed as described in section 3.3.1.

Supplementary Table 3 - Standard curve for guanine. MRM: 152 → 135 (qualifier 152→110).

Concentration		MRM Response
$ng \cdot mL^{-1}$	μM	(peak area)
7.8125	0.05	2886.552555
15.625	0.10	5574.710522
31.25	0.21	10713.81487
62.5	0.41	20131.95285
125	0.83	41643.73026
250	1.65	82666.48054
500	3.31	167170.7723

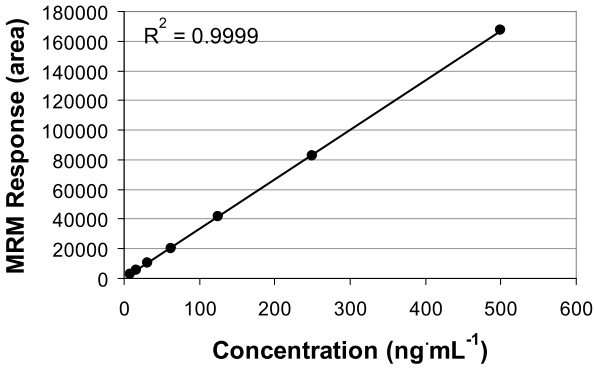

Supplementary Figure 3 - Standard curve for guanine performed as described in section 3.3.1.

Supplementary Table 4 - Standard curve for guanosine. MRM: 152 → 135 (qualifier 152→110).

Concentration		MRM Response
$ng \cdot mL^{-1}$	μM	(peak area)
7.8125	0.03	784.285834
15.625	0.06	2137.588201
31.25	0.11	4121.238908
62.5	0.22	8550.040254
125	0.44	17046.03666
250	0.88	33958.85961
500	1.77	66762.87776

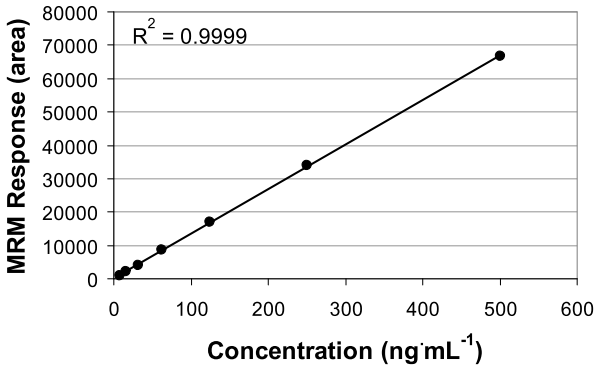

Supplementary Figure 4 - Standard curve for guanosine performed as described in section 3.3.1.

Supplementary Table 5 - Standard curve for AMP. MRM: 348 → 136 (qualifier 348→97).

Concentration		MRM Response
$ng \cdot mL^{-1}$	μM	(peak area)
15.625	0.05	11014.81093
31.25	0.09	21119.63391
62.5	0.18	42675.59577
125	0.36	86890.16284
250	0.72	175074.7389
500	1.44	351198.607

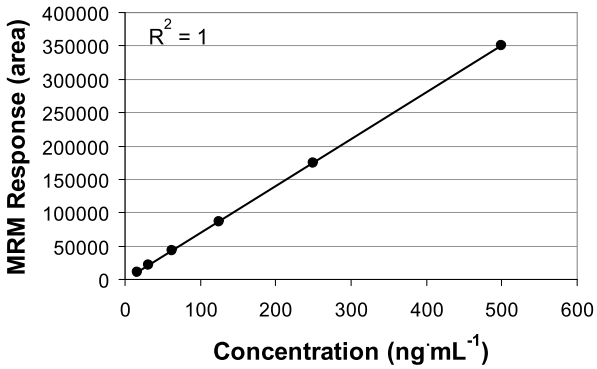

Supplementary Figure 5 - Standard curve for AMP performed as described in section 3.3.1

Supplementary Table 6 - Measured and corrected ^{13}C enrichment of purine nucleosides in DNA, RNA and supernatants from hBD-challenged *E. coli*. Values were obtained by GC-IRMS and corrected as described in section 3.4.7.

Source Glu (C isotope)	Sample	Nucleoside (C_{10})	TMS (C_3) Derivatization: groups added (x)	TMS (C_3) Derivatization: Total C (n_{dc})[a]	R ($^{13}C/^{12}C$)	$\delta^{13}C$ Eqn. (1)	Fractional Abundance (F_{dc}) Eqn. (3)	Corrected F (F_c) Eqn.(4)	Corrected R (R_c) Eqn. (5)	Corrected δ ($\delta^{13}C_c$) Eqn. (6)
-	*TMS*	-	-	-	*0.01082*	*-36.83*	*0.01071*	-	-	-
^{12}C	DNA	dAdo	3	19	0.01098	-23.08	0.01086	0.01099	0.01112	-10.69
	RNA	Ado	4	22	0.01095	-25.64	0.01083	0.01098	0.01110	-12.20
	S.N.	Ado	4	22	0.01131	6.08	0.01118	0.01175	0.01188	57.62
^{13}C	DNA	dAdo	3	19	0.10846	8651.84	0.09784	0.17626	0.21401	18044.61
	RNA	Ado	4	22	0.10486	8331.17	0.09490	0.19594	0.24370	20686.72
	S.N.	Ado	4	22	0.09695	7627.96	0.08838	0.18160	0.22189	18746.29
^{12}C	DNA	dGuo	4	22	0.01102	-19.26	0.01090	0.01113	0.01126	1.82
	RNA	Guo	5	25	0.01100	-21.22	0.01088	0.01114	0.01126	2.20
	S.N.	Guo	5	25	0.01109	-13.32	0.01097	0.01135	0.01148	21.97
^{13}C	DNA	dGuo	4	22	0.06565	4841.80	0.06160	0.12267	0.13983	11443.36
	RNA	Guo	5	25	0.09129	7123.88	0.08365	0.19307	0.23928	20293.85
	S.N.	Guo	5	25	0.09865	7779.23	0.08959	0.20790	0.26488	22571.41

[a] total carbon moles in the derivatized compound = C moles in the nucleoside (10) + [C moles in TMS (3) x number of TMS groups added]

Eqn. (1) $\delta^{13}C = [(R_{SAMPLE}/R_{PDB})-1] \times 10^3$; $R_{PDB} = 0.0112372$

Eqn. (3) $F_{dc} = R/(1+R)$

Eqn. (4) $F_c = [(n_{dc} F_{dc}) - (x\, n_d F_d)] / n_c$; $n_d = 3$; $n_c = 10$; $F_d = 0.01071$

Eqn. (5) $R_c = F_c/(1-F_c)$

Eqn. (6) $\delta\, ^{13}C_c = [(R_c/R_{PDB})-1] \times 10^3$; $R_{PDB} = 0.0112372$

7.3. Equipments

7.3.1. Chromatographers and mass spectrometers

6460 TripleQuad LC/MS system (Agilent Technologies, Santa Clara, CA, USA)

Varian GC-MS system 450GC/240MS ion trap mass spectrometer (Varian Inc., Agilent Technologies)

GC IsoLink system (combustion interface) MAT 253 stable isotope ratio MS
(Thermo Scientific, Rockford, IL, USA)

7.3.2. Microscopes

TEM910 transmission electron microscope (Carl Zeiss, Oberkochen, Germany)
with Slow-Scan CCD-Camera (ProScan, Scheuring, Germany)

Axio Imager A1 epifluorescence microscope (Zeiss Imaging Solutions GmBH, Göttingen, Germany)

Zeiss Photo microscope (Carl Zeiss, Oberkochen, Germany)

DMI6000 CS microscope with confocal unit Leica TCS SP5
(Leica Microsystems GmbH, Wetzlar, Germany)

Stereomicroscope (Carl Zeiss AG, Oberkochen, Germany).

Light microscope (Nikon Eclipse TS100, Nikon Instruments, Inc., Melville, NY, USA).

7.3.3. Electrophoresis and gel imaging systems

Wide- and Mini Horizontal Gel System (Starlab International, GmbH, Ahrensburg Germany).

Mini-Protean ® Tetra system Mini with Trans-Blot cell
(Bio-Rad Laboratories, Inc., Hercules, CA, USA)

E.A.S.Y. Win32 gel documentation system (Herolab GmbH, Wiesloch, Germany).

Optimax Typ TR developing machine (MS-L GmbH, Wiesloch, Germany)

Photo Scanner HP Scanjet G4050 (Hewlett-Packard Company, Palo Alto, CA, USA)

7.3.4. Photometers and plate readers

BioscreenC automated microbiology growth analysis system (Oy Growth Curves)

NanoDrop 2000c spectrophotometer (Thermo Scientific, Rockford, IL, USA).

Victor^{TM} X3 2030 multilabel reader (PerkinElmer, Turku, Finland)

μQuant microplate spectrophotometer (Bio-Tek Instruments, Inc., Winooski, VT, USA)

VICTOR^2 Wallac 1420 multilabel counter (PerkinElmer)

7.3.5. Additional equipment

Flow cytometer Becton Dickinson FACSCalibur (BD Bioscience, San Jose, CA, USA)

Autoclave Bioclav 32-2-3 (KSG Sterilisator GmbH, Olching, Germany)

Termocycler Mastercycler (Eppendorf, Hamburg, Germany)

3130*xl* Genetic Analyzer (Applied Biosystems, Darmstadt, Germany).

Microbiological safety cabinets HERAsafe (ThermoScientific-Heraeus, Hanau. Germany)

Shaker incubator Certomat BS-1 (Sartorius Stedim Biotech GmbH, Göttingen, Germany)

CO_2 incubator C200 (Labotect Labor-Technik Göttingen GmbH, Göttingen, Germany)

Centrifuge DuPont Sorvall RC3C (ThermoScientific-DuPont, Newtown, CT, USA)

Centrifuge Eppendorf 5415R (Eppendorf, Hamburg, Germany)

Shaker platform Assistent (Karl Hecht KG, Sondheim, Germany)

8. REFERENCES

Abraham, W.R., Hesse, C. and Pelz, O. (1998). Ratios of carbon isotopes in microbial lipids as an indicator of substrate usage. Applied and Environmental Microbiology *64*, 4202-4209.

Abraham, W.R., Strompl, C., Meyer, H., Lindholst, S., Moore, E.R., Christ, R., Vancanneyt, M., Tindall, B.J., Bennasar, A., Smit, J. and Tesar, M. (1999). Phylogeny and polyphasic taxonomy of *Caulobacter* species. Proposal of *Maricaulis* gen. nov. with *Maricaulis maris* (Poindexter) comb. nov. as the type species, and emended description of the genera *Brevundimonas* and *Caulobacter*. International Journal of Systematic Bacteriology *49 Pt 3*, 1053-1073.

Abreu, M.T., Vora, P., Faure, E., Thomas, L.S., Arnold, E.T. and Arditi, M. (2001). Decreased expression of Toll-Like Receptor-4 and MD-2 correlates with intestinal epithelial cell protection against dysregulated proinflammatory gene expression in response to bacterial lipopolysaccharide. Journal of Immunology *167*, 1609-1616.

Ades, S.E. (2008). Regulation by destruction: design of the sigmaE envelope stress response. Current Opinion in Microbiology *11*, 535-540.

Al-Awadi, F.M. and Khan, I. (1999). Studies on purine enzymes in experimental colitis. Molecular and Cellular Biochemistry *194*, 17-22.

Al-Awadi, F.M. and Khan, I. (2001). Blood purine and energy status in rats with colitis. Digestive Diseases and Sciences *46*, 443-448.

Alam, M.S., Kurtz, C.C., Rowlett, R.M., Reuter, B.K., Wiznerowicz, E., Das, S., Linden, J., Crowe, S.E. and Ernst, P.B. (2009a). CD73 is expressed by human regulatory T helper cells and suppresses proinflammatory cytokine production and *Helicobacter felis*-induced gastritis in mice. Journal of Infectious Diseases *199*, 494-504.

Alam, M.S., Kurtz, C.C., Wilson, J.M., Burnette, B.R., Wiznerowicz, E.B., Ross, W.G., Rieger, J.M., Figler, R.A., Linden, J., Crowe, S.E. and Ernst, P.B. (2009b). A_{2A} adenosine receptor (AR) activation inhibits pro-inflammatory cytokine production by human $CD4^+$ helper T cells and regulates *Helicobacter*-induced gastritis and bacterial persistence. Mucosal Immunology *2*, 232-242.

Aldhous, M.C., Noble, C.L. and Satsangi, J. (2009). Dysregulation of human beta-defensin-2 protein in inflammatory bowel disease. PLoS One *4*, e6285.

Alkalay, I., Yaron, A., Hatzubai, A., Orian, A., Ciechanover, A. and Ben-Neriah, Y. (1995). Stimulation-dependent I kappa B alpha phosphorylation marks the NF-kappa B inhibitor for degradation via the ubiquitin-proteasome pathway. Proceedings of the National Academy of Sciences of the United States of America *92*, 10599-10603.

Allwood, J.W., Clarke, A., Goodacre, R. and Mur, L.A. (2010). Dual metabolomics: a novel approach to understanding plant-pathogen interactions. Phytochemistry *71*, 590-597.

Alverdy, J., Holbrook, C., Rocha, F., Seiden, L., Wu, R.L., Musch, M., Chang, E., Ohman, D. and Suh, S. (2000). Gut-derived sepsis occurs when the right pathogen with the right

virulence genes meets the right host: evidence for *in vivo* virulence expression in *Pseudomonas aeruginosa*. Annals of Surgery *232*, 480-489.

Antonioli, L., Fornai, M., Colucci, R., Ghisu, N., Blandizzi, C. and Del Tacca, M. (2006). A2a receptors mediate inhibitory effects of adenosine on colonic motility in the presence of experimental colitis. Inflammatory Bowel Diseases *12*, 117-122.

Antonioli, L., Fornai, M., Colucci, R., Ghisu, N., Da Settimo, F., Natale, G., Kastsiuchenka, O., Duranti, E., Virdis, A., Vassalle, C., La Motta, C., Mugnaini, L., Breschi, M.C., Blandizzi, C. and Del Taca, M. (2007). Inhibition of adenosine deaminase attenuates inflammation in experimental colitis. Journal of Pharmacology and Experimental Therapeutics *322*, 435-442.

Antonioli, L., Fornai, M., Colucci, R., Ghisu, N., Tuccori, M., Del Tacca, M. and Blandizzi, C. (2008). Pharmacological modulation of adenosine system: novel options for treatment of inflammatory bowel diseases. Inflammatory Bowel Diseases *14*, 566-574.

Antonioli, L., Fornai, M., Colucci, R., Awwad, O., Ghisu, N., Tuccori, M., Da Settimo, F., La Motta, C., Natale, G., Duranti, E., Virdis, A. and Blandizzi, C. (2010). The blockade of adenosine deaminase ameliorates chronic experimental colitis through the recruitment of adenosine A_{2A} and A_3 receptors. Journal of Pharmacology and Experimental Therapeutics *335*, 434-442.

Antonioli, L., Fornai, M., Colucci, R., Awwad, O., Ghisu, N., Tuccori, M., Del Tacca, M. and Blandizzi, C. (2011). Differential recruitment of high affinity A_1 and A_{2A} adenosine receptors in the control of colonic neuromuscular function in experimental colitis. European Journal of Pharmacology *650*, 639-649.

APD The Antimicrobial Peptide Database: http://aps.unmc.edu/AP/main.php.

Artis, D. (2008). Epithelial-cell recognition of commensal bacteria and maintenance of immune homeostasis in the gut. Nature Reviews Immunology *8*, 411-420.

Arumugam, M., Raes, J., Pelletier, E., Le Paslier, D., Yamada, T., Mende, D.R., Fernandes, G.R., Tap, J., Bruls, T., Batto, J.M., Bertalan, M., Borruel, N., Casellas, F., Fernandez, L., Gautier, L., Hansen, T., Hattori, M., Hayashi, T., Kleerebezem, M., Kurokawa, K., Leclerc, M., Levenez, F., Manichanh, C., Nielsen, H.B., Nielsen, T., Pons, N., Poulain, J., Qin, J., Sicheritz-Ponten, T., Tims, S., Torrents, D., Ugarte, E., Zoetendal, E.G., Wang, J., Guarner, F., Pedersen, O., de Vos, W.M., Brunak, S., Dore, J., Antolin, M., Artiguenave, F., Blottiere, H.M., Almeida, M., Brechot, C., Cara, C., Chervaux, C., Cultrone, A., Delorme, C., Denariaz, G., Dervyn, R., Foerstner, K.U., Friss, C., van de Guchte, M., Guedon, E., Haimet, F., Huber, W., van Hylckama-Vlieg, J., Jamet, A., Juste, C., Kaci, G., Knol, J., Lakhdari, O., Layec, S., Le Roux, K., Maguin, E., Merieux, A., Melo Minardi, R., M'Rini, C., Muller, J., Oozeer, R., Parkhill, J., Renault, P., Rescigno, M., Sanchez, N., Sunagawa, S., Torrejon, A., Turner, K., Vandemeulebrouck, G., Varela, E., Winogradsky, Y., Zeller, G., Weissenbach, J., Ehrlich, S.D. and Bork, P. (2011). Enterotypes of the human gut microbiome. Nature *473*, 174-180.

Atarashi, K., Nishimura, J., Shima, T., Umesaki, Y., Yamamoto, M., Onoue, M., Yagita, H., Ishii, N., Evans, R., Honda, K. and Takeda, K. (2008). ATP drives lamina propria T_H17 cell differentiation. Nature *455*, 808-812.

Backhed, F., Ding, H., Wang, T., Hooper, L.V., Koh, G.Y., Nagy, A., Semenkovich, C.F. and Gordon, J.I. (2004). The gut microbiota as an environmental factor that regulates fat storage. Proceedings of the National Academy of Sciences of the United States of America *101*, 15718-15723.

Backhed, F., Ley, R.E., Sonnenburg, J.L., Peterson, D.A. and Gordon, J.I. (2005). Host-bacterial mutualism in the human intestine. Science *307*, 1915-1920.

Backhed, F., Manchester, J.K., Semenkovich, C.F. and Gordon, J.I. (2007). Mechanisms underlying the resistance to diet-induced obesity in germ-free mice. Proceedings of the National Academy of Sciences of the United States of America *104*, 979-984.

Baggott, J.E., Vaughn, W.H. and Hudson, B.B. (1986). Inhibition of 5-aminoimidazole-4-carboxamide ribotide transformylase, adenosine deaminase and 5'-adenylate deaminase by polyglutamates of methotrexate and oxidized folates and by 5-aminoimidazole-4-carboxamide riboside and ribotide. Biochemical Journal *236*, 193-200.

Bai, A., Ma, A.G., Yong, M., Weiss, C.R., Ma, Y., Guan, Q., Bernstein, C.N. and Peng, Z. (2010). AMPK agonist downregulates innate and adaptive immune responses in TNBS-induced murine acute and relapsing colitis. Biochemical Pharmacology *80*, 1708-1717.

Baker, M. (2011). Metabolomics: from small molecules to big ideas. Nature Methods *8*, 117-121.

Bals, R., Wang, X., Wu, Z., Freeman, T., Bafna, V., Zasloff, M. and Wilson, J.M. (1998). Human beta-defensin 2 is a salt-sensitive peptide antibiotic expressed in human lung. Journal of Clinical Investigation *102*, 874-880.

Barclay, A.R., Morrison, D.J. and Weaver, L.T. (2008). What is the role of the metabolic activity of the gut microbiota in inflammatory bowel disease? Probing for answers with stable isotopes. Journal of Pediatric Gastroenterology and Nutrition *46*, 486-495.

Barnich, N., Carvalho, F.A., Glasser, A.L., Darcha, C., Jantscheff, P., Allez, M., Peeters, H., Bommelaer, G., Desreumaux, P., Colombel, J.F. and Darfeuille-Michaud, A. (2007). CEACAM6 acts as a receptor for adherent-invasive *E. coli*, supporting ileal mucosa colonization in Crohn disease. Journal of Clinical Investigation *117*, 1566-1574.

Barrett, J.C., Hansoul, S., Nicolae, D.L., Cho, J.H., Duerr, R.H., Rioux, J.D., Brant, S.R., Silverberg, M.S., Taylor, K.D., Barmada, M.M., Bitton, A., Dassopoulos, T., Datta, L.W., Green, T., Griffiths, A.M., Kistner, E.O., Murtha, M.T., Regueiro, M.D., Rotter, J.I., Schumm, L.P., Steinhart, A.H., Targan, S.R., Xavier, R.J., Libioulle, C., Sandor, C., Lathrop, M., Belaiche, J., Dewit, O., Gut, I., Heath, S., Laukens, D., Mni, M., Rutgeerts, P., Van Gossum, A., Zelenika, D., Franchimont, D., Hugot, J.-P., de Vos, M., Vermeire, S., Louis, E., Cardon, L.R., Anderson, C.A., Drummond, H., Nimmo, E., Ahmad, T., Prescott, N.J., Onnie, C.M., Fisher, S.A., Marchini, J., Ghori, J., Bumpstead, S., Gwilliam, R., Tremelling, M., Deloukas, P., Mansfield, J., Jewell, D., Satsangi, J., Mathew, C.G., Parkes, M., Georges, M. and Daly, M.J. (2008). Genome-wide association defines more than 30 distinct susceptibility loci for Crohn's disease. Nature Genetics *40*, 955-962.

Baumgart, D.C. and Sandborn, W.J. (2007). Inflammatory bowel disease: clinical aspects and established and evolving therapies. Lancet *369*, 1641-1657.

Berney, M., Hammes, F., Bosshard, F., Weilenmann, H.U. and Egli, T. (2007). Assessment and interpretation of bacterial viability by using the LIVE/DEAD BacLight Kit in combination with flow cytometry. Applied and Environmental Microbiology *73*, 3283-3290.

Bhatti, A.R., DeVoe, I.W. and Ingram, J.M. (1976). The release and characterization of some periplasm-located enzymes of *Pseudomonas aeruginosa*. Canadian Journal of Microbiology *22*, 1425-1429.

Biragyn, A., Ruffini, P.A., Leifer, C.A., Klyushnenkova, E., Shakhov, A., Chertov, O., Shirakawa, A.K., Farber, J.M., Segal, D.M., Oppenheim, J.J. and Kwak, L.W. (2002). Toll-like receptor 4-dependent activation of dendritic cells by beta-defensin 2. Science *298*, 1025-1029.

Boman, H.G. (1995). Peptide Antibiotics and their Role in Innate Immunity. Annual Review of Immunology *13*, 61-92.

Boniotto, M., Jordan, W.J., Eskdale, J., Tossi, A., Antcheva, N., Crovella, S., Connell, N.D. and Gallagher, G. (2006). Human beta-defensin 2 induces a vigorous cytokine response in peripheral blood mononuclear cells. Antimicrobial Agents and Chemotherapy *50*, 1433-1441.

Borenshtein, D., Fry, R.C., Groff, E.B., Nambiar, P.R., Carey, V.J., Fox, J.G. and Schauer, D.B. (2008). Diarrhea as a cause of mortality in a mouse model of infectious colitis. Genome Biology *9*, R122.

Botsford, J.L. and Harman, J.G. (1992). Cyclic AMP in prokaryotes. Microbiological Reviews *56*, 100-122.

Boudeau, J., Glasser, A.L., Masseret, E., Joly, B. and Darfeuille-Michaud, A. (1999). Invasive ability of an *Escherichia coli* strain isolated from the ileal mucosa of a patient with Crohn's disease. Infection and Immunity *67*, 4499-4509.

Boudeau, J., Glasser, A.L., Julien, S., Colombel, J.F. and Darfeuille-Michaud, A. (2003). Inhibitory effect of probiotic *Escherichia coli* strain Nissle 1917 on adhesion to and invasion of intestinal epithelial cells by adherent-invasive *E. coli* strains isolated from patients with Crohn's disease. Alimentary pharmacology & therapeutics *18*, 45-56.

Bouma, G. and Strober, W. (2003). The immunological and genetic basis of inflammatory bowel disease. Nature Reviews Immunology *3*, 521-533.

Breeuwer, P. and Abee, T. (2000). Assessment of viability of microorganisms employing fluorescence techniques. International Journal of Food Microbiology *55*, 193-200.

Broad, D.F. and Smith, J.T. (1981). *Escherichia coli* 5'-nucleotidase: purification, properties and its release by osmotic shock. Journal of General Microbiology *123*, 241-247.

Brogden, K.A. (2005). Antimicrobial peptides: pore formers or metabolic inhibitors in bacteria? Nature Reviews Microbiology *3*, 238-250.

Brotz, H., Bierbaum, G., Leopold, K., Reynolds, P.E. and Sahl, H.G. (1998). The lantibiotic mersacidin inhibits peptidoglycan synthesis by targeting lipid II. Antimicrobial Agents and Chemotherapy *42*, 154-160.

Canny, G., Cario, E., Lennartsson, A., Gullberg, U., Brennan, C., Levy, O. and Colgan, S.P. (2006). Functional and biochemical characterization of epithelial bactericidal/permeability-increasing protein. American Journal of Physiology Gastrointestinal and Liver Physiology *290*, G557-567.

Castellanos, M., Wilson, D.B. and Shuler, M.L. (2004). A modular minimal cell model: purine and pyrimidine transport and metabolism. Proceedings of the National Academy of Sciences of the United States of America *101*, 6681-6686.

Cavalcante, I.C., Castro, M.V., Barreto, A.R., Sullivan, G.W., Vale, M., Almeida, P.R., Linden, J., Rieger, J.M., Cunha, F.Q., Guerrant, R.L., Ribeiro, R.A. and Brito, G.A. (2006). Effect of novel A_{2A} adenosine receptor agonist ATL 313 on *Clostridium difficile* toxin A-induced murine ileal enteritis. Infection and Immunity *74*, 2606-2612.

Cerf-Bensussan, N. and Gaboriau-Routhiau, V. (2010). The immune system and the gut microbiota: friends or foes? Nature Reviews Immunology *10*, 735-744.

Chan, E.S. and Cronstein, B.N. (2002). Molecular action of methotrexate in inflammatory diseases. Arthritis Research *4*, 266-273.

Chang, A.H. and Parsonnet, J. (2010). Role of bacteria in oncogenesis. Clinical Microbiology Reviews *23*, 837-857.

Chassaing, B. and Darfeuille-Michaud, A. (2011). The commensal microbiota and enteropathogens in the pathogenesis of inflammatory bowel diseases. Gastroenterology *140*, 1720-1728 e1723.

Chitnis, S.N. and Prasad, K.S. (1990). Seminalplasmin, an antimicrobial protein from bovine seminal plasma, inhibits peptidoglycan synthesis in *Escherichia coli*. FEMS Microbiology Letters *60*, 281-284.

Cho, J.H. (2008). The genetics and immunopathogenesis of inflammatory bowel disease. Nature Reviews Immunology *8*, 458-466.

Christofi, F.L., Zhang, H., Yu, J.G., Guzman, J., Xue, J., Kim, M., Wang, Y.Z. and Cooke, H.J. (2001). Differential gene expression of adenosine A1, A2a, A2b, and A3 receptors in the human enteric nervous system. Journal of Comparative Neurology *439*, 46-64.

Collier-Hyams, L.S., Zeng, H., Sun, J., Tomlinson, A.D., Bao, Z.Q., Chen, H., Madara, J.L., Orth, K. and Neish, A.S. (2002). Cutting edge: *Salmonella* AvrA effector inhibits the key proinflammatory, anti-apoptotic NF-kappa B pathway. Journal of Immunology *169*, 2846-2850.

Crain, P.F. (1990). Preparation and enzymatic hydrolysis of DNA and RNA for mass spectrometry. Methods in Enzymology *193*, 782-790.

Crane, J.K., Olson, R.A., Jones, H.M. and Duffey, M.E. (2002). Release of ATP during host cell killing by enteropathogenic *E. coli* and its role as a secretory mediator. American Journal of Physiology Gastrointestinal and Liver Physiology *283*, G74-86.

Crane, J.K., Shulgina, I. and Naeher, T.M. (2007). Ecto-5'-nucleotidase and intestinal ion secretion by enteropathogenic *Escherichia coli*. Purinergic Signalling *3*, 233-246.

Crane, J.K. and Shulgina, I. (2009). Feedback effects of host-derived adenosine on enteropathogenic *Escherichia coli*. FEMS Immunology and Medical Microbiology *57*, 214-228.

Cronstein, B.N., Daguma, L., Nichols, D., Hutchison, A.J. and Williams, M. (1990). The adenosine/neutrophil paradox resolved: human neutrophils possess both A_1 and A_2 receptors that promote chemotaxis and inhibit O_2 generation, respectively. Journal of Clinical Investigation *85*, 1150-1157.

Cronstein, B.N., Levin, R.I., Philips, M., Hirschhorn, R., Abramson, S.B. and Weissmann, G. (1992). Neutrophil adherence to endothelium is enhanced via adenosine A_1 receptors and inhibited via adenosine A_2 receptors. Journal of Immunology *148*, 2201-2206.

Daniel, P.B., Walker, W.H. and Habener, J.F. (1998). Cyclic AMP signaling and gene regulation. Annual Review of Nutrition *18*, 353-383.

Davey, H.M., Kell, D.B., Weichart, D.H. and Kaprelyants, A.S. (2004). Estimation of microbial viability using flow cytometry. Current Protocols in Cytometry *Chapter 11*, Unit 11 13.

Dayie, T.K. and Thakur, C.S. (2010). Site-specific labeling of nucleotides for making RNA for high resolution NMR studies using an *E. coli* strain disabled in the oxidative pentose phosphate pathway. Journal of Biomolecular NMR *47*, 19-31.

de Araujo Junqueira, A.F., Dias, A.A., Vale, M.L., Spilborghs, G.M., Bossa, A.S., Lima, B.B., Carvalho, A.F., Guerrant, R.L., Ribeiro, R.A. and Brito, G.A. (2011). Adenosine deaminase inhibition prevents *Clostridium difficile* toxin A-induced enteritis in mice. Infection and Immunity *79*, 653-662.

Deaglio, S., Dwyer, K.M., Gao, W., Friedman, D., Usheva, A., Erat, A., Chen, J.F., Enjyoji, K., Linden, J., Oukka, M., Kuchroo, V.K., Strom, T.B. and Robson, S.C. (2007). Adenosine generation catalyzed by CD39 and CD73 expressed on regulatory T cells mediates immune suppression. Journal of Experimental Medicine *204*, 1257-1265.

Desrosiers, M.D., Cembrola, K.M., Fakir, M.J., Stephens, L.A., Jama, F.M., Shameli, A., Mehal, W.Z., Santamaria, P. and Shi, Y. (2007). Adenosine deamination sustains dendritic cell activation in inflammation. Journal of Immunology *179*, 1884-1892.

Dicksved, J., Halfvarson, J., Rosenquist, M., Jarnerot, G., Tysk, C., Apajalahti, J., Engstrand, L. and Jansson, J.K. (2008). Molecular analysis of the gut microbiota of identical twins with Crohn's disease. ISME Journal *2*, 716-727.

Domach, M.M., Leung, S.K., Cahn, R.E., Cocks, G.G. and Shuler, M.L. (1984). Computer model for glucose-limited growth of a single cell of *Escherichia coli* B/r-A. Biotechnology and Bioengineering *26*, 203-216.

Duchmann, R., Kaiser, I., Hermann, E., Mayet, W., Ewe, K. and Meyer zum Buschenfelde, K.H. (1995). Tolerance exists towards resident intestinal flora but is broken in active inflammatory bowel disease (IBD). Clinical and Experimental Immunology *102*, 448-455.

Duerr, R.H., Taylor, K.D., Brant, S.R., Rioux, J.D., Silverberg, M.S., Daly, M.J., Steinhart, A.H., Abraham, C., Regueiro, M., Griffiths, A., Dassopoulos, T., Bitton, A., Yang, H., Targan, S., Datta, L.W., Kistner, E.O., Schumm, L.P., Lee, A.T., Gregersen, P.K., Barmada, M.M., Rotter, J.I., Nicolae, D.L. and Cho, J.H. (2006). A genome-wide association study identifies *IL23R* as an inflammatory bowel disease gene. Science *314*, 1461-1463.

Duncan, S.H., Louis, P. and Flint, H.J. (2007). Cultivable bacterial diversity from the human colon. Letters in Applied Microbiology *44*, 343-350.

Dürr, U.H.N., Sudheendra, U.S. and Ramamoorthy, A. (2006). LL-37, the only human member of the cathelicidin family of antimicrobial peptides. Biochimica et Biophysica Acta (BBA) - Biomembranes *1758*, 1408-1425.

Eckburg, P.B., Bik, E.M., Bernstein, C.N., Purdom, E., Dethlefsen, L., Sargent, M., Gill, S.R., Nelson, K.E. and Relman, D.A. (2005). Diversity of the human intestinal microbial flora. Science *308*, 1635-1638.

Eckmann, L., Nebelsiek, T., Fingerle, A.A., Dann, S.M., Mages, J., Lang, R., Robine, S., Kagnoff, M.F., Schmid, R.M., Karin, M., Arkan, M.C. and Greten, F.R. (2008). Opposing functions of IKKbeta during acute and chronic intestinal inflammation. Proceedings of the National Academy of Sciences of the United States of America *105*, 15058-15063.

Eisenhut, M. (2006). Changes in ion transport in inflammatory disease. Journal of Inflammation *3*, 5.

Erdmann, A.A., Gao, Z.G., Jung, U., Foley, J., Borenstein, T., Jacobson, K.A. and Fowler, D.H. (2005). Activation of Th1 and Tc1 cell adenosine A_{2A} receptors directly inhibits IL-2 secretion in vitro and IL-2-driven expansion in vivo. Blood *105*, 4707-4714.

Ermolaeva, M.D. (2001). Synonymous codon usage in bacteria. Current Issues in Molecular Biology *3*, 91-97.

Estrela, A.B. and Abraham, W.R. (2011). Adenosine in the inflamed gut: a janus faced compound. Current Medicinal Chemistry *18*, 2791-2815.

Evershed, R.P., Crossman, Z.M., Bull, I.D., Mottram, H., Dungait, J.A., Maxfield, P.J. and Brennand, E.L. (2006). ^{13}C-Labelling of lipids to investigate microbial communities in the environment. Current Opinion in Biotechnology *17*, 72-82.

Fellermann, K., Stange, D.E., Schaeffeler, E., Schmalzl, H., Wehkamp, J., Bevins, C.L., Reinisch, W., Teml, A., Schwab, M., Lichter, P., Radlwimmer, B. and Stange, E.F. (2006). A chromosome 8 gene-cluster polymorphism with low human beta-defensin 2 gene copy number predisposes to Crohn disease of the colon. American Journal of Human Genetics *79*, 439-448.

Feoktistov, I., Ryzhov, S., Goldstein, A.E. and Biaggioni, I. (2003). Mast cell-mediated stimulation of angiogenesis: cooperative interaction between A_{2B} and A_3 adenosine receptors. Circulation Research *92*, 485-492.

Fiebich, B.L., Akundi, R.S., Biber, K., Hamke, M., Schmidt, C., Butcher, R.D., van Calker, D. and Willmroth, F. (2005). IL-6 expression induced by adenosine A2b receptor stimulation

in U373 MG cells depends on p38 mitogen activated kinase and protein kinase C. Neurochemistry International *46*, 501-512.

Fiehn, O. (2002). Metabolomics – the link between genotypes and phenotypes. Plant Molecular Biology *48*, 155-171.

Finlay, B.B. and McFadden, G. (2006). Anti-immunology: evasion of the host immune system by bacterial and viral pathogens. Cell *124*, 767-782.

Flach, T.L., Pang, W., Chau, E.M., Desrosiers, M.D. and Shi, Y. (2009). Adenosine primes resting stage dendritic cells before their activation. Biochemical and Biophysical Research Communications *380*, 748-751.

Fortin, A., Harbour, D., Fernandes, M., Borgeat, P. and Bourgoin, S. (2006). Differential expression of adenosine receptors in human neutrophils: up-regulation by specific Th1 cytokines and lipopolysaccharide. Journal of Leukocyte Biology *79*, 574-585.

Frank, D.N., St. Amand, A.L., Feldman, R.A., Boedeker, E.C., Harpaz, N. and Pace, N.R. (2007). Molecular-phylogenetic characterization of microbial community imbalances in human inflammatory bowel diseases. Proceedings of the National Academy of Sciences of the United States of America *104*, 13780-13785.

Frank, D.N., Robertson, C.E., Hamm, C.M., Kpadeh, Z., Zhang, T., Chen, H., Zhu, W., Sartor, R.B., Boedeker, E.C., Harpaz, N., Pace, N.R. and Li, E. (2011). Disease phenotype and genotype are associated with shifts in intestinal-associated microbiota in inflammatory bowel diseases. Inflammatory Bowel Diseases *17*, 179-184.

Fredholm, B.B., AP, I.J., Jacobson, K.A., Klotz, K.N. and Linden, J. (2001a). International Union of Pharmacology. XXV. Nomenclature and classification of adenosine receptors. Pharmacology Reviews *53*, 527-552.

Fredholm, B.B., Irenius, E., Kull, B. and Schulte, G. (2001b). Comparison of the potency of adenosine as an agonist at human adenosine receptors expressed in Chinese hamster ovary cells. Biochemical Pharmacology *61*, 443-448.

Frick, J.S., MacManus, C.F., Scully, M., Glover, L.E., Eltzschig, H.K. and Colgan, S.P. (2009). Contribution of adenosine A2B receptors to inflammatory parameters of experimental colitis. Journal of Immunology *182*, 4957-4964.

Friedman, D.J., Kunzli, B.M., YI, A.R., Sevigny, J., Berberat, P.O., Enjyoji, K., Csizmadia, E., Friess, H. and Robson, S.C. (2009). From the Cover: CD39 deletion exacerbates experimental murine colitis and human polymorphisms increase susceptibility to inflammatory bowel disease. Proceedings of the National Academy of Sciences of the United States of America *106*, 16788-16793.

Friedrich, M.W. (2006). Stable-isotope probing of DNA: insights into the function of uncultivated microorganisms from isotopically labeled metagenomes. Current Opinion in Biotechnology *17*, 59-66.

Fujimura, K.E., Slusher, N.A., Cabana, M.D. and Lynch, S.V. (2010). Role of the gut microbiota in defining human health. Expert Review of Anti-infective Therapy *8*, 435-454.

Gadangi, P., Longaker, M., Naime, D., Levin, R.I., Recht, P.A., Montesinos, M.C., Buckley, M.T., Carlin, G. and Cronstein, B.N. (1996). The anti-inflammatory mechanism of sulfasalazine is related to adenosine release at inflamed sites. Journal of Immunology *156*, 1937-1941.

Ganz, T. (2003). Defensins: antimicrobial peptides of innate immunity. Nature Reviews Immunology *3*, 710-720.

Gessi, S., Varani, K., Merighi, S., Ongini, E. and Borea, P.A. (2000). A_{2A} adenosine receptors in human peripheral blood cells. British Journal of Pharmacology *129*, 2-11.

Gessi, S., Merighi, S., Varani, K., Cattabriga, E., Benini, A., Mirandola, P., Leung, E., Mac Lennan, S., Feo, C., Baraldi, S. and Borea, P.A. (2007). Adenosine receptors in colon carcinoma tissues and colon tumoral cell lines: focus on the A_3 adenosine subtype. Journal of Cellular Physiology *211*, 826-836.

Ghosh, D., Porter, E., Shen, B., Lee, S.K., Wilk, D., Drazba, J., Yadav, S.P., Crabb, J.W., Ganz, T. and Bevins, C.L. (2002). Paneth cell trypsin is the processing enzyme for human defensin-5. Nature Immunology *3*, 583-590.

Giacometti, A., Cirioni, O., Barchiesi, F., Del Prete, M.S., Fortuna, M., Caselli, F. and Scalise, G. (2000). *In vitro* susceptibility tests for cationic peptides: comparison of broth microdilution methods for bacteria that grow aerobically. Antimicrobial Agents and Chemotherapy *44*, 1694-1696.

Gill, S.R., Pop, M., Deboy, R.T., Eckburg, P.B., Turnbaugh, P.J., Samuel, B.S., Gordon, J.I., Relman, D.A., Fraser-Liggett, C.M. and Nelson, K.E. (2006). Metagenomic analysis of the human distal gut microbiome. Science *312*, 1355-1359.

Glick, J. and Garber, N. (1983). The Intracellular Localization of *Pseudomonas aeruginosa* Lectins. Journal of General Microbiology *129*, 3085-3090.

Gosalbes, M.J., Durban, A., Pignatelli, M., Abellan, J.J., Jimenez-Hernandez, N., Perez-Cobas, A.E., Latorre, A. and Moya, A. (2011). Metatranscriptomic approach to analyze the functional human gut microbiota. PLoS One *6*, e17447.

Graca da Silveira, M., Vitoria San Romao, M., Loureiro-Dias, M.C., Rombouts, F.M. and Abee, T. (2002). Flow cytometric assessment of membrane integrity of ethanol-stressed *Oenococcus oeni* cells. Applied and Environmental Microbiology *68*, 6087-6093.

Gradel, K.O., Nielsen, H.L., Schonheyder, H.C., Ejlertsen, T., Kristensen, B. and Nielsen, H. (2009). Increased short- and long-term risk of inflammatory bowel disease after *Salmonella* or *Campylobacter* gastroenteritis. Gastroenterology *137*, 495-501.

Greenwell-Wild, T., Vazquez, N., Sim, D., Schito, M., Chatterjee, D., Orenstein, J.M. and Wahl, S.M. (2002). *Mycobacterium avium* infection and modulation of human macrophage gene expression. Journal of Immunology *169*, 6286-6297.

Guarner, F. and Schaafsma, G.J. (1998). Probiotics. International Journal of Food Microbiology *39*, 237-238.

Gullberg, U., Bengtsson, N., Bulow, E., Garwicz, D., Lindmark, A. and Olsson, I. (1999). Processing and targeting of granule proteins in human neutrophils. Journal of Immunological Methods *232*, 201-210.

Guzman, J., Yu, J.G., Suntres, Z., Bozarov, A., Cooke, H., Javed, N., Auer, H., Palatini, J., Hassanain, H.H., Cardounel, A.J., Javed, A., Grants, I., Wunderlich, J.E. and Christofi, F.L. (2006). ADOA3R as a therapeutic target in experimental colitis: proof by validated high-density oligonucleotide microarray analysis. Inflammatory Bowel Diseases *12*, 766-789.

Hafez, M., Hayes, K., Goldrick, M., Grencis, R.K. and Roberts, I.S. (2010). The K5 capsule of *Escherichia coli* strain Nissle 1917 is important in stimulating expression of Toll-like receptor 5, CD14, MyD88, and TRIF together with the induction of interleukin-8 expression via the mitogen-activated protein kinase pathway in epithelial cells. Infection and Immunity *78*, 2153-2162.

Halme, L., Paavola-Sakki, P., Turunen, U., Lappalainen, M., Farkkila, M. and Kontula, K. (2006). Family and twin studies in inflammatory bowel disease. World Journal of Gastroenterology *12*, 3668-3672.

Hampe, J., Franke, A., Rosenstiel, P., Till, A., Teuber, M., Huse, K., Albrecht, M., Mayr, G., De La Vega, F.M., Briggs, J., Gunther, S., Prescott, N.J., Onnie, C.M., Hasler, R., Sipos, B., Folsch, U.R., Lengauer, T., Platzer, M., Mathew, C.G., Krawczak, M. and Schreiber, S. (2007). A genome-wide association scan of nonsynonymous SNPs identifies a susceptibility variant for Crohn disease in *ATG16L1*. Nature Genetics *39*, 207-211.

Hancock, R.E. and Scott, M.G. (2000). The role of antimicrobial peptides in animal defenses. Proceedings of the National Academy of Sciences of the United States of America *97*, 8856-8861.

Hancock, R.E. and Rozek, A. (2002). Role of membranes in the activities of antimicrobial cationic peptides. FEMS Microbiology Letters *206*, 143-149.

Harder, J., Bartels, J., Christophers, E. and Schroder, J.M. (1997). A peptide antibiotic from human skin. Nature *387*, 861.

Harder, J., Bartels, J., Christophers, E. and Schroder, J.M. (2001). Isolation and characterization of human beta -defensin-3, a novel human inducible peptide antibiotic. Journal of Biological Chemistry *276*, 5707-5713.

Hart, M.L., Jacobi, B., Schittenhelm, J., Henn, M. and Eltzschig, H.K. (2009). Cutting Edge: A2B Adenosine receptor signaling provides potent protection during intestinal ischemia/reperfusion injury. Journal of Immunology *182*, 3965-3968.

Hasko, G., Kuhel, D.G., Chen, J.F., Schwarzschild, M.A., Deitch, E.A., Mabley, J.G., Marton, A. and Szabo, C. (2000). Adenosine inhibits IL-12 and TNF-[alpha] production via adenosine A2a receptor-dependent and independent mechanisms. The FASEB Journal *14*, 2065-2074.

Hasko, G. and Cronstein, B.N. (2004). Adenosine: an endogenous regulator of innate immunity. Trends in Immunology *25*, 33-39.

Hasko, G., Linden, J., Cronstein, B. and Pacher, P. (2008). Adenosine receptors: therapeutic aspects for inflammatory and immune diseases. Nature Reviews Drug Discovery *7*, 759-770.

Hattori, M. and Taylor, T.D. (2009). The human intestinal microbiome: a new frontier of human biology. DNA Research *16*, 1-12.

Heazlewood, C.K., Cook, M.C., Eri, R., Price, G.R., Tauro, S.B., Taupin, D., Thornton, D.J., Png, C.W., Crockford, T.L., Cornall, R.J., Adams, R., Kato, M., Nelms, K.A., Hong, N.A., Florin, T.H., Goodnow, C.C. and McGuckin, M.A. (2008). Aberrant mucin assembly in mice causes endoplasmic reticulum stress and spontaneous inflammation resembling ulcerative colitis. PLoS Medicine *5*, e54.

Hong, R.W., Shchepetov, M., Weiser, J.N. and Axelsen, P.H. (2003). Transcriptional profile of the *Escherichia coli* response to the antimicrobial insect peptide cecropin A. Antimicrobial Agents and Chemotherapy *47*, 1-6.

Hooper, L.V., Stappenbeck, T.S., Hong, C.V. and Gordon, J.I. (2003). Angiogenins: a new class of microbicidal proteins involved in innate immunity. Nature Immunology *4*, 269-273.

Hoover, D.M., Rajashankar, K.R., Blumenthal, R., Puri, A., Oppenheim, J.J., Chertov, O. and Lubkowski, J. (2000). The structure of human beta-defensin-2 shows evidence of higher order oligomerization. Journal of Biological Chemistry *275*, 32911-32918.

Hormannsperger, G. and Haller, D. (2010). Molecular crosstalk of probiotic bacteria with the intestinal immune system: clinical relevance in the context of inflammatory bowel disease. International Journal of Medical Microbiology *300*, 63-73.

Huebner, C., Ding, Y., Petermann, I., Knapp, C. and Ferguson, L.R. (2011). The probiotic *Escherichia coli* Nissle 1917 reduces pathogen invasion and modulates cytokine expression in Caco-2 cells infected with Crohn's disease-associated *E. coli* LF82. Applied and Environmental Microbiology *77*, 2541-2544.

Hughes, D.T. and Sperandio, V. (2008). Inter-kingdom signalling: communication between bacteria and their hosts. Nature Reviews Microbiology *6*, 111-120.

Hugot, J.P., Chamaillard, M., Zouali, H., Lesage, S., Cezard, J.P., Belaiche, J., Almer, S., Tysk, C., O'Morain, C.A., Gassull, M., Binder, V., Finkel, Y., Cortot, A., Modigliani, R., Laurent-Puig, P., Gower-Rousseau, C., Macry, J., Colombel, J.F., Sahbatou, M. and Thomas, G. (2001). Association of NOD2 leucine-rich repeat variants with susceptibility to Crohn's disease. Nature *411*, 599-603.

Hwang, K.K., Hall, C.S., Spielman, W.S. and Sparks, H.V. (2001). FK506 promotes adenosine release from endothelial cells via inhibition of adenosine kinase. European Journal of Pharmacology *425*, 85-93.

Ivanov, II, Atarashi, K., Manel, N., Brodie, E.L., Shima, T., Karaoz, U., Wei, D., Goldfarb, K.C., Santee, C.A., Lynch, S.V., Tanoue, T., Imaoka, A., Itoh, K., Takeda, K., Umesaki, Y., Honda, K. and Littman, D.R. (2009). Induction of intestinal Th17 cells by segmented filamentous bacteria. Cell *139*, 485-498.

Izcue, A., Coombes, J.L. and Powrie, F. (2009). Regulatory lymphocytes and intestinal inflammation. Annual Review of Immunology *27*, 313-338.

Jackson, J.R., Seed, M.P., Kircher, C.H., Willoughby, D.A. and Winkler, J.D. (1997). The codependence of angiogenesis and chronic inflammation. The FASEB Journal *11*, 457-465.

Jacobson, K.A. and Gao, Z.G. (2006). Adenosine receptors as therapeutic targets. Nature Reviews Drug Discovery *5*, 247-264.

Jijon, H.B., Walker, J., Hoentjen, F., Diaz, H., Ewaschuk, J., Jobin, C. and Madsen, K.L. (2005). Adenosine is a negative regulator of NF-kappaB and MAPK signaling in human intestinal epithelial cells. Cellular Immunology *237*, 86-95.

Kaderbhai, N.N., Broadhurst, D.I., Ellis, D.I., Goodacre, R. and Kell, D.B. (2003). Functional genomics via metabolic footprinting: monitoring metabolite secretion by *Escherichia coli* tryptophan metabolism mutants using FT-IR and direct injection electrospray mass spectrometry. Comparative and Functional Genomics *4*, 376-391.

Kaper, J.B., Nataro, J.P. and Mobley, H.L.T. (2004). Pathogenic *Escherichia coli*. Nature Reviews Microbiology *2*, 123-140.

Kaser, A., Zeissig, S. and Blumberg, R.S. (2010). Inflammatory bowel disease. Annual Review of Immunology *28*, 573-621.

KEEG Kyoto Encyclopedia of Genes and Genomes : http://www.genome.jp/kegg/pathway/map/map00230.html.

Kell, D.B., Brown, M., Davey, H.M., Dunn, W.B., Spasic, I. and Oliver, S.G. (2005). Metabolic footprinting and systems biology: the medium is the message. Nature Reviews Microbiology *3*, 557-565.

Kelly, D., Campbell, J.I., King, T.P., Grant, G., Jansson, E.A., Coutts, A.G.P., Pettersson, S. and Conway, S. (2004). Commensal anaerobic gut bacteria attenuate inflammation by regulating nuclear-cytoplasmic shuttling of PPAR-γ and RelA. Nature Immunology *5*, 104-112.

Kelly, D., Conway, S. and Aminov, R. (2005). Commensal gut bacteria: mechanisms of immune modulation. Trends in Immunology *26*, 326-333.

Khoa, N.D., Montesinos, M.C., Reiss, A.B., Delano, D., Awadallah, N. and Cronstein, B.N. (2001). Inflammatory cytokines regulate function and expression of adenosine A_{2A} receptors in human monocytic THP-1 cells. Journal of Immunology *167*, 4026-4032.

Kim, Y.G., Park, J.H., Shaw, M.H., Franchi, L., Inohara, N. and Nunez, G. (2008). The cytosolic sensors Nod1 and Nod2 are critical for bacterial recognition and host defense after exposure to Toll-like receptor ligands. Immunity *28*, 246-257.

Kobie, J.J., Shah, P.R., Yang, L., Rebhahn, J.A., Fowell, D.J. and Mosmann, T.R. (2006). T regulatory and primed uncommitted CD4 T cells express CD73, which suppresses effector CD4 T cells by converting 5'-adenosine monophosphate to adenosine. Journal of Immunology *177*, 6780-6786.

Kohlgraf, K.G., Ackermann, A., Lu, X., Burnell, K., Belanger, M., Cavanaugh, J.E., Xie, H., Progulske-Fox, A. and Brogden, K.A. (2010a). Defensins attenuate cytokine responses yet enhance antibody responses to *Porphyromonas gingivalis* adhesins in mice. Future Microbiology *5*, 115-125.

Kohlgraf, K.G., Pingel, L.C., Dietrich, D.E. and Brogden, K.A. (2010b). Defensins as anti-inflammatory compounds and mucosal adjuvants. Future Microbiology *5*, 99-113.

Kolachala, V., Asamoah, V., Wang, L., Obertone, T.S., Ziegler, T.R., Merlin, D. and Sitaraman, S.V. (2005a). TNF-alpha upregulates adenosine 2b (A2b) receptor expression and signaling in intestinal epithelial cells: a basis for A2bR overexpression in colitis. Cellular and Molecular Life Sciences *62*, 2647-2657.

Kolachala, V., Asamoah, V., Wang, L., Srinivasan, S., Merlin, D. and Sitaraman, S.V. (2005b). Interferon-gamma down-regulates adenosine 2b receptor-mediated signaling and short circuit current in the intestinal epithelia by inhibiting the expression of adenylate cyclase. Journal of Biological Chemistry *280*, 4048-4057.

Kolachala, V., Ruble, B., Vijay-Kumar, M., Wang, L., Mwangi, S., Figler, H., Figler, R., Srinivasan, S., Gewirtz, A., Linden, J., Merlin, D. and Sitaraman, S. (2008a). Blockade of adenosine A_{2B} receptors ameliorates murine colitis. British Journal of Pharmacology *155*, 127-137.

Kolachala, V.L., Vijay-Kumar, M., Dalmasso, G., Yang, D., Linden, J., Wang, L., Gewirtz, A., Ravid, K., Merlin, D. and Sitaraman, S.V. (2008b). A_{2B} adenosine receptor gene deletion attenuates murine colitis. Gastroenterology *135*, 861-870.

Koshiba, M., Kojima, H., Huang, S., Apasov, S. and Sitkovsky, M.V. (1997). Memory of extracellular adenosine A_{2A} purinergic receptor-mediated signaling in murine T cells. Journal of Biological Chemistry *272*, 25881-25889.

Kreckler, L.M., Wan, T.C., Ge, Z.D. and Auchampach, J.A. (2006). Adenosine inhibits tumor necrosis factor-alpha release from mouse peritoneal macrophages via A_{2A} and A_{2B} but not the A_3 adenosine receptor. Journal of Pharmacology and Experimental Therapeutics *317*, 172-180.

Krishnakumari, V., Singh, S. and Nagaraj, R. (2006). Antibacterial activities of synthetic peptides corresponding to the carboxy-terminal region of human beta-defensins 1-3. Peptides *27*, 2607-2613.

Lakatos, P.L. (2006). Recent trends in the epidemiology of inflammatory bowel diseases: up or down? World Journal of Gastroenterology *12*, 6102-6108.

Lan, Y., Ye, Y., Kozlowska, J., Lam, J.K.W., Drake, A.F. and Mason, A.J. (2010). Structural contributions to the intracellular targeting strategies of antimicrobial peptides. Biochimica et Biophysica Acta (BBA) - Biomembranes *1798*, 1934-1943.

Langrish, C.L., McKenzie, B.S., Wilson, N.J., de Waal Malefyt, R., Kastelein, R.A. and Cua, D.J. (2004). IL-12 and IL-23: master regulators of innate and adaptive immunity. Immunological Reviews *202*, 96-105.

Lappas, C.M., Rieger, J.M. and Linden, J. (2005). A_{2A} adenosine receptor induction inhibits IFN-gamma production in murine $CD4^+$ T cells. Journal of Immunology *174*, 1073-1080.

Lawrance, I.C., Fiocchi, C. and Chakravarti, S. (2001). Ulcerative colitis and Crohn's disease: distinctive gene expression profiles and novel susceptibility candidate genes. Human Molecular Genetics *10*, 445-456.

Lee, H.Y., Andalibi, A., Webster, P., Moon, S.K., Teufert, K., Kang, S.H., Li, J.D., Nagura, M., Ganz, T. and Lim, D.J. (2004). Antimicrobial activity of innate immune molecules against *Streptococcus pneumoniae*, *Moraxella catarrhalis* and nontypeable *Haemophilus influenzae*. BMC Infectious Diseases *4*, 12.

Lee, J., Mo, J.H., Katakura, K., Alkalay, I., Rucker, A.N., Liu, Y.T., Lee, H.K., Shen, C., Cojocaru, G., Shenouda, S., Kagnoff, M., Eckmann, L., Ben-Neriah, Y. and Raz, E. (2006). Maintenance of colonic homeostasis by distinctive apical TLR9 signalling in intestinal epithelial cells. Nature Cell Biology *8*, 1327-1336.

Lee, J.C. and Parkes, M. (2011). Genome-wide association studies and Crohn's disease. Briefings in Functional Genomics *10*, 71-76.

Lehrer, R.I., Barton, A., Daher, K.A., Harwig, S.S., Ganz, T. and Selsted, M.E. (1989). Interaction of human defensins with *Escherichia coli.* Mechanism of bactericidal activity. Journal of Clinical Investigation *84*, 553-561.

Lehrer, R.I., Rosenman, M., Harwig, S.S., Jackson, R. and Eisenhauer, P. (1991). Ultrasensitive assays for endogenous antimicrobial polypeptides. Journal of Immunological Methods *137*, 167-173.

Lehrer, R.I., Lichtenstein, A.K. and Ganz, T. (1993). Defensins: antimicrobial and cytotoxic peptides of mammalian cells. Annual Review of Immunology *11*, 105-128.

Lehrer, R.I. and Ganz, T. (2002). Cathelicidins: a family of endogenous antimicrobial peptides. Current Opinion in Hematology *9*, 18-22.

Lehrer, R.I. (2004). Primate defensins. Nature Reviews Microbiology *2*, 727-738.

Lencer, W.I., Cheung, G., Strohmeier, G.R., Currie, M.G., Ouellette, A.J., Selsted, M.E. and Madara, J.L. (1997). Induction of epithelial chloride secretion by channel-forming cryptdins 2 and 3. Proceedings of the National Academy of Sciences of the United States of America *94*, 8585-8589.

Levine, B. and Deretic, V. (2007). Unveiling the roles of autophagy in innate and adaptive immunity. Nature Reviews Immunology *7*, 767-777.

Ley, R.E., Backhed, F., Turnbaugh, P., Lozupone, C.A., Knight, R.D. and Gordon, J.I. (2005). Obesity alters gut microbial ecology. Proceedings of the National Academy of Sciences of the United States of America *102*, 11070-11075.

Ley, R.E., Peterson, D.A. and Gordon, J.I. (2006a). Ecological and evolutionary forces shaping microbial diversity in the human intestine. Cell *124*, 837-848.

Ley, R.E., Turnbaugh, P.J., Klein, S. and Gordon, J.I. (2006b). Microbial ecology: Human gut microbes associated with obesity. Nature *444*, 1022-1023.

Ley, R.E., Lozupone, C.A., Hamady, M., Knight, R. and Gordon, J.I. (2008). Worlds within worlds: evolution of the vertebrate gut microbiota. Nature Reviews Microbiology *6*, 776-788.

Li, P. and Hotamisligil, G.S. (2010). Metabolism: Host and microbes in a pickle. Nature *464*, 1287-1288.

Lin, P.W., Simon, P.O., Jr., Gewirtz, A.T., Neish, A.S., Ouellette, A.J., Madara, J.L. and Lencer, W.I. (2004). Paneth cell cryptdins act in vitro as apical paracrine regulators of the innate inflammatory response. Journal of Biological Chemistry *279*, 19902-19907.

Linder, J.U. (2010). cGMP production in bacteria. Molecular and Cellular Biochemistry *334*, 215-219.

Link, A.A., Kino, T., Worth, J.A., McGuire, J.L., Crane, M.L., Chrousos, G.P., Wilder, R.L. and Elenkov, I.J. (2000). Ligand-activation of the adenosine A2a receptors inhibits IL-12 production by human monocytes. Journal of Immunology *164*, 436-442.

Loffler, M., Morote-Garcia, J.C., Eltzschig, S.A., Coe, I.R. and Eltzschig, H.K. (2007). Physiological roles of vascular nucleoside transporters. Arteriosclerosis, Thrombosis, and Vascular Biology *27*, 1004-1013.

Louis, N.A., Robinson, A.M., MacManus, C.F., Karhausen, J., Scully, M. and Colgan, S.P. (2008). Control of IFN-alphaA by CD73: implications for mucosal inflammation. Journal of Immunology *180*, 4246-4255.

Luckey, T.D. (1972). Introduction to intestinal microecology. American Journal of Clinical Nutrition *25*, 1292-1294.

Ma, D., Forsythe, P. and Bienenstock, J. (2004). Live *Lactobacillus reuteri* is essential for the inhibitory effect on tumor necrosis factor alpha-induced interleukin-8 expression. Infection and Immunity *72*, 5308-5314.

Mabley, J., Soriano, F., Pacher, P., Hasko, G., Marton, A., Wallace, R., Salzman, A. and Szabo, C. (2003a). The adenosine A_3 receptor agonist, N6-(3-iodobenzyl)-adenosine-5'-N-methyluronamide, is protective in two murine models of colitis. European Journal of Pharmacology *466*, 323-329.

Mabley, J.G., Pacher, P., Liaudet, L., Soriano, F.G., Hasko, G., Marton, A., Szabo, C. and Salzman, A.L. (2003b). Inosine reduces inflammation and improves survival in a murine model of colitis. American Journal of Physiology Gastrointestinal and Liver Physiology *284*, G138-144.

Macallan, D.C., Fullerton, C.A., Neese, R.A., Haddock, K., Park, S.S. and Hellerstein, M.K. (1998). Measurement of cell proliferation by labeling of DNA with stable isotope-labeled glucose: studies *in vitro*, in animals, and in humans. Proceedings of the National Academy of Sciences of the United States of America *95*, 708-713.

MacMaster, J.F., Dambach, D.M., Lee, D.B., Berry, K.K., Qiu, Y., Zusi, F.C. and Burke, J.R. (2003). An inhibitor of IkappaB kinase, BMS-345541, blocks endothelial cell adhesion

molecule expression and reduces the severity of dextran sulfate sodium-induced colitis in mice. Inflammation Research *52*, 508-511.

Madison, M.N., Kleshchenko, Y.Y., Nde, P.N., Simmons, K.J., Lima, M.F. and Villalta, F. (2007). Human defensin alpha-1 causes *Trypanosoma cruzi* membrane pore formation and induces DNA fragmentation, which leads to trypanosome destruction. Infect Immun *75*, 4780-4791.

Maeda, S., Hsu, L.C., Liu, H., Bankston, L.A., Iimura, M., Kagnoff, M.F., Eckmann, L. and Karin, M. (2005). Nod2 mutation in Crohn's disease potentiates NF-kappaB activity and IL-1beta processing. Science *307*, 734-738.

Magalhaes, J.G., Tattoli, I. and Girardin, S.E. (2007). The intestinal epithelial barrier: how to distinguish between the microbial flora and pathogens. Seminars in Immunology *19*, 106-115.

Mangoni, M.L., Papo, N., Barra, D., Simmaco, M., Bozzi, A., Di Giulio, A. and Rinaldi, A.C. (2004). Effects of the antimicrobial peptide temporin L on cell morphology, membrane permeability and viability of *Escherichia coli*. Biochemical Journal *380*, 859-865.

Manichanh, C., Rigottier-Gois, L., Bonnaud, E., Gloux, K., Pelletier, E., Frangeul, L., Nalin, R., Jarrin, C., Chardon, P., Marteau, P., Roca, J. and Dore, J. (2006). Reduced diversity of faecal microbiota in Crohn's disease revealed by a metagenomic approach. Gut *55*, 205-211.

Mapelli, V., Olsson, L. and Nielsen, J. (2008). Metabolic footprinting in microbiology: methods and applications in functional genomics and biotechnology. Trends in Biotechnology *26*, 490-497.

Marchesi, J.R., Holmes, E., Khan, F., Kochhar, S., Scanlan, P., Shanahan, F., Wilson, I.D. and Wang, Y. (2007). Rapid and noninvasive metabonomic characterization of inflammatory bowel disease. Journal of Proteome Research *6*, 546-551.

Martin, L., Pingle, S.C., Hallam, D.M., Rybak, L.P. and Ramkumar, V. (2006). Activation of the adenosine A_3 receptor in RAW 264.7 cells inhibits lipopolysaccharide-stimulated tumor necrosis factor-alpha release by reducing calcium-dependent activation of nuclear factor-kappaB and extracellular signal-regulated kinase 1/2. Journal of Pharmacology and Experimental Therapeutics *316*, 71-78.

Martinez-Medina, M., Aldeguer, X., Lopez-Siles, M., Gonzalez-Huix, F., Lopez-Oliu, C., Dahbi, G., Blanco, J.E., Blanco, J., Garcia-Gil, L.J. and Darfeuille-Michaud, A. (2009). Molecular diversity of *Escherichia coli* in the human gut: new ecological evidence supporting the role of adherent-invasive *E. coli* (AIEC) in Crohn's disease. Inflammatory Bowel Diseases *15*, 872-882.

Mashego, M.R., Rumbold, K., De Mey, M., Vandamme, E., Soetaert, W. and Heijnen, J.J. (2007). Microbial metabolomics: past, present and future methodologies. Biotechnology Letters *29*, 1-16.

Masseret, E., Boudeau, J., Colombel, J.F., Neut, C., Desreumaux, P., Joly, B., Cortot, A. and Darfeuille-Michaud, A. (2001). Genetically related *Escherichia coli* strains associated with Crohn's disease. Gut *48*, 320-325.

Matsuo, M., Oogai, Y., Kato, F., Sugai, M. and Komatsuzawa, H. (2011). Growth-phase dependence of susceptibility to antimicrobial peptides in *Staphylococcus aureus*. Microbiology *157*, 1786-1797.

Matsuzaki, K. (1999). Why and how are peptide-lipid interactions utilized for self-defense? Magainins and tachyplesins as archetypes. Biochimica et Biophysica Acta *1462*, 1-10.

Melmed, G., Thomas, L.S., Lee, N., Tesfay, S.Y., Lukasek, K., Michelsen, K.S., Zhou, Y., Hu, B., Arditi, M. and Abreu, M.T. (2003). Human intestinal epithelial cells are broadly unresponsive to Toll-like receptor 2-dependent bacterial ligands: implications for host-microbial interactions in the gut. Journal of Immunology *170*, 1406-1415.

Méndez-Ortiz, M.M., Hyodo, M., Hayakawa, Y. and Membrillo-Hernández, J. (2006). Genome-wide Transcriptional Profile of *Escherichia coli* in Response to High Levels of the Second Messenger 3′,5′-Cyclic Diguanylic Acid. Journal of Biological Chemistry *281*, 8090-8099.

Menendez, A. and Brett Finlay, B. (2007). Defensins in the immunology of bacterial infections. Current Opinion in Immunology *19*, 385-391.

METLIN Metabolite and tandem MS database, from Scripps Center for Metabolomics http://metlin.scripps.edu/.

Meyer-Hoffert, U., Hornef, M.W., Henriques-Normark, B., Axelsson, L.G., Midtvedt, T., Putsep, K. and Andersson, M. (2008). Secreted enteric antimicrobial activity localises to the mucus surface layer. Gut *57*, 764-771.

Mondel, M., Schroeder, B.O., Zimmermann, K., Huber, H., Nuding, S., Beisner, J., Fellermann, K., Stange, E.F. and Wehkamp, J. (2009). Probiotic *E. coli* treatment mediates antimicrobial human beta-defensin synthesis and fecal excretion in humans. Mucosal Immunology *2*, 166-172.

Montesinos, M.C., Desai, A., Delano, D., Chen, J.F., Fink, J.S., Jacobson, M.A. and Cronstein, B.N. (2003). Adenosine A_{2A} or A_3 receptors are required for inhibition of inflammation by methotrexate and its analog MX-68. Arthritis and Rheumatism *48*, 240-247.

Montesinos, M.C., Takedachi, M., Thompson, L.F., Wilder, T.F., Fernandez, P. and Cronstein, B.N. (2007). The antiinflammatory mechanism of methotrexate depends on extracellular conversion of adenine nucleotides to adenosine by ecto-5'-nucleotidase: findings in a study of ecto-5'-nucleotidase gene-deficient mice. Arthritis and Rheumatism *56*, 1440-1445.

Morote-Garcia, J.C., Rosenberger, P., Nivillac, N.M., Coe, I.R. and Eltzschig, H.K. (2009). Hypoxia-inducible factor-dependent repression of equilibrative nucleoside transporter 2 attenuates mucosal inflammation during intestinal hypoxia. Gastroenterology *136*, 607-618.

Mowat, A.M. (2003). Anatomical basis of tolerance and immunity to intestinal antigens. Nature Reviews Immunology *3*, 331-341.

Müller, C., Autenrieth, I. and Peschel, A. (2005). Intestinal epithelial barrier and mucosal immunity. Cellular and Molecular Life Sciences *62*, 1297-1307.

Muto, A. and Osawa, S. (1987). The guanine and cytosine content of genomic DNA and bacterial evolution. Proceedings of the National Academy of Sciences of the United States of America *84*, 166-169.

Naganuma, M., Wiznerowicz, E.B., Lappas, C.M., Linden, J., Worthington, M.T. and Ernst, P.B. (2006). Cutting edge: Critical role for A_{2A} adenosine receptors in the T cell-mediated regulation of colitis. Journal of Immunology *177*, 2765-2769.

Nakav, S., Chaimovitz, C., Sufaro, Y., Lewis, E.C., Shaked, G., Czeiger, D., Zlotnik, M. and Douvdevani, A. (2008). Anti-inflammatory preconditioning by agonists of adenosine A1 receptor. PLoS One *3*, e2107.

Naumann, M. and Scheidereit, C. (1994). Activation of NF-kappa B *in vivo* is regulated by multiple phosphorylations. EMBO Journal *13*, 4597-4607.

Neish, A.S., Gewirtz, A.T., Zeng, H., Young, A.N., Hobert, M.E., Karmali, V., Rao, A.S. and Madara, J.L. (2000). Prokaryotic Regulation of Epithelial Responses by Inhibition of IκB-α Ubiquitination. Science *289*, 1560-1563.

Nell, S., Suerbaum, S. and Josenhans, C. (2010). The impact of the microbiota on the pathogenesis of IBD: lessons from mouse infection models. Nature Reviews Microbiology *8*, 564-577.

Nemeth, Z.H., Lutz, C.S., Csoka, B., Deitch, E.A., Leibovich, S.J., Gause, W.C., Tone, M., Pacher, P., Vizi, E.S. and Hasko, G. (2005). Adenosine augments IL-10 production by macrophages through an A_{2B} receptor-mediated posttranscriptional mechanism. Journal of Immunology *175*, 8260-8270.

Nenci, A., Becker, C., Wullaert, A., Gareus, R., van Loo, G., Danese, S., Huth, M., Nikolaev, A., Neufert, C., Madison, B., Gumucio, D., Neurath, M.F. and Pasparakis, M. (2007). Epithelial NEMO links innate immunity to chronic intestinal inflammation. Nature *446*, 557-561.

Neshat, S., deVries, M., Barajas-Espinosa, A.R., Skeith, L., Chisholm, S.P. and Lomax, A.E. (2009). Loss of purinergic vascular regulation in the colon during colitis is associated with upregulation of CD39. American Journal of Physiology Gastrointestinal and Liver Physiology *296*, G399-405.

Neu, H.C. (1968). The 5'-nucleotidases (uridine diphosphate sugar hydrolases) of the *Enterobacteriaceae*. Biochemistry *7*, 3766-3773.

Neufeld, J.D., Wagner, M. and Murrell, J.C. (2007). Who eats what, where and when? Isotope-labelling experiments are coming of age. ISME Journal *1*, 103-110.

Neurath, M.F., Pettersson, S., Meyer zum Buschenfelde, K.H. and Strober, W. (1996). Local administration of antisense phosphorothioate oligonucleotides to the p65 subunit of NF-kappa B abrogates established experimental colitis in mice. Nature Medicine *2*, 998-1004.

Nguyen, D.K., Montesinos, M.C., Williams, A.J., Kelly, M. and Cronstein, B.N. (2003). Th1 cytokines regulate adenosine receptors and their downstream signaling elements in human microvascular endothelial cells. Journal of Immunology *171*, 3991-3998.

Nicolas, P. (2009). Multifunctional host defense peptides: intracellular-targeting antimicrobial peptides. FEBS Journal *276*, 6483-6496.

Niyonsaba, F., Iwabuchi, K., Matsuda, H., Ogawa, H. and Nagaoka, I. (2002). Epithelial cell-derived human beta-defensin-2 acts as a chemotaxin for mast cells through a pertussis toxin-sensitive and phospholipase C-dependent pathway. International Immunology *14*, 421-426.

Niyonsaba, F., Ogawa, H. and Nagaoka, I. (2004). Human beta-defensin-2 functions as a chemotactic agent for tumour necrosis factor-alpha-treated human neutrophils. Immunology *111*, 273-281.

Nizet, V. (2006). Antimicrobial peptide resistance mechanisms of human bacterial pathogens. Current Issues in Molecular Biology *8*, 11-26.

Novitskiy, S.V., Ryzhov, S., Zaynagetdinov, R., Goldstein, A.E., Huang, Y., Tikhomirov, O.Y., Blackburn, M.R., Biaggioni, I., Carbone, D.P., Feoktistov, I. and Dikov, M.M. (2008). Adenosine receptors in regulation of dendritic cell differentiation and function. Blood *112*, 1822-1831.

Nyström, T. (2001). Not quite dead enough: on bacterial life, culturability, senescence, and death. Archives of Microbiology *176*, 159-164.

O'Hara, A.M. and Shanahan, F. (2006). The gut flora as a forgotten organ. EMBO Reports *7*, 688-693.

O'Neil, D.A., Porter, E.M., Elewaut, D., Anderson, G.M., Eckmann, L., Ganz, T. and Kagnoff, M.F. (1999). Expression and Regulation of the Human ß-Defensins hBD-1 and hBD-2 in Intestinal Epithelium. Journal of Immunology *163*, 6718-6724.

O'Neil, D.A. (2003). Regulation of expression of beta-defensins: endogenous enteric peptide antibiotics. Molecular Immunology *40*, 445-450.

Odashima, M., Bamias, G., Rivera-Nieves, J., Linden, J., Nast, C.C., Moskaluk, C.A., Marini, M., Sugawara, K., Kozaiwa, K., Otaka, M., Watanabe, S. and Cominelli, F. (2005). Activation of A_{2A} adenosine receptor attenuates intestinal inflammation in animal models of inflammatory bowel disease. Gastroenterology *129*, 26-33.

Ogura, Y., Bonen, D.K., Inohara, N., Nicolae, D.L., Chen, F.F., Ramos, R., Britton, H., Moran, T., Karaliuskas, R., Duerr, R.H., Achkar, J.P., Brant, S.R., Bayless, T.M., Kirschner, B.S., Hanauer, S.B., Nunez, G. and Cho, J.H. (2001). A frameshift mutation in NOD2 associated with susceptibility to Crohn's disease. Nature *411*, 603-606.

Ohta, A. and Sitkovsky, M. (2001). Role of G-protein-coupled adenosine receptors in downregulation of inflammation and protection from tissue damage. Nature *414*, 916-920.

Okamura, S., Maruyama, H.B. and Yanagita, T. (1973). Ribosome degradation and degradation products in starved *Escherichia coli*. VI. Prolonged culture during glucose starvation. Journal of Biochemistry *73*, 915-922.

Otvos, L., O, I., Rogers, M.E., Consolvo, P.J., Condie, B.A., Lovas, S., Bulet, P. and Blaszczyk-Thurin, M. (2000). Interaction between Heat Shock Proteins and Antimicrobial Peptides. Biochemistry *39*, 14150-14159.

Pallen, M.J. and Wren, B.W. (2007). Bacterial pathogenomics. Nature *449*, 835-842.

Panther, E., Idzko, M., Herouy, Y., Rheinen, H., Gebicke-Haerter, P.J., Mrowietz, U., Dichmann, S. and Norgauer, J. (2001). Expression and function of adenosine receptors in human dendritic cells. The FASEB Journal *15*, 1963-1970.

Panyutich, A.V., Szold, O., Poon, P.H., Tseng, Y. and Ganz, T. (1994). Identification of defensin binding to C1 complement. FEBS Letters *356*, 169-173.

Park, C.B., Kim, H.S. and Kim, S.C. (1998). Mechanism of action of the antimicrobial peptide buforin II: buforin II kills microorganisms by penetrating the cell membrane and inhibiting cellular functions. Biochemical and Biophysical Research Communications *244*, 253-257.

Park, C.B., Yi, K.S., Matsuzaki, K., Kim, M.S. and Kim, S.C. (2000). Structure-activity analysis of buforin II, a histone H2A-derived antimicrobial peptide: the proline hinge is responsible for the cell-penetrating ability of buforin II. Proceedings of the National Academy of Sciences of the United States of America *97*, 8245-8250.

Parkes, M., Barrett, J.C., Prescott, N.J., Tremelling, M., Anderson, C.A., Fisher, S.A., Roberts, R.G., Nimmo, E.R., Cummings, F.R., Soars, D., Drummond, H., Lees, C.W., Khawaja, S.A., Bagnall, R., Burke, D.A., Todhunter, C.E., Ahmad, T., Onnie, C.M., McArdle, W., Strachan, D., Bethel, G., Bryan, C., Lewis, C.M., Deloukas, P., Forbes, A., Sanderson, J., Jewell, D.P., Satsangi, J., Mansfield, J.C., Cardon, L. and Mathew, C.G. (2007). Sequence variants in the autophagy gene *IRGM* and multiple other replicating loci contribute to Crohn's disease susceptibility. Nature Genetics *39*, 830-832.

Patrzykat, A., Friedrich, C.L., Zhang, L., Mendoza, V. and Hancock, R.E. (2002). Sublethal concentrations of pleurocidin-derived antimicrobial peptides inhibit macromolecular synthesis in *Escherichia coli*. Antimicrobial Agents and Chemotherapy *46*, 605-614.

Pazgier, M., Hoover, D.M., Yang, D., Lu, W. and Lubkowski, J. (2006). Human beta-defensins. Cellular and Molecular Life Sciences *63*, 1294-1313.

Petrof, E.O., Claud, E.C., Sun, J., Abramova, T., Guo, Y., Waypa, T.S., He, S.-M., Nakagawa, Y. and Chang, E.B. (2009). Bacteria-free solution derived from *Lactobacillus plantarum* inhibits multiple NF-kappaB pathways and inhibits proteasome function. Inflammatory Bowel Diseases *15*, 1537-1547.

Pettengill, M.A., Lam, V.W. and Ojcius, D.M. (2009). The danger signal adenosine induces persistence of chlamydial infection through stimulation of A2b receptors. PLoS One *4*, e8299.

Pingel, L.C., Kohlgraf, K.G., Hansen, C.J., Eastman, C.G., Dietrich, D.E., Burnell, K.K., Srikantha, R.N., Xiao, X., Belanger, M., Progulske-Fox, A., Cavanaugh, J.E., Guthmiller, J.M., Johnson, G.K., Joly, S., Kurago, Z.B., Dawson, D.V. and Brogden, K.A. (2008). Human beta-defensin 3 binds to hemagglutinin B (rHagB), a non-fimbrial adhesin from *Porphyromonas gingivalis*, and attenuates a pro-inflammatory cytokine response. Immunology and Cell Biology *86*, 643-649.

Powers, J.-P.S. and Hancock, R.E.W. (2003). The relationship between peptide structure and antibacterial activity. Peptides *24*, 1681-1691.

Qin, J., Li, R., Raes, J., Arumugam, M., Burgdorf, K.S., Manichanh, C., Nielsen, T., Pons, N., Levenez, F., Yamada, T., Mende, D.R., Li, J., Xu, J., Li, S., Li, D., Cao, J., Wang, B., Liang, H., Zheng, H., Xie, Y., Tap, J., Lepage, P., Bertalan, M., Batto, J.M., Hansen, T., Le Paslier, D., Linneberg, A., Nielsen, H.B., Pelletier, E., Renault, P., Sicheritz-Ponten, T., Turner, K., Zhu, H., Yu, C., Jian, M., Zhou, Y., Li, Y., Zhang, X., Qin, N., Yang, H., Wang, J., Brunak, S., Dore, J., Guarner, F., Kristiansen, K., Pedersen, O., Parkhill, J., Weissenbach, J., Bork, P. and Ehrlich, S.D. (2010). A human gut microbial gene catalogue established by metagenomic sequencing. Nature *464*, 59-65.

Rahimian, R., Fakhfouri, G., Daneshmand, A., Mohammadi, H., Bahremand, A., Rasouli, M.R., Mousavizadeh, K. and Dehpour, A.R. (2010). Adenosine A_{2A} receptors and uric acid mediate protective effects of inosine against TNBS-induced colitis in rats. European Journal of Pharmacology *649*, 376-381.

Razani, B. and Cheng, G. (2010). NF-kappaB: much learned, much to learn. Science Signaling *3*, pe29.

Ren, T., Grants, I., Alhaj, M., McKiernan, M., Jacobson, M., Hassanain, H.H., Frankel, W., Wunderlich, J. and Christofi, F.L. (2011). Impact of disrupting adenosine A_3 receptors ($A_3^{-/-}$ AR) on colonic motility or progression of colitis in the mouse. Inflammatory Bowel Diseases *17*, 1698-1713.

Rescigno, M. (2011). The intestinal epithelial barrier in the control of homeostasis and immunity. Trends in Immunology *32*, 256-264.

Rhee, K.J., Wu, S., Wu, X., Huso, D.L., Karim, B., Franco, A.A., Rabizadeh, S., Golub, J.E., Mathews, L.E., Shin, J., Sartor, R.B., Golenbock, D., Hamad, A.R., Gan, C.M., Housseau, F. and Sears, C.L. (2009). Induction of persistent colitis by a human commensal, enterotoxigenic *Bacteroides fragilis*, in wild-type C57BL/6 mice. Infection and Immunity *77*, 1708-1718.

Rhodius, V.A., Suh, W.C., Nonaka, G., West, J. and Gross, C.A. (2006). Conserved and variable functions of the sigmaE stress response in related genomes. PLoS Biology *4*, e2.

Rieley, G. (1994). Derivatization of organic compounds prior to gas chromatographic-combustion-isotope ratio mass spectrometric analysis: identification of isotope fractionation processes. Analyst *119*, 915-919.

Riksen, N.P., Barrera, P., van den Broek, P.H., van Riel, P.L., Smits, P. and Rongen, G.A. (2006). Methotrexate modulates the kinetics of adenosine in humans *in vivo*. Annals of Rheumatic Diseases *65*, 465-470.

Riley, M.A. and Wertz, J.E. (2002). Bacteriocin diversity: ecological and evolutionary perspectives. Biochimie *84*, 357-364.

Rinas, U., Hellmuth, K., Kang, R., Seeger, A. and Schlieker, H. (1995). Entry of *Escherichia coli* into stationary phase is indicated by endogenous and exogenous accumulation of nucleobases. Applied and Environmental Microbiology *61*, 4147-4151.

Rogler, G., Brand, K., Vogl, D., Page, S., Hofmeister, R., Andus, T., Knuechel, R., Baeuerle, P.A., Scholmerich, J. and Gross, V. (1998). Nuclear factor kappaB is activated in

macrophages and epithelial cells of inflamed intestinal mucosa. Gastroenterology *115*, 357-369.

Rook, G.A.W. and Brunet, L.R. (2005). Microbes, immunoregulation, and the gut. Gut *54*, 317-320.

Routsias, J.G., Karagounis, P., Parvulesku, G., Legakis, N.J. and Tsakris, A. (2010). *In vitro* bactericidal activity of human beta-defensin 2 against nosocomial strains. Peptides *31*, 1654-1660.

Rudner, R. and LeDoux, M. (1974). Distribution of pyrimidine oligonucleotides in complementary strand fractions of *Escherichia coli* deoxyribonucleic acid. Biochemistry *13*, 118-125.

Rybaczyk, L., Rozmiarek, A., Circle, K., Grants, I., Needleman, B., Wunderlich, J.E., Huang, K. and Christofi, F.L. (2009). New bioinformatics approach to analyze gene expressions and signaling pathways reveals unique purine gene dysregulation profiles that distinguish between CD and UC. Inflammatory Bowel Diseases *15*, 971-984.

Ryzhov, S., Zaynagetdinov, R., Goldstein, A.E., Novitskiy, S.V., Blackburn, M.R., Biaggioni, I. and Feoktistov, I. (2008a). Effect of A_{2B} adenosine receptor gene ablation on adenosine-dependent regulation of proinflammatory cytokines. Journal of Pharmacology and Experimental Therapeutics *324*, 694-700.

Ryzhov, S., Zaynagetdinov, R., Goldstein, A.E., Novitskiy, S.V., Dikov, M.M., Blackburn, M.R., Biaggioni, I. and Feoktistov, I. (2008b). Effect of A_{2B} adenosine receptor gene ablation on proinflammatory adenosine signaling in mast cells. Journal of Immunology *180*, 7212-7220.

Salzman, N.H., Ghosh, D., Huttner, K.M., Paterson, Y. and Bevins, C.L. (2003). Protection against enteric salmonellosis in transgenic mice expressing a human intestinal defensin. Nature *422*, 522-526.

Salzman, N.H., Hung, K., Haribhai, D., Chu, H., Karlsson-Sjoberg, J., Amir, E., Teggatz, P., Barman, M., Hayward, M., Eastwood, D., Stoel, M., Zhou, Y., Sodergren, E., Weinstock, G.M., Bevins, C.L., Williams, C.B. and Bos, N.A. (2010). Enteric defensins are essential regulators of intestinal microbial ecology. Nature Immunology *11*, 76-83.

Sansonetti, P.J. (2011). To be or not to be a pathogen: that is the mucosally relevant question. Mucosal Immunology *4*, 8-14.

Sartor, R.B. (2006). Mechanisms of disease: pathogenesis of Crohn's disease and ulcerative colitis. Nature Clinical Practice Gastroenterology & Hepatology *3*, 390-407.

Sartor, R.B. (2008). Microbial influences in inflammatory bowel diseases. Gastroenterology *134*, 577-594.

Savage, D.C. (1977). Microbial ecology of the gastrointestinal tract. Annual Review of Microbiology *31*, 107-133.

Savkovic, S.D., Koutsouris, A. and Hecht, G. (1997). Activation of NF-kappaB in intestinal epithelial cells by enteropathogenic *Escherichia coli*. American Journal of Physiology Cell Physiology *273*, C1160-1167.

Schlee, M., Wehkamp, J., Altenhoefer, A., Oelschlaeger, T.A., Stange, E.F. and Fellermann, K. (2007). Induction of human beta-defensin 2 by the probiotic *Escherichia coli* Nissle 1917 is mediated through flagellin. Infection and Immunity *75*, 2399-2407.

Schneider, J.J., Unholzer, A., Schaller, M., Schafer-Korting, M. and Korting, H.C. (2005). Human defensins. Journal of Molecular Medicine *83*, 587-595.

Schroder, J.M. (1999). Epithelial antimicrobial peptides: innate local host response elements. Cellular and Molecular Life Sciences *56*, 32-46.

Schultz, M. (2008). Clinical use of *E. coli* Nissle 1917 in inflammatory bowel disease. Inflammatory Bowel Diseases *14*, 1012-1018.

Sellon, R.K., Tonkonogy, S., Schultz, M., Dieleman, L.A., Grenther, W., Balish, E., Rennick, D.M. and Sartor, R.B. (1998). Resident enteric bacteria are necessary for development of spontaneous colitis and immune system activation in interleukin-10-deficient mice. Infection and Immunity *66*, 5224-5231.

Selmeczy, Z., Csoka, B., Pacher, P., Vizi, E.S. and Hasko, G. (2007). The adenosine A_{2A} receptor agonist CGS 21680 fails to ameliorate the course of dextran sulphate-induced colitis in mice. Inflammation Research *56*, 204-209.

Selsted, M.E. and Ouellette, A.J. (2005). Mammalian defensins in the antimicrobial immune response. Nature Immunology *6*, 551-557.

Sessions, A.L. (2006). Isotope-ratio detection for gas chromatography. Journal of Separation Science *29*, 1946-1961.

Shi, J. (2007). Defensins and Paneth cells in inflammatory bowel disease. Inflammatory Bowel Diseases *13*, 1284-1292.

Shi, J., Aono, S., Lu, W., Ouellette, A.J., Hu, X., Ji, Y., Wang, L., Lenz, S., van Ginkel, F.W., Liles, M., Dykstra, C., Morrison, E.E. and Elson, C.O. (2007). A novel role for defensins in intestinal homeostasis: regulation of IL-1beta secretion. Journal of Immunology *179*, 1245-1253.

Shiner, E.K., Rumbaugh, K.P. and Williams, S.C. (2005). Interkingdom signaling: Deciphering the language of acyl homoserine lactones. FEMS Microbiology Reviews *29*, 935-947.

Siegmund, B., Rieder, F., Albrich, S., Wolf, K., Bidlingmaier, C., Firestein, G.S., Boyle, D., Lehr, H.A., Loher, F., Hartmann, G., Endres, S. and Eigler, A. (2001). Adenosine kinase inhibitor GP515 improves experimental colitis in mice. Journal of Pharmacology and Experimental Therapeutics *296*, 99-105.

Simms, L.A., Doecke, J.D., Walsh, M.D., Huang, N., Fowler, E.V. and Radford-Smith, G.L. (2008). Reduced alpha-defensin expression is associated with inflammation and not NOD2 mutation status in ileal Crohn's disease. Gut *57*, 903-910.

Singh, U.P., Singh, S., Singh, R., Karls, R.K., Quinn, F.D., Potter, M.E. and Lillard, J.W., Jr. (2007). Influence of *Mycobacterium avium* subsp. *paratuberculosis* on colitis development and specific immune responses during disease. Infection and Immunity *75*, 3722-3728.

Sitaraman, S.V., Merlin, D., Wang, L., Wong, M., Gewirtz, A.T., Si-Tahar, M. and Madara, J.L. (2001). Neutrophil-epithelial crosstalk at the intestinal lumenal surface mediated by reciprocal secretion of adenosine and IL-6. Journal of Clinical Investigation *107*, 861-869.

Smith, P.K., Krohn, R.I., Hermanson, G.T., Mallia, A.K., Gartner, F.H., Provenzano, M.D., Fujimoto, E.K., Goeke, N.M., Olson, B.J. and Klenk, D.C. (1985). Measurement of protein using bicinchoninic acid. Analytical Biochemistry *150*, 76-85.

Sokol, H. and Seksik, P. (2010). The intestinal microbiota in inflammatory bowel diseases: time to connect with the host. Current Opinion in Gastroenterology *26*, 327-331.

Soler, C., James, K.J. and Picó, Y. (2007). Capabilities of different liquid chromatography tandem mass spectrometry systems in determining pesticide residues in food: Application to estimate their daily intake. Journal of Chromatography A *1157*, 73-84.

Sperandio, V., Torres, A.G., Jarvis, B., Nataro, J.P. and Kaper, J.B. (2003). Bacteria-host communication: the language of hormones. Proceedings of the National Academy of Sciences of the United States of America *100*, 8951-8956.

Spurr, A.R. (1969). A low-viscosity epoxy resin embedding medium for electron microscopy. Journal of Ultrastructure Research *26*, 31-43.

Spychala, J. and Mitchell, B.S. (2002). Cyclosporin A and FK506 decrease adenosine kinase activity and adenosine uptake in T-lymphocytes. Journal of Laboratory and Clinical Medicine *140*, 84-91.

Stanley, P.E. (1989). A review of bioluminescent ATP techniques in rapid microbiology. Journal of Bioluminescence and Chemiluminescence *4*, 375-380.

Stecher, B., Macpherson, A.J., Hapfelmeier, S., Kremer, M., Stallmach, T. and Hardt, W.D. (2005). Comparison of *Salmonella enterica* serovar Typhimurium colitis in germfree mice and mice pretreated with streptomycin. Infection and Immunity *73*, 3228-3241.

Stecher, B. and Hardt, W.D. (2008). The role of microbiota in infectious disease. Trends in Microbiology *16*, 107-114.

Strauber, H. and Muller, S. (2010). Viability states of bacteria--specific mechanisms of selected probes. Cytometry Part A : Journal of the International Society for Analytical Cytology *77*, 623-634.

Strober, W., Fuss, I. and Mannon, P. (2007). The fundamental basis of inflammatory bowel disease. Journal of Clinical Investigation *117*, 514-521.

Strohmeier, G.R., Reppert, S.M., Lencer, W.I. and Madara, J.L. (1995). The A2b adenosine receptor mediates cAMP responses to adenosine receptor agonists in human intestinal epithelia. Journal of Biological Chemistry *270*, 2387-2394.

Strohmeier, G.R., Lencer, W.I., Patapoff, T.W., Thompson, L.F., Carlson, S.L., Moe, S.J., Carnes, D.K., Mrsny, R.J. and Madara, J.L. (1997). Surface expression, polarization, and functional significance of CD73 in human intestinal epithelia. Journal of Clinical Investigation *99*, 2588-2601.

Stroinigg, N. and Srivastava, M.D. (2005). Modulation of toll-like receptor 7 and LL-37 expression in colon and breast epithelial cells by human beta-defensin-2. Allergy and Asthma Proceedings *26*, 299-309.

Suau, A., Bonnet, R., Sutren, M., Godon, J.-J., Gibson, G.R., Collins, M.D. and Dore, J. (1999). Direct Analysis of Genes Encoding 16S rRNA from Complex Communities Reveals Many Novel Molecular Species within the Human Gut. Applied and Environmental Microbiology *65*, 4799-4807.

Sun, J., Gunzer, F., Westendorf, A.M., Buer, J., Scharfe, M., Jarek, M., Gößling, F., Blöcker, H. and Zeng, A.-P. (2005). Genomic peculiarity of coding sequences and metabolic potential of probiotic *Escherichia coli* strain Nissle 1917 inferred from raw genome data. Journal of Biotechnology *117*, 147-161.

Sundaram, U., Hassanain, H., Suntres, Z., Yu, J.G., Cooke, H.J., Guzman, J. and Christofi, F.L. (2003). Rabbit chronic ileitis leads to up-regulation of adenosine *A1/A3* gene products, oxidative stress, and immune modulation. Biochemical Pharmacology *65*, 1529-1538.

Swidsinski, A., Ladhoff, A., Pernthaler, A., Swidsinski, S., Loening-Baucke, V., Ortner, M., Weber, J., Hoffmann, U., Schreiber, S., Dietel, M. and Lochs, H. (2002). Mucosal flora in inflammatory bowel disease. Gastroenterology *122*, 44-54.

Takahashi, H.K., Iwagaki, H., Hamano, R., Wake, H., Kanke, T., Liu, K., Yoshino, T., Tanaka, N. and Nishibori, M. (2007). Effects of adenosine on adhesion molecule expression and cytokine production in human PBMC depend on the receptor subtype activated. British Journal of Pharmacology *150*, 816-822.

Territo, M.C., Ganz, T., Selsted, M.E. and Lehrer, R. (1989). Monocyte-chemotactic activity of defensins from human neutrophils. Journal of Clinical Investigation *84*, 2017-2020.

Thakur, C.S., Brown, M.E., Sama, J.N., Jackson, M.E. and Dayie, T.K. (2010). Growth of wildtype and mutant *E. coli* strains in minimal media for optimal production of nucleic acids for preparing labeled nucleotides. Applied Microbiology and Biotechnology *88*, 771-779.

Thammavongsa, V., Kern, J.W., Missiakas, D.M. and Schneewind, O. (2009). *Staphylococcus aureus* synthesizes adenosine to escape host immune responses. Journal of Experimental Medicine *206*, 2417-2427.

Thomas, C.M. and Versalovic, J. (2010). Probiotics-host communication: Modulation of signaling pathways in the intestine. Gut Microbes *1*, 148-163.

Trautmann, A. (2009). Extracellular ATP in the immune system: more than just a "danger signal". Science Signaling *2*, pe6.

Turnbaugh, P.J., Ley, R.E., Mahowald, M.A., Magrini, V., Mardis, E.R. and Gordon, J.I. (2006). An obesity-associated gut microbiome with increased capacity for energy harvest. Nature *444*, 1027-1031.

Turnbaugh, P.J. and Gordon, J.I. (2009). The core gut microbiome, energy balance and obesity. Journal of Physiology *587*, 4153-4158.

UC Davis ChemWiki by University of California, Davis http://chemwiki.ucdavis.edu/Analytical_Chemistry/Instrumental_Analysis/Gas_Chromatography.

Valore, E.V., Martin, E., Harwig, S.S. and Ganz, T. (1996). Intramolecular inhibition of human defensin HNP-1 by its propiece. Journal of Clinical Investigation *97*, 1624-1629.

van den Berg, R.H., Faber-Krol, M.C., van Wetering, S., Hiemstra, P.S. and Daha, M.R. (1998). Inhibition of activation of the classical pathway of complement by human neutrophil defensins. Blood *92*, 3898-3903.

van Dieren, J.M., Kuipers, E.J., Samsom, J.N., Nieuwenhuis, E.E. and van der Woude, C.J. (2006). Revisiting the immunomodulators tacrolimus, methotrexate, and mycophenolate mofetil: their mechanisms of action and role in the treatment of IBD. Inflammatory Bowel Diseases *12*, 311-327.

Veldhuizen, E.J.A., Rijnders, M., Claassen, E.A., van Dijk, A. and Haagsman, H.P. (2008). Porcine [beta]-defensin 2 displays broad antimicrobial activity against pathogenic intestinal bacteria. Molecular Immunology *45*, 386-394.

Vieira, G., Sabarly, V., Bourguignon, P.Y., Durot, M., Le Fevre, F., Mornico, D., Vallenet, D., Bouvet, O., Denamur, E., Schachter, V. and Medigue, C. (2011). Core and panmetabolism in *Escherichia coli*. Journal of Bacteriology *193*, 1461-1472.

Villas-Boas, S.G., Rasmussen, S. and Lane, G.A. (2005). Metabolomics or metabolite profiles? Trends in Biotechnology *23*, 385-386.

Voss, E., Wehkamp, J., Wehkamp, K., Stange, E.F., Schroder, J.M. and Harder, J. (2006). NOD2/CARD15 mediates induction of the antimicrobial peptide human beta-defensin-2. Journal of Biological Chemistry *281*, 2005-2011.

Vylkova, S., Sun, J.N. and Edgerton, M. (2007). The role of released ATP in killing *Candida albicans* and other extracellular microbial pathogens by cationic peptides. Purinergic Signalling *3*, 91-97.

Walia, B., Castaneda, F.E., Wang, L., Kolachala, V.L., Bajaj, R., Roman, J., Merlin, D., Gewirtz, A.T. and Sitaraman, S.V. (2004). Polarized fibronectin secretion induced by adenosine regulates bacterial-epithelial interaction in human intestinal epithelial cells. Biochemical Journal *382*, 589-596.

Wang, Y., Hoenig, J.D., Malin, K.J., Qamar, S., Petrof, E.O., Sun, J., Antonopoulos, D.A., Chang, E.B. and Claud, E.C. (2009). 16S rRNA gene-based analysis of fecal microbiota from preterm infants with and without necrotizing enterocolitis. ISME Journal *3*, 944-954.

Wang, Z. and Wang, G. (2004). APD: the Antimicrobial Peptide Database. Nucleic Acids Research *32*, D590-592.

Watanabe, K., Fukumoto, H. and Isoi, K. (1986). Intracellular localization of ATP:AMP phosphotransferase in *Escherichia coli*. Biochemical and Biophysical Research Communications *134*, 527-531.

Watanabe, K., Tomioka, S., Tanimura, K., Oku, H. and Isoi, K. (2011). Uptake of AMP, ADP, and ATP in *Escherichia coli* W. Bioscience, Biotechnology, and Biochemistry *75*, 7-12.

Watanabe, T., Kitani, A., Murray, P.J., Wakatsuki, Y., Fuss, I.J. and Strober, W. (2006). Nucleotide binding oligomerization domain 2 deficiency leads to dysregulated TLR2 signaling and induction of antigen-specific colitis. Immunity *25*, 473-485.

Wehkamp, J., Fellermann, K., Herrlinger, K.R., Baxmann, S., Schmidt, K., Schwind, B., Duchrow, M., Wohlschlager, C., Feller, A.C. and Stange, E.F. (2002). Human beta-defensin 2 but not beta-defensin 1 is expressed preferentially in colonic mucosa of inflammatory bowel disease. European Journal of Gastroenterology & Hepatology *14*, 745-752.

Wehkamp, J., Harder, J., Weichenthal, M., Mueller, O., Herrlinger, K.R., Fellermann, K., Schroeder, J.M. and Stange, E.F. (2003). Inducible and constitutive beta-defensins are differentially expressed in Crohn's disease and ulcerative colitis. Inflammatory Bowel Diseases *9*, 215-223.

Wehkamp, J., Harder, J., Wehkamp, K., Wehkamp-von Meissner, B., Schlee, M., Enders, C., Sonnenborn, U., Nuding, S., Bengmark, S., Fellermann, K., Schroder, J.M. and Stange, E.F. (2004). NF-kappaB- and AP-1-mediated induction of human beta defensin-2 in intestinal epithelial cells by *Escherichia coli* Nissle 1917: a novel effect of a probiotic bacterium. Infection and Immunity *72*, 5750-5758.

Wehkamp, J., Salzman, N.H., Porter, E., Nuding, S., Weichenthal, M., Petras, R.E., Shen, B., Schaeffeler, E., Schwab, M., Linzmeier, R., Feathers, R.W., Chu, H., Lima, H., Jr., Fellermann, K., Ganz, T., Stange, E.F. and Bevins, C.L. (2005). Reduced Paneth cell alpha-defensins in ileal Crohn's disease. Proceedings of the National Academy of Sciences of the United States of America *102*, 18129-18134.

Wen, L., Ley, R.E., Volchkov, P.Y., Stranges, P.B., Avanesyan, L., Stonebraker, A.C., Hu, C., Wong, F.S., Szot, G.L., Bluestone, J.A., Gordon, J.I. and Chervonsky, A.V. (2008). Innate immunity and intestinal microbiota in the development of Type 1 diabetes. Nature *455*, 1109-1113.

Werner, E., Heilier, J.F., Ducruix, C., Ezan, E., Junot, C. and Tabet, J.C. (2008). Mass spectrometry for the identification of the discriminating signals from metabolomics: current status and future trends. Journal of Chromatography B, Analytical Technologies in the Biomedical and Life Sciences *871*, 143-163.

Whitman, W.B., Coleman, D.C. and Wiebe, W.J. (1998). Prokaryotes: the unseen majority. Proceedings of the National Academy of Sciences of the United States of America *95*, 6578-6583.

WHO (2001). FAO/WHO. Health and nutritional properties of probiotics in food including powder milk with live lactic acid bacteria. Basel, Switzerland: World Health Organization 2001.

Wiechert, W. (2001). ^{13}C metabolic flux analysis. Metabolic Engineering *3*, 195-206.

Wilson, C.L., Ouellette, A.J., Satchell, D.P., Ayabe, T., Lopez-Boado, Y.S., Stratman, J.L., Hultgren, S.J., Matrisian, L.M. and Parks, W.C. (1999). Regulation of intestinal alpha-defensin activation by the metalloproteinase matrilysin in innate host defense. Science *286*, 113-117.

Wilson, J.M., Ross, W.G., Agbai, O.N., Frazier, R., Figler, R.A., Rieger, J., Linden, J. and Ernst, P.B. (2009). The A_{2B} adenosine receptor impairs the maturation and immunogenicity of dendritic cells. Journal of Immunology *182*, 4616-4623.

Wimley, W.C., Selsted, M.E. and White, S.H. (1994). Interactions between human defensins and lipid bilayers: evidence for formation of multimeric pores. Protein Science *3*, 1362-1373.

Wohlgemuth, S., Haller, D., Blaut, M. and Loh, G. (2009). Reduced microbial diversity and high numbers of one single *Escherichia coli* strain in the intestine of colitic mice. Environmental Microbiology *11*, 1562-1571.

Xaus, J., Mirabet, M., Lloberas, J., Soler, C., Lluis, C., Franco, R. and Celada, A. (1999). IFN-gamma up-regulates the A_{2B} adenosine receptor expression in macrophages: a mechanism of macrophage deactivation. Journal of Immunology *162*, 3607-3614.

Xavier, R.J. and Podolsky, D.K. (2007). Unravelling the pathogenesis of inflammatory bowel disease. Nature *448*, 427-434.

Xi, C. and Wu, J. (2010). dATP/ATP, a multifunctional nucleotide, stimulates bacterial cell lysis, extracellular DNA release and biofilm development. PLoS One *5*, e13355.

Yang, A., Mucsi, A.D., Desrosiers, M.D., Chen, J.F., Schnermann, J.B., Blackburn, M.R. and Shi, Y. (2010). Adenosine mediated desensitization of cAMP signaling enhances T-cell responses. European Journal of Immunology *40*, 449-459.

Yang, D., Chertov, O., Bykovskaia, S.N., Chen, Q., Buffo, M.J., Shogan, J., Anderson, M., Schroder, J.M., Wang, J.M., Howard, O.M. and Oppenheim, J.J. (1999). Beta-defensins: linking innate and adaptive immunity through dendritic and T cell CCR6. Science *286*, 525-528.

Yang, D., Chen, Q., Chertov, O. and Oppenheim, J.J. (2000). Human neutrophil defensins selectively chemoattract naive T and immature dendritic cells. Journal of Leukocyte Biology *68*, 9-14.

Yasuda, Y., Saito, M., Yamamura, T., Yaguchi, T. and Nishizaki, T. (2009). Extracellular adenosine induces apoptosis in Caco-2 human colonic cancer cells by activating caspase-9/-3 via A_{2a} adenosine receptors. Journal of Gastroenterology *44*, 56-65.

Ye, J.H. and Rajendran, V.M. (2009). Adenosine: an immune modulator of inflammatory bowel diseases. World Journal of Gastroenterology *15*, 4491-4498.

Ye, Z., Petrof, E.O., Boone, D., Claud, E.C. and Sun, J. (2007). *Salmonella* effector AvrA regulation of colonic epithelial cell inflammation by deubiquitination. American Journal of Pathology *171*, 882-892.

Yeaman, M.R. and Yount, N.Y. (2003). Mechanisms of antimicrobial peptide action and resistance. Pharmacological Reviews *55*, 27-55.

Yenugu, S., Hamil, K.G., Radhakrishnan, Y., French, F.S. and Hall, S.H. (2004). The androgen-regulated epididymal sperm-binding protein, human beta-defensin 118 (DEFB118) (formerly ESC42), is an antimicrobial beta-defensin. Endocrinology *145*, 3165-3173.

Yonezawa, A., Kuwahara, J., Fujii, N. and Sugiura, Y. (1992). Binding of tachyplesin I to DNA revealed by footprinting analysis: significant contribution of secondary structure to DNA binding and implication for biological action. Biochemistry *31*, 2998-3004.

Yoshida, N., McNiven, S.J., Morita, T., Nakamura, H. and Karube, I. (2002). A simple, multiple simultaneous spectrophotometric method for BOD determination using DCIP as the redox color indicator. Analytical Letters *35*, 1541 - 1549.

Zaph, C., Troy, A.E., Taylor, B.C., Berman-Booty, L.D., Guild, K.J., Du, Y., Yost, E.A., Gruber, A.D., May, M.J., Greten, F.R., Eckmann, L., Karin, M. and Artis, D. (2007). Epithelial-cell-intrinsic IKK-[bgr] expression regulates intestinal immune homeostasis. Nature *446*, 552-556.

Zasloff, M. (2002). Antimicrobial peptides of multicellular organisms. Nature *415*, 389-395.

Zhao, C., Wang, I. and Lehrer, R.I. (1996). Widespread expression of beta-defensin hBD-1 in human secretory glands and epithelial cells. FEBS Letters *396*, 319-322.

Zhu, B.D., Feng, Y., Huang, N., Wu, Q. and Wang, B.Y. (2003). *Mycobacterium bovis* bacille Calmette-Guerin (BCG) enhances human beta-defensin-1 gene transcription in human pulmonary gland epithelial cells. Acta Pharmacologica Sinica *24*, 907-912.

Zilbauer, M., Dorrell, N., Boughan, P.K., Harris, A., Wren, B.W., Klein, N.J. and Bajaj-Elliott, M. (2005). Intestinal innate immunity to *Campylobacter jejuni* results in induction of bactericidal human beta-defensins 2 and 3. Infection and Immunity *73*, 7281-7289.

ACKNOWLEDGEMENTS

I am indebted to the skilful scientists who contributed directly to this work. First of all to my supervisor, Dr. Wolf-Rainer Abraham, for opening the first door, believing in my capacity and continuously giving me opportunities to develop it. To Dr. Gabriella Molinari, Dr. Dieco Würdemann and the Environmental Microbiology group, for introducing me to the defensins. To Dr. Maximiliano Gutierrez and his group, for precious guidance while working with human cells. To Dr. Manfred Rohde and his group, for generating the electron microscopy images. To Eng. Esther Surges, for her efficient assistance with our chromatographers and mass spectrometers and for the measurements at the IRMS. To Ignacio Poblete for his support with flow cytometry analysis. To Dr. Melissa Wos-Oxley for critically reading the thesis.

Also, I acknowledge the examiners of this work for their time and receptiveness: Prof. Dr. Katharina Riedel, Prof. Dr. Dietmar Schomburg and Prof. Dr. Kenneth Timmis, my doktorvater, to whom I am particularly thankful for his kindness during these three years.

I would like to thank my lovely teammates in CMIK, our department secretaries Conni and Ladina, and also colleagues from other groups, who offered me help and goodwill when I needed, especially the ones who additionally provided cheerful moments and open friendship. Special thanks to the whole Brazilian/latin “gang” (and multinational sympathizers) for the best laughter, the best food and the best mood, people who can smooth even the hardest times. A giant Obrigada! to Amélia, Daiana, Maira and my amazing crew of nutritionists; to Marcela for the outgoing experienced support and to Marcelinho for helping optimize my time with the computer. I thank the friends who encouraged me to embrace this project in the first place, and assisted me from the distance, especially Adriana, Alexandre and Prof. Termignoni.

Finally, I wish to thank my beloved family, and my parents above all, for the confidence, support and love so great that reaches me overseas. Thanks to my friends Aline e Ricardo, who share with me the dream of a PhD abroad, since the time when it seemed too big a step for my legs.

I gratefully dedicate this thesis to Marcelo Gehara, the man with whom I share not only my dreams, but my life and love, for being here for me, my haven and my inspiration.

ESTRELA, Andréia Bergamo

Persönliche Daten

Geburtsdatum:	01.12.1984
Geburtsort:	Porto Alegre – Brasilien
Addresse:	Helmstedter Str. 144 38102 – Braunschweig, DE
e-mail:	Andreia.Estrela@Helmholtz-hzi.de an_estrela@yahoo.com.br

Ausbildung

Seit 2008	Promotion (Fachgebiet Biologie, Mikrobiologie) Arbeitsgruppe Chemische Mikrobiologie Helmholtz-Zentrum für Infektionsforschung Braunschweig – Deutschland
2007– 2008	Master in Zell- und Molekularbiologie Thema: "Protein digestion in cattle tick, *Ripicephalus (B.) microplus*, larvae." Postgraduierten-Programm: Zell- und Molekularbiologie Universität: Universidade Federal do Rio Grande do Sul Porto Alegre – Brasilien
2002 – 2006	Abschluss in Biologie Diplomarbeitsthema: "A cysteine-endopeptidase from *Boophilus microplus* larvae with vitellin digestion activity." Institut für Lebenswissenschaft Universität: Universidade Federal do Rio Grande do Sul Porto Alegre – Brasilien

Sprachkenntnisse

Portugiesisch – Muttersprache

Englisch – fließend in Wort und Schrift

Spanisch – fließend in Wort, sehr gut in Schrift

Deutsch – befriedigend in Wort und Schrift

Praktika ----------

März 2002 – Dezember 2006	Wissenschaftliches Stipendiat – Forschungsthema: "Purification and characterization of a vitellin degrading enzyme, involved in larval nutrition during starvation. Physiologically important molecules as potential targets to an anti-tick vaccine." Universität: Universidade Federal do Rio Grande do Sul Porto Alegre - Brasilien
Februar 2006 – März 2006	Trainee (360 Std) – Projekt: "Behavioural studies associated to semiochemicals, using advanced tools to develop pest-management methods. Morphological and ultra-structural analysis of soybean-pest insects' antenna.Introduction to Tranmission and Scanning Electron Microscopy." Zentrum: Centro Nacional de Pesquisa de Recursos Genéticos e Biotecnologia (CENARGEN - EMBRAPA) Brasília - Brasilien

Veröffentlichungen ----------

1. ESTRELA, A.B.; Abraham, W.R. Adenosine in the inflamed gut: a janus faced compound. *Current Medicinal Chemistry* 18(18):2791-2815. **2011**.

2. ESTRELA A.B.; Seixas A.;Teixeira V.O.; Pinto A.F.; Termignoni C.Vitellin- and hemoglobin-digesting enzymes in *Rhipicephalus (Boophilus) microplus* larvae and females. *Comparative Biochemistry and Physiology B: Biochemistry and Molecular Biology.* 157(4):326-335. **2010**.

3. Seixas, A.; ESTRELA, A.; Pontes, E.; Ceolato, J.; Lara, F.; Gondin, K.; Termignoni, C. Distribution and functional studies of a *Rhipicephalus Boophilus microplus* Vitellin-Degrading Cysteine Endopeptidase. *Parasitology* 137(12):1819-1831. **2010**.

4. ESTRELA, A. B.; Abraham, W.R. Proposal of *Brevundimonas vancanneytii* sp. nov. isolated from blood of a patient with endocarditis. *International Journal of Systematic and Evolutionary Microbiology* 60(Pt 9):2129-2134. **2010**.

5. Abraham, W.R.; ESTRELA, A.B.; Nikitin, D.I.; Smit, J.; Vancanneyt, M. Proposal of *Brevundimonas halotolerans* sp. nov., *Brevundimonas poindexterae* sp. nov. and *Brevundimonas staleyi* sp. nov., prosthecate bacteria from aquatic habitats. *International Journal of Systematic and Evolutionary Microbiology* 60(Pt 8):1837-1843. **2010**.

6. ESTRELA A. B.; Heck, M. G.; Abraham W.R. Novel approaches to control biofilm infections. *Current Medicinal Chemistry* 16(12):1512-1530. **2009**.

7. ESTRELA, A.; Seixas, A.; Termignoni, C. A cysteine endopeptidase from tick (*Rhipicephalus (Boophilus) microplus*) larvae with vitellin digestion activity. *Comparative Biochemistry and Physiology: B, Biochemistry and Molecular Biology* 148: 410 – 416. **2007**.